UNFOLDED PROTEIN RESPONSE (UPR): AN IMPENDING TARGET FOR MULTIPLE NEUROLOGICAL DISORDERS

EDITED BY: Safikur Rahman, Arif Tasleem Jan, Khurshid Ahmad and Rinki Minakshi

PUBLISHED IN: Frontiers in Aging Neuroscience and Frontiers in Cellular Neuroscience

frontiers Research Topics

ISSN 1664-8714
ISBN 978-2-83250-430-7
DOI 10.3389/978-2-83250-430-7

About Frontiers

Frontiers is more than just an open-access publisher of scholarly articles: it is a pioneering approach to the world of academia, radically improving the way scholarly research is managed. The grand vision of Frontiers is a world where all people have an equal opportunity to seek, share and generate knowledge. Frontiers provides immediate and permanent online open access to all its publications, but this alone is not enough to realize our grand goals.

Frontiers Journal Series

The Frontiers Journal Series is a multi-tier and interdisciplinary set of open-access, online journals, promising a paradigm shift from the current review, selection and dissemination processes in academic publishing. All Frontiers journals are driven by researchers for researchers; therefore, they constitute a service to the scholarly community. At the same time, the Frontiers Journal Series operates on a revolutionary invention, the tiered publishing system, initially addressing specific communities of scholars, and gradually climbing up to broader public understanding, thus serving the interests of the lay society, too.

Dedication to Quality

Each Frontiers article is a landmark of the highest quality, thanks to genuinely collaborative interactions between authors and review editors, who include some of the world's best academicians. Research must be certified by peers before entering a stream of knowledge that may eventually reach the public - and shape society; therefore, Frontiers only applies the most rigorous and unbiased reviews.
Frontiers revolutionizes research publishing by freely delivering the most outstanding research, evaluated with no bias from both the academic and social point of view. By applying the most advanced information technologies, Frontiers is catapulting scholarly publishing into a new generation.

What are Frontiers Research Topics?

Frontiers Research Topics are very popular trademarks of the Frontiers Journals Series: they are collections of at least ten articles, all centered on a particular subject. With their unique mix of varied contributions from Original Research to Review Articles, Frontiers Research Topics unify the most influential researchers, the latest key findings and historical advances in a hot research area! Find out more on how to host your own Frontiers Research Topic or contribute to one as an author by contacting the Frontiers Editorial Office: frontiersin.org/about/contact

UNFOLDED PROTEIN RESPONSE (UPR): AN IMPENDING TARGET FOR MULTIPLE NEUROLOGICAL DISORDERS

Topic Editors:
Safikur Rahman, Babasaheb Bhimrao Ambedkar Bihar University, India
Arif Tasleem Jan, Baba Ghulam Shah Badshah University, India
Khurshid Ahmad, Yeungnam University, South Korea
Rinki Minakshi, University of Delhi, India

Citation: Rahman, S., Jan, A. T., Ahmad, K., Minakshi, R., eds. (2022). Unfolded Protein Response (UPR): An Impending Target for Multiple Neurological Disorders. Lausanne: Frontiers Media SA. doi: 10.3389/978-2-83250-430-7

Table of Contents

frontiers | Frontiers in Aging Neuroscience

TYPE Editorial
PUBLISHED 23 September 2022
DOI 10.3389/fnagi.2022.1014450

OPEN ACCESS

EDITED AND REVIEWED BY
Jorge Busciglio,
University of California, Irvine,
United States

*CORRESPONDENCE
Arif Tasleem Jan
atasleem@bgsbu.ac.in

SPECIALTY SECTION
This article was submitted to Cellular and Molecular Mechanisms of Brain-aging, a section of the journal Frontiers in Aging Neuroscience

RECEIVED 08 August 2022
ACCEPTED 22 August 2022
PUBLISHED 23 September 2022

CITATION
Jan AT, Rahman S, Ahmad K and Minakshi R (2022) Editorial: Unfolded protein response (UPR): An impending target for multiple neurological disorders.
Front. Aging Neurosci. 14:1014450.
doi: 10.3389/fnagi.2022.1014450

Editorial: Unfolded protein response (UPR): An impending target for multiple neurological disorders

Arif Tasleem Jan[1]*, Safikur Rahman[2], Khurshid Ahmad[3] and Rinki Minakshi[4]

[1]Gene Expression Lab, School of Biosciences and Biotechnology, Baba Ghulam Shah Badshah University, Rajouri, India, [2]Department of Botany, Munshi Singh College, BR Ambedkar Bihar University, Muzaffarpur, Bihar, India, [3]Department of Medical Biotechnology, Yeungnam University, Gyeongsan, South Korea, [4]Department of Microbiology, Swami Shraddhanand College, University of Delhi, New Delhi, India

KEYWORDS

aggregation, endoplasmic reticulum stress, neurological disorders, protein folding, proteinopathies, unfolded protein response

Editorial on the Research Topic
Unfolded protein response (UPR): An impending target for multiple neurological disorders

Introduction

The endoplasmic reticulum (ER) is responsible for carrying out the process of folding, maturation, and trafficking of proteins, following their synthesis in the cell. The function of the ER can be disrupted by environmental insults, resulting in the accumulation of misfolded or unfolded cargo in its lumen, a condition referred to as ER stress. The ER normally has a rescue pathway to take care of the damaged or misfolded protein overload, which involves halting the translational machinery, upregulating the expression of the chaperones, and diverting misfolded or unfolded proteins to degradation pathways, called ER-associated degradation (ERAD). If this rescue pathway fails, the protein aggregates will be sensed by PERK1, IRE1, and ATF6 in the ER, resulting in the activation of an extremely conserved signaling pathway called the ER unfolded protein response (UPR^{ER}). If the accumulation of misfolded proteins and the stress and damaging conditions associated with them persist for a long time, the resulting cellular injury can manifest itself in the form of a variety of etiologies in the brain, including Alzheimer's disease (AD), Parkinson's disease (PD), and amyotrophic lateral sclerosis (ALS). In this context, it has become increasingly important to: (a) decipher the pathophysiology of neurodegenerative disorders (NDs), (b) put up a multidimensional assessment of the genetic mechanisms underlying these disorders, (c) identify mechanisms that link stress responses to neuronal function, (d) set

up preventive interventions to reduce the occurrence of these diseases, and (e) strategize pharmacological interventions to ameliorate the effects of neurological disorders, as an optimal method for extending the survival of affected individuals.

With our call for articles, we provided an interface for authors to share their views and further explore the fundamental aspects of the UPR^{ER} in the pathophysiological regulation of neuronal disorders. This Research Topic is a multifaceted collection of analyses contributed by clinicians, neuroscientists, and academicians. It highlights recent advancements in the methodological approaches, pharmacological interventions, and conceptual issues that can be of immense use in dealing with different neurological disorders. Our goal was to make valuable contributions to deciphering different aspects of the occurrence of neurological disorders. This includes interrogating the interplay of UPR^{ER}-based signaling modules and the mechanism of their entanglement with neuronal abnormalities, as well as offering perspectives on designing different therapeutics against neurological diseases.

This issue contains review (five articles) and original research (four articles) covering recent advances on different aspects of the ER unfolded protein response and protein aggregation, and a series of papers covering different aspects of the physiological and pathological consequences of UPR^{ER} that lead to the development of NDs.

Zhao et al. review the complex interplay of ER stress and UPR^{ER} in ALS and TDP-43-associated pathology. ALS, a disease characterized by degeneration of the motor system, was found to exert its effects through dysregulation of the proteostasis, progressing through the aberrant build-up of misfolded/unfolded proteins in the ER lumen.

The article by Yasmeen et al. focuses on deciphering the link between UPR^{ER} signaling and microRNA in the pathogenesis of AD. In their study, they extensively elaborated ER stress and UPR in the dysregulation of microRNAs and the resulting consequences in the pathogenesis of AD.

The article by Alam and Akhter studies the occurrence diabetic retinopathy, a challenging eye disease, and then discusses its association with ER stress and UPR^{ER}. The authors also point out the key cellular programs in the development of diabetic retinopathy, thus providing a better understanding and elaborative view of the molecular and cellular basis of the development of this condition.

Fernandez et al. sought to explore this association further by investigating the role of UPR^{ER} in the development and function of immune cells. In this article, the authors studied the capacity of UPR^{ER} to set the threshold between cell survival and death and tried to establish the potential contributions of UPR^{ER} in brain-associated immune cells in the context of the development of an ND. This topic is discussed further in the article by Mukherjee et al. who reviewed the literature and summarized observations to ultimately present evidence that curcumin slows the progression of ND. The study established a relationship between curcumin levels, UPR^{ER}, and chance of ND development.

The original articles submitted to this issue present a range of relatively simple and pragmatically implementable pharmacological approaches toward promoting health and improving interventional strategies as part of reducing the development of ND. Pathak et al. studied the role of ofloxacin (a broad-spectrum antibiotic) as a possible drug molecule for use in the treatment of ND. The study both employed *in silico* modules and made use of biophysical techniques to uncover the dynamics of actin polymerization. The authors report that actin polymerization is disrupted upon binding with ofloxacin in a concentration-dependent manner, and thus holds great promise for use in the treatment of neurological disorders.

Warepam et al. address differences in the deposition levels of toxic protein inclusions in the presence and/or absence of an important brain metabolite, N-acetylaspartate (NAA). They report that NAA, whose levels have been reported to be altered in a variety of neurological disorders, acts as a potential protein stabilizer with the capacity to inhibit the aggregation of carbonic anhydrase and catalase. However, the authors debate whether an increase in alpha-synuclein is fueled by decreasing concentrations of NAA. They propose that NAA, with its potential to suppress protein aggregation, may offer benefits in terms of solubilizing the protein aggregates associated with the development of NDs.

Chen et al. integrated experimental and computational methods to show the expression pattern and potential implications of ER stress in the development of intracranial aneurysm (IA). The authors observed that the majority of the differentially expressed genes in the Gene Expression Omnibus and RNA sequencing datasets they studied are associated with ER stress, autophagy, and metabolism. The authors predicted a total of nine targets, all associated with ER stress, that can act as potential drug targets for use in delaying the formation and progression of IA.

Li et al. examined the neuroprotective effects of exercise after stroke and elucidated the role of SIRT1 in attributing neuroprotection. The authors used an ischemia/reperfusion rat model to investigate the effects of a post-stroke exercise regimen and its potential to regulate reactive oxygen species (ROS)/ER stress through the involvement of SIRT1. They established that SIRT1 is associated with the regulation of neuronal functioning and brain health and elucidated that mild exercise post-stroke, as well as intense exercise, might play a beneficial role in attributing neuroprotection. This comes as a significant finding in that the inclusion of exercise and regular follow-up assessments can be understood as a preventive step against the development of ND.

Conclusion

The articles published under this Research Topic cover a broad range of subjects that are directly related to the pathogenesis of ND, as well as its diagnosis and potential therapeutics. Other articles highlight the role and functionality of UPR^{ER} as well as lifestyle changes that affect the development of ND.

Author contributions

AJ prepared the initial draft of this editorial. SR, KA, and RM carefully revised the draft. All authors contributed to the contents of this article and approved the final version.

Funding

This work was supported by the Department of Science and Technology, India under Science and Engineering Research Board (DST-SERB) Grant No. CRG/2019/004106 and J&K Science Technology and Innovation Council (J&K ST&IC), India Grant No. (JK ST&IC/SRE/996-998).

Conflict of interest

The authors declare that the research was conducted in the absence of any commercial or financial relationships that could be construed as a potential conflict of interest.

Publisher's note

frontiers in Aging Neuroscience

ORIGINAL RESEARCH
published: 06 October 2020
doi: 10.3389/fnagi.2020.591579

Ofloxacin as a Disruptor of Actin Aggresome "Hirano Bodies": A Potential Repurposed Drug for the Treatment of Neurodegenerative Diseases

*Samridhi Pathak, Haifa Parkar, Sarita Tripathi and Avinash Kale**

School of Chemical Sciences, University of Mumbai - Department of Atomic Energy Center for Excellence in Basic Sciences, University of Mumbai, Vidyanagari Campus, Mumbai, India

There is a growing number of aging populations that are more prone to the prevalence of neuropathological disorders. Two major diseases that show a late onset of the symptoms include Alzheimer's disorder (AD) and Parkinson's disorder (PD), which are causing an unexpected social and economic impact on the families. A large number of researches in the last decade have focused upon the role of amyloid precursor protein, Aβ-plaque, and intraneuronal neurofibrillary tangles (tau-proteins). However, there is very few understanding of actin-associated paracrystalline structures formed in the hippocampus region of the brain and are called Hirano bodies. These actin-rich inclusion bodies are known to modulate the synaptic plasticity and employ conspicuous effects on long-term potentiation and paired-pulse paradigms. Since the currently known drugs have very little effect in controlling the progression of these diseases, there is a need to develop therapeutic agents, which can have improved efficacy and bioavailability, and can transport across the blood–brain barrier. Moreover, finding novel targets involving compound screening is both laborious and is an expensive process in itself followed by equally tedious Food and Drug Administration (FDA) approval exercise. Finding alternative functions to the already existing FDA-approved molecules for reversing the progression of age-related proteinopathies is of utmost importance. In the current study, we decipher the role of a broad-spectrum general antibiotic (Ofloxacin) on actin polymerization dynamics using various biophysical techniques like right-angle light scattering, dynamic light scattering, circular dichroism spectrometry, isothermal titration calorimetry, scanning electron microscopy, etc. We have also performed *in silico* docking studies to deduce a plausible mechanism of the drug binding to the actin. We report that actin gets disrupted upon binding to Ofloxacin in a concentration-dependent manner. We have inferred that Ofloxacin, when attached to a drug delivery system, can act as a good candidate for the treatment of neuropathological diseases.

Keywords: ofloxacin, neurodegenerative diseases, actin, repurposable drugs, biophysical studies, SEM, *in silico*

OPEN ACCESS

Edited by:
Safikur Rahman, Munshi Singh College, Babasaheb Bhimrao Ambedkar Bihar University, India

Reviewed by:
Md Tabish Rehman, King Saud University, Saudi Arabia
Nitesh Kumar Poddar, Invertis University, India

***Correspondence:**
Avinash Kale
avinash.kale@cbs.ac.in

Received: *04 August 2020*
Accepted: *09 September 2020*
Published: *06 October 2020*

Citation:
Pathak S, Parkar H, Tripathi S and Kale A (2020) Ofloxacin as a Disruptor of Actin Aggresome "Hirano Bodies": A Potential Repurposed Drug for the Treatment of Neurodegenerative Diseases. Front. Aging Neurosci. 12:591579. doi: 10.3389/fnagi.2020.591579

INTRODUCTION

Neurodegenerative disorders (NDs) are the subset of brain disorders defined by the obliteration of neuronal cells resulting from the accumulation of protein aggregates (Perl et al., 1995). Deaths related to NDs are second-most around the globe and a prominent cause of disability worldwide (Feigin et al., 2019). An estimated 12 million Americans will be suffering from NDs by 2030, of which patients suffering from Alzheimer's disease would be on top of the list (Chanfreau et al., 2005; Gammon, 2014). The biological factors that are known to cause NDs are attributed to oxidative stress, cytoskeletal protein aggregation, abnormal ubiquitination of protein, mitochondrial dysfunction, etc. (Trends and Disorders, 2018). Diseases like Alzheimer's disorder (AD), Parkinson's disease (PD), Huntington's disease (HD), amyotrophic lateral sclerosis (ALS), frontal temporal dementia (FTD) falls under the category of NDs and a major contributor to the socioeconomic problems associated with it (Subramaniam, 2019). Various factors have been associated to be the causative agent behind NDs, but a prominent one is still far from the search. Depending on the type of NDs, it could be either familial or sporadic (Przedborski et al., 2003). The current treatment regime focuses on slowing the manifestations of the symptoms and providing temporary relief toward these symptoms, thus, causing a severe lack of procedure to slow the disease progression and eventual death (Trends and Disorders, 2018).

Cytoskeletal protein has a major role to play in neuronal functioning by providing flexibility and maintaining the neuronal circuit (Muñoz-Lasso et al., 2020b). Certain proteins that are widely studied for their role in NDs are prion, tau, β-amyloid, α-synuclein, and Huntington (Gitler et al., 2017). It is implicated that misfolding of these proteins leads to their aggregation in the neuronal cells resulting in neurodegeneration (Ross and Poirier, 2004; Santa-Mara et al., 2008; Goebel, 2009; Spears et al., 2014; Koistinen et al., 2017). However, the role of cytoskeletal protein actin in the manifestation of NDs have been far from understood. Actin is reported to be the driving force in controlling synaptic plasticity and maintaining the structural integrity of the synapses (Kim and Lisman, 1999; Luo, 2002; Fukazawa et al., 2003; Bourne and Harris, 2008; Okada and Soderling, 2009). It functions by changing its morphology in response to different types of neural activity (Svennberg, 2006; Gordon-Weeks and Fournier, 2014; Spence and Soderling, 2015; Szabó et al., 2016; Pelucchi et al., 2020). Defects in the regulation of actin protein is one of the contributing factors leading to neurological disorders (Kim and Lisman, 1999; Luo, 2002; Bourne and Harris, 2008; Okada and Soderling, 2009).

Actin cytoskeletal remodeling and rearrangement play an important role at different sites in the brain cells and different stages of brain activity (Kevenaar and Hoogenraad, 2015; Yamada and Kuba, 2016). In the axonal cells, actin occurs as a meshwork of branched filaments (Yamada and Kuba, 2016). During polarization of neurons, actin and its regulators control the assembly and disassembly of F-actin filament in order to regulate the axonal elongation and contribute to the formation of axonal filopodia (Kevenaar and Hoogenraad, 2015). Aberrations in the axonal cytoskeletal-dependent process lead to defects in axonal transport, outgrowth, targeting, and synapse functioning, which, in turn, is associated with ALS (Kevenaar and Hoogenraad, 2015). In the mature neurons, actin is associated with regulating the presynaptic functions such as conscripting and repositioning of a synaptic vesicle, maintaining exocytosis and endocytosis. Mis-regulated actin in mature neurons has been implicated in various mental illnesses such as intellectual disability and schizophrenia (Ogawa and Rasband, 2008). Actin polymerization dynamics has a major role in sustaining the morphology of the spine and is associated with long-term memory via activation of long-term potentiation (LTP) or long-term depression (LTD) of excitatory signal transmission (Kim and Lisman, 1999; Luo, 2002; Bourne and Harris, 2008; Okada and Soderling, 2009). Also, actin rods are involved in the progression of axonal sensory neuropathy: a condition where neurons are damaged as observed in frataxin-deficient dorsal root ganglion (DRG) neurons (Muñoz-Lasso et al., 2020a).

The presence of F-actin aggregates has also been found in Hirano bodies, which are one of the causes of AD (Sabo et al., 2001; Maselli et al., 2003; Melidone et al., 2011; Furgerson et al., 2012; Yao and Khan, 2013). Hirano bodies are cytoplasmic inclusion bodies, rod-shaped eosinophilic in nature. It was first found in the hippocampus region of the aged brain in patients suffering from ALS and PD (Goldman, 1983; Sabo et al., 2001; Maselli et al., 2003; Melidone et al., 2011; Furgerson et al., 2012; Yao and Khan, 2013). The protein aggregate was filamentous, paracrystalline in nature, and thin filaments of 6 mm in size were observed. Actin depolymerization factor (ADF)/cofilin, an actin-binding protein, which helps sever F-actin, is severely reduced under stress conditions thereby enhancing the formation of aggregates (Yang et al., 2010; Muñoz-Lasso et al., 2020a,b). This leads to the development of rod-like structures of actin filaments widely present in neurons of patients with AD and PD (Furukawa and Fechheimer, 1997; Yang et al., 2010).

Owing to the aforementioned problems associated with actin misfolding, dysregulation, and its subsequent aggregation, it can form a potential therapeutic target for neurological disorders. A previous study by Pathak et al. (2020) elucidates the effect of the tetracycline group of antibiotics on F-actin protein aggregate. It has paved a way to think toward the detection of targeted therapies against F-actin aggregates. Due to this, the use of Food and Drug Administration (FDA)-approved drugs could form a potential alternative to act against actin aggregates responsible for neurodegenerative and neurodevelopmental disorders. Drug repositioning has become one of the widely used approaches in recent times, as it is highly efficient, economical, and less vulnerable. This may have a major impact on the reduction of financial burden, the progression of the disease, and subsequently lower the time taken for the drug discovery (Eira et al., 2016; Pushpakom et al., 2019; Pathak et al., 2020).

Ofloxacin is a broad-spectrum antibiotic widely used to treat infections caused due to *Staphylococcus aureus*, *methicillin-resistant Staphylococcus aureus (MRSA)*, *Streptococcus* spp., *Enterococcus faecalis*, Enterobacteriaceae, and *Pseudomonas aeruginosa*. It comes under the class of fluoroquinolones and structurally, it is a tricyclic ring that has a methyl group

being attached to the C-3 position (asymmetric carbon) on the oxazine ring (Morrissey et al., 1996). Owing to the safety of this drug, which has passed all the clinical trial phases, our study has identified it as a molecular entity with a new function. In the current study, we have investigated the role of Ofloxacin on F-actin aggregates using various biophysical techniques such as right-angle light scattering (RLS), dynamic light scattering (DLS), circular dichroism spectroscopy (CD), and kinetics study. The imaging studies using scanning electron microscopy (SEM) were also carried out, and the plausible mode of binding of Ofloxacin to F-actin protein was studied using isothermal titration calorimetry (ITC) and *in silico* studies. We have proposed a plausible mode of binding of Ofloxacin to actin and its subsequent disruption into the smaller oligomeric state. We thus propose that actin aggregates can be broken into smaller oligomers and be made available for new rounds of polymerization using Ofloxacin, if we have a proper drug delivery system in place, which is capable of crossing the blood–brain barrier (BBB).

MATERIALS AND METHODS

Purification and Characterization of Actin

All chemicals used for the experiment were procured from S.D Fine (Mumbai, India) except for DTT and Ofloxacin (PubChem CID: 4583), which were procured from Sigma Aldrich (Mumbai, India). Acetone powder from pig thigh muscle (*Sus scrofa domesticus*) was prepared following a standard protocol (Solomon et al., 2010). Actin was purified using the method developed by Spudich et al. in the year 1971 for rabbit skeletal muscle (Solomon et al., 2010) with minor modifications. In brief, acetone powder was homogenized in G-actin buffer (GB) (composition: 2 mM Tris–HCl, 0.2 mM ATP, 0.5 mM DTT, and 0.2 mM $CaCl_2$) followed by treatment with polymerization buffer (PB: Composition: 800 mM KCl and 5 mM $MgCl_2$). It was then kept for overnight polymerization with constant stirring at 4°C, followed by ultracentrifugation at 75,000 rpm for 90 min. The ultracentrifuge used was a tabletop model from Beckman Coulter XP-100 at Bombay College of Pharmacy (BCP), Mumbai, India. Purified polymer actin (F-actin) was characterized on MALDI-TOF (Bruker Daltonik GmbH) (Chavan et al., 2016) at the Advanced Centre for Treatment, Research, and Education in Cancer (ACTREC), Navi Mumbai, India. In order to exchange the solvent system from PB to either GB or water, the F-actin pellet was resuspended in the respective solvent and was dialyzed against the desired solvent system for 72 h at 4°C with buffer change every 12 h.

Light-Scattering Measurements

To avoid any interference in the scattering analysis, independent constant wavelength synchronous fluorescence (CWSF) measurements were carried out on actin and Ofloxacin in the polymerization buffer system. All the aforementioned compounds were procured from Himedia (Mumbai, India) and Sigma Aldrich. All these measurements were carried out on Cary Eclipse Fluorescence Spectrophotometer from Agilent technologies with the following parameters while keeping the difference between excitation and emission wavelength ($\Delta\lambda$) at zero: excitation wavelength: 200–700 nm, emission wavelength: 200–700 nm, excitation slit width: 5, emission slit width: 5, excitation filter: auto, emission filter: auto, temperature: room temperature, time points: T0, T3, T6, T24, T48, and T72 h. It should be noted that we have shown data only up to 48 h for clarity purposes. The concentration of actin was fixed at 3 μM, whereas, for Ofloxacin, measurements were carried out for the highest concentration of 3,000 μM to ensure that there is no concentration-dependent aggregation of the compound. The synchronous curves are depicted in **Figure 1**. Likewise, measurements were also carried out for water and G-actin buffer systems.

Based on the findings of the synchronous measurements, all the scattering experiments were carried out using the following parameters: excitation wavelength: 350 nm, emission wavelength: 350 nm, excitation slit width: 5, emission slit width: 5, excitation filter: auto, emission filter: auto. The concentration of actin protein was kept constant at 3 μM and was incubated with varying concentrations (3, 30, 150, 300, 750, 1,500, and 3,000 μM) of Ofloxacin. Scattering measurements were carried out at the following time points: T0, T3, T6, T12, T18, T24, T36, T48, and T72 h. These measurements were done in the three different solvent systems, namely, PB, GB, and water.

Dynamic Light Scattering Studies

The effect of Ofloxacin on the oligomeric state and heterogeneity of F-actin was measured using DLS. The experiments were performed on Malvern Panalytical (United Kingdom) at the Department of Biophysics, University of Mumbai, India. The position of the attenuator was set at 4.65, which was determined automatically based on the size and the concentration of the actin polymer in association with the respective compounds. The samples were taken in a polystyrene disposable sizing cuvette, and folded capillary zeta cell was used for the measurement of zeta potential. F-actin was prepared in PB buffer, and the concentration was kept constant at 3 μM. The concentration of Ofloxacin was maintained at 300 μM (compound ratio to actin was kept at 1:100). At least two measurements were carried out for each of the interactions between F-actin and the drug. A detection angle of 90° was used for the measurement of the size. The analysis was carried out on a zeta sizer Nano-ZS90 DLS system at 25°C, equipped with red (633 nm) laser and avalanche photodiode detector (quantum efficiency > 50% at 633 nm). The software associated with this DLS machine was Dispersion Technology Software (DTS) version 7.0, which was used to analyze the z-average hydrodynamic radius, intensity distribution, volume distribution, polydispersity index (PDI), autocorrelation function, and zeta potential (Liu et al., 2012).

Circular Dichroism Spectroscopy

The changes in the secondary structure of F-actin in the three different solvent systems, namely, PB, GB, and water were monitored using CD spectroscopy. All measurements were carried out between 260 and 200 nm using a JASCO-J-815

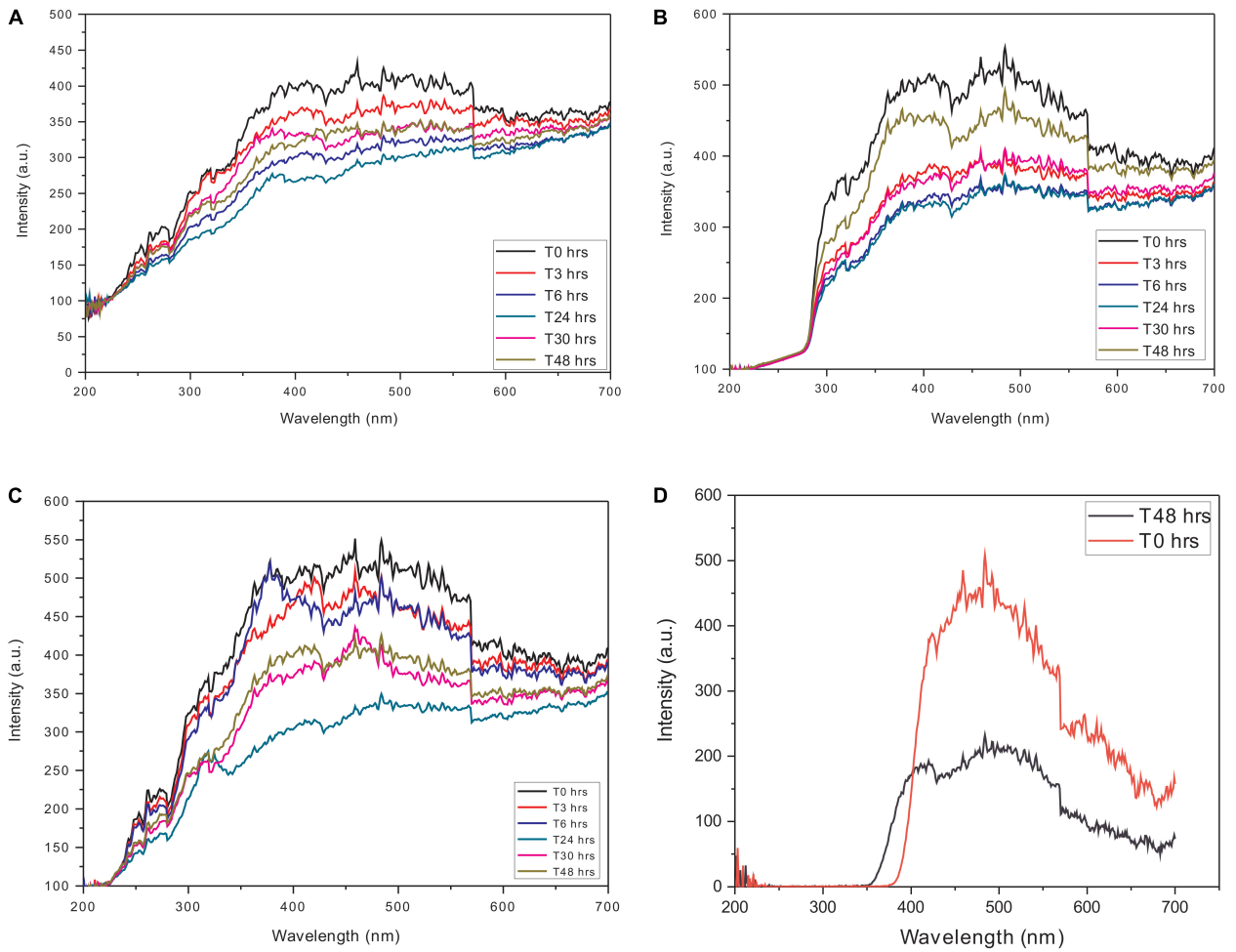

FIGURE 1 | Constant wavelength synchronous analysis (CWSF) profile for actin control in **(A)** polymerization buffer (PB), **(B)** G-actin buffer (GB), **(C)** water, and **(D)** Ofloxacin control in PB. Black color represents CWSF at 0 h, red color represents CWSF at 3 h, blue color represents CWSF at 6 h, green color represents CWSF at 24 h, pink color represents CWSF at 30 h, and the cyan color represents CWSF at T48 h.

spectropolarimeter at the National Centre for Cell Sciences (NCCS), Pune, India. The protein was prepared in the respective buffer, and the concentration was fixed at 5 μM. The ratio of protein:drug Ofloxacin was taken as 1:5 (25 μM), 1:10 (50 μm), 1:20 (100 μM) 1:50 (250 μM), and 1:100 (500 μM). The parameters used in the experiment were as follows: the bandwidth was maintained at 1.00 nm, and the cell of 1 mm path length was used. The data were presented as mean residue ellipticity $[\theta]$ in deg cm^2 $dmol^{-1}$, which is defined by equation 1 below:

$$[\theta] = CD/10 \times n \times 1 \times Cp) \quad (1)$$

where CD is in millidegree, n is the number of amino acid residues, 1 is the path length of the cell in cm, and Cp is the molar concentration of the protein (Sonavane et al., 2017). The K2D2 (Perez-Iratxeta and Andrade-Navarro, 2008) software was used, and further analysis of the data was done using CAPITO (Wiedemann et al., 2013).

Imagining Studies Using Scanning Electron Microscopy

The SEM analysis was carried out on a ZEISS microscope using the following parameters: EHT (3 kV) and signal (SE2). It should be noted that all the imaging assays were performed in GB buffer, and water as PB buffer was high in salt concentration, thereby, limiting us for imaging in PB buffer. SEM imaging was carried out at the Tata Institute of Fundamental Research (TIFR), Mumbai.

Kinetic Measurements for Actin Aggregation

The rate of depolymerization of F-actin in the presence and absence of Ofloxacin was performed using different concentrations of drugs ranging from 3 to 90 μM. The concentration of actin was fixed at 3 μM and was prepared in PB. The effect of the drug on the depolymerization kinetics of actin was measured using RLS on spectrofluorimeter (Agilent technology) (Borana et al., 2014). These measurements were

performed at room temperature with excitation and emission wavelengths fixed at 350 nm. In each case, the slit width for both excitation and emission was kept at 5 nm. The measurements were carried out for 30 min to ensure the attainment of saturation points for the respective compounds. The above parameter for the kinetic analysis was derived based upon our initial synchronous experiments with the offset value of zero (Borana et al., 2014).

All the kinetic traces were adequately fit to a single exponential decay curve as defined by the following equation (Equation 2):

$$y = y0 + A2 \times \exp\left(-\frac{x}{t1}\right) \quad (2)$$

where A2 stands for the amplitude, y0 stands for the maximum degradation/depolymerization, and t1 stands for the time constant. Depolymerization rate constant K_{app} was apparently calculated as the inverse of the apparent rate constant.

$$K_{app} = 1/t$$

Since all of the traces showed nearly to be a two-phased reaction, the amplitude of the first phase reaction was calculated by the following equation (Equation 3):

$$A1 = y_{\max} - A2 \quad (3)$$

where y_{max} is the RLS value in the absence of drugs.

Isothermal Titration Calorimetric Measurements

Isothermal titration calorimetric (ITC) experiments were carried out to understand the association constant (Ka), thermodynamic parameters of binding (ΔH), entropy (ΔS), and the stoichiometry (n) of the interaction of the drug with F-actin. The protein was prepared in PB buffer and kept for dialysis for 72 h at 4°C on a magnetic stirrer. All the measurements were carried out on a Malvern MicroCal ITC 200. The following parameters were used for the analysis: the total number of injections for Ofloxacin was 19, cell temperature was kept at 25°C, reference power was kept at 10, the initial delay was 180, cell concentration (F-actin): 0.067 mM, syringe concentration for Ofloxacin was 1.34 mM (20×).

In silico Data Analysis

Actin interaction with that of Ofloxacin was carried out in order to predict the site of binding of the drug to the actin oligomer (Hexamer). For all our analyses, we had used the ADP bound actin monomer (PDB ID: 1J6Z) (Otterbein et al., 2001). The structure was carefully observed and was duly corrected for incomplete residual side chains using the simple mutate function of the WinCoot tool (Crystallographic Object-Oriented Toolkit) (Emsley et al., 2010; Debreczeni and Emsley, 2012). This modified monomer was used to prepare a hexametric polymer using the cryo-EM structure, 3J0S as a template molecule using the SSM superpose function of the WinCoot. Subsequently, the hexamer was energy minimized using the online Gromacs Minimizer 5.0 tool (Abraham et al., 2015). The 3D structure of Ofloxacin was downloaded from PubChem (CID: 4583) and saved as an SDF file. This SDF file was then converted to PDB using the Discovery Studio 2019 Client (BIOVIA Discovery Studio Visualizer).

AutoDockTools-1.5.6 was used to prepare the ".pdbqt" files for both actin polymer and Ofloxacin. AutoDock Vina 4.2.6. was used for carrying out the docking studies of the actin with the drug utilizing the standard search parameters (Trott and Olson, 2010). Obtained results were analyzed using Pymol as a visualization tool.

RESULTS

Purification and Characterization of Actin

Our sequence analysis showed that human actin was having more than 90% similarity to that of pig actin. Actin being highly conserved across the higher eukaryotes, the pig (*S. scrofa domesticus*) thigh muscle was used for the purification of actin. In order to purify actin, acetone powder was prepared from pig thigh muscle and stored at −80°C. Actin was purified using the protocol as mentioned and modified by Pathak et al. (2020) in batches for all our assays. The purified actin had a mass of 42 kDa as observed in our SDS page analysis, which was also confirmed by excising the aforementioned band from the gel and subjecting it to mass spectrometric analysis.

Constant Wavelength Synchronous Analysis

In order to perform RLS analysis for the actin–Ofloxacin interaction, it was important for us to know the parameters for the same. We performed CWSF for both the drug molecule (Ofloxacin) as well as actin in three different buffer systems viz: PB, GB, and Water. It was observed in our results (**Figures 1A–C**) that actin in all the three buffer systems shows a very high scattering from 250 to 700 nm up to 48 h. Ofloxacin has negligible scattering observed up to 390 nm beyond, which starts showing a very high scattering as observed in **Figure 1D**. Owing to our CWSF data, we performed all our right-angle scattering analysis at a wavelength of around 350 nm, as actin in all the three buffer systems showed significant scattering, while Ofloxacin did not show any scattering. This would, hence, avoid any interference from the drug while collecting the data for right-angle scattering.

Right-Angle Light Scattering Measurements

Actin–Ofloxacin interaction was studied using RLS at the different concentrations for up to 48 h in the three aforementioned buffer systems. We observed that actin control in buffer systems showed a very high scattering of around 700 nm in PB and water and around 450 nm in GB. This high intensity was directly proportional to the size of the aggregate present in our control systems. Both PB and water has polymerized filamentous actin as well as aggregated actin, while GB has oligomeric actin present in them indicating the three different morphological states of the protein as found in the *in vivo* system. Also, there was very little drop in the measured intensity

of the actin controls with respect to time, which was indicative of actin's intrinsic property to polymerize and depolymerize. Upon treatment with different concentrations of Ofloxacin as observed in **Figures 2A–C**, there was a proportional drop in the scattering intensity as the function of its concentration as well as the time of treatment. At higher concentrations from 30 to 3,000 μM, the scattering intensity is very low in all the three buffer systems indicating that Ofloxacin upon interaction with either the polymerized actin, higher oligomeric actin, or aggregated actin gets disintegrated to smaller oligomeric and subsequently to monomeric actin. This interaction is also shown to be irreversible as there was no rise in the scattering intensity even after 48–96 h.

Dynamic Light Scattering for Actin Compound Interaction Studies

As observed from **Figures 3A,C,E**, actin control in the three solvent systems *viz*, PB, GB, and water shows the presence of a heterogeneous population of actin aggregates, which varies in size. The two peaks vary in the size of aggregated actin present in each of the three solvent systems. In PB, the size was deciphered to be around 90–150 d nm for the first peak, from 350 to 800 d nm. In GB, the size of the two peaks has been deduced to be 80–120 and 300–400 d nm while in water, the size of the two peaks was more than 1,000 d nm. This size variance and heterogeneity of the peaks show that actin control has a different morphology in the three different solvent systems. However, upon treatment with Ofloxacin, actin in PB, GB, and water were disintegrated into a homogenous population of smaller monomeric/oligomeric state actin as observed in **Figures 3B,D,F** respectively. The size of the homogenous peaks was deduced to be 70–80 d nm in PB, 450–500 d nm in GB, and 100–120 d nm in water.

CD Spectrophotometric Analysis of the Actin Compound Interaction Studies

We also performed circular dichroism spectroscopic analysis (CD) for both untreated actin control and treated actin with Ofloxacin in PB, GB, and water, respectively. The CD data obtained in mdeg was analyzed using the CAPITO software. As observed in **Figures 4A–C**, actin control in PB, GB, and water shows the curve to have a single peak dip at 212 nm indicative of the presence of more polymeric, filamentous, or aggregated structures. However, upon treatment with Ofloxacin, actin in all the three respective buffer system shows the change in the curve profile to contain more α-helical structure closer to globular actin monomer with two dips observed at 211 and 220 nm.

Our CAPITO analysis as observed in **Figures 4A–C** also suggests the compactness of the actin protein upon treatment with different concentrations of Ofloxacin either as globule, molten globule, premolten globule, or unfolded protein. Untreated actin in PB exists as molten globule, which is indicative of compact partially folded conformation with near-native compression, whereas in GB and water, it exists as a globular structure. As soon as we treat actin in the PB buffer system with Ofloxacin at 50 and 100 μM, a concentration-dependent change in the structural content of the actin was observed. At 50 μM, the actin oligomer lies between the conformation of the molten globule and globular protein indicating the presence of a larger oligomeric actin with increasingly exposed hydrophobic residues (Perera et al., 2016). However, as soon as the concentration is increased to 100 μM, actin, which is further disrupted to either small oligomers or monomers, has a compact near-native structure with substantial α-helical content and more organized tertiary structure. Similarly, when actin in GB was treated with Ofloxacin, there was a structural change observed with respect to the concentration of the drug molecule. At a lower concentration of 50 μM, actin is disintegrated into smaller oligomers and monomers prevailing as a molten globular protein with partially exposed hydrophobic residues rich in α-helix. However, as soon as the concentration is increased, the partially folded actin protein is switched back to the more globular structure. In water, where the actin exists as an amorphous aggregate, the structural premise of the protein is more globular. As soon as it is treated with Ofloxacin at a concentration of 50 μM, it occurs as a molten globule and changes to a more globular structure at a higher concentration of 100 μM. This structural change in actin in water is quite contrary to that observed in actin treated in PB and GB.

We also analyzed the same set of data using BESTSEL software to calculate the percentage of α-helical and β-structure present in

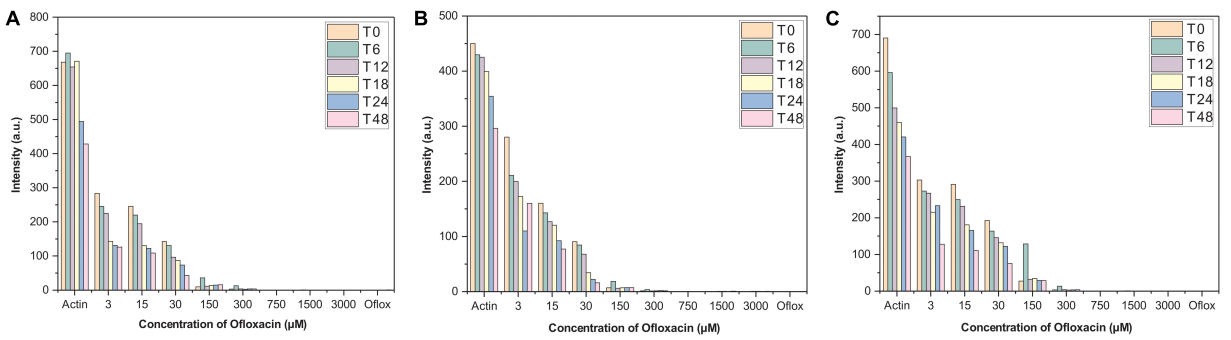

FIGURE 2 | Right-angle light scattering (RLS) profile for actin control and actin treated with Ofloxacin in **(A)** PB, **(B)** GB, and **(C)** water. The orange bar stands for actin aggregates at 0 h, green for 6 h, purple for 12 h, yellow for 18 h, blue for 24 h, and pink for 48 h.

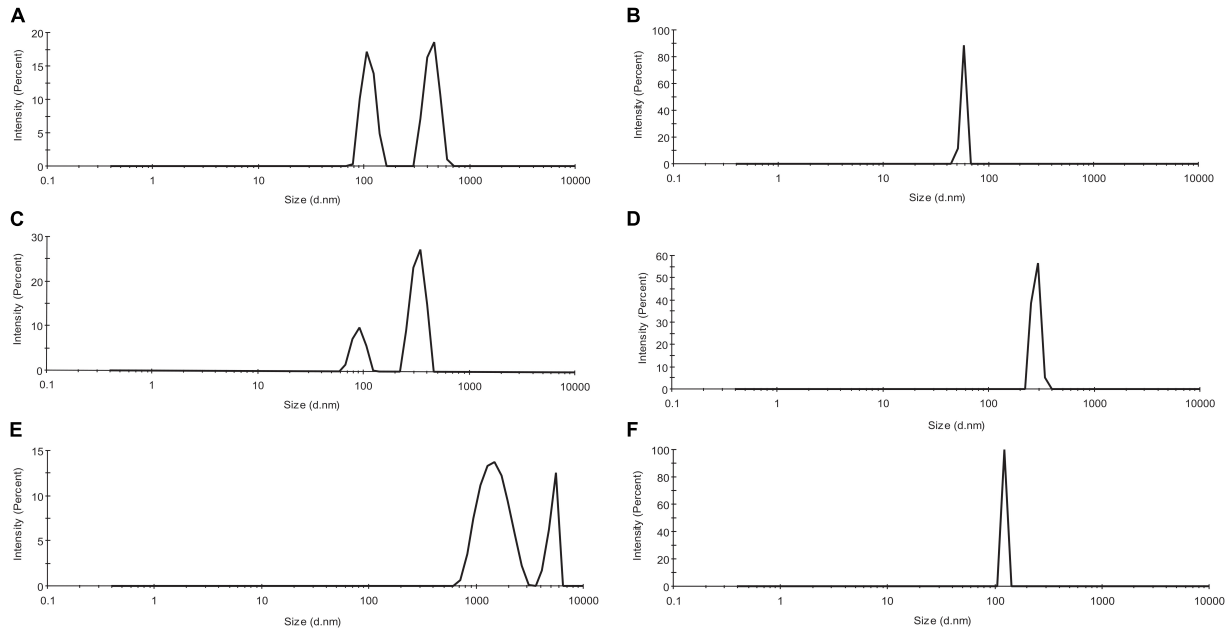

FIGURE 3 | Profile for dynamic light scattering (DLS) scattering of **(A)** untreated actin in PB; **(B)** actin treated with Ofloxacin in PB; **(C)** untreated actin control in GB; **(D)** actin treated with Ofloxacin in GB; **(E)** untreated actin control in water; and **(F)** treated actin with Ofloxacin at 300 μM.

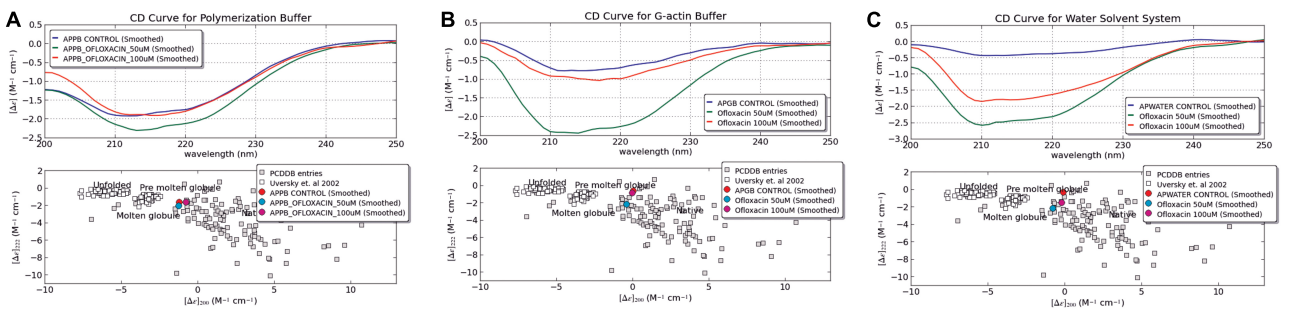

FIGURE 4 | CD Spectroscopic data analyzed for actin control and actin treated with Ofloxacin using CAPITO software. **(A)** PB; **(B)** GB; and **(C)** water. The blue curve is representative of actin control, whereas the green curve is representative of actin treated with Ofloxacin at 50 μM, and the red curve is representative of actin treated with Ofloxacin at 100 μM in the respective buffer.

untreated and treated actin. Our BESTSEL analysis as observed in **Figure 5A**, is that actin control in polymerization buffer has 9.9% of α-helix, 26.2 β-sheet, 16.3% turns, and 45.5% other non-organized structures. However, upon treatment with Ofloxacin in PB as observed in **Figure 5B**, the content of α-helix was increased to 17.4%, β-sheet was increased to 35.3%, while turns and other unorganized structures were reduced to 13.3 and 33.4%, respectively. Similarly, for the G-actin buffer, it was observed in **Figures 5C,D** that actin control had the presence of α-helix of around 3.6%, β-sheet, around 37.2%, turn, 14.2%, and other structures, 45.1%. However, the treated actin had an α-helix of around 18.3%, β-sheet 37.6%, turn, 9.5%, and other structures, 34.7%. Also, for actin control in water as observed in **Figure 5E**, we observed α-helix to be around 4.5%, β-sheet, 37.5%, turn, 14.9%, and other structures, 43.2%. However, upon treatment, the structural change was reported to comprise 16% α-helix, 25.3% β-sheet, 12.4% turn, and 46.3% other unorganized structure as observed in **Figure 5F**. Our result of the BESTSEL analysis indicates that posttreatment of polymerized/aggregated actin resulted in actin enriched in α-helical content which is likely to be closer to the globular actin molecule.

SEM Imaging for the Actin Compound Interaction

Scanning electron microscopy was performed for both treated and untreated actin in GB as well as water. PB was not used for these imaging studies due to the presence of high salt concentration in the buffer (800 mM KCl), which gave rise to more salt crystals to be observed in the SEM image. As observed in **Figures 6a,c**, untreated actin dialyzed against GB and water showed the presence of filamentous actin as well as

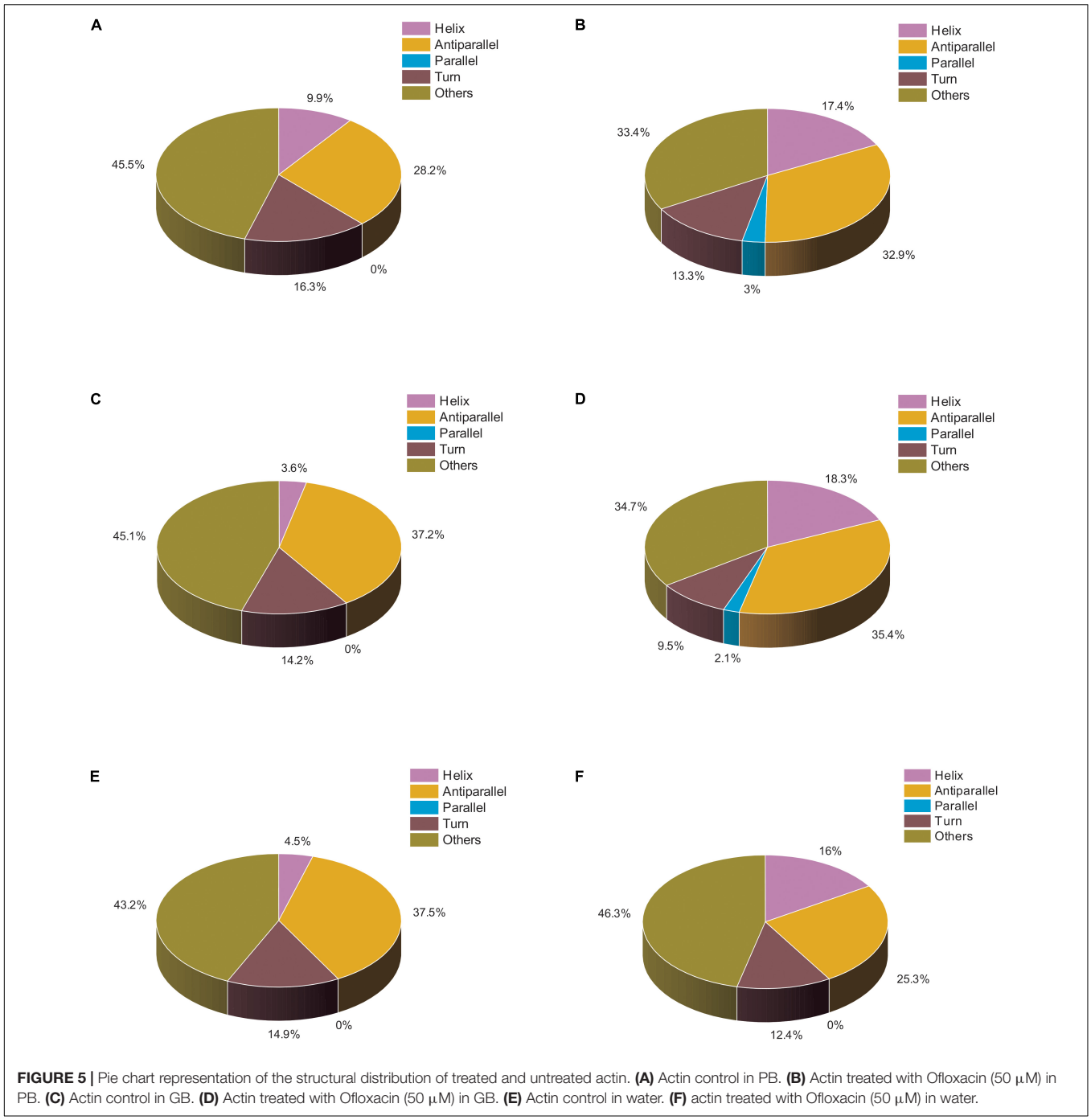

FIGURE 5 | Pie chart representation of the structural distribution of treated and untreated actin. **(A)** Actin control in PB. **(B)** Actin treated with Ofloxacin (50 μM) in PB. **(C)** Actin control in GB. **(D)** Actin treated with Ofloxacin (50 μM) in GB. **(E)** Actin control in water. **(F)** actin treated with Ofloxacin (50 μM) in water.

amorphous actin aggregates, which when treated with Ofloxacin gets broken down to a smaller oligomeric protein as observed in **Figures 6b,d**.

Kinetic Analysis of Actin Depolymerization

We monitored the kinetic parameters for actin interactions with Ofloxacin in polymerization buffer as a function of right-angle scattering, which was measured every 5 s for up to 100 min. It is a known fact that right-angle scattering is proportionate to the size of the molecule. As observed in **Figures 7A–I**, the graph shows actin control in PB and the effect of Ofloxacin with its varying concentrations, which was analyzed and fit using a single exponential decay function of the kinetics. Three different parameters were reported through this fitting viz: (1) kagg, (2) amplitude (A2), and (3) y0. kagg stands for rate constant representing the speed of the reaction upon the interaction of actin polymer and Ofloxacin. A2 stands for amplitude indicating the amount of smaller actin oligomers formed upon

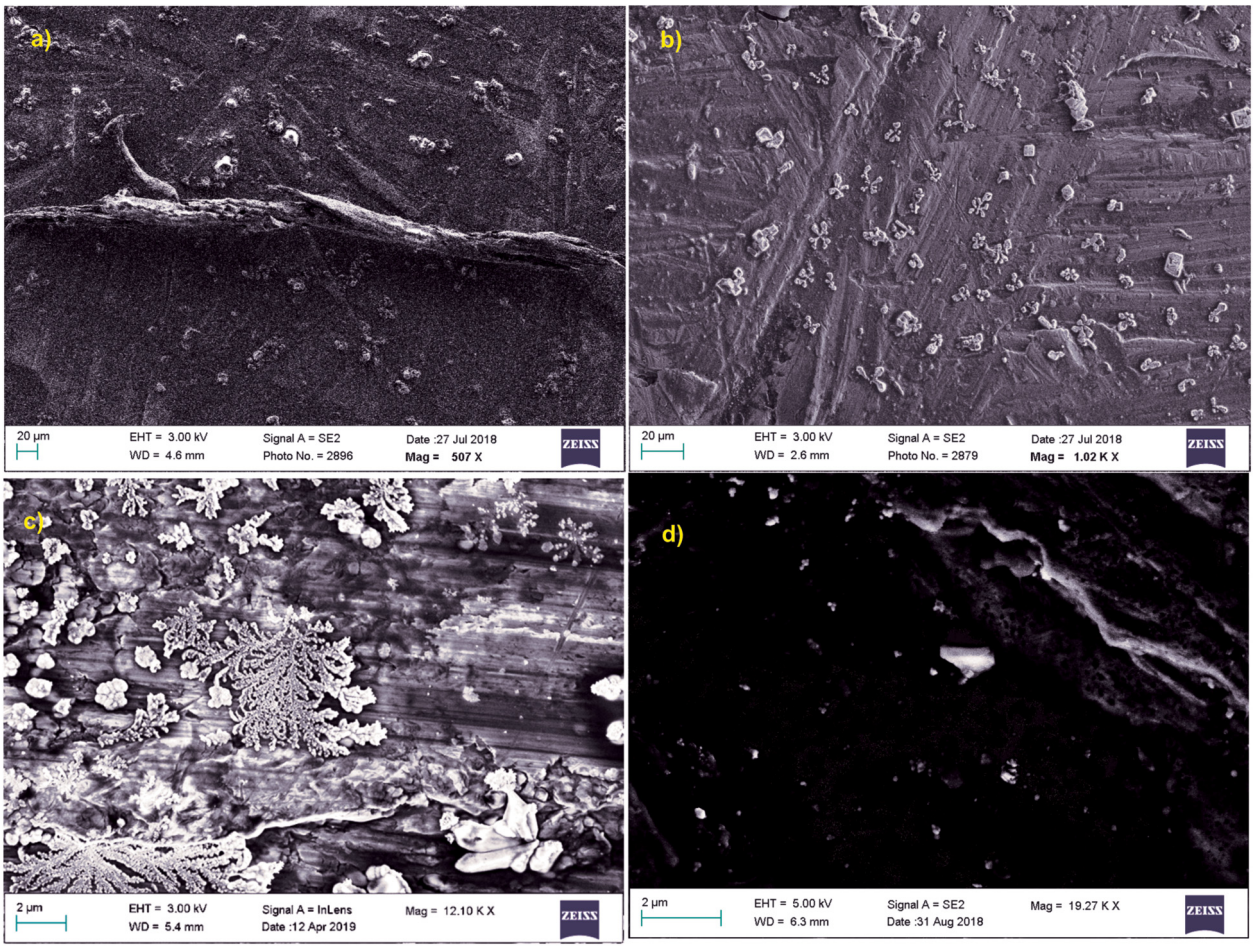

FIGURE 6 | SEM images for actin **(a)** dialyzed in G-actin buffer 20 μm; **(b)** treated with Ofloxacin in G-actin buffer 20 μm; **(c)** dialyzed in water 2 μM; and **(d)** treated with Ofloxacin in water 2 μM.

interaction with Ofloxacin. y0 stands for the extent to which the depolymerization has occurred upon interaction with the drug at the infinite (∞) time. The R^2 value for the single exponential decay fit was calculated to be between 0.97 and 0.72 as analyzed for varying concentrations of Ofloxacin interaction with actin.

The kinetics of polymerized F-actin in PB was measured for 100 min of its intrinsic polymerization and depolymerization dynamics that occur at the barbed end and the pointed end, respectively. We observed (**Figures 7A**, **8A**) that actin control in polymerization buffer is quite stable and does not disintegrate substantially with the values for amplitude observed as 64.64 a.u., y0, 416.35 a.u., and t1, 1,820.99 s. However, upon treatment with Ofloxacin with a stoichiometric ratio of 1:1 as observed in **Figure 7B**, the amplitude was calculated as 100.12 a.u., y0 was calculated as 271.80 a.u., and t1 was calculated as 2,693.98 s. With increasing concentration, a tremendous decrease in the intensity of the amplitude was observed indicating that Ofloxacin works to break down the highly aggregated actin into smaller oligomers. This process is concentration dependent. It was observed in our analysis that increasing concentration of Ofloxacin led to the decrease in the time required for breaking down the highly aggregated actin to smaller oligomers as well as the increase in the number of smaller oligomers formed. We also report the mode of interaction of the actin polymer with that of Ofloxacin, which follows a two-phased reaction. The first phase is quite faster than the second phase wherein an intermediate product is formed before the formation of the final product. The amplitude of the first phase (A1) can be calculated using Eq. (3) and is concentration dependent, while the second phase is not dependent upon the concentration of the Ofloxacin treatment.

Furthermore, we plotted the amplitude for the second phase reaction (A2), the time constant (t1), and y0 against the concentration of Ofloxacin. A graph of the extent of disintegration (y0) against the concentration of Ofloxacin shows (**Figure 8B**) that as the concentration of the drug molecule increases, there is also an increase in the disintegrated product. We observed (**Figure 8C**) that the amount of the smaller oligomer formed is highest at a very high concentration of around 90 μM. Our graphical analysis for rate constant shows that the speed of interaction of Ofloxacin with that of actin polymer and

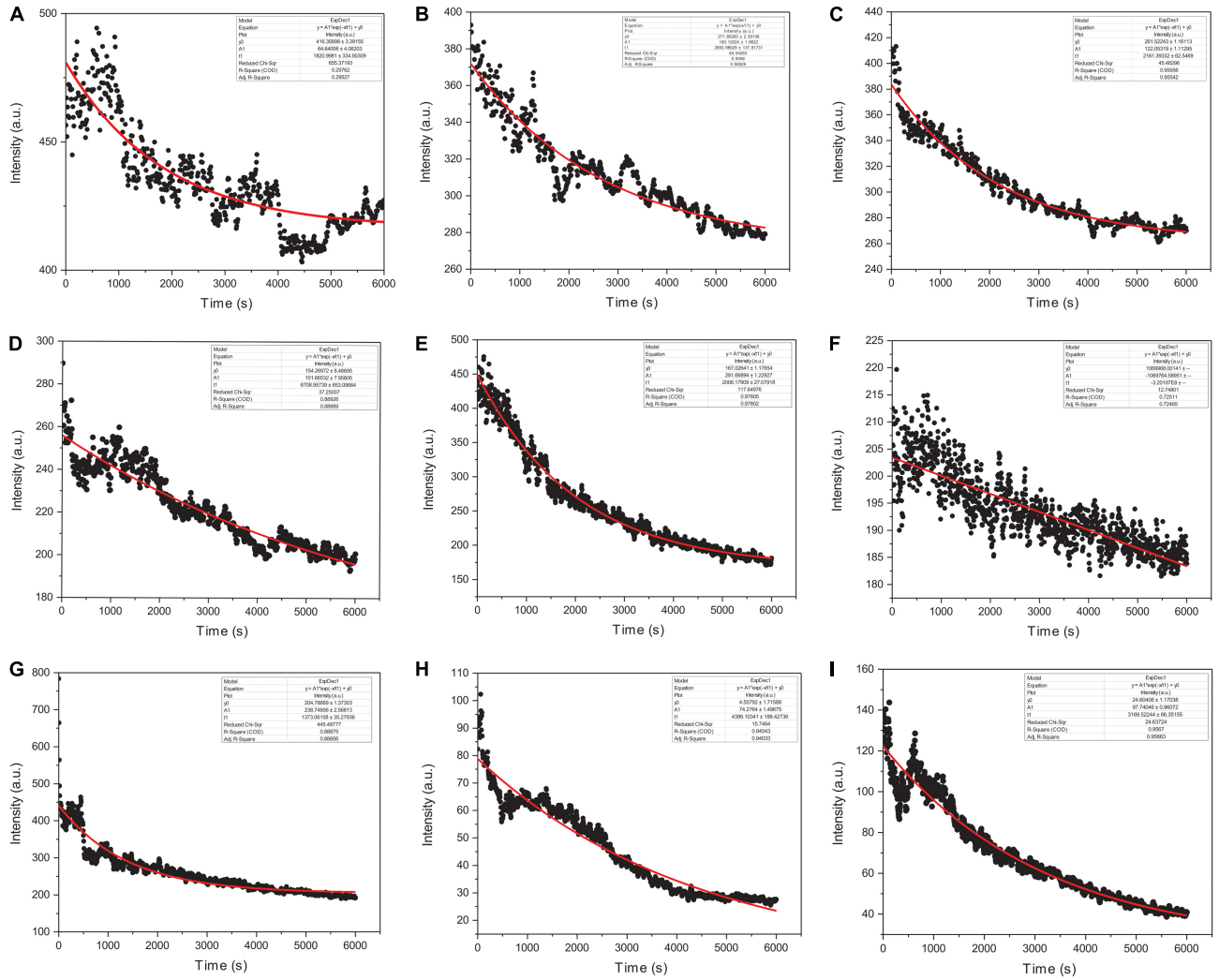

FIGURE 7 | Graphical representation of actin polymerization dynamics in the presence and absence of Ofloxacin at different concentrations observed in PB. **(A)** Actin control; **(B)** treated actin at 3 μM; **(C)** treated actin at 6 μM; **(D)** treated actin at 9 μM; **(E)** treated actin at 15 μM; **(F)** treated actin at 30 μM; **(G)** treated actin at 45 μM; **(H)** treated actin at 60 μM; **(I)** treated actin at 90 μM. The red straight line indicates the single exponential curve fit analysis while the black dots represent the RLS intensity recorded every 5 s of actin–Ofloxacin interaction.

its subsequent breakdown increases with the increase in the concentration of Ofloxacin as observed in **Figure 8D**.

Isothermal Titration Calorimetry Analysis for Actin Compound Interaction

We carried out our interaction study of actin polymer and Ofloxacin using ITC in order to deduce the thermodynamic parameters for the reaction as well as the mode of binding. **Figures 9A–D** show the ITC profile for the actin aggregates interacting with Ofloxacin in polymerization buffer analyzed and tailored using a different model system. The upper panel represents the endothermic heat pulse with the first injection of around 0.4 μl followed by 18 injections of 2 μl each of 1.34 mM Ofloxacin into the actin aggregate solution of 0.067 mM. The lower panel illustrates the integrated heat data indicative of the differential binding curve that was fit with using one-site binding, two-site sequential binding, three-site sequential binding, and four-site sequential binding model system. Although all the fit for the ITC data as seen in **Table 1** shows binding to the actin of Ofloxacin strongly, the best fit was observed for the two-site sequential binding with the chi-square value of 1.373E5. The values of ΔH, ΔS, and K have been reported for all the four-binding models in **Table 1**. All of our binding fit shows that the reaction is both enthalpically as well as entropically driven. Two-site sequential binding of the drug molecule to the actin filament is enthalpically driven at both the sites of binding. This specifies that actin polymer/aggregate disruption upon binding of Ofloxacin is quite spontaneous and exothermic. Our data is indicative that Ofloxacin might be binding the actin polymer at multiple sites; however, two major sites on the actin polymer would

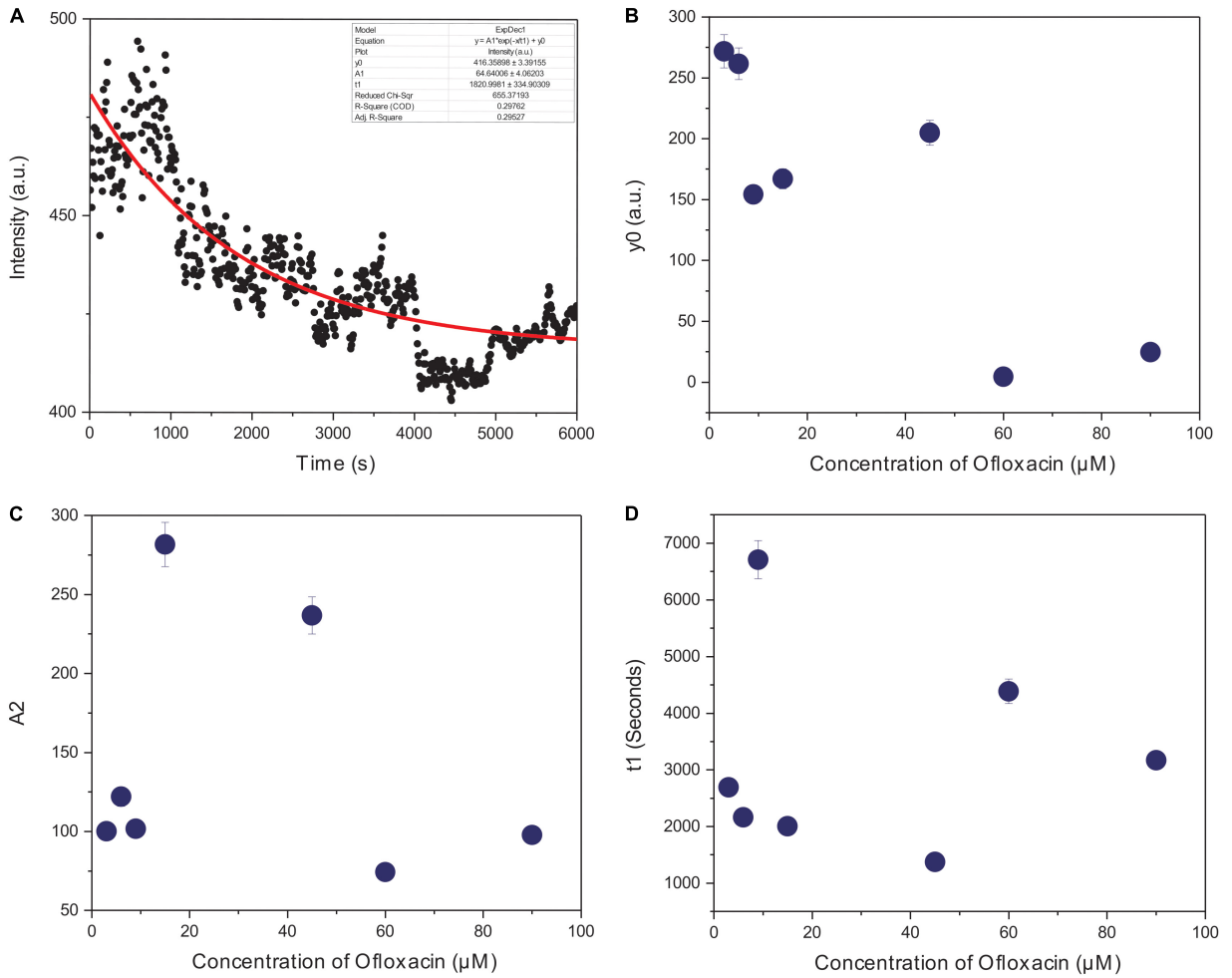

FIGURE 8 | Graphical representation of representative kinetic profiles in PB for actin treated with Ofloxacin: **(A)** Actin control; **(B)** extent of disintegration (y0); **(C)** amplitude (A2); and **(D)** time constant (t1).

be more favorable for Ofloxacin binding than the rest of the other binding sites.

In silico Data Analysis

We performed autodocking studies for hexameric actin interaction with Ofloxacin in order to deduce the possible mode of binding of the drug molecule to that of the filament. We observed in **Figure 10** that most of the clusters of the Ofloxacin drug bind to the lateral interface of the actin timer. Various previous studies have suggested that actin during nucleation forms a rigid nucleus known for producing a critical concentration to promote the process of elongation of the filament (Cooper and Schafer, 2000; Vavylonis et al., 2005; Bugyi and Carlier, 2010; Blanchoin et al., 2014; Cell Signaling, 2014; De La Cruz and Gardel, 2015; Galkin et al., 2015; Coutts and La Thangue, 2016; Carlier and Shekhar, 2017). Our docking studies suggest that Ofloxacin tries to either inhibit by binding to the lateral interface as observed for Cluster 1, Site 2, Site 3, and Site 4 or disrupts the already formed nuclei in the system. It has also been observed in our data that the drug molecule is also getting associated with SD-2 of actin, which is rich in coiled coil as is prevalent in Cluster 2. It is an already known fact that these SD-2 of the actin monomer are responsible for the major conformational changes that drive the dynamics of actin polymerization (Blanchoin et al., 2014; Galkin et al., 2015; Carlier and Shekhar, 2017). We speculate that actin might be undergoing major conformational change upon Ofloxacin binding at SD-2, thereby, disintegrating the actin molecule. This data is quite in consensus with our ITC where the thermodynamics of the interaction reaction supports two-site sequential binding of the drug to actin.

DISCUSSION

Ofloxacin is one of the widely used broad-spectrum fluoroquinolone antibiotic used against several bacterial infections such as bronchitis, pneumonia, chlamydia, gonorrhea, skin infections, urinary tract infections, and infections of

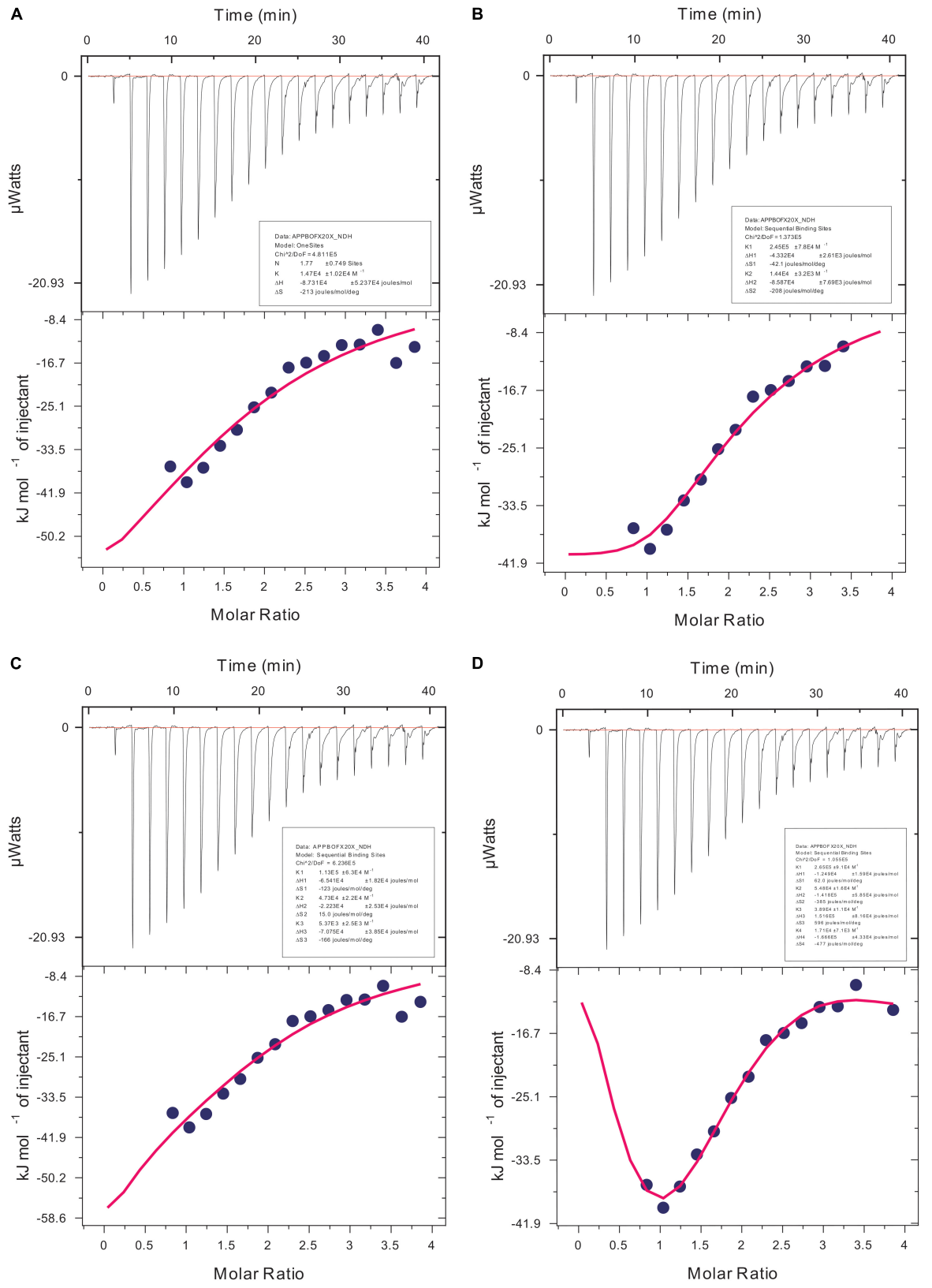

FIGURE 9 | Isothermal calorimetric profile for actin aggregates treated with Ofloxacin in PB. **(A)** Model: one-site binding; **(B)** model: sequential two-site binding; **(C)** model: sequential three-site binding; and **(D)** model: sequential four-site binding.

TABLE 1 | Thermodynamic parameters obtained using isothermal titration calorimetry (ITC) for Ofloxacin.

Parameters	One-site binding	Sequential two-site binding	Sequential three-site binding	Sequential four-site binding
Chi^2/DoF	4.811 E5	1.373E5	6.236E5	1.055E5
K1	1.47E4 ± 1.02E4 M^{-1}	2.45E5 ± 7.8E4 M^{-1}	1.13E5 ± 6.3E4 M^{-1}	2.65E5 ± 9.1E4 M^{-1}
ΔH1	−8.731E4 ± 5.237E4 J/mol	−4.332E4 ± 2.61E3 J/mol	−6.541E4 ± 1.82E4 J/mol	−1.249E4 ± 1.59E4 J/mol
ΔS1	−213 J/mol/deg	−42.1 J/mol/deg	−123 J/mol/deg	62.0 J/mol/deg
K2		1.44E4 ± 3.2E3 M^{-1}	4.73E4 ± 2.2E4 M^{-1}	5.48E4 ± 1.6E4 M^{-1}
ΔH2		−8.587E4 ± 7.69E3 J/mol	−2.223E4 ± 2.53E4 J/mol	−1.418E5 ± 5.85E4 J/mol
ΔS2		−208 J/mol/deg	15.0 J/mol/deg	−385 J/mol/deg
K3			5.37E3 ± 2.5E3 M^{-1}	3.89E4 ± 1.1E4 M^{-1}
ΔH3			−7.075E4 ± 3.85E4 J/mol	1.516E5 ± 8.16E4 J/mol
ΔS3			−166 J/mol/deg	596 J/mol/deg
K4				1.71E4 ± 7.1E3 M^{-1}
ΔH4				−1.666E5 ± 4.33E4 J/mol
ΔS4				−477 J/mol/deg
	Enthalpically driven	Enthalpically driven	Enthalpically driven	Enthalpically and entropically driven

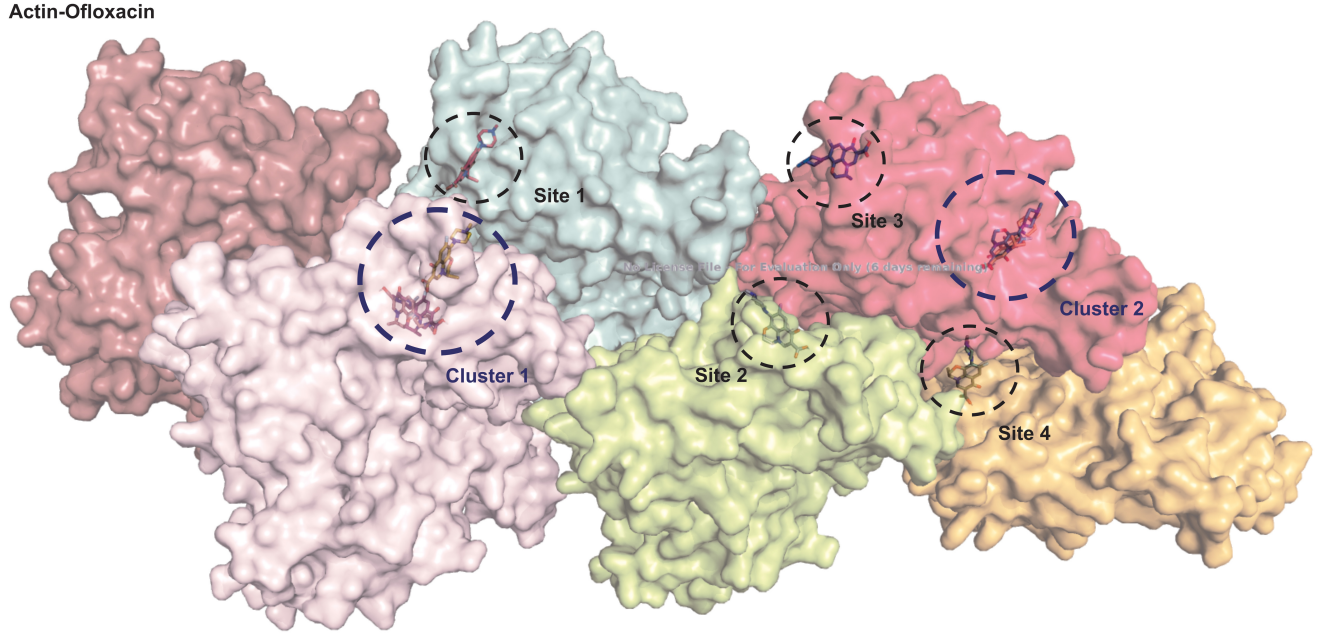

FIGURE 10 | Actin polymer interaction with Ofloxacin. Hexamer actin. ChainA is shown salmon, ChainB in purple, ChainC in cyan, ChainD in lemon, ChainE in pink, and ChainF in orange.

the prostate (Administration, n.d.; Kern et al., 1987; Eron and Gentry, 1992). Drug repositioning is a new approach that has been emerging recently for the treatment of various diseases as any lead molecule under a *de novo* drug discovery program, which takes around 10–15 years to come into the market and probably has a success rate of less than 10%. It has been a known fact that the FDA has approved different molecules against 400 human proteins (Pillaiyar et al., 2020). These proteins are classified under the umbrella of enzymes, transporters, G protein-coupled receptors (GPCRs), cluster of differentiation (CD) markers, voltage-gated ion channels, and nuclear receptors (Pillaiyar et al., 2020). Actin is one of the globular proteins with an ATPase binding cleft and an intrinsic property to polymerize (Oda et al., 2009; McKayed and Simpson, 2013). This polymerization dynamics that has been regulated by various actin-binding protein forms the driving force for many cellular processes such as cellular motility, cellular niche formation, and transport of biological molecules (Shekhar et al., 2016; Carlier and Shekhar, 2017). It has been observed that aberrations in the actin polymerization–depolymerization cycle lead to aggregation of the actin molecule leading to various diseased conditions (Lambrechts et al., 2004; Fletcher and Mullins, 2010; Muñoz-Lasso et al., 2020b). The unregulated actin dynamics has been implicated into the various neuropathological conditions, which manifest with the aging process among

humans (Lambrechts et al., 2004; Gourlay and Ayscough, 2005; Goebel, 2009; Yao and Khan, 2012).

These neuropathological conditions are difficult to treat and lead to a decline in the quality of life. Thus, there is a widespread need for molecules with low cell toxicity to be identified for its ability to control and monitor cytoskeletal protein especially actin whose pathology has been implicated in arising cases of neurological apathies. Our current study emphasizes upon identifying a molecule, which can depolymerize the actin aggregates to smaller oligomers and prevent subsequent neuronal cell death that arises due to these aggregate formations. We utilized various biophysical techniques to study the role of Ofloxacin, a broad-spectrum antibiotic with a very low level of cell toxicity on actin polymerization–depolymerization dynamics. We also utilized *in silico* docking study in order to understand the mechanism of binding of Ofloxacin to actin and its subsequent role in breaking down the highly amorphous or polymerized actin to smaller aggregates.

Owing to the fact that human actin is closer to pig (*S. scrofa*) actin, we purified actin from the acetone powder of pig thigh muscle. The protein was purified upon several polymerization and depolymerization cycles in PB buffer rich in salt concentration and GB buffer, which has the presence of a reducing agent and ATP. The purified protein was isolated and separated at 42-kDa molecular weight on the SDS page. It was also confirmed using the excised band for mass spectrometric analysis to be actin. This protein was then used for further interaction studies with the drug Ofloxacin. We performed constant wavelength synchronous analysis to observe for the scattering profile for the three morphological states of actin in PB, GB, and water and the drug molecule in PB. This data was measured for up to 48 h. The measured data for the actin in three different buffers had the presence of high scattering intensity from 250 to 700 nm indicating toward the fact that all three morphological states of the actin remain in the filamentous, oligomeric, and aggregated state. However, when we did the same analysis for the drug, it was observed that actin shows negligible scattering up to 395 nm beyond, which starts self-aggregating resulting in a very high scattering intensity from 400 to 700 nm. Hence, for our further right-angle scattering measurement, we used 350 nm. Furthermore, we carried out a right-angle scattering measurement for actin–Ofloxacin interaction with varying concentrations of the drug molecule up to 48 h. We observed through our RLS measurement that actin controls in all the three buffer systems, which was having very high scattering intensity due to the presence of a higher molecular weight aggregate that gets disrupted to a smaller oligomeric size with low scattering intensity as the function of the concentration of Ofloxacin. This binding and disruption in all the three buffer systems were irreversible as no increase in the scattering intensity was observed posttreatment even after the 48 h of incubation.

We performed dynamic light measurement in order to deduce the particle size obtained posttreatment with Ofloxacin. It was observed that the heterogenous peak representing variations in shape and size of the actin aggregate in three different solvent systems was transformed to a homogenous peak of a smaller size indicating the breakdown of the actin polymer/aggregate to a smaller oligomeric or monomeric state. The structural change in the actin morphology pre- and posttreatment was analyzed using the CD spectrometric measurement, the data for which was collected in mdeg. The data for the untreated actin control as well as the treated actin in the three buffer systems were analyzed both manually using two different software viz: CAPITO (Wiedemann et al., 2013) and BESTSEL (Micsonai et al., 2018). The information obtained through our analysis indicated an increase in the structural population of the α-helix in treated actin compared to their untreated counterparts. The oligomers/monomers obtained posttreatment had a structural component closer to the content of globular actin, which is also rich in α-helix (Pathak et al., 2020). Actin in PB is more polymeric or filamentous with highly exposed hydrophobic residues and has near-native compactness, while actin in GB is more globular with native compactness of the protein and substantially a higher α-helix structure. This distinct feature of GB is due to the fact that this buffer is capable of disrupting the actin aggregate/polymer into a smaller oligomeric size of the actin. At a lower concentration of Ofloxacin, around 25 μM, we do not observe much change in the structural content from that of the treated actin. Thus, we choose to have the concentration of the drug molecule with a ratio of 1:10 and above. One of the important findings of our CD data using our CAPITO analysis was that treated actin in PB and GB brings about a concentration-dependent change from molten globule to that of the more globular structure. On the contrary, actin in water, which occurs as an amorphous aggregate, was seen to be occurring as a globular structure. Treated actin at 50 μM occurs as a molten globular structure with a more exposed hydrophobic structure with near-native compactness (Perera et al., 2016). As soon as the concentration is increased to 100 μM. actin changes from a molten globular structure to a more globular structure. This change, which is typical of water, is because of the amorphous aggregate that has a more unorganized structure, which is more spherical and compact, with relatively less exposed hydrophobic structure and a detectable tertiary structure. However, at a lower concentration of Ofloxacin, actin is disrupted as a more linear polymeric or large oligomeric secondary structure occurring as a molten globule with near-native compactness. At the increased concentration of 100 μM, actin is disrupted to monomeric or lower oligomeric structure rich in α-helix with near-native compactness and less exposed hydrophobic residues. Although we tried to increase the concentration of Ofloxacin with a ratio up to 1:50, it leads to the saturation of the CD detector.

We then also perform imaging studies to observe for the morphological difference in the treated and untreated actin. Control actin dialyzed against GB and water shows the presence of filamentous actin as well as amorphous actin aggregate. However, upon treatment with Ofloxacin, this highly filamentous as well as amorphous aggregate is converted to the morphology of smaller oligomers and monomers. We also performed the kinetic study for the actin–Ofloxacin interaction as a function of right-angle scattering measured against the varying concentrations of Ofloxacin. We tried to deduce three basic parameters from our study viz, y0, which represents the extent to which disintegration

occurs, the time constant (t1), which is the time taken to break down and stabilize the reaction, as well as amplitude (A2), which represents the number of lower oligomers formed posttreatment with actin in polymerization buffer. Our analyzed data revealed that actin itself undergoes constant recycling of polymerization and depolymerization as a result of its intrinsic property as was observed for the actin control in PB. However, upon the treatment, we deduced that the amount of actin oligomeric content (A2) increased with an increase in the concentration of Ofloxacin, thereby, decreasing the content of highly aggregated actin in the system with each increasing concentration. We also see that actin polymer/aggregate upon treatment with Ofloxacin follows a two-phased reaction of which the first phase of the reaction remains tremendously fast compared to the second phase, which is relatively very slow. We observed that an intermediate product is formed before the formation of the end product in our kinetic analysis. The time required to stabilize the reaction was as short as 30 min, although our measurement was carried out up to 100 min and more. Most of the interaction was found to occur in the first phase, which is concentration dependent beyond which, as we enter the second phase post the intermediate product formation, actin disruption is independent of the concentration of Ofloxacin.

We then studied our interaction of actin–Ofloxacin in PB using ITC to deduce the thermodynamic parameters for the reaction and its mode of binding. Although our result shows binding for one site and multiple site sequential binding, the best fit was observed for two-site binding with low error values indicating that there are two major sites on actin polymer/aggregate, which favors the binding of Ofloxacin and subsequent disintegration of the actin molecule to a lower oligomeric size. We also observed that, on both of these sites, the interaction is enthalpically as well as entropically driven. Our *in silico* data shows two prevalent sites for binding of Ofloxacin to that of actin hexamer. These sites include the lateral interface, which is important for actin monomer interaction to form the nuclei, and the other site is near SD-2. We speculate that actin might undergo conformation change in its three-dimensional lattice upon Ofloxacin binding at SD-2 as well as inhibits the interaction of the actin monomer at the interface, which are responsible for nuclei formation as shown in **Figure 11**. This data agrees with our ITC data, which show a preferential mode of binding to the two-site sequential binding. The plausible mechanism that we have deduced is that Ofloxacin binds the actin at the aforementioned sites viz, cluster 1 and cluster 2, thereby, bringing about conformational change and destabilizing the larger aggregates. This is followed by the disintegration of large actin aggregates into the oligomeric structure. The accumulation of smaller nuclei or monomeric actin might prevent the obliteration of neuronal cells due to the inclusion bodies of actin.

CONCLUSION

In the current study, Ofloxacin, which is a widely used broad-spectrum antibiotic for various bacterial infections, is elucidated as a potential candidate for drug repurposing. We studied actin aggregate as a significant therapeutic target site to treat various neurodegenerative as well as neurodevelopmental disorders. In order to study the role that Ofloxacin plays on these protein molecules, we purified actin from the pig thigh muscle (*S. scrofa domesticus*) in three different solvent systems. The three solvent systems, namely, PB, GB, and water mimic the *in vivo* morphology of the actin protein inside a human cell. These result in the actin being purified as a long filamentous polymer when dialyzed against PB, as smaller oligomers when dialyzed against GB, whereas in water, it formed amorphous aggregates. Pig thigh muscle was used as it is highly homologous with that of human actin with a 95% identity. Throughout the initial high-throughput screening of Ofloxacin on different morphologies of actin, we observed that the drug molecule was indeed disrupting large actin molecules.

In order to understand the actual role of Ofloxacin on actin aggregates, we performed CWSF analysis. During this assay,

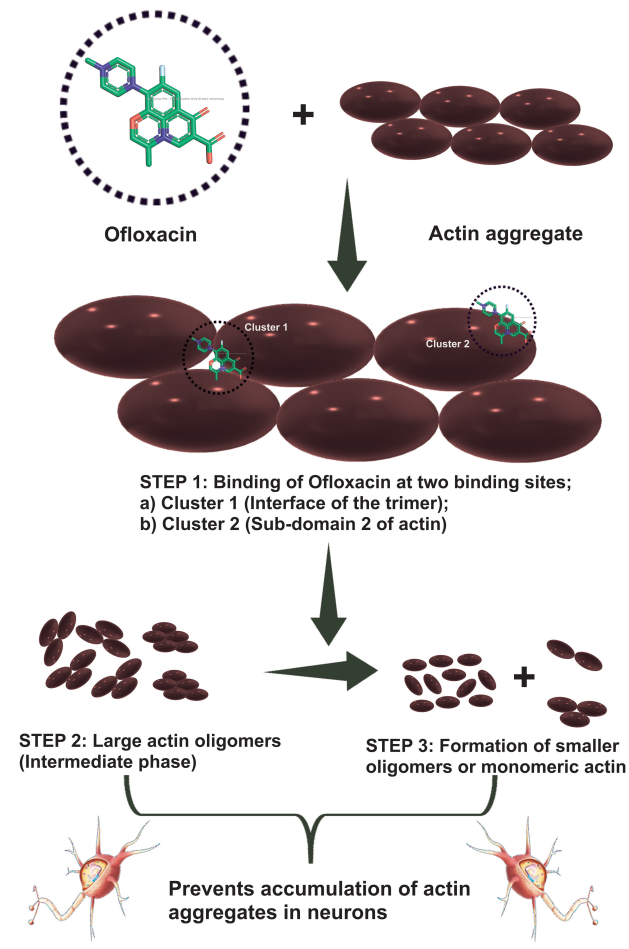

FIGURE 11 | Cartoon representation of the mechanism of action of Ofloxacin on actin aggregates. Actin aggregates upon treatment with Ofloxacin result in binding at two sites on actin. Large oligomers are formed in the intermediate phase followed by the formation of smaller-sized oligomers of monomeric actin.

we observed that actin in all the three buffer systems shows higher scattering from 250 to 700 nm for 48–72 h without any drops. This indicates that actin remains as a large molecular-sized polymer, oligomer, or amorphous aggregate for a long period of time. We then performed the same assay for the drug up to 72 h, which resulted in Ofloxacin showing scattering post 400 nm wavelength. In order to avoid any major interference from the drug molecule during our RLS measurement, we used a wavelength of 350 nm as the scattering of the drug up to 390 nm remains negligible. During the right-angle scattering, we observed that there was a concentration-dependent drop in the scattering intensity of the actin molecule in all the three solvent systems. Since this drop in the intensity was observed up until 72 h, we concluded that Ofloxacin causes an irreversible disruption of larger actin aggregates. We then performed DLS, which resulted in the convergence of heterogenous peaks of actin aggregates in PB, GB, and water to a homologous peak of smaller sizes indicating the change in the actin morphology and abundance of either smaller actin oligomers or monomers.

We also performed CD spectroscopic analysis in all the three-buffer systems, which indicates a shift of a highly polymeric structure of untreated actin into an actin rich in α-helix posttreatment. This analysis leads us to conclude that differential actin aggregate changed to globular actin. In order to observe the morphological changes in actin, we also performed SEM analysis. Through our data, we reported that the disintegration of actin occurred in both GB and water upon treatment with Ofloxacin. Our kinetic data analysis of Ofloxacin interaction with that of actin polymer in polymerization buffer indicates that the disruption of larger actin aggregates followed a two-phase reaction. During the first phase of the reaction, which is much faster than the second phase, a large molecule of actin aggregate is formed into a smaller actin nuclei, which is further disrupted into a smaller oligomer or monomeric actin. The second phase of the reaction, which is relatively slow, does not show much change in activity upon the increase in the concentration of Ofloxacin. We thus concluded that only the first phase of the reaction, which forms the intermediate product of actin aggregates, is concentration dependent. Isothermal calorimetry data suggested that the best binding occurred with two set sequential bindings with the interaction being enthalpically and entropically driven. The interaction was further studied using *in silico* analysis of actin–drug association. It was understood from the auto-dock data that Ofloxacin binds to actin at two major sites viz, Sub-domain 2 as well as at the interface of the actin nuclei. Ofloxacin was supposedly found to interfere with both the longitudinal as well as lateral interactions between two associating actin monomers.

Through our biophysical and mechanistic understanding of actin–Ofloxacin interaction, we suggest that the drug could be used as a potential candidate against the prognosis and treatment of several neurodegenerative as well as a neurodevelopmental disorders. In order to make it to the market, much further work in the area of drug dosage and drug delivery of this molecule is required. A molecular vehicle, either organic or nanomaterial, capable of encapsulating the drug as well as crossing the BBB would prove to be beneficial in targeting the dysregulated actin aggregate formed in the neuronal cells.

DATA AVAILABILITY STATEMENT

All datasets presented in this study are included in the article/supplementary material.

AUTHOR CONTRIBUTIONS

SP executed the experiment, analyzed the data, and wrote the manuscript. HP executed the experiment and wrote the manuscript. ST executed the experiments. AK conceptualized the work, analyzed the data, and wrote the manuscript. All authors contributed to the article and approved the submitted version.

FUNDING

We would like to acknowledge Department of Biotechnology (DBT), Government of India (Grant number: BT/PR16325/NER/95/117/2015) for partial financial support.

REFERENCES

Abraham, M. J., Murtola, T., Schulz, R., Páll, S., Smith, J. C., Hess, B., et al. (2015). Gromacs: high-performance molecular simulations through multi-level parallelism from laptops to supercomputers. *SoftwareX* 1–2, 19–25. doi: 10.1016/j.softx.2015.06.001

Blanchoin, L., Boujemaa-Paterski, R., Sykes, C., and Plastino, J. (2014). Actin dynamics, architecture, and mechanics in cell motility. *Physiol. Rev.* 94, 235–263. doi: 10.1152/physrev.00018.2013

Borana, M. S., Mishra, P., Pissurlenkar, R. R. S., Hosur, R. V., and Ahmad, B. (2014). Curcumin and kaempferol prevent lysozyme fibril formation by modulating aggregation kinetic parameters. *Biochim. Biophys. Acta* 1844, 670–680. doi: 10.1016/j.bbapap.2014.01.009

Bourne, J. N., and Harris, K. M. (2008). Balancing structure and function at hippocampal dendritic Spines. *Annu. Rev. Neurosci.* 31, 47–67. doi: 10.1146/annurev.neuro.31.060407.125646

Bugyi, B., and Carlier, M. -F. (2010). Control of actin filament treadmilling in cell motility. *Annu. Rev. Biophys.* 39, 449–470. doi: 10.1146/annurev-biophys-051309-103849

Carlier, M. F., and Shekhar, S. (2017). Global treadmilling coordinates actin turnover and controls the size of actin networks. *Na. Rev. Mol. Cell Biol.* 18, 389–401. doi: 10.1038/nrm.2016.172

Cell Signaling (2014). *Regulation of Actin Dynamics*. Danvers, MA: Cell Signaling Technology, Inc.

Chanfreau, G. F., Gourlay, C. W., Carpp, L. N., Timpson, P., Winder, S. J., Ayscough, K. R., et al. (2005). Impact and prevention of neurodegenerative diseases in society: alzheimer and Parkinson. *Trends Cell Biol.* 118:460.

Chavan, R., Mukherjee, S., Dahake, R., Colvin, D., Kale, A., and Chowdhary, A. (2016). Differential proteomic analysis of respiratory samples from patients suffering from influenza. *VirusDisease* 27, 226–233. doi: 10.1007/s13337-016-0332-x

Cooper, J. A., and Schafer, D. A. (2000). Control of actin assembly and disassembly at filament ends. *Curr. Opin. Cell Biol.* 12, 97–103. doi: 10.1016/S0955-0674(99)00062-9

Coutts, A. S., and La Thangue, N. B. (2016). Regulation of actin nucleation and autophagosome formation. *Cell. Mol. Life Sci.* 73, 3249–3263. doi: 10.1007/s00018-016-2224-z

De La Cruz, E. M., and Gardel, M. L. (2015). Actin mechanics and fragmentation. *J. Biol. Chem.* 290, 17137–17144. doi: 10.1074/jbc.R115.636472

Debreczeni, J. É, and Emsley, P. (2012).). Handling ligands with Coot. *Acta Crystallogr. Sect. D* 68, 425–430. doi: 10.1107/S0907444912000200

Eira, J., Silva, C. S., Sousa, M. M., and Liz, M. A. (2016). The cytoskeleton as a novel therapeutic target for old neurodegenerative disorders. *Prog. Neurobiol.* 141, 61–82. doi: 10.1016/j.pneurobio.2016.04.007

Emsley, P., Lohkamp, B., Scott, W. G., and Cowtan, K. (2010). Features and development of Coot. *Acta Crystallogr. Sect. D* 66, 486–501. doi: 10.1107/S0907444910007493

Eron, L. J., and Gentry, L. O. (1992). Oral ofloxacin for infections caused by bacteria resistant to oral antimicrobial agents. *Diagn. Microbiol. Infect. Dis.* 15, 435–439. doi: 10.1016/0732-8893(92)90085-8

Feigin, V. L., Nichols, E., Alam, T., Bannick, M. S., Beghi, E., Blake, N., et al. (2019). Global, regional, and national burden of neurological disorders, 1990–2016: a systematic analysis for the Global Burden of Disease Study 2016. *Lancet Neurol.* 18, 459–480. doi: 10.1016/S1474-4422(18)30499-X

Fletcher, D. A., and Mullins, R. D. (2010). Cell mechanisms and cytoskeleton. *Nature* 463, 485–492. doi: 10.1038/nature08908.Cell

Food and Drug Administration (n.d.). *FLOXIN Tablets*, Vol. 7. 1–32. Avaliable at: https://www.accessdata.fda.gov/drugsatfda_docs/label/2007/019735s057lbl.pdf (accessed September, 2008).

Fukazawa, Y., Saitoh, Y., Ozawa, F., Ohta, Y., Mizuno, K., and Inokuchi, K. (2003). Hippocampal LTP is accompanied by enhanced F-actin content within the dendritic spine that is essential for late LTP maintenance in vivo. *Neuron* 38, 447–460. doi: 10.1016/s0896-6273(03)00206-x

Furgerson, M., Fechheimer, M., and Furukawa, R. (2012). Model hirano bodies protect against tau-independent and tau-dependent cell death initiated by the amyloid precursor protein intracellular domain. *PLoS One* 7:e0044996. doi: 10.1371/journal.pone.0044996

Furukawa, R., and Fechheimer, M. (1997). The structure, function, and assembly of actin filament bundles. *Int. Re. Cytol.* 175, 29–90. doi: 10.1016/s0074-7696(08)62125-7

Galkin, V. E., Orlova, A., Vos, M. R., Schröder, G. F., and Egelman, E. H. (2015). Near-atomic resolution for one state of F-Actin. *Structure* 23, 173–182. doi: 10.1016/j.str.2014.11.006

Gammon, K. (2014). Neurodegenerative disease: brain windfall. *Nature* 515, 299–300. doi: 10.1038/nj7526-299a

Gitler, A. D., Dhillon, P., and Shorter, J. (2017). Neurodegenerative disease: models, mechanisms, and a new hope. *DMM Dis. Models Mech.* 10, 499–502. doi: 10.1242/dmm.030205

Goebel, H. H. (2009). Protein aggregate myopathies: introduction. *Brain Pathol.* 19, 480–482. doi: 10.1111/j.1750-3639.2009.00291.x

Goldman, J. E. (1983). The association of actin with hirano bodies. *J. Neuropathol. Exp. Neurol.* 42, 146–152. doi: 10.1097/00005072-198303000-00004

Gordon-Weeks, P. R., and Fournier, A. E. (2014). Neuronal cytoskeleton in synaptic plasticity and regeneration. *J. Neurochem.* 129, 206–212. doi: 10.1111/jnc.12502

Gourlay, C. W., and Ayscough, K. R. (2005). The actin cytoskeleton in ageing and apoptosis. *FEMS Yeast Res.* 5, 1193–1198. doi: 10.1016/j.femsyr.2005.08.001

Kern, W., Kurrle, E., and Vanek, E. (1987). Ofloxacin for prevention of bacterial infections in granulocytopenic patients. *Infection* 15, 427–432. doi: 10.1007/BF01647222

Kevenaar, J. T., and Hoogenraad, C. C. (2015). The axonal cytoskeleton: from organization to function. *Front. Mol. Neurosci.* 8:44. doi: 10.3389/fnmol.2015.00044

Kim, C., and Lisman, J. E. (1999). A role of actin filament in synaptic transmission and long-term potentiation. *J. Neurosci.* 19, 4314–4324. doi: 10.1523/jneurosci.19-11-04314.1999

Koistinen, N. A., Edlund, A. K., Menon, P. K., Ivanova, E. V., Bacanu, S., and Iverfeldt, K. (2017). Nuclear localization of amyloid-β precursor protein-binding protein Fe65 is dependent on regulated intramembrane proteolysis. *PLoS One* 12:e0173888. doi: 10.1371/journal.pone.0173888

Lambrechts, A., Van Troys, M., and Ampe, C. (2004). The actin cytoskeleton in normal and pathological cell motility. *Int. J. Biochem. Cell Biol.* 36, 1890–1909. doi: 10.1016/j.biocel.2004.01.024

Liu, H., Pierre-Pierre, N., and Huo, Q. (2012). Dynamic light scattering for gold nanorod size characterization and study of nanorod-protein interactions. *Gold Bull.* 45, 187–195. doi: 10.1007/s13404-012-0067-4

Luo, L. (2002). Actin cytoskeleton regulation in neuronal morphogenesis and structural plasticity. *Annu. Rev. Cell Dev. Biol.* 18, 601–635. doi: 10.1146/annurev.cellbio.18.031802.150501

Maselli, A., Furukawa, R., Thomson, S. A. M., Davis, R. C., and Fechheimer, M. (2003). Formation of hirano bodies induced by expression of an actin cross-linking protein with a gain-of-function mutation. *Eukaryotic Cell* 2, 778–787. doi: 10.1128/ec.2.4.778-787.2003

McKayed, K., and Simpson, J. (2013). Actin in action: imaging approaches to study cytoskeleton structure and function. *Cells* 2, 715–731. doi: 10.3390/cells2040715

Melidone, R., Keating, J. H., Pfannl, R., and Alroy, J. (2011). Cerebral hirano-like bodies in an alpaca (*Vicugna pacos*). *Vet. Pathol.* 49, 723–726. doi: 10.1177/0300985811406886

Micsonai, A., Wien, F., Bulyáki, É, Kun, J., Moussong, É, Lee, Y. H., et al. (2018). BeStSel: a web server for accurate protein secondary structure prediction and fold recognition from the circular dichroism spectra. *Nucleic Acids Res.* 46, W315–W322. doi: 10.1093/nar/gky497

Morrissey, I., Hoshino, K., Sato, K., Yoshida, A., Hayakawa, I., Bures, M. G., et al. (1996). Mechanism of differential activities of ofloxacin enantiomers? *Antimicrob. Agents nd Chemother.* 40, 1775–1784. doi: 10.1128/aac.40.8.1775

Muñoz-Lasso, D. C., Mollá, B., Calap-Quintana, P., García-Giménez, J. L., Pallardo, F. V. V., Palau, F., et al. (2020a). Cofilin dysregulation alters actin turnover in frataxin-deficient neurons. *Sci. Rep.* 10, 1–10. doi: 10.1038/s41598-020-62050-7

Muñoz-Lasso, D. C., Romá-Mateo, C., Pallardó, F. V., and Gonzalez-Cabo, P. (2020b). Much more than a scaffold: cytoskeletal proteins in neurological disorders. *Cells* 9:358. doi: 10.3390/cells9020358

Oda, T., Iwasa, M., Aihara, T., Maéda, Y., and Narita, A. (2009). The nature of the globular- to fibrous-actin transition. *Nature* 457, 441–445. doi: 10.1038/nature07685

Ogawa, Y., and Rasband, M. N. (2008). The functional organization and assembly of the axon initial segment. *Curr. Opin. Neurobiol.* 18, 307–313. doi: 10.1016/j.conb.2008.08.008

Okada, H., and Soderling, S. H. (2009). Signaling through actin to regulate spine formation and function. *Open Neurosci. J.* 3, 97–107. doi: 10.2174/1874082000903020097

Otterbein, L. R., Graceffa, P., and Dominguez, R. (2001). The crystal structure of uncomplexed actin in the ADR state. *Science* 293, 708–711. doi: 10.1126/science.1059700

Pathak, S., Tripathi, S., Deori, N., Ahmad, B., Verma, H., Lokhande, R., et al. (2020). Effect of tetracycline family of antibiotics on actin aggregation, resulting in the formation of Hirano bodies responsible for neuropathological disorders. *J. Biomol. Struct. Dyn.* 1–18. doi: 10.1080/07391102.2020.1717629 [Epub ahead of print].

Pelucchi, S., Stringhi, R., and Marcello, E. (2020). Dendritic spines in alzheimer's disease: how the actin cytoskeleton contributes to synaptic failure. *Int. J. Mol. Sci.* 21, 1–23. doi: 10.3390/ijms21030908

Perera, S. P., McIntosh, T. C., and Wanasundara, J. P. D. (2016). Structural properties of cruciferin and napin of brassica napus (Canola) show distinct responses to changes in ph and temperature. *Plants* 5:36. doi: 10.3390/plants5030036

Perez-Iratxeta, C., and Andrade-Navarro, M. A. (2008). K2D2: estimation of protein secondary structure from circular dichroism spectra. *BMC Struct. Biol.* 8:25. doi: 10.1186/1472-6807-8-25

Perl, D. P., Davidson, M., Haroutunian, V., and Davis, K. L. (1995). Alzheimer's disease and related neurodegenerative diseases in elderly schizophrenic patients. *J. Neuropathol. Exp. Neurol.* 54:460. doi: 10.1097/00005072-199505000-00211

Pillaiyar, T., Meenakshisundaram, S., and Manickam, M. (2020). A medicinal chemistry perspective of drug repositioning: recent advances and challenges in drug discovery. *Eur. J. Med. Chem.* 195:112275. doi: 10.1016/j.ejmech.2020.112275

Przedborski, S., Vila, M., and Jackson-Lewis, V. (2003). Neurodegeneration: what is it and where are we? *J. Clin. Invest.* 111, 3–10. doi: 10.1172/JCI200317522

Pushpakom, S., Iorio, F., Eyers, P. A., Escott, K. J., Hopper, S., Wells, A., et al. (2019). Drug repurposing: progress, challenges and recommendations. *Nat. Rev. Drug Discov.* 18, 41–58. doi: 10.1038/nrd.2018.168

Ross, C. A., and Poirier, M. A. (2004). Protein aggregation and neurodegenerative disease. *Nat. Med.* 10:S10. doi: 10.1038/nm1066

Sabo, S. L., Ikin, A. F., Buxbaum, J. D., and Greengard, P. (2001). The Alzheimer amyloid precursor protein (APP) and FE65, an APP-binding protein, regulate cell movement. *J. Cell Biol.* 153, 1403–1414. doi: 10.1083/jcb.153.7.1403

Santa-Mara, I., Santpere, G., MacDonald, M. J., Gomez De Barreda, E., Hernandez, F., Moreno, F. J., et al. (2008). Coenzyme Q induces tau aggregation, tau filaments, and Hirano bodies. *J. Neuropathol. Exp. Neurol.* 67, 428–434. doi: 10.1097/NEN.0b013e31816fc9b6

Shekhar, S., Pernier, J., and Carlier, M.-F. (2016). Regulators of actin filament barbed ends at a glance. *J. Cell Sci.* 129, 1085–1091. doi: 10.1242/jcs.179994

Solomon, E. I., Augustine, A. J., and Yoon, J. (2010). Rapid and efficient purification of actin from nonmuscle sources. *Cell Motil. Cytoskeleton* 39, 3921–3932. doi: 10.1039/b800799c.O

Sonavane, S., Haider, S. Z., Kumar, A., and Ahmad, B. (2017). Hemin is able to disaggregate lysozyme amyloid fibrils into monomers. *Biochim. Biophys. Acta* 1865, 1315–1325. doi: 10.1016/j.bbapap.2017.07.017

Spears, W., Furgerson, M., Sweetnam, J. M., Evans, P., Gearing, M., Fechheimer, M., et al. (2014). Hirano bodies differentially modulate cell death induced by tau and the amyloid precursor protein intracellular domain. *BMC Neurosci.* 15:74. doi: 10.1186/1471-2202-15-74

Spence, E. F., and Soderling, S. H. (2015). Actin out: regulation of the synaptic cytoskeleton. *J. Biol. Chem.* 290, 28613–28622. doi: 10.1074/jbc.R115.655118

Subramaniam, S. (2019). Selective neuronal death in neurodegenerative diseases: the ongoing mystery. *Yale J. Biol. Med.* 92, 695–705.

Svennberg, K. (2006). Moisture Buffering in the Indoor Environment. *Physics* 67, 184–192. doi: 10.1016/j.brainresrev.2011.01.003.Impaired

Szabó, E. C., Manguinhas, R., and Fonseca, R. (2016). The interplay between neuronal activity and actin dynamics mimic the setting of an LTD synaptic tag. *Sci. Rep.* 6, 1–14. doi: 10.1038/srep33685

Trends, C. M., and Disorders, N. (2018). Current medication trendsand global impact on neurodegenerative disorders. *J. Pharmaceut. Pharmacol.* 6, 01–09. doi: 10.13188/2327-204x.1000024

Trott, O., and Olson, A. J. (2010). AutoDock Vina: improving the speed and accuracy of docking with a new scoring function, efficient optimization, and multithreading. *J. Comput. Chem.* 31, 455–461. doi: 10.1002/jcc.21334

Vavylonis, D., Yang, Q., and O'Shaughnessy, B. (2005). Actin polymerization kinetics, cap structure, and fluctuations. *Proc. Natl. Acad. Sci. U.S.A.* 102, 8543–8548. doi: 10.1073/pnas.0501435102

Wiedemann, C., Bellstedt, P., and Görlach, M. (2013). CAPITO - A web server-based analysis and plotting tool for circular dichroism data. *Bioinformatics* 29, 1750–1757. doi: 10.1093/bioinformatics/btt278

Yamada, R., and Kuba, H. (2016). Structural and functional plasticity at the axon initial segment. *Front. Cell. Neurosci.* 10:250. doi: 10.3389/fncel.2016.00250

Yang, G., Sau, C., Lai, W., Cichon, J., and Li, W. (2010). ADF/cofilin-actin rods in neurodegenerative diseases J.R. *Curr. Alzheimer Res.* 7, 241–250. doi: 10.1126/science.1249098.Sleep

Yao, J., and Khan, A. N. (2012). Involvement of actin pathology in Alzheimer's Disease. *Cell Dev. Biol.* 02, 2–4. doi: 10.4172/2168-9296.1000e121

Yao, J., and Khan, A. N. (2013). Involvement of actin pathology in Alzheimer's Disease. *Cell Dev. Biol.* 02, 2–4.

Conflict of Interest: The authors declare that the research was conducted in the absence of any commercial or financial relationships that could be construed as a potential conflict of interest.

frontiers in Cellular Neuroscience

MINI REVIEW
published: 03 February 2021
doi: 10.3389/fncel.2020.615125

The Impacts of Unfolded Protein Response in the Retinal Cells During Diabetes: Possible Implications on Diabetic Retinopathy Development

Kaiser Alam and Yusuf Akhter*

Department of Biotechnology, School of Life Sciences, Babasaheb Bhimrao Ambedkar University, Lucknow, India

Diabetic retinopathy (DR) is a vision-threatening, chronic, and challenging eye disease in the diabetic population. Despite recent advancements in the clinical management of diabetes, DR remains the major cause of blindness in working-age adults. A better understanding of the molecular and cellular basis of DR development will aid in identifying therapeutic targets. Emerging pieces of evidence from recent research in the field of ER stress have demonstrated a close association between unfolded protein response (UPR)-associated cellular activities and DR development. In this minireview article, we shall provide an emerging understating of how UPR influences DR pathogenesis at the cellular level.

Keywords: unfolded protein response, diabetic retinopathy, retinal vascular cell, retinal glial cell, retinal pigment epithelium, retinal neuronal cell

OPEN ACCESS

Edited by:
Arif Tasleem Jan, Baba Ghulam Shah Badshah University, India

Reviewed by:
Vasudharani Devanathan, Indian Institute of Science Education and Research, India
Victoria P. Connaughton, American University, United States

****Correspondence:***
Kaiser Alam
alamkaiser@gmail.com

Specialty section:
This article was submitted to Cellular Neuropathology, a section of the journal Frontiers in Cellular Neuroscience

Received: *09 October 2020*
Accepted: *23 December 2020*
Published: *03 February 2021*

Citation:
Alam K and Akhter Y (2021) The Impacts of Unfolded Protein Response in the Retinal Cells During Diabetes: Possible Implications on Diabetic Retinopathy Development. Front. Cell. Neurosci. 14:615125. doi: 10.3389/fncel.2020.615125

INTRODUCTION

In the worldwide-rising diabetic population, diabetic retinopathy (DR) remains one of the major eye diseases leading to visual impairment and in severe cases even blindness. DR causes noticeable socioeconomic costs for the family of patients and the healthcare system because it significantly affects the working-age population. Epidemiological studies have suggested that about one-third of diabetic patients have some degree of DR and about 10% of them have severe forms of DR, such as diabetic macular edema (DME) and proliferative diabetic retinopathy (PDR). The current DR treatments, such as laser therapy, anti-vascular endothelial growth factor (VEGF) agents, and corticosteroids, usually lead to adverse side effects and are applied only in patients with severe forms of DR (Antonetti et al., 2012; Jenkins et al., 2015).

Besides carrying out many important cellular functions, such as lipid synthesis, calcium ions (Ca^{2+}) homeostasis, and storage, the endoplasmic reticulum (ER) is involved especially in protein homeostasis, proteostasis, of membrane and secretory pathway-associated proteins that account for at least one-third of the proteins that are synthesized in the higher organism (Zhang and Kaufman, 2008; Hotamisligil, 2010; Walter and Ron, 2011). To ascertain quality control of protein folding, eukaryotic organisms regulate ER–protein processing activities of misfolded/unfolded proteins at the cellular level known as unfolded protein response (UPR). The activation of UPR results in several outcomes, such as attenuation of global protein translation, enhanced degradation of ER

luminal unfolded or misfolded protein, and increased amount of ER-localized chaperones (Rao et al., 2004). Thus, UPR tries to restore ER homeostasis that is essential for cell survival. However, if ER stress is chronic and severe because of unrestorable aggregation of unfolded proteins, UPR induces cell death (Zhang and Kaufman, 2008). Studies in the area of ER stress have implicated dysfunctional UPR on the onset and progression of many diseases including diabetes and its associated complications in various organs, such as the kidney (diabetic nephropathy), neurons (diabetic neuropathy), and eyes (DR; Hotamisligil, 2010).

The retina of the eye is a light-sensitive, greatly complex, and highly organized neural tissue. Recent insight into the physiology of the retina suggests that proper functioning of the retina depends on the close association between neural, glial, and specialized vasculature as a neurovascular unit or neurovascular coupling (Alarcon-Martinez et al., 2020). Communications between different types of the cells in such a neurovascular unit inside the retina are essential for efficient visual function. The retina is considered as an immune-privileged tissue, which is mainly maintained by the blood–retinal barrier (BRB) that safeguards the retinal tissue functions from the systemic immune responses. The BRB prevents easy access of blood constituents to the retina by the complexes of tight junctional (TJ) proteins at two levels, first, between endothelial cells of retinal capillaries that nourish the inner retina (inner BRB) and second, between retinal pigment epithelium (RPE) cells that maintain a barrier for choroidal capillaries nourishing the outer retina (outer BRB; Cunha-Vaz et al., 2011). It has been well documented that prolonged diabetes deteriorates the tiny blood vessels of the eye leading to the breakdown of the BRB. In severe cases, small blood capillaries get occluded to cause ischemia, hypoxia, and finally neovascularization. The advanced and vision-threatening stage of DR is known as PDR, which is characterized by retinal growth of new blood vessels (neovascularization) and epiretinal membrane at the vitreous surface of the retina. These pathological changes can cause vitreous hemorrhage and tractional retinal detachment resulting in the severe loss of vision (Maugh, 1976). Clinical findings and assessment of different stages of DR are based mainly on compromised vasculature in the retina (Antonetti et al., 2012; Jenkins et al., 2015). As DR remains clinically asymptomatic until significantly advanced, new diagnostic tools and therapeutic strategies for the initial stages of its development are urgently needed. In this scenario, the UPR pathways are extremely promising targets to prevent and treat DR at the early stages of its development.

UPR is known to be a group of phylogenetically conserved intracellular signaling responses and has at least three parallelly or sequentially operated pathways with unique mechanisms of action (**Figure 1**). Some excellent recent reviews have been published on this subject in the context of various pathophysiological conditions including ocular diseases (Hetz et al., 2013; Zhang et al., 2015; Grootjans et al., 2016; Hetz and Saxena, 2017; Kroeger et al., 2019). Each pathway is named after its ER transmembrane protein, namely, activating transcription factor 6 (ATF6), inositol requiring enzyme 1 (IRE1), and double-stranded RNA-activated protein kinase (PKR)-like ER kinase (PERK). These transmembrane proteins act as sensors of ER luminal unfolded or misfolded proteins. Under normal conditions, 78-kDa glucose-regulated protein (GRP78), a heat shock family-related chaperone protein, binds these sensor proteins in their ER luminal domain, keeping them inactive (Bertolotti et al., 2000). However, during various stress conditions, GRP78 preferably binds to unfolded or misfolded proteins rather than the sensor proteins in the ER lumen, which leads to the activation of the UPR pathways. The downstream signaling of the GRP78-released sensors is well studied and is found to be different within each of the three UPR pathways. In the ATF6 pathways, GRP78-released ATF6 moves to the Golgi apparatus where it is cleaved at different sites by a serine protease and a metalloprotease. Cleaved ATF6 is an active transcription factor that enters the nucleus and activates the promoter of its cognate target genes, such as calreticulin, GRP78, and 94-kDa glucose-regulated protein (GRP94). On the other hand, GRP78-released IRE1, as well as PERK, is activated only after autophosphorylation and oligomerization (Ron and Walter, 2007). In the IRE1 pathway, activated IRE1 acts as a dual activity protein with both kinase and ribonuclease functions. Activated IRE1 removes the internal 28 base pairs segment from X-box binding protein 1 (XBP1) mRNA, generating an alternative splice variant protein XBP1s (Zhang et al., 2015). XBP1s is a transcription factor that either alone or in conjunction with ATF6α upregulates the expression of various ER-localized chaperones and proteins involved in ER-associated protein degradation (ERAD; Lee et al., 2003). It can also rapidly degrade some specific subset of mRNAs depending on their sequence and localization (Hollien and Weissman, 2006). It is pertinent to note that the IRE1 pathway is conserved from lower eukaryotes to higher mammal organisms. Finally, in the PERK pathways, GRP78-released PERK after its autophosphorylation and oligomerization suppresses the activity of translational initiation factor 2 (eIF2) complex by phosphorylating its α subunit. This change in the eIF2 complex not only attenuates the rate of global translation initiation and protein synthesis but also favors the translation of some mRNA, such as activating transcription factor 4 (ATF4; Blais et al., 2004). ATF4 protein is a versatile transcription factor paradoxically involved in both cell survival and apoptosis dependent on the state of ER stress. During acute ER stress, ATF4 induces the genes responsible for adaption; however, under chronic ER stress condition, it promotes apoptosis by upregulating genes, such as CCAAT enhancer-binding protein homologous protein (CHOP; Rozpedek et al., 2016). Additionally, CHOP also contributes to calcium homeostasis in a reactive oxidative stress-dependent manner (Tabas and Ron, 2011). These three pathways either in parallel or in sequence attenuate ER stress.

In recent years, increased mechanistic studies in the field of UPR have suggested that not only different tissues but also different cell types within the organ are represented by different UPR branches (Mori, 2009; Walter and Ron, 2011; Simó and Hernández, 2014; Wang and Kaufman, 2016). However, the activation of the UPR pathways during diabetic conditions in

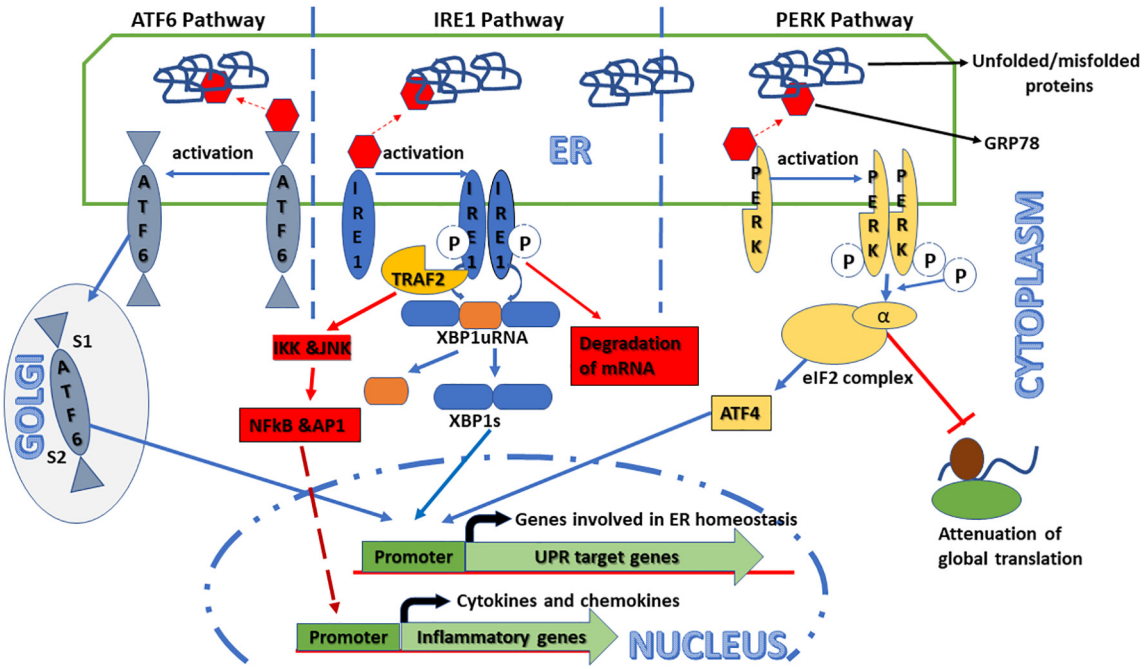

FIGURE 1 | Schematic representation of the signaling pathways activated in the unfolded protein response (UPR). Endoplasmic reticulum (ER) stress can trigger UPR that consists of at least three independent pathways identified by their transmembrane sensor proteins, namely, activating transcription factor 6 (ATF6), inositol requiring enzyme 1 (IRE1), and double-stranded RNA-activated protein kinase (PKR)-like ER kinase (PERK). Under normal conditions, these sensor proteins are inactive because of their association with an ER-resident chaperone protein, 78-kDa glucose-regulated protein (GRP78). However, in ER stress conditions, GRP78 preferentially binds to unfolded/misfolded proteins in the ER lumen leading to the release and activation of the sensor proteins that, in turn, induce their respective downstream signaling pathways. In the ATF6 pathway, GRP78-released ATF6 moves to the Golgi apparatus and is cleaved by both serine proteases and metalloproteases at S1 and S2 sites, respectively. Cleaved ATF6 acts as a transcription factor that binds to the promoters of UPR target genes, such as GRP78 and X-box binding protein 1 (XBP1), and upregulates their expression. In the IRE1 pathway, after its autophosphorylation and oligomerization, GRP78-released IRE1 processes the XBP1 mRNA to generate spliced XBP1 (XBP1s) that, in turn, induces UPR target genes to restore ER homeostasis. Additionally, activated IRE1 also induces the expression and secretion of inflammatory cytokines, such as tumor necrosis factor-α (TNF-α) and interleukin-1β (IL-1β), through the TNF receptor-associated factor 2–IκB kinase–c Jun N-terminal kinase (TRAF2–IKK–JNK) signaling axis. Under some circumstances, it can rapidly degrade some specific subset of mRNAs. In the PERK pathway, after its autophosphorylation and oligomerization, GRP78-released PERK globally attenuates mRNAs to protein translation by phosphorylating the α-subunit of translational initiation factor (eIF2) complex. Additionally, increased eIF2α phosphorylation also modulates the pro- and anti-apoptotic pathways by activating the alternative transcription factor 4-C/EBP homologous protein (ATF4–CHOP) signaling axis.

different types of the retinal cells is not properly reviewed, which is the focus of this review.

UPR ACTIVATION AND ITS IMPACTS ON THE RETINAL CELLS IN DR

In diabetes, chronic hyperglycemia-associated metabolic abnormalities impair the ER functions in many tissues including the retina (Oshitari et al., 2008; Roy et al., 2013). Data from recent research in DR implicate UPR to be activated very early in various retinal cells leading to diabetes-associated cellular dysfunctions and visual impairment.

Retinal Vascular Cell Dysfunctions

In studies using experimental animal models and patients with diabetes, observed enhanced vascular permeability and neovascularization in DR are closely associated with endothelial dysfunctions and pericyte cell death (Kowluru et al., 2007; Chan et al., 2010; Santos and Kowluru, 2011). The retinal microvascular endothelial cells (RMECs) are one of the principal cells that maintain the inner BRB constituted by TJ complexes composed of transmembrane proteins, such as occludin, claudin, zona occludens, and adhesion molecules (Metea and Newman, 2007). Changes in the expression/activity of these proteins can compromise the integrity of the TJ complex, leading to the breakdown of the BRB, which is a clinically important phenomenon in DR pathogenesis (Klaassen et al., 2009). Several studies have implicated ER stress-mediated retinal inflammation in vascular dysfunctions associated with the development of DR (Adachi et al., 2011). For example, Adachi and colleagues demonstrated that the permeability of externally added fluorescein isothiocyanate (FITC) dextran was significantly increased in the human RMECs treated with ER stress-inducing drugs, such as thapsigargin and tunicamycin. Similarly, these drugs can reduce transendothelial electrical resistance and levels of claudin 5 of TJ complex protein in the RMEC (Adachi et al., 2012).

In DR, enhanced permeability and neovascularization is shown to be critically mediated by VEGF and inflammatory cytokines/chemokines. Several studies have suggested that

the activation of UPR regulates VEGF expression and secretion. Li and colleagues reported that in the cultured human RMECs, hypoxia-induced and tumor necrosis factor (TNF)-α expressions were parallelly associated with the activation of UPR with enhanced GRP78, ATF4 levels, and the phosphorylation of IRE1, as well as eIF2α. They also demonstrated that 4-phenylbutyric acid (PBA), a chemical chaperone and attenuator of ER stress, ameliorated these activities (Li et al., 2009). Using rat retinal capillary EC line (TR-iBRB), Chen et al. (2012) showed that high glucose-induced inflammatory cytokines and VEGF expressions were mediated by the activation of the PERK pathway through signal transducer and activator of transcription 3 (STAT3) signaling. Furthermore, Liu et al. (2013) reported that in the human RMECs, diabetic-mimetic conditions increased the expression levels of XBP1/IRE1, ATF6, and a heat shock chaperone α-crystallin B (CRYAB) that consequently upregulate VEGF and knockdown of any of them (IRE1a, ATF6, or CRYAB) by siRNA degrade VEGF (Liu et al., 2013). Recently, Lenin et al. demonstrated that in the human retinal endothelial cell (HREC), hyperglycemia plus TNF treatment decreased transendothelial resistance and the expression of vascular endothelial (VE)-cadherin, which was rescued by ER stress inhibitor drug tauroursodeoxycholic acid (TUDCA; Lenin et al., 2018).

Pericytes are mural cells that partially cover all the blood vessel capillaries. The density of pericytes in retinal capillaries is higher than that in other locations, which suggests their important functional role in the retina. In the adult retina, pericytes are terminally differentiated; therefore, they do not replicate at this site, and their degeneration results in thickening of the basement membrane, increased permeability, and edema (Mandarino, 1992). DR is the only known disease that is strongly correlated to pericyte loss. The pericytes deficiency in the retinal capillaries can lead either to endothelial cell proliferation resulting in microaneurysm (Hammes et al., 2002) or to their degeneration resulting in acellular capillaries, one of the earliest morphological signs of vascular abnormalities in DR. It is worthy to note here that the measurement of acellular capillaries is one of the most reliable markers in experimental DR stages in an animal model.

Several reports implicated UPR activation in retinal pericytes exposed to a fluctuated concentration of glucose. For instance, the UPR pathways were strongly activated not by hyperglycemia but by hypoglycemia or no glucose at all in retinal pericytes leading to their apoptosis (Ikesugi et al., 2006). Similarly, expression levels of transcription factor ATF4 of the PERK pathway of UPR and its target genes CHOP and monocyte chemoattractant protein 1 (MCP-1), an inflammatory molecule, were increased by intermittent high glucose but not by constant high glucose. These glucose fluctuated activities in pericytes were attenuated by a chemical chaperone (Zhong et al., 2012b). In contrary to the above findings, using conditionally immortalized rat retinal pericyte, one report suggests that GRP78 activation and apoptosis were induced by total depletion rather than fluctuations of cellular glucose levels (Makita et al., 2011).

One of the important risk factors for DR onset in type 1 diabetic patients is the increased serum levels of the complexes of oxidatively modified low-density lipoprotein (oxLDL) and its auto-antibodies, oxLDL immune complexes (Ox-LDL-IC; Lopes-Virella et al., 2012). Fu et al. (2014) demonstrated that Ox-LDL-IC was cytotoxic to retinal pericytes. Ox-LDL-IC-induced apoptosis of pericytes was mediated also by ER stress, which was triggered by scavenger and IgG receptors. Recently, it was reported that advanced glycation end product (AGE) or modified low-density lipoprotein induced the PERK pathway of UPR in human retinal pericytes, which was ameliorated by a chemical chaperone, ursodeoxycholic acid (UDCA; Chung et al., 2017).

Retinal Glial Cell Dysfunctions

The retinal glial cells, also considered as innate immune cells of the retina, are composed of three types, namely, astrocytes, microglia, and Müller cells (MCs). They are the main producer of proinflammatory cytokines, such as TNF-α, interleukin (IL)-1β, and IL-6 (Yang et al., 2008; Kochan et al., 2012). The predominant glial cell types in the retina are MCs that span all across the retina from the outer limiting membrane to the inner limiting membrane (Newman and Reichenbach, 1996; Ahmad et al., 2011). MCs are involved in many critical retinal functions, such as ion homeostasis regulation, structural stabilization, neuronal survival, and neurotransmitter recycling (Reichenbach et al., 1993; Chan-Ling, 1994; Kim et al., 2006). Furthermore, they are involved in providing trophic and anti-oxidative support to neurons and maintaining the BRB. MCs function as a soft protector for neurons, keeping them safe from external injuries, such as mechanical trauma. They are proposed to be living optical fibers that transduce light through the internal neuron, preventing the scattering of light thereby enhancing signal/noise ratio (Reichenbach and Bringmann, 2013). During stress conditions, MCs absorb glucose and nutrients from the blood and store them as glycogen that can be utilized as an energy source. They also uptake and detoxify glutamate and provide glutamine and lactate as metabolites to neurons (Zahs et al., 2003; Zahs and Ceelen, 2006). Furthermore, MCs remove retinal fluid to prevent retinal edema, which is an extremely important function because the retina does not have a lymphatic drainage system (Zhao et al., 2010, 2011). However, when retinal homeostasis is disturbed due to various pathophysiological conditions, such as diabetes, MCs get activated and undergo reactive gliosis (Bringmann et al., 2009).

The activation of MCs was found to be one of the main factors for DR onset and progression (Feit-Leichman et al., 2005; Wong et al., 2011), which is crucially dependent on the activation of the UPR pathways and the expression/secretion of VEGF and inflammatory cytokines. For example, Zhong et al. (2012a) reported that high glucose exposed MCs upregulated the expression of VEGF and the activation of ATF4, a PERK pathway transcription factor. Using rat MC line, Wu et al. (2019) recently reported that both hyperglycemia and its osmotic control mannitol activated

the UPR pathways to upregulate the expression of VEGF. They demonstrated that all three pathways of UPR were interdependent on one another for their VEGF upregulation function. Recently, Yang and colleagues have demonstrated that primary MCs derived from genetically Xbp1 knockout (Xbp1 Müller−/−) mice expressed higher levels of VEGF, TNF-α, phosphorylated c-Jun N-terminal kinase (p-JNK), and ER stress markers (except GRP78) and intensified inflammation and ER stress when exposed to high glucose or hypoxia than MCs derived from control mice. They further demonstrated that the chemical chaperones both PBA and trimethylamine N-oxide (TMAO) suppressed glucose or hypoxia-induced VEGF and TNF-α from Xbp1 knockout MCs (Yang et al., 2019).

RPE Cell Dysfunctions

The RPE cells are pigmented in nature and constitute the outer BRB of the retina. Its long apical microvilli enclose a light-sensitive neural segment of the retina. The basolateral part of the RPE cells touches the Bruch's membrane, which separates choriocapillaris fenestrated endothelium (Strauss, 2005). The RPE cells are involved in many activities important for proper visual functions, such as the transformation of all-trans-retinal into 11-cis-retinal, necessary for visual cycles, shed photoreceptor membrane phagocytosis, extra-light absorption, and protection from photooxidation (Simó et al., 2010). Although relatively fewer studies on DR focus on the RPE cells than on the RMECs for DR-associated dysfunctions, such as vascular leakage and changes on TJ proteins, they indeed suggested that diabetes damages the RPE cells of the retina (Kirber et al., 1980; Vinores et al., 1989; Xu and Le, 2011).

Several studies reported that the expression and secretion of VEGF in diabetic retinal RPE cells were mediated by the activation of the UPR pathways (Zhang et al., 2015; Salminen et al., 2010). One group reported that homocysteine-induced VEGF in the RPE cells was mediated by the ATF4 transcription factor of the PERK pathway (Roybal et al., 2004). Similarly, the phosphorylation of eIF2α indicating the activation of the PERK pathway is reported in the RPE cells of patients with the non-proliferative stage of DR (Miranda et al., 2012). Du et al. (2013) demonstrated that the RPE cells of diabetic patients with retinopathy had more levels of GRP78 chaperone than those of diabetic patients without retinopathy, suggesting the involvement of UPR of the RPE cells in DR development.

Additionally, several traditional herbal drugs were shown to ameliorate diabetic-mimetic condition-induced UPR activation in the RPE cells. It was reported that beta-glucogallin, an aldose reductase inhibitor isolated from Indian gooseberry fruit,

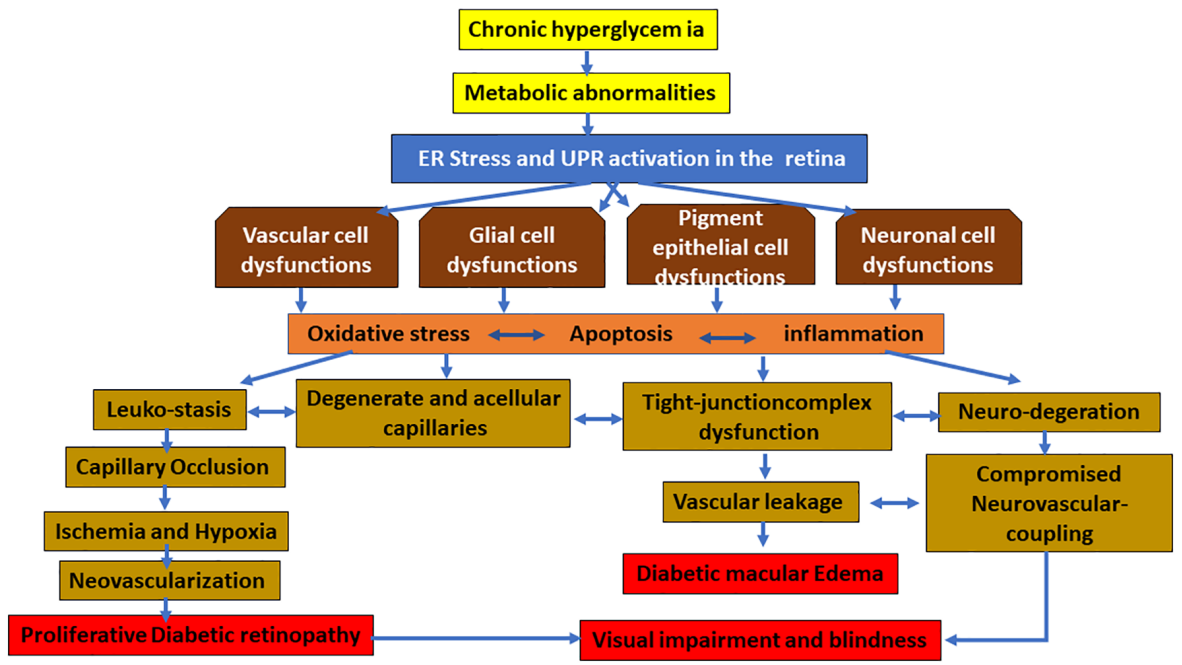

FIGURE 2 | Hypothesized schematic representation of the UPR pathways causing damage to the vascular, glial, pigment epithelial, and neuronal cells of the retina in diabetic retinopathy (DR). In diabetes, chronic hyperglycemia and its associated metabolic abnormalities lead to ER stress in the retinal cells. While temporary and mild ER stress can be overcome by the adaptive UPR, persistent ER stress and the consequent UPR activation can follow different pathways to activate the proinflammatory and proapoptotic signaling pathways. This results in damage to various cells of the retina. The characteristic changes of early diabetic retinas may be glial cell activation, which, in turn, leads to vascular changes leading to apoptosis and dropout of pericyte, as well as dysfunctional tight junctional complex proteins of endothelial and pigment epithelial cells resulting in the inner and outer blood–retinal barrier (BRB) breakdown, respectively. Furthermore, neuronal abnormalities lead to compromised neurovascular coupling and finally neovascularization and hemorrhage, resulting in vision-threatening DR such as macular edema and proliferative diabetic retinopathy.

was shown to ameliorate GRP78 induced by hyperglycemia in the RPE cells (Chang et al., 2015). Furthermore, in the ARPE-19 cell line, grape polyphenol was shown to attenuate the thapsigargin-induced activation of the UPR pathways, VEGF expression, and apoptosis (Ha et al., 2014). Kang et al. (2018) demonstrated that in the RPE cells, chrysin, a flavone-type flavonoid, attenuated diabetic-mimetic conditions, or ER stress inducer drugs mediated the induction of ATF6, IRE1α (Kang et al., 2018). Recently, Peng et al. (2020) demonstrated that in the RPE cells, astragalus polysaccharide, a traditional Chinese medicine, ameliorates UPR activation, as well as apoptosis, *via* the regulation of the miR-204/SIRT1 signaling axis in an *in vitro* metabolic memory model (Peng et al., 2020).

Retinal Neuronal Cell Dysfunctions

The neural retina is composed of many cell types, such as rods, cones, and horizontal, bipolar, amacrine, and ganglion cells. Although the first clinical signs of DR are vascular changes, diabetes can damage the neuronal retina resulting in alterations in retinal functions (Shirao and Kawasaki, 1998; Li et al., 2002; Phipps et al., 2006). Among the retinal neuron, the retinal ganglion cells (RGCs) are widely investigated concerning the effect of diabetes (Kern and Barber, 2008). Several reports have demonstrated RGCs loss in the retina of diabetic patients or experimental animal models (Barber et al., 1998; Martin et al., 2004; Oshitari et al., 2008).

Cell death of the ganglion cells was proposed to be a relatively early phenomenon in DR, which is dependent on the activation of the UPR pathways. Oshitari et al. (2011) reported that apoptosis of RGCs from the diabetic retina or non-diabetic retina *in vitro* exposed to high glucose correlated the activation of the PERK pathway with increased levels of CHOP. Using an STZ-induced diabetic animal model, Yang and colleagues reported that although CHOP of the PERK pathways was significantly increased all along with the nerve fiber and ganglion cell of the retina, JNK and caspase 12 protein, molecules critically involved in apoptosis, were found to be increased and restricted in the ganglion cell layer. They also reported that the intraperitoneal injection of the drug TUDCA ameliorated levels of all these molecules, as well as DR-associated dysfunctions (Yang et al., 2013). Using the transformed mouse RGC cell line (mRGC), Zhang et al. (2018) demonstrated that ganglion cell apoptosis in the context of DR was mediated by PERK pathways activation through ATF4 and CHOP, which is ameliorated by a Chinese herbal medicine He-Ying-Qing-Re Herbal Formula (HF).

SUMMARY AND CONCLUSION

Although the pathogenesis of DR is extremely involved, it is becoming clearer that the UPR can either protect the diabetic retina from retinopathy or promote it to the initiation, progression, and aggravation of retinopathy. Early events of DR pathogenesis include gliosis of MCs, apoptosis/degeneration of vascular (pericytes), and neuronal (ganglion) cells, precipitating vascular abnormalities. Research in the field of DR has provided a body of evidence indicating the activation of the UPR pathways in most of the retinal cells. In the RMECs and RPE cells, DR condition-exposed increased VEGF and cytokine expressions are reported to be mediated by the PERK and IRE1 pathways of UPR. Moreover, diabetic-mimetic conditions mediated RGC and pericytes cell death are demonstrated to be medicated by the PERK pathways through CHOP and ATF4. Furthermore, all three pathways of UPR are reported to be necessary for VEGF and cytokines mediated MCs activation. Additionally, several chemical and herbal drugs were reported to ameliorate diabetic-mimetic condition-induced UPR activation and DR development.

However, it is not clear how different pathways of UPR in different types of the cells are temporally and spatially interrelated and altered in the neurovascular unit of the retina during diabetes. Published studies suggest that the early activation of UPR in the glial cells, such as MCs, triggers the proinflammatory and/or proangiogenic pathways in an oxidative stress-dependent manner resulting in the expression and secretion of various neurodegenerative, proinflammatory, and proangiogenic growth factors, cytokines, and chemokines, which, in turn, lead to vascular abnormalities observed in PDR (**Figure 2**). Additional studies are needed for deeper understanding and determining the best preventive and therapeutic target of DR in the UPR pathways.

AUTHOR CONTRIBUTIONS

KA conceived and designed the work, analyzed the published data, wrote, critically reviewed and revised the manuscript. YA analyzed the published data, critically reviewed and revised the manuscript. Both authors contributed to the article and approved the submitted version.

REFERENCES

Adachi, T., Teramachi, M., Yasuda, H., Kamiya, T., and Hara, H. (2012). Contribution of p38 MAPK, NF-κB and glucocorticoid signaling pathways to ER stress-induced increase in retinal endothelial permeability. *Arch. Biochem. Biophys.* 520, 30–35. doi: 10.1016/j.abb.2012.01.014

Adachi, T., Yasuda, H., Nakamura, S., Kamiya, T., Hara, H., Hara, H., et al. (2011). Endoplasmic reticulum stress induces retinal endothelial permeability of extracellular-superoxide dismutase. *Free Radic. Res.* 45, 1083–1092. doi: 10.3109/10715762.2011.595408

Ahmad, I., del Debbio, C. B., Das, A. V., and Parameswaran, S. (2011). Müller glia: a promising target for therapeutic regeneration. *Invest. Ophthalmol. Vis. Sci.* 52, 5758–5764. doi: 10.1167/iovs.11-7308

Alarcon-Martinez, L., Villafranca-Baughman, D., Quintero, H., Kacerovsky, J. B., Dotigny, F., Murai, K. K., et al. (2020). Interpericyte tunnelling nanotubes regulate neurovascular coupling. *Nature* 585, 91–95. doi: 10.1038/s41586-020-2589-x

Antonetti, D. A., Klein, R., and Gardner, T. W. (2012). Diabetic retinopathy. *N. Engl. J. Med.* 366, 1227–1239. doi: 10.1056/NEJMra1005073

Barber, A. J., Lieth, E., Khin, S. A., Antonetti, D. A., Buchanan, A. G., and Gardner, T. W. (1998). Neural apoptosis in the retina during experimental and human diabetes: early onset and effect of insulin. *J. Clin. Invest.* 102, 783–791. doi: 10.1172/JCI2425

Bertolotti, A., Zhang, Y., Hendershot, L. M., Harding, H. P., and Ron, D. (2000). Dynamic interaction of BiP and ER stress transducers in the unfolded-protein response. *Nat. Cell Biol.* 2, 326–332. doi: 10.1038/35014014

Blais, J. D., Filipenko, V., Bi, M., Harding, H. P., Ron, D., Koumenis, C., et al. (2004). Activating transcription factor 4 is translationally regulated by hypoxic stress. *Mol. Cell. Biol.* 24, 7469–7482. doi: 10.1128/MCB.24.17.7469-7482.2004

Bringmann, A., Iandiev, I., Pannicke, T., Wurm, A., Hollborn, M., Wiedemann, P., et al. (2009). Cellular signaling and factors involved in Müller cell gliosis: neuroprotective and detrimental effects. *Prog. Retin. Eye Res.* 28, 423–451. doi: 10.1016/j.preteyeres.2009.07.001

Chan, P. S., Kanwar, M., and Kowluru, R. A. (2010). Resistance of retinal inflammatory mediators to suppress after reinstitution of good glycemic control: novel mechanism for metabolic memory. *J. Diabetes Complications* 24, 55–63. doi: 10.1016/j.jdiacomp.2008.10.002

Chan-Ling, T. (1994). Glial, neuronal and vascular interactions in the mammalian retina. *Prog. Retin. Eye Res.* 51, 1–40. doi: 10.1016/j.preteyeres.2015.06.003

Chang, K. C., Snow, A., Labarbera, D. V., and Petrash, J. M. (2015). Aldose reductase inhibition alleviates hyperglycemic effects on human retinal pigment epithelial cells. *Chem. Biol. Interact.* 234, 254–260. doi: 10.1016/j.cbi.2014.10.007

Chen, Y., Wang, J. J., Li, J., Hosoya, K. I., Ratan, R., Townes, T., et al. (2012). Activating transcription factor 4 mediates hyperglycaemia-induced endothelial inflammation and retinal vascular leakage through activation of STAT3 in a mouse model of type 1 diabetes. *Diabetologia* 55, 2533–2545. doi: 10.1007/s00125-012-2594-1

Chung, Y. R., Choi, J. A., Koh, J. Y., and Yoon, Y. H. (2017). Ursodeoxycholic acid attenuates endoplasmic reticulum stress-related retinal pericyte loss in streptozotocin-induced diabetic mice. *J. Diabetes Res.* 2017:1763292. doi: 10.1155/2017/1763292

Cunha-Vaz, J., Bernardes, R., and Lobo, C. (2011). Blood-retinal barrier. *Eur. J. Ophthalmol.* 21, S3–S9. doi: 10.5301/EJO.2010.6049

Du, M., Wu, M., Fu, D., Yang, S., Chen, J., Wilson, K., et al. (2013). Effects of modified LDL and HDL on retinal pigment epithelial cells: a role in diabetic retinopathy? *Diabetologia* 56, 2318–2328. doi: 10.1007/s00125-013-2986-x

Feit-Leichman, R. A., Kinouchi, R., Takeda, M., Fan, Z., Mohr, S., Kern, T. S., et al. (2005). Vascular damage in a mouse model of diabetic retinopathy: relation to neuronal and glial changes. *Invest. Ophthalmol. Vis. Sci.* 46, 4281–4287. doi: 10.1167/iovs.04-1361

Fu, D., Yu, J. Y., Wu, M., Du, M., Chen, Y., Abdelsamie, S. A., et al. (2014). Immune complex formation in human diabetic retina enhances toxicity of oxidized LDL towards retinal capillary pericytes. *J. Lipid Res.* 55, 860–869. doi: 10.1194/jlr.M045401

Grootjans, J., Kaser, A., Kaufman, R. J., and Blumberg, R. S. (2016). The unfolded protein response in immunity and inflammation. *Nat. Rev. Immunol.* 16, 469–484. doi: 10.1038/nri.2016.62

Ha, J. H., Shil, P. K., Zhu, P., Gu, L., Li, Q., and Chung, S. (2014). Ocular inflammation and endoplasmic reticulum stress are attenuated by supplementation with grape polyphenols in human retinal pigmented epithelium cells and in C57BL/6 mice. *J. Nutr.* 144, 799–806. doi: 10.3945/jn.113.186957

Hammes, H. P., Lin, J., Renner, O., Shani, M., Lundqvist, A., Betsholtz, C., et al. (2002). Pericytes and the pathogenesis of diabetic retinopathy. *Diabetes* 51, 3107–3112. doi: 10.2337/diabetes.51.10.3107

Hetz, C., Chevet, E., and Harding, H. P. (2013). Targeting the unfolded protein response in disease. *Nat. Rev. Drug Discov.* 12, 703–719. doi: 10.1038/nrd3976

Hetz, C., and Saxena, S. (2017). ER stress and the unfolded protein response in neurodegeneration. *Nat. Rev. Neurol.* 13, 477–491. doi: 10.1038/nrneurol.2017.99

Hollien, J., and Weissman, J. S. (2006). Decay of endoplasmic reticulum-localized mRNAs during the unfolded protein response. *Science* 313, 104–107. doi: 10.1126/science.1129631

Hotamisligil, G. S. (2010). Endoplasmic reticulum stress and the inflammatory basis of metabolic disease. *Cell* 140, 900–917. doi: 10.1016/j.cell.2010.02.034

Ikesugi, K., Mulhern, M. L., Madson, C. J., Hosoya, K. I., Terasaki, T., Kador, P. F., et al. (2006). Induction of endoplasmic reticulum stress in retinal pericytes by glucose deprivation. *Curr. Eye Res.* 31, 947–953. doi: 10.1080/02713680600966785

Jenkins, A. J., Joglekar, M. V., Hardikar, A. A., Keech, A. C., O'Neal, D. N., and Januszewski, A. S. (2015). Biomarkers in diabetic retinopathy. *Rev. Diabet. Stud.* 12, 159–195. doi: 10.1900/RDS.2015.12.159

Kang, M. K., Lee, E. J., Kim, Y. H., Kim, D. Y., Oh, H., Kim, S.-I., et al. (2018). Chrysin ameliorates malfunction of retinoid visual cycle through blocking activation of age-rage-er stress in glucose-stimulated retinal pigment epithelial cells and diabetic eyes. *Nutrients* 10:1046. doi: 10.3390/nu10081046

Kern, T. S., and Barber, A. J. (2008). Retinal ganglion cells in diabetes. *J. Physiol.* 586, 4401–4408. doi: 10.1113/jphysiol.2008.156695

Kim, J. H., Kim, J. H., Park, J. A., Lee, S.-W., Kim, W. J., Yu, Y. S., et al. (2006). Blood-neural barrier: intercellular communication at glio-vascular interface. *J. Biochem. Mol. Biol.* 39, 339–345. doi: 10.5483/bmbrep.2006.39.4.339

Kirber, W. M., Nichols, C. W., Grimes, P. A., Winegrad, A. I., and Laties, A. M. (1980). A permeability defect of the retinal pigment epithelium: occurrence in early streptozocin diabetes. *Arch. Ophthalmol.* 98, 725–728. doi: 10.1001/archopht.1980.01020030719015

Klaassen, I., Hughes, J. M., Vogels, I. M. C., Schalkwijk, C. G., Van Noorden, C. J. F., and Schlingemann, R. O. (2009). Altered expression of genes related to blood-retina barrier disruption in streptozotocin-induced diabetes. *Exp. Eye Res.* 89, 4–15. doi: 10.1016/j.exer.2009.01.006

Kochan, T., Singla, A., Tosi, J., and Kumar, A. (2012). Toll-like receptor 2 ligand pretreatment attenuates retinal microglial inflammatory response but enhances phagocytic activity toward *Staphylococcus aureus*. *Infect. Immun.* 80, 2076–2088. doi: 10.1128/IAI.00149-12

Kowluru, R. A., Kanwar, M., and Kennedy, A. (2007). Metabolic memory phenomenon and accumulation of peroxynitrite in retinal capillaries. *Exp. Diabetes Res.* 2007:21976. doi: 10.1155/2007/21976

Kroeger, H., Chiang, W. C., Felden, J., Nguyen, A., and Lin, J. H. (2019). ER stress and unfolded protein response in ocular health and disease. *FEBS J.* 286, 399–412. doi: 10.1111/febs.14522

Lee, A.-H., Iwakoshi, N. N., and Glimcher, L. H. (2003). XBP-1 regulates a subset of endoplasmic reticulum resident chaperone genes in the unfolded protein response. *Mol. Cell. Biol.* 23, 7448–7459. doi: 10.1128/mcb.23.21.7448-7459.2003

Lenin, R., Nagy, P. G., Alli, S., Rao, V. R., Clauss, M. A., Kompella, U. B., et al. (2018). Critical role of endoplasmic reticulum stress in chronic endothelial activation-induced visual deficits in tie2-tumor necrosis factor mice. *J. Cell. Biochem.* 119, 8460–8471. doi: 10.1002/jcb.27072

Li, J., Wang, J. J., Yu, Q., Wang, M., and Zhang, S. X. (2009). Endoplasmic reticulum stress is implicated in retinal inflammation and diabetic retinopathy. *FEBS Lett.* 583, 1521–1527. doi: 10.1016/j.febslet.2009.04.007

Li, Q., Zemel, E., Miller, B., and Perlman, I. (2002). Early retinal damage in experimental diabetes: electroretinographical and morphological observations. *Exp. Eye Res.* 74, 615–625. doi: 10.1006/exer.2002.1170

Liu, L., Qi, X., Chen, Z., Shaw, L., Cai, J., Smith, L. H., et al. (2013). Targeting the IRE1α/XBP1 and ATF6 arms of the unfolded protein response enhance VEGF blockade to prevent retinal and choroidal neovascularization. *Am. J. Pathol.* 182, 1412–1424. doi: 10.1016/j.ajpath.2012.12.020

Lopes-Virella, M. F., Jenkins, A. J., Baker, N. L., Virella, G., Hunt, K. J., and Lyons, T. J. (2012). High concentrations of AGE-LDL and oxidized LDL in circulating immune complexes are associated with progression of retinopathy in type 1 diabetes. *Diabetes Care* 35, 1333–1340. doi: 10.2337/dc11-2040

Makita, J., Hosoya, K. I., Zhang, P., and Kador, P. F. (2011). Response of rat retinal capillary pericytes and endothelial cells to glucose. *J. Ocul. Pharmacol. Ther.* 27, 7–15. doi: 10.1089/jop.2010.0051

Mandarino, L. J. (1992). Current hypotheses for the biochemical basis of diabetic retinopathy. *Diabetes Care* 15, 1892–1901. doi: 10.2337/diacare.15.12.1892

Martin, P. M., Roon, P., Van Ells, T. K., Ganapathy, V., and Smith, S. B. (2004). Death of retinal neurons in streptozotocin-induced diabetic mice. *Invest. Ophthalmol. Vis. Sci.* 45, 3330–3336. doi: 10.1167/iovs.04-0247

Maugh, T. H. (1976). Diabetic retinopathy: new ways to prevent blindness. *Science* 192, 539–540. doi: 10.1126/science.192.4239.539

Metea, M. R., and Newman, E. A. (2007). Signalling within the neurovascular unit in the mammalian retina. *Exp. Physiol.* 92, 635–640. doi: 10.1113/expphysiol.2006.036376

Miranda, S., González-Rodríguez, á., García-Ramírez, M., Revuelta-Cervantes, J., Hernández, C., Simó, R., et al. (2012). Beneficial effects of fenofibrate in retinal pigment epithelium by the modulation of stress and survival signaling under diabetic conditions. *J. Cell. Physiol.* 227, 2352–2362. doi: 10.1002/jcp.22970

Mori, K. (2009). Signalling pathways in the unfolded protein response: development from yeast to mammals. *J. Biochem* 146, 743–750. doi: 10.1093/jb/mvp166

Newman, E., and Reichenbach, A. (1996). The Muller cell: a functional element of the retina. *Trends Neurosci.* 19, 307–312. doi: 10.1016/0166-2236(96)10040-0

Oshitari, T., Yamamoto, S., Hata, N., and Roy, S. (2008). Mitochondria- and caspase-dependent cell death pathway involved in neuronal degeneration in diabetic retinopathy. *Br. J. Ophthalmol.* 92, 552–556. doi: 10.1136/bjo.2007.132308

Oshitari, T., Yoshida-Hata, N., and Yamamoto, S. (2011). Effect of neurotrophin-4 on endoplasmic reticulum stress-related neuronal apoptosis in diabetic and high glucose exposed rat retinas. *Neurosci. Lett.* 501, 102–106. doi: 10.1016/j.neulet.2011.06.057

Peng, Q. H., Tong, P., Gu, L. M., and Li, W. J. (2020). Astragalus polysaccharide attenuates metabolic memory-triggered ER stress and apoptosis *via* regulation of miR-204/SIRT1 axis in retinal pigment epithelial cells. *Biosci. Rep.* 40:BSR20192121. doi: 10.1042/BSR20192121

Phipps, J. A., Yee, P., Fletcher, E. L., and Vingrys, A. J. (2006). Rod photoreceptor dysfunction in diabetes: activation, deactivation and dark adaptation. *Invest. Ophthalmol. Vis. Sci.* 47, 3187–3194. doi: 10.1167/iovs.05-1493

Rao, R. V., Ellerby, H. M., and Bredesen, D. E. (2004). Coupling endoplasmic reticulum stress to the cell death program. *Cell Death Differ.* 11, 372–380. doi: 10.1038/sj.cdd.4401378

Reichenbach, A., and Bringmann, A. (2013). New functions of Müller cells. *Glia* 61, 651–678. doi: 10.1002/glia.22477

Reichenbach, A., Stolzenburg, J. U., Eberhardt, W., Chao, T. I., Dettmer, D., and Hertz, L. (1993). What do retinal Müller (glial) cells do for their neuronal "small siblings"? *J. Chem. Neuroanat.* 6, 201–213. doi: 10.1016/0891-0618(93)90042-3

Ron, D., and Walter, P. (2007). Signal integration in the endoplasmic reticulum unfolded protein response. *Nat. Rev. Mol. Cell Biol.* 8, 519–529. doi: 10.1038/nrm2199

Rozpedek, W., Pytel, D., Mucha, B., Leszczynska, H., Diehl, J. A., and Majsterek, I. (2016). The role of the PERK/eIF2α/ATF4/CHOP signaling pathway in tumor progression during endoplasmic reticulum stress. *Curr. Mol. Med.* 16, 533–544. doi: 10.2174/1566524016666160523143937

Roy, S., Trudeau, K., Roy, S., Tien, T., and Barrette, K. F. (2013). Mitochondrial dysfunction and endoplasmic reticulum stress in diabetic retinopathy: mechanistic insights into high glucose-induced retinal cell death. *Curr. Clin. Pharmacol.* 8, 278–284. doi: 10.2174/1574884711308040003

Roybal, C. N., Yang, S., Sun, C. W., Hurtado, D., Vander Jagt, D. L., Townes, T. M., et al. (2004). Homocysteine increases the expression of vascular endothelial growth factor by a mechanism involving endoplasmic reticulum stress and transcription factor ATF4. *J. Biol. Chem.* 279, 14844–14852. doi: 10.1074/jbc.M312948200

Salminen, A., Kauppinen, A., Hyttinen, J. M. T., Toropainen, E., and Kaarniranta, K. (2010). Endoplasmic reticulum stress in age-related macular degeneration: trigger for neovascularization. *Mol. Med.* 16, 535–542. doi: 10.2119/molmed.2010.00070

Santos, J. M., and Kowluru, R. A. (2011). Role of mitochondria biogenesis in the metabolic memory associated with the continued progression of diabetic retinopathy and its regulation by lipoic acid. *Invest. Ophthalmol. Vis. Sci.* 52, 8791–8798. doi: 10.1167/iovs.11-8203

Shirao, Y., and Kawasaki, K. (1998). Electrical responses from diabetic retina. *Prog. Retin. Eye Res.* 17, 59–76. doi: 10.1016/s1350-9462(97)00005-0

Simó, R., and Hernández, C. (2014). Neurodegeneration in the diabetic eye: new insights and therapeutic perspectives. *Trends Endocrinol. Metab.* 25, 23–33. doi: 10.1016/j.tem.2013.09.005

Simó, R., Villarroel, M., Corraliza, L., Hernández, C., and Garcia-Ramírez, M. (2010). The retinal pigment epithelium: something more than a constituent of the blood-retinal barrier-implications for the pathogenesis of diabetic retinopathy. *J. Biomed. Biotechnol.* 2010:190724. doi: 10.1155/2010/190724

Strauss, O. (2005). The retinal pigment epithelium in visual function. *Physiol. Rev.* 85, 845–881. doi: 10.1152/physrev.00021.2004

Tabas, I., and Ron, D. (2011). Integrating the mechanisms of apoptosis induced by endoplasmic reticulum stress. *Nat. Cell Biol.* 13, 184–190. doi: 10.1038/ncb0311-184

Vinores, S. A., Gadegbeku, C., Campochiaro, P. A., and Green, W. R. (1989). Immunohistochemical localization of blood-retinal barrier breakdown in human diabetics. *Am. J. Pathol.* 134, 231–235.

Walter, P., and Ron, D. (2011). The unfolded protein response: from stress pathway to homeostatic regulation. *Science* 334, 1081–1086. doi: 10.1126/science.1209038

Wang, M., and Kaufman, R. J. (2016). Protein misfolding in the endoplasmic reticulum as a conduit to human disease. *Nature* 529, 326–335. doi: 10.1038/nature17041

Wong, V. H. Y., Vingrys, A. J., and Bui, B. V. (2011). Glial and neuronal dysfunction in streptozotocin-induced diabetic rats. *J. Ocul. Biol. Dis. Infor.* 4, 42–50. doi: 10.1007/s12177-011-9069-3

Wu, S., Zhu, X., Guo, B., Zheng, T., Ren, J., Zeng, W., et al. (2019). Unfolded protein response pathways correlatively modulate endoplasmic reticulum stress responses in rat retinal Müller cells. *J. Ophthalmol.* 2019:9028483. doi: 10.1155/2019/9028483

Xu, H., and Le, Y. (2011). Significance of outer blood–retina barrier breakdown in diabetes and ischemia. *Invest. Ophthalmol. Vis. Sci.* 52, 2160–2164. doi: 10.1167/iovs.10-6518

Yang, J., Chen, C., McLaughlin, T., Wang, Y., Le, Y. Z., Wang, J. J., et al. (2019). Loss of X-box binding protein 1 in Müller cells augments retinal inflammation in a mouse model of diabetes. *Diabetologia* 62, 531–543. doi: 10.1007/s00125-018-4776-y

Yang, Z., Stratton, C., Francis, P. J., Kleinman, M. E., Tan, P. L., Gibbs, D., et al. (2008). Toll-like receptor 3 and geographic atrophy in age-related macular degeneration. *N. Engl. J. Med.* 359, 1456–1463. doi: 10.1056/NEJMoa0802437

Yang, L. P., Wu, L. M., Wang, D. M., Li, Y., Dou, H. L., Tso, M. O. M., et al. (2013). Role of endoplasmic reticulum stress in the loss of retinal ganglion cells in diabetic retinopathy. *Neural Regen. Res.* 8, 3148–3158. doi: 10.3969/j.issn.1673-5374.2013.33.009

Zahs, K. R., and Ceelen, P. W. (2006). Gap junctional coupling and connexin immunoreactivity in rabbit retinal glia. *Visual Neuroscience* 23, 1–10. doi: 10.1017/S0952523806231018

Zahs, K. R., Kofuji, P., Meier, C., and Dermietzel, R. (2003). Connexin immunoreactivity in glial cells of the rat retina. *J. Comp. Neurol.* 455, 531–546. doi: 10.1002/cne.10524

Zhang, K., and Kaufman, R. J. (2008). From endoplasmic-reticulum stress to the inflammatory response. *Nature* 454, 455–462. doi: 10.1038/nature07203

Zhang, S. X., Ma, J. H., Bhatta, M., Fliesler, S. J., and Wang, J. J. (2015). The unfolded protein response in retinal vascular diseases: implications and therapeutic potential beyond protein folding. *Prog. Retin. Eye Res.* 45, 111–131. doi: 10.1016/j.preteyeres.2014.12.001

Zhang, C., Xu, Y., Tan, H. Y., Li, S., Wang, N., Zhang, Y., et al. (2018). Neuroprotective effect of He-Ying-Qing-Re formula on retinal ganglion cell in diabetic retinopathy. *J. Ethnopharmacol.* 214, 179–189. doi: 10.1016/j.jep.2017.12.018

Zhao, M., Bousquet, E., Valamanesh, F., Farman, N., Jeanny, J. C., Jaisser, F., et al. (2011). Differential regulations of AQP4 and Kir4.1 by triamcinolone acetonide and dexamethasone in the healthy and inflamed retina. *Invest. Ophthalmol. Vis. Sci.* 52, 6340–6347. doi: 10.1167/iovs.11-7675

Zhao, M., Valamanesh, F., Celerier, I., Savoldelli, M., Jonet, L., Jeanny, J., et al. (2010). The neuroretina is a novel mineralocorticoid target: aldosterone

up–regulates ion and water channels in Müller glial cells. *FASEB J.* 24, 3405–3415. doi: 10.1096/fj.09-154344

Zhong, Y., Li, J., Chen, Y., Wang, J. J., Ratan, R., and Zhang, S. X. (2012a). Activation of endoplasmic reticulum stress by hyperglycemia is essential for Müller cell-derived inflammatory cytokine production in diabetes. *Diabetes* 61, 492–504. doi: 10.1016/j.bja.2019.03.040

Zhong, Y., Wang, J. J., and Zhang, S. X. (2012b). Intermittent but not constant high glucose induces ER stress and inflammation in human retinal pericytes. *Adv. Exp. Med. Biol.* 723, 285–292. doi: 10.1007/978-1-4614-0631-0_37

Conflict of Interest: The authors declare that the research was conducted in the absence of any commercial or financial relationships that could be construed as a potential conflict of interest.

frontiers in Cellular Neuroscience

ORIGINAL RESEARCH
published: 05 February 2021
doi: 10.3389/fncel.2021.617308

Brain Metabolite, N-Acetylaspartate Is a Potent Protein Aggregation Inhibitor

Marina Warepam[1†], Awdhesh Kumar Mishra[2†], Gurumayum Suraj Sharma[3], Kritika Kumari[4], Snigdha Krishna[4], Mohd Sajjad Ahmad Khan[5], Hamidur Rahman[1] and Laishram Rajendrakumar Singh[4]*

[1] Department of Biotechnology, Manipur University, Manipur, India, [2] Department of Biotechnology, Yeungnam University, Gyeongsan-si, South Korea, [3] Department of Botany, Bhaskaracharya College of Applied Sciences, University of Delhi, New Delhi, India, [4] Dr. B. R. Ambedkar Center for Biomedical Research, University of Delhi, New Delhi, India, [5] Department of Basic Sciences, Deanship of Preparatory Year and Supporting Studies, Imam Abdulrahman Bin Faisal University, Dammam, Saudi Arabia

Deposition of toxic protein inclusions is a common hallmark of many neurodegenerative disorders including Alzheimer's disease, Parkinson disease etc. N-acetylaspartate (NAA) is an important brain metabolite whose levels got altered under various neurodegenerative conditions. Indeed, NAA has been a widely accepted biological marker for various neurological disorders. We have also reported that NAA is a protein stabilizer. In the present communication, we investigated the role of NAA in modulating the aggregation propensity on two model proteins (carbonic anhydrase and catalase). We discovered that NAA suppresses protein aggregation and could solubilize preformed aggregates.

Keywords: protein aggregation, light scattering, protein stability, protein denaturation, neurological disorders

OPEN ACCESS

Edited by:
Rinki Minakshi, Swami Shraddhanand College, University of Delhi, India

Reviewed by:
Hiroaki Kaku, Western Michigan University, United States
Gulam Rabbani, Yeungnam University, South Korea

***Correspondence:**
Laishram Rajendrakumar Singh
lairksingh@gmail.com

[†] These authors have contributed equally to this work

Specialty section:
This article was submitted to Cellular Neuropathology, a section of the journal Frontiers in Cellular Neuroscience

Received: *22 October 2020*
Accepted: *08 January 2021*
Published: *05 February 2021*

Citation:
Warepam M, Mishra AK, Sharma GS, Kumari K, Krishna S, Khan MSA, Rahman H and Singh LR (2021) Brain Metabolite, N-Acetylaspartate Is a Potent Protein Aggregation Inhibitor. Front. Cell. Neurosci. 15:617308. doi: 10.3389/fncel.2021.617308

INTRODUCTION

The amino acid, N-acetylaspartate (NAA) is synthesized in the brain from aspartate and acetyl-coenzyme A by the enzyme L-aspartate N-acetyltransferase via acetylation of aspartate by acetyl coenzyme A. On the other hand, it is also catabolized by the enzyme, aspartoacylase (Birnbaum et al., 1952; Goldstein, 1959; Knizley, 1967; Truckenmiller et al., 1985). NAA is found at exceptionally high concentrations in various regions of the brain and can attain up to 10 mM or more (Miyake et al., 1981; Blüml, 1999; Pan and Takahashi, 2005), making it the most concentrated amino acid in brain. The exact functional role of NAA in neurons and its significance of high concentrations have not been known. However, evidences indicate that NAA is an important precursor of the neuropeptide, N-acetylaspartylglutamate (NAAG) (Moffett et al., 2007). Other proposed cellular roles of NAA include osmoregulation of neuronal cells and axon-glial signaling, maintenance of nitrogen balance in brain, basic source of acetate required for myelin lipid biosynthesis in oligodendrocytes, and facilitation of energy metabolism in neuronal mitochondria etc. (Taylor et al., 1995; Clark, 1998; Baslow, 2003; Baslow et al., 2003; Madhavarao et al., 2005; Moffett et al., 2007). NAA is also a significant brain specific biomarker (Rael et al., 2004). The reduction in NAA (obtained from magnetic resonance spectroscopy, MRS of NAA) level has been used as an index of the extent of brain injury following a traumatic injury (Danielsen and Ross, 1999). Almost all neurological disorders involving neuronal loss or dysfunction (e.g., including amyotrophic lateral sclerosis, alzheimers, multiple sclerosis, epilepsy, schizophrenia,

cerebral ischemia, and glioblastoma) are associated with alterations in NAA levels (Paley et al., 1996; Danielsen and Ross, 1999; Kantarci and Jack, 2003; Kalra and Arnold, 2004; Briellmann et al., 2005; Abbott and Bustillo, 2006; Criste and Trapp, 2006). Altered level of NAA is also associated with two inborn error of metabolism namely, Canavan disease (CD), in which there is a build-up of NAA (hyperacetylaspartia) and spongiform leukodystrophy (hypoacetylaspartia), caused due to the lack of aspartoacylase activity, where the enzyme that synthesizes NAA is apparently absent (Burlina et al., 1994; Boltshauser et al., 2004).

It has been known from various studies that NAA is an osmolyte in the brain cells responsible for the removal of water from neurons (Taylor et al., 1994, 1995). Most recently, our laboratory also reported that NAA exhibit strong stabilizing effect on different proteins (due to increase in T_m and ΔG_D°) (Warepam et al., 2020). Furthermore as mentioned above, there is alteration in the NAA levels under various neurodegenerative conditions. Since various neurodegenerative conditions are associated with toxic protein inclusions (which are in fact, aggregates, high order oligomers or amyloidogenic species), we thought, NAA could be a modulator of protein aggregation or proteopathic conditions. To address this issue, we have initiated our study on two different proteins (carbonic anhydrase, CA, and catalase), whose folding and aggregation pathways are well-known. We discovered that NAA is a potential inhibitor of protein aggregation. The results indicate that cellular overexpression or treatment of affected brain region with NAA can prevent brain cells from deposition of toxic protein inclusions.

MATERIALS AND METHODS

Materials

Commercially lyophilized CA (catalog number C2624) and catalase (C9322) were purchased from Sigma. NAA was also obtained from the Sigma. Urea was purchased from MP Biomedicals. These chemicals were used without further purification as they are of analytical grade.

Methods

Preparation of Protein Stock Solutions and Determination of Concentrations

CA and catalase solutions were dialyzed extensively against 0.1 M KCl at pH 7.0 and 4°C. The dialyzed protein stock solutions were filtered using 0.22 μm millipore syringe filter. A single protein band during polyacrylamide gel electrophoresis was obtained for both the proteins. Concentration of carbonic anhydrase and catalase solutions were determined experimentally using molar absorption coefficient, ε (M^{-1} cm^{-1}) value of 57,000 at 280 nm for CA (Yazdanparast et al., 2005) and 3.24×10^5 at 405 nm for catalase (Haber et al., 1993). For optical measurements all the proteins and buffer solutions were prepared in degassed double distilled water containing 0.1 M KCl. pH of the protein solutions remained similar even after addition of NAA.

Protein Aggregation Studies for CA and Catalase

CA (0.1 mg/ml in 0.05 M potassium phosphate buffer pH 7.0) was incubated overnight in presence of various concentrations of NAA at room temperature. Catalase (0.2 mg/ml) was also incubated with NAA for 1 h. Then, aggregation profiles were monitored by measuring the change in the light scattering intensity (at 500 nm) at 63°C for 15 min using Jasco V-660 UV/Vis spectrophotometer equipped with a Peltier type controller (ETCS-761) (for CA) and at 55°C for 70 min using Cary Eclipse Fluorescence Spectrophotometer (equipped with a single cell peltier) (for catalase). The measurements were carried out for at least three times. Kinetic parameters (lag time, k_{app} and I_f) of CA and catalase aggregation were analyzed using the equation:

$$I = I_o + \frac{I_f}{1 + e^{-\left(\frac{t-t_o}{b}\right)}} \quad (1)$$

where I is the light scattering intensity at time t, and t_o is the time at 50% maximal light scattering, I_o and I_f represent the initial base line and final plateau line, respectively, b is a constant. Thus, the apparent rate constant, k_{app} for the formation of aggregates is given by $1/b$ and the lag time is given by t_o-$2b$ (Nielsen et al., 2001). Each curve was independently analyzed for the respective kinetic parameters and mean was calculated. The deviations (standard error) from the mean was then analyzed.

Transmission Electron Microscopy (TEM) of Carbonic Anhydrase

Protein samples incubated at 63°C in the presence and absence of NAA (1 M) were pelleted. Pelleted samples (10 μl) were placed on a copper grid and were air dried for 5–10 min. For negative staining of the samples, 1% of uranyl acetate solution was added on to the copper grid and again allowed to air dried. Samples were then examined under FEI Tecnai G2-200 kV HRTA transmission electron microscopy operating at 200 kV.

Temperature-Dependent Aggregation Studies

Temperature dependent aggregation of CA was monitored by measuring the change in the light scattering intensity at 500 nm using Jasco V-660 UV/Vis spectrophotometer equipped with a Peltier type controller (ETCS-761) with a heating rate of 1°C/min. This scan rate was found to provide adequate time for equilibration. Each sample was heated from 20 to 80°C. The measurements were repeated for three times. The temperature dependent aggregation curve of carbonic anhydrase was analyzed using the following empirical equation (Senisterra et al., 2006, 2010):

$$I = \frac{I_f}{1 + e^{\left[\frac{T_{agg}-T}{b}\right]}} \quad (2)$$

where I is the light scattering intensity at temperature T, I_f is the limiting value of light scattering at higher temperatures. T_{agg} is the temperature corresponding to the middle point of the transition, i.e., a temperature at which $I = I_f/2$ and b is constant. Each curve was independently analyzed for the

respective aggregation parameters and mean was calculated. The deviations (standard error) from the mean was then analyzed.

Urea-Induced Denaturation Measurements

Urea-induced denaturation of CA (0.125 μM) in presence and absence of NAA were followed by measuring changes at 355 nm as a function of urea concentration using Perkin Elmer-LS 55. Protein solutions at each urea concentration were kept for 6 h to allow equilibration. The optical transition data were converted into ΔG_D, Gibbs energy change using the equation:

$$\Delta G_D = -RTln\{(y - y_N)/(y_D - y)\} \quad (3)$$

where R is the universal gas constant, T is the temperature in Kelvin, y is the observed optical property and y_N and y_D are, respectively, the optical properties of the native and denatured protein molecules under the same experimental condition in which y has been determined. We then use linear extrapolation method for the analysis of ΔG_D° (Pace, 1975; Santoro and Bolen, 1988), using the following equation:

$$\Delta G_D = \Delta G_D^\circ - m_d[\text{GdmCl}], \quad (4)$$

where ΔG_D° is the value of ΔG_D at 0 M denaturant, and m_d gives the linear dependence of ΔG_D on the [Urea]. Each curve was independently analyzed for the respective thermodynamic parameters and mean was calculated. The deviations (standard error) from the mean was then analyzed.

Structural Measurements

Near-UV CD spectra of native state of CA were measured in the presence and absence of NAA at least three times in a J-810 (Jasco spectropolarimeter) equipped with a Peltier-type temperature controller (Jasco PTC-424S). Necessary subtraction for the contribution of blank from each spectrum of protein was performed. Protein concentration used was 0.5 mg/ml. The path length of the cuvette used was 10 mm. Routinely calibration of the CD instrument was done with D-10-camphorsulfonic acid.

Intrinsic fluorescence of carbonic anhydrase was measured in a Perkin Elmer-LS 55 at least for three times in absence and presence of NAA. Protein concentration used was 3 μM. The excitation wavelength was 297 nm. Necessary blank subtraction was made.

AC (0.1 mg/ml) was titrated with the desired concentrations of NAA and incubated overnight at room temperature. ANS (16-fold molar excess over CA concentration) is added on each CA samples and then incubated at 63°C for 15 min for equilibration. The fluorescence spectra of CA aggregates formed in the presence and absence of NAA were recorded from 380 to 600 nm with an excitation wavelength of 345 nm on a Perkin Elmer-LS 55 (Fluorescence spectrometer) using a quartz cuvette of 5 mm path length. All necessary background corrections were made. The measurements were carried out for at least three times.

Reversal of Protein Aggregation

Aggregation of CA was carried out at 63°C using a heating block (Indogenix) for 15 min in the absence of NAA. Light scattering intensity (at 500 nm) at 63°C was measured immediately after addition of NAA using UV-visible spectrophotometer. All necessary subtraction of blank solutions was made.

TABLE 1 | Kinetic parameters of CA aggregation in the absence and presence of NAA.

	Concentration (M)	Lag time (min)	$k_{app(min^{-1})}$	I_f
NAA	0.00	2.9 ± 0.16	1.63 ± 0.09	0.94 ± 0.05
	0.25	3.2 ± 0.17	1.46 ± 0.08	0.86 ± 0.05
	0.50	3.5 ± 0.17	0.95 ± 0.06	0.69 ± 0.05
	0.75	3.7 ± 0.19	0.55 ± 0.04	0.49 ± 0.04
	1.00	4.1 ± 0.24	0.45 ± 0.03	0.33 ± 0.03

"±" represents standard error of three independent measurements.

RESULTS

NAA Affects the Aggregation Kinetics of CA and Catalase

To investigate the effect of NAA on protein aggregation process, we have chosen CA as its folding behavior and aggregation kinetics have been extensively studied (Kundu and Guptasarma, 2002; Rana et al., 2008). A high content of β-sheet and a single domain structure protein make it highly prone to aggregate at an unfolding temperature of 63°C (Lavecchia and Zugaro, 1991; Sarraf et al., 2004). To study the effect of NAA on the aggregation of CA, we monitored the kinetic processes of CA aggregation at 63°C and pH 7.0 in the presence and absence of different concentrations of NAA by observing changes in the light scattering intensity at 500 nm. **Figure 1A** shows aggregation profile of CA as a function of time in absence and presence of different concentration of NAA. It is seen in this figure that there is decrease in the final magnitude of the aggregates suggesting its inhibitory effect. The aggregation kinetic parameters (lag time, k_{app} and I_f) of CA in the absence and presence of different NAA concentrations were analyzed using Equation (1). The estimated values are given in **Table 1**. Results presented in this table show (i) an increase in lag phase in the presence of NAA and (ii) slower aggregation growth rates than those of the protein alone (control) and (iii) decrease in the I_f (final magnitude of aggregates formed). To further confirm the decrease in the extent of CA aggregation in presence of NAA, we have taken TEM images of CA aggregates in the presence of 1 M NAA concentration (**Figure 1C**). The large difference observed in the density of aggregates formed in the presence of NAA and that of the control (absence of NAA) suggest that NAA is able to decrease protein aggregation to a large extent.

We have also examined the ability of NAA on inhibiting the aggregation of another protein, catalase (**Figure 2**). The aggregation kinetic profiles were analyzed using equation (1) for the aggregation parameters (shown in **Table 2**). It is seen in this Table that NAA suppresses the aggregation of catalase and the behavior of inhibitory mechanism is similar to that observed for CA. The results indicate that NAA inhibits protein aggregation in general via common mechanism.

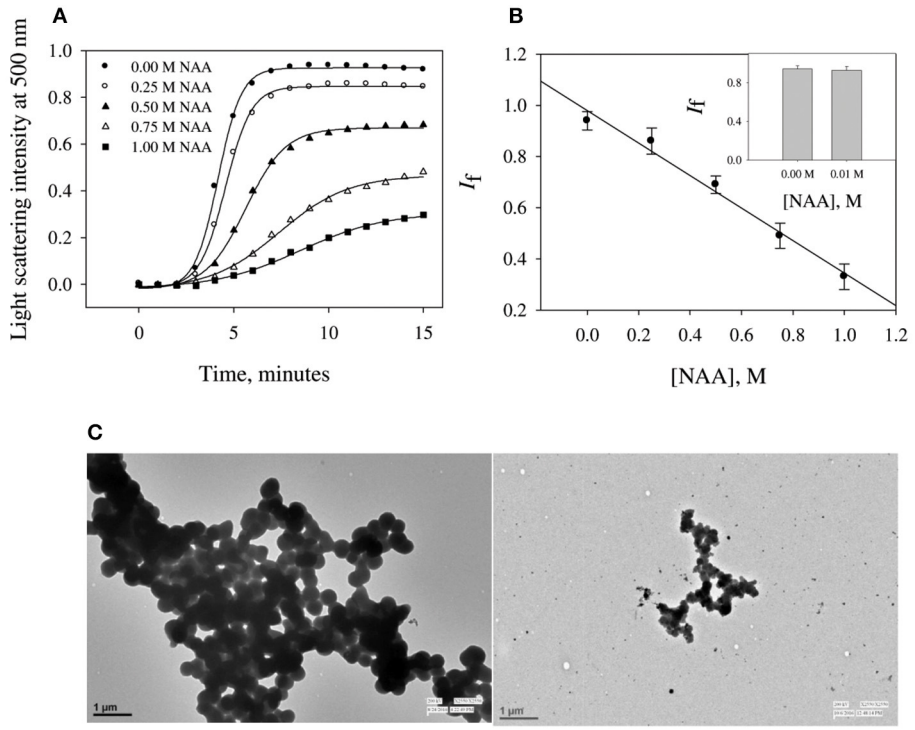

FIGURE 1 | Time dependent aggregation profiles of carbonic anhydrase**. (A)** Aggregation kinetics of CA monitored by observing changes in the light scattering intensity at 500 nm in presence and absence of NAA. The lines present the best fits of the data using Equation (1). Results shown are representative of at least three independent measurements and mean error of the best fits are given in **Table 1**. **(B)** Plots of I_f vs. NAA concentrations. Error bars represents the standard errors of the mean. **(C)** Transmission electron microscopy images of CA in absence of NAA (left panel) and in presence (right panel) of 1 M NAA.

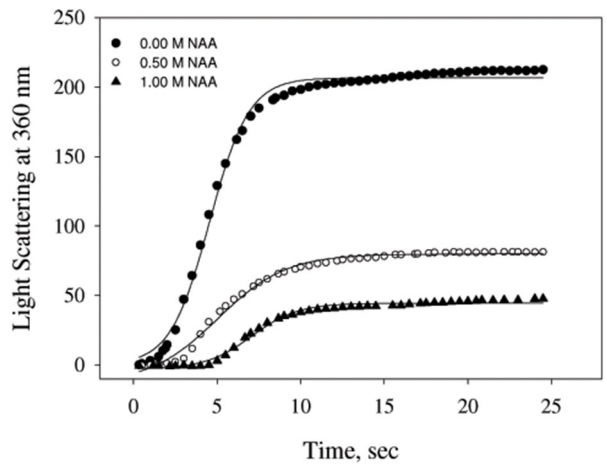

FIGURE 2 | Time dependent aggregation profiles of catalase. Aggregation kinetics of catalase monitored by observing changes in the light scattering intensity at 360 nm in presence and absence of NAA. The lines present the best fits of the data using Equation (1). Results shown are representative of at least three independent measurements and mean error of the three independent best fits are given in **Table 2**.

TABLE 2 | Kinetic parameters of catalase aggregation in the absence and presence of NAA.

	Concentration (M)	Lag time (min)	$k_{app(min^{-1})}$	I_f
NAA	0.00	2.4 ± 0.14	0.9 ± 0.04	206.33 ± 14
	0.50	3.7 ± 0.19	0.9 ± 0.05	81.28 ± 7
	1.00	4.5 ± 0.22	0.8 ± 0.05	45.86 ± 4

"±" represents standard error of three independent measurements.

NAA Increases the $\Delta G_D°$ and T_{agg} of CA

We have further investigated the effect of NAA on temperature-dependent aggregation of CA. **Figure 3A** shows the aggregation of CA as a function of temperature at pH 7.0 in the presence and absence of various concentrations of NAA. It is seen in the figure that CA initiates aggregation when it reaches 63°C in absence of NAA which is consistent with the earlier reports (Lavecchia and Zugaro, 1991; Sarraf et al., 2004). However, in the presence of NAA the aggregation starts at higher temperature. The parameters, T_{agg} and I_f of temperature-dependent aggregation of CA were further analyzed using appropriate equations (Equation 2). The evaluated values are given in **Table 3**. It is seen in the table that NAA is able to decrease CA aggregation by decreasing the I_f with increasing NAA concentration indicating that the extent of formation of aggregates is reduced. Accordingly, we also observed an increase in the T_{agg} value as a function of NAA concentration indicating stabilizing of the native protein by NAA. To directly estimate the changes in thermodynamic parameters, we have performed urea-induced denaturation of CA in presence of NAA (**Figure 4**) and

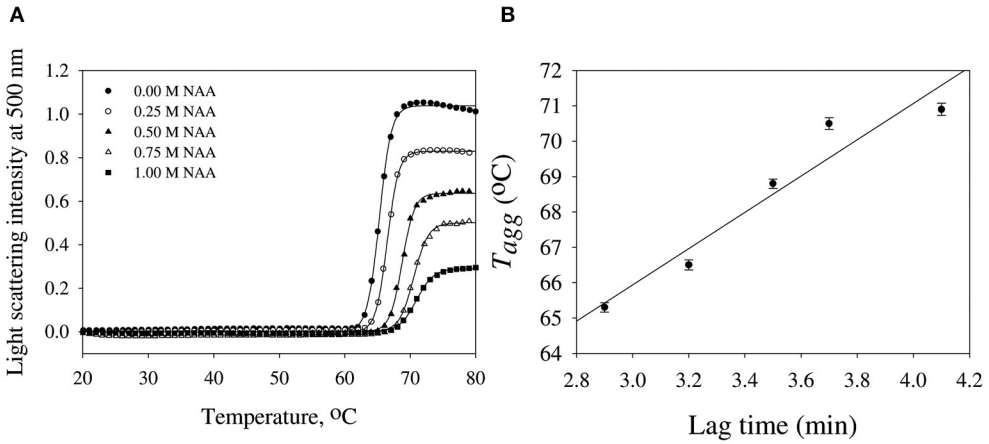

FIGURE 3 | Temperature dependent aggregation profiles of carbonic anhydrase. **(A)** Temperature dependent aggregation kinetics of CA monitored by observing changes in the light scattering intensity at 500 nm in presence and absence of NAA. The lines present the best fits of the data using Equation (2). Results shown are representative of at least three independent measurements and mean error of the three independent best fits are given in **Table 3**. **(B)** Plots of T_{agg} vs. lag time.

TABLE 3 | Parameters of temperature dependent aggregation of CA in the absence and presence of NAA.

	Concentration (M)	T_{agg} (°C)	I_f
NAA	0.00	65.3 ± 0.26	1.00 ± 0.06
	0.25	66.5 ± 0.22	0.83 ± 0.04
	0.50	68.8 ± 0.23	0.64 ± 0.04
	1.00	70.5 ± 0.18	0.50 ± 0.03
	1.50	70.9 ± 0.21	0.29 ± 0.02
	2.00	71.4 ± 0.24	0.24 ± 0.02

"±" represents standard error of three independent measurements.

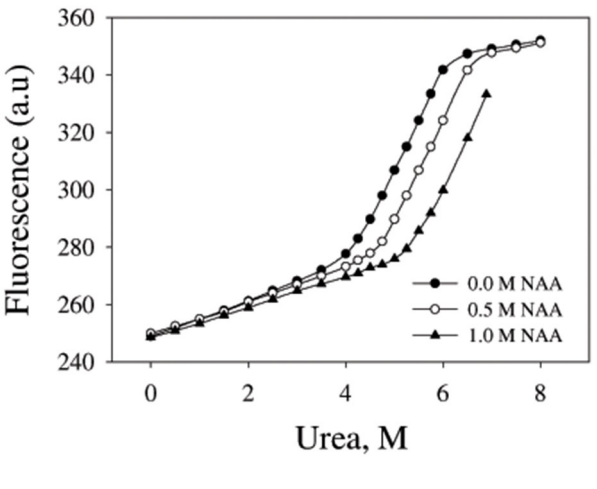

FIGURE 4 | Urea denaturation profiles of CA. Denaturation of CA by observing changes at 355 nm using different concentration of urea in presence and absence of NAA. Excitation wavelength was 280 nm. Results shown are representative of at least three independent measurements and mean error of the three independent best fits are given in **Table 4**.

the evaluated parameters (using Equations 3 and 4) are shown in **Table 4**. However, it should be noted that at 1 M NAA, a complete urea-induced transition curve could not be obtained due to experimental constraints and therefore y_D was unknown. Since y_D is independent of the molar concentration of NAA, we have analyzed this incomplete transition curve by using property of y_D for the control (in the absence of NAA). It is seen in **Table 4** that there is increase in the C_m and ΔG_D° of the CA in presence of NAA in a concentration dependent manner. There is around 25% increases in the ΔG_D° in presence of 1 M NAA.

NAA Induces Partial Structural Alteration on Native CA

We have further investigated the effect of NAA on the structural differences between the NAA treated and untreated CA. **Figure 5** shows the near-UV CD, tryptophan fluorescence and ANS fluorescence spectra of the CA in absence and presence of CA. Far-UV CD spectra could not be collected due to experimental constraints. It is seen in the Figure that CA exhibit three different peaks in the near-UV region (270, 287, and 296 nm) which are characteristics peaks originated from the trp47, trp97, and trp245, respectively. There is no observed alteration in any of the peaks in presence of NAA. However, tryptophan spectra shows little decrease in the λ_{max} of the CA indicating that some of the tryptophan residues are partly in a polar environment relative to the NAA untreated samples. ANS measurement revealed that native CA does not bind ANS but the NAA treated CA exhibit partial binding of ANS.

NAA Partially Reverses Preformed CA Aggregates

We were interested to investigate if NAA could reverse the preformed CA aggregates. For this we monitored the change in light scattering intensity (at 500 nm) of the various CA

aggregated samples diluted in buffer alone and in presence of NAA. **Figure 6** shows the plot of light scattering intensity vs. NAA concentrations. It is seen in the figure that NAA is able to partly reverse the preformed CA aggregates.

DISCUSSION

NAA is not only the most abundant amino acid in brain cells (as compared to the other amino acids) but also seems to play an important role in the proteopathic conditions as its level is altered under disease conditions associated with the proteopathies (Moffett et al., 2007). Our results revealed that NAA exhibits pronounce inhibitory effect on the aggregation behavior of CA (see **Figures 1A,B**) as evident from the decrease in final magnitude of the aggregates in a concentration dependent manner. However, physiological concentration of NAA could not offer any inhibitory effect (see inset **Figure 1B**). TEM images further confirmed that CA forms spherical aggregates and there is several fold decrease in amount of aggregates formed (**Figure 1C**). The observed inhibitory effects on catalase aggregation (**Figure 2**) also indicate that aggregation suppressing effect of NAA is not confined to CA but may be generally true. It has been well-understood that deposition of Aβ or alpha-synuclein oligomers is the common pathology associated with Alzheimer or Parkinson, respectively (Rabbani and Choi, 2018). Our results indicate that in the presence of NAA, Aβ or alpha-synuclein aggregation should be prevented. In support, it has been reported that NAA suppresses the aggregation of Aβ42 (Dollé et al., 2018). Thus, it appears that increase in the Aβ or alpha synuclein aggregation under the pathologic conditions, is due to decrease in the NAA concentration making it insufficient

TABLE 4 | Thermodynamic stability parameter of carbonic anhydrase in presence of NAA.

[NAA], M	C_m (M)	$\Delta G_D°$ (kcal/mol)
0.0	5.2 ± 0.06	7.9 ± 0.39
0.5	5.7 ± 0.05	8.6 ± 0.43
1.0	6.3 ± 0.08	9.9 ± 0.47

"±" represents standard error of three independent measurements.

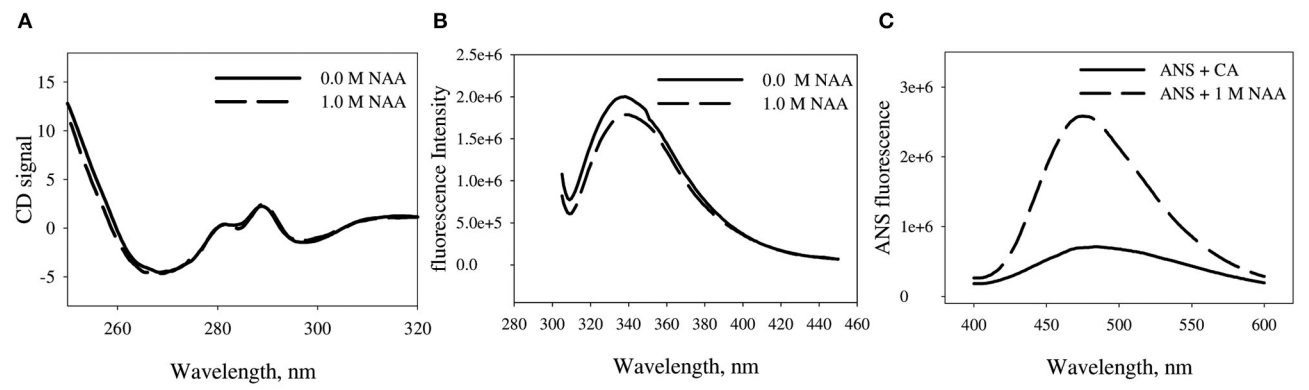

FIGURE 5 | Effect of NAA on native state conformation of CA. **(A)** Near UV-CD spectra (tertiary structure) of CA in absence and presence of NAA **(B)** Intrinsic fluorescence emission spectra of CA in absence and presence of NAA **(C)** ANS emission fluorescence spectra of CA. The spectra shown are representative of three independent measurements.

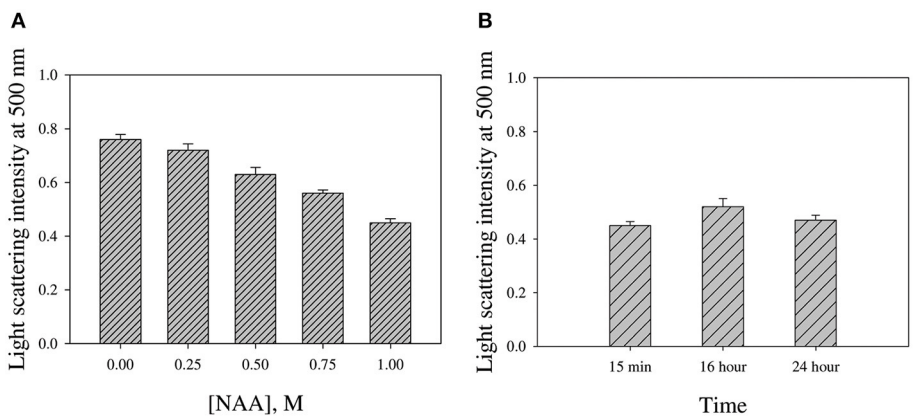

FIGURE 6 | NAA effect on reversing preformed CA aggregates. **(A)** Light scattering intensities of aggregated CA in the presence of different NAA concentrations **(B)** Intensities upon prolong incubations in presence of 1.0 M NAA. Error bars represent standard error of the mean.

to modulate aggregation pathway. Furthermore, increase in intracellular level of myo-inositol under the neurodegenerative conditions might also be an attempt to augment the aggregation of Aβ or alpha synuclein. It is likely that cells undergo genetic and epigenetic alteration due to the pathological conditions that is in favor of aggregate formation.

We then investigated the mechanism of suppression of CA aggregation by NAA. For this first of all, NAA-induced aggregation profiles were analyzed for its effect on the various steps of the oligomerization process (as shown in **Table 1**). In general protein aggregation profile is exemplified by a sigmoidal curve consisting of lag phase (or nucleation step), log phase (oligomerization step), and final stationary phase (or formation of mature aggregates). The general belief is that native protein exists in dynamic equilibrium with aggregation prone species (APS) formed by undergoing certain conformational changes in the native protein. Nucleation phase comprises of the conversion of the native protein to the APS. The APS then self-associates to form various high order oligomers in the log phase. High order oligomers further assemble in an ordered (producing amyloidogenic species) or disordered (producing amorphous oligomers) manner to form mature aggregated species (maturation step). It is also evident in table that inhibitory effect of NAA on the CA aggregation pathway is largely due to its effect on the nucleation step (as evident from the pronounce increase in the lag time), which subsequently reduces the oligomerization step (k_{app}). Since native and APS exists in a dynamic equilibrium, the observed effect of the nucleation step perhaps, be due to stabilization of the native state thereby shifting the equilibrium, Native ↔ APS toward the left. This hypothesis was established firstly by monitoring the temperature-dependence of CA aggregation process using light scattering as a probe (see **Figure 3A** and **Table 3**). Shifting of the temperature-dependent aggregation curve to higher temperatures (or T_{agg}) in a NAA concentration-dependent manner is a signature for the stabilization of the native protein or reduction of the APS population (Mittal and Singh, 2014). To further confirm, we have plotted T_{agg} as a function of the lag phase (**Figure 3B**). A strong correlation between the two parameters confirms that the decrease in I_f is a result of the effect of NAA on the nucleation phase. A direct evidence came from the urea-induced unfolding studies of CA in the **Figure 4**. It is seen in **Table 4** that ΔG_D° of CA increases in presence of NAA suggesting the stabilization of CA native state by NAA. NAA has also been shown to increase the T_m and ΔG_D° of lysozyme and RNase-A (Warepam et al., 2020). Taken together, the results led us to conclude that stabilization of the native state might have therefore disfavoured partial unfolding of CA and thus the formation of APS.

We were further interested to investigate the conformational alteration on CA due to NAA treatment that results in inhibition of CA aggregation. For this we have measured the conformation of CA in presence of NAA using multiple spectroscopic techniques. It is seen in **Figure 5A** that there is no significant alteration in the gross tertiary structure of the proteins due to NAA (as evident from near-UV CD studies). On the other hand, tryptophan fluorescence studies revealed that there is slight changes in the environment of the tryptophan (as evident from the slight hypochromicity) (**Figure 5B**). Such structural change affecting tryptophan micro-environment might have affected the exposition pattern of hydrophobic clusters to the solvent (Rabbani et al., 2012). ANS is a dye that specifically binds to the exposed hydrophobic clusters to the solvent (Rabbani et al., 2011, 2014, 2015). It is seen in **Figure 5C** that there no apparent binding of ANS in presence of NAA but significant binding with little shift in λ_{max} in absence indicating little compaction of the hydrophobic groups. Taken together, the results indicate that NAA treatment induces minute conformational alteration to the CA bringing about large increase in native state stability.

We were further interested to investigate if NAA could also dissolve the preformed aggregates. For this we have intentionally treated the pre-aggregated CA with different concentrations of NAA and analyzed the aggregation status using light scattering. It is evident in **Figure 6A** that there is partial decrease in the light scattering intensity in presence of NAA. However, there is no complete reversal of the aggregates even upon longer time incubations (**Figure 6B**). On molecular level, it is possible that the CH_3 groups in NAA compete with the CH_3-CH_3 interaction between any two adhering polypeptides in the oligomer resulting in the disruption of the intermolecular hydrophobic interaction and hence masking off the exposed hydrophobic groups of the monomeric units upon dissociation from the oligomer. Taken together, we conclude that NAA not only suppresses protein aggregation but also partly dissolve preformed aggregates. Thus, our study clearly indicates that NAA is not only a protein stabilizer but also a potent inhibitor of protein aggregation. The inhibition of protein aggregation is via its effect on the nucleation step of the aggregation kinetics. Under pathological conditions of Alzheimers and Parkinson, NAA is highly lowered. Thus, attempt to increase intracellular NAA concentration would be a viable strategy toward the therapeutic intervention of amyloidogenic condition of brain. Nevertheless, NAA may also be employed in other cell types wherein deposition of protein inclusion is the main cause of the pathophysiology.

Similar to our observation on NAA, other protein chaperones including yeast HSP104 and human HSP40/HSP70/HSP110 or Fas apoptosis inhibitory molecule also have the ability to solubilize preformed aggregates *in vivo* in ATP dependent or ATP independent manners respectively (Shorter, 2011; Kaku et al., 2020). As compared to the other protein chaperones which work by their catalytic ability, NAA is a small molecule metabolite that perhaps bring about solubilization of oligomers by virtue of its ability to bind to the hydrophobic groups exposed in the protein aggregates. The observations indicate there might be existence of different disaggregases in the cellular environment.

DATA AVAILABILITY STATEMENT

The original contributions presented in the study are included in the article/supplementary material, further inquiries can be directed to the corresponding author/s.

AUTHOR CONTRIBUTIONS

LS was responsible for the conception, design, interpretation of the results, and writing manuscript. MW for conducting

experiments. LS, MW, and AM involved in data analysis. GS, KK, SK, MK, and HR was involved in editing the final manuscript. AM and MK were involved in critically revising and editing the final manuscript. All authors contributed to the article and approved the submitted version.

FUNDING

This work is supported partly by the research grant from the SERB, Department of Science and Technology (PDF/2015/001090), Indian Council of Medical Research (45/34/2018-BIO/BMS) provided to MW. This research work is also partly supported by grant obtained from UGC-SAP and DST-PURSE Delhi University.

ACKNOWLEDGMENTS

MW also thanks Central Instrumentation Facility, ACBR, University of Delhi for providing CD facility.

REFERENCES

Abbott, C., and Bustillo, J. (2006). What have we learned from proton magnetic resonance spectroscopy about schizophrenia? A critical update. *Curr. Opin. Psychiatry* 19, 135–139. doi: 10.1097/01.yco.0000214337.29378.cd

Baslow, M. H. (2003). Brain N-acetylaspartate as a molecular water pump and its role in the etiology of Canavan disease: a mechanistic explanation. *J. Mol. Neurosci.* 21, 185–190. doi: 10.1385/JMN:21:3:185

Baslow, M. H., Suckow, R. F., Gaynor, K., Bhakoo, K. K., Marks, N., Saito, M., et al. (2003). Brain damage results in down-regulation of N-acetylaspartate as a neuronal osmolyte. *Neuromol. Med.* 3, 95–104. doi: 10.1385/NMM:3:2:95

Birnbaum, S. M., Levintow, L., Kingsley, R. B., and Greenstein, J. P. (1952). Specificity of amino acid acylases. *J. Biol. Chem.* 194, 455–470. doi: 10.1016/S0021-9258(18)55898-1

Blüml, S. (1999). *In vivo* quantitation of cerebral metabolite concentrations using natural abundance 13C MRS at 1.5 T. *J. Magn. Reson.* 136, 219–225. doi: 10.1006/jmre.1998.1618

Boltshauser, E., Schmitt, B., Wevers, R. A., Engelke, U., Burlina, A. B., and Burlina, A. P. (2004). Follow-up of a child with hypoacetylaspartia. *Neuropediatrics* 35, 255–258. doi: 10.1055/s-2004-821036

Briellmann, R. S., Wellard, R. M., and Jackson, G. D. (2005). Seizure-associated abnormalities in epilepsy: evidence from MR imaging. *Epilepsia* 46, 760–766. doi: 10.1111/j.1528-1167.2005.47604.x

Burlina, A. P., Corazza, A., Ferrari, V., Erhard, P., Künnecke, B., Seelig, J., et al. (1994). Detection of increased urinary N-acetylaspartylglutamate in Canavan disease. *Eur. J. Pediatr.* 153, 538–539. doi: 10.1007/BF01957015

Clark, J. B. (1998). N-acetyl aspartate: a marker for neuronal loss or mitochondrial dysfunction. *Dev. Neurosci.* 20, 271–276. doi: 10.1159/000017321

Criste, G., and Trapp, B. (2006). N-acetyl-L-aspartate in multiple sclerosis. *Adv. Exp. Med. Biol.* 576, 199–214. doi: 10.1007/0-387-30172-0_14

Danielsen, E., and Ross, B. (1999). *Magnetic Resonance Spectroscopy Diagnosis of Neurological Diseases*.New York, NY: Marcel Dekker.

Dollé, J. P., Rodgers, J. M., Browne, K. D., Troxler, T., Gai, F., and Smith, D. H. (2018). Newfound effect of N-acetylaspartate in preventing and reversing aggregation of amyloid-beta *in vitro*. *Neurobiol. Dis.* 117, 161–169. doi: 10.1016/j.nbd.2018.05.023

Goldstein, F. B. (1959). Biosynthesis of N-acetyl-L-aspartic acid. *J.Biol.Chem.* 234, 2702–2706. doi: 10.1016/S0021-9258(18)69763-7

Haber, J., Maślakiewicz, P., Rodakiewicz-Nowak, J., and Walde, P. (1993). Activity and spectroscopic properties of bovine liver catalase in sodium bis(2-ethylhexyl)sulfosuccinate/isooctane reverse micelles. *Eur. J. Biochem.* 217, 567–573. doi: 10.1111/j.1432-1033.1993.tb18278.x

Kaku, H., Ludlow, A. V., Gutknecht, M. F., and Rothstein, T. L. (2020). FAIM opposes aggregation of mutant SOD1 that typifies some forms of familial amyotrophic lateral sclerosis. *Front. Neurosci.* 14:110. doi: 10.3389/fnins.2020.00110

Kalra, S., and Arnold, D. L. (2004). ALS surrogate markers MRS Amyotroph Lateral Scler Other. *Motor Neuron Disord.* 5, 111–114. doi: 10.1080/17434470410019861

Kantarci, K., and Jack, C. R. Jr. (2003). Neuroimaging in Alzheimer disease: an evidence-based review. *Neuroimaging Clin. N. Am.* 13, 197–209. doi: 10.1016/S1052-5149(03)00025-X

Knizley, H. Jr. (1967). The enzymatic synthesis of N-acetyl-L-aspartic acid by a water insoluble preparation of a cat brain acetone powder. *J. Biol. Chem.* 242, 4619–4622. doi: 10.1016/S0021-9258(18)99502-5

Kundu, B., and Guptasarma, P. (2002). Use of a hydrophobic dye to indirectly probe the structural organization and conformational plasticity of molecules in amorphous aggregates of carbonic anhydrase. *Biochem. Biophys. Res. Commun.* 293, 572–577. doi: 10.1016/S0006-291X(02)00257-7

Lavecchia, R., and Zugaro, M. (1991). Thermal denaturation of erythrocyte carbonic anhydrase. *FEBS Lett.* 292, 162–164. doi: 10.1016/0014-5793(91)80858-Z

Madhavarao, C. N., Arun, P., Moffett, J. R., Szucs, S., Surendran, S., Matalon, R., et al. (2005). Defective N-acetylaspartate catabolism reduces brain acetate levels and myelin lipid synthesis in Canavan's disease. *Proc. Natl. Acad. Sci. U. S. A.* 102, 5221–5226. doi: 10.1073/pnas.0409184102

Mittal, S., and Singh, L. R. (2014). Macromolecular crowding decelerates aggregation of a β-rich protein, bovine carbonic anhydrase: a case study. *J. Biochem.* 156, 273–282. doi: 10.1093/jb/mvu039

Miyake, M., Kakimoto, Y., and Sorimachi, M. (1981). A gas chromatographic method for the determination of N-acetyl-L-aspartic acid, N-acetyl-aspartylglutamic acid and beta-citryl-L-glutamic acid and their distributions in the brain and other organs of various species of animals. *J. Neurochem.* 36, 804–810. doi: 10.1111/j.1471-4159.1981.tb01665.x

Moffett, J. R., Ross, B., Arun, P., Madhavarao, C. N., and Namboodiri, A. M. (2007). N-Acetylaspartate in the CNS: from neurodiagnostics to neurobiology. *Prog Neurobiol.* 81, 89–131. doi: 10.1016/j.pneurobio.2006.12.003

Nielsen, L., Khurana, R., Coats, A., Frokjaer, S., Brange, J., Vyas, S., et al. (2001). Effect of environmental factors on the kinetics of insulin fibril formation: elucidation of the molecular mechanism. *Biochemistry* 40, 6036–6046. doi: 10.1021/bi002555c

Pace, C. N. (1975). The stability of globular proteins. *CRC Crit. Rev. Biochem.* 3, 1–43. doi: 10.3109/10409237509102551

Paley, M., Cozzone, P. J., Alonso, J., Vion-Dury, J., Confort-Gouny, S., Wilkinson, I. D., et al. (1996). A multicenter proton magnetic resonance spectroscopy study of neurological complications of AIDS. *AIDS Res. Hum. Retroviruses* 12, 213–222. doi: 10.1089/aid.1996.12.213

Pan, J. W., and Takahashi, K. (2005). Interdependence of N-acetyl aspartate and high-energy phosphates in healthy human brain. *Ann. Neurol.* 57, 92–97. doi: 10.1002/ana.20317

Rabbani, G., Ahmad, E., Vahid Khan, M., Ashraf, M. T., Bhat, R., and Khan, R. H. (2015). Impact of structural stability of cold adapted Candida antarctica lipase B (caLB): in relation to pH, chemical and thermal denaturation. *RSC Adv.* 5, 20115–20131. doi: 10.1039/C4RA17093H

Rabbani, G., Ahmad, E., Zaidi, N., Fatima, S., and Khan, R. H. (2012). pH-induced molten globule state of rhizopus niveus lipase is more resistant against thermal and chemical denaturation than its native state. *Cell Biochem. Biophys.* 62, 487–499. doi: 10.1007/s12013-011-9335-9

Rabbani, G., Ahmad, E., Zaidi, N., and Khan, R. H. (2011). pH-dependent conformational transitions in conalbumin (Ovotransferrin), a metalloproteinase from hen egg white. *Cell Biochem. Biophys.* 61, 551–560. doi: 10.1007/s12013-011-9237-x

Rabbani, G., and Choi, I. (2018). Roles of osmolytes in protein folding and aggregation in cells and their biotechnological applications. *Int. J. Biol. Macromol.* 109, 483–491. doi: 10.1016/j.ijbiomac.2017.12.100

Rabbani, G., Kaur, J., Ahmad, E., Khan, R. H., and Jain, S. K. (2014). Structural characteristics of thermostable immunogenic outer membrane protein from *Salmonella enterica* serovar Typhi. *Appl. Biochem. Biotechnol*. 98, 2533–2543. doi: 10.1007/s00253-013-5123-3

Rael, L. T., Thomas, G. W., Bar-Or, R., Craun, M. L., and Bar-Or, D. (2004). An anti-inflammatory role for N-acetly aspartate in stimulated human astroglial cells. *Biochem. Biophys. Res. Commun*. 319, 847–853. doi: 10.1016/j.bbrc.2004.04.200

Rana, A., Gupta, T. P., Bansal, S., and Kundu, B. (2008). Formation of amyloid fibrils by bovine carbonic anhydrase. *Biochim. Biophys. Acta* 1784, 930–935. doi: 10.1016/j.bbapap.2008.02.020

Santoro, M. M., and Bolen, D. W. (1988). Unfolding free energy changes determined by the linear extrapolation method. 1. Unfolding of phenylmethanesulfonyl alpha-chymotrypsin using different denaturants. *Biochemistry*. 27, 8063–8068. doi: 10.1021/bi00421a014

Sarraf, N. S., Saboury, A. A., Ranjbar, B., and Moosavi-Movahedi, A. A. (2004). Structural and functional changes of bovine carbonic anhydrase as a consequence of temperature. *Acta Biochim. Pol*. 51, 665–671. doi: 10.18388/abp.2004_3551

Senisterra, G. A., Ghanei, H., Khutoreskaya, G., Dobrovetsky, E., Edwards, A. M., Privé, G. G., et al. (2010). Assessing the stability of membrane proteins to detect ligand binding using differential static light scattering. *J. Biomol. Screen*. 15, 314–320. doi: 10.1177/1087057109357117

Senisterra, G. A., Markin, E., Yamazaki, K., Hui, R., Vedadi, M., and Awrey, D. E. (2006). Screening for ligands using a generic and high-throughput light-scattering-based assay. *J. Biomol. Screen*. 11, 940–948. doi: 10.1177/1087057106294699

Shorter, J. (2011). The mammalian disaggregase machinery:Hsp110 synergizes with Hsp70 and Hsp40 to catalyse protein disaggregation and reactivation in a cell-free system. *PLoS One*. 6:e26319. doi: 10.1371/journal.pone.0026319

Taylor, D. L., Davies, S. E., Obrenovitch, T. P., Doheny, M. H., Patsalos, P. N., Clark, J. B., et al. (1995). Investigation into the role of N-acetylaspartate in cerebral osmoregulation. *J. Neurochem*. 65, 275–281. doi: 10.1046/j.1471-4159.1995.65010275.x

Taylor, D. L., Davies, S. E., Obrenovitch, T. P., Urenjak, J., Richards, D. A., Clark, J. B., et al. (1994). Extracellular Nacetylaspartate in the rat brain: *in vivo* determination of basal levels and changes evoked by high K+. *J. Neurochem*. 62, 2349–2355. doi: 10.1046/j.1471-4159.1994.62062349.x

Truckenmiller, M. E., Namboodiri, M. A., Brownstein, M. J., and Neale, J. H. (1985). N-Acetylation of L-aspartate in the nervous system: differential distribution of a specific enzyme. *J.Neurochem*. 45, 1658–1662. doi: 10.1111/j.1471-4159.1985.tb07240.x

Warepam, M., Ahmad, K., Rahman, S., Rahaman, H., Kumari, K., and Singh, L. R. (2020). N-Acetylaspartate is an important brain osmolyte. *Biomolecules* 10, 286. doi: 10.3390/biom10020286

Yazdanparast, R., Khodarahmi, R., and Soori, E. (2005). Comparative studies of the artificial chaperone-assisted refolding of thermally denatured bovine carbonic anhydrase using different capturing ionic detergents and beta-cyclodextrin. *Arch. Biochem. Biophys*. 437, 178–185. doi: 10.1016/j.abb.2005.03.003

Conflict of Interest: The authors declare that the research was conducted in the absence of any commercial or financial relationships that could be construed as a potential conflict of interest.

frontiers in Cellular Neuroscience

ORIGINAL RESEARCH
published: 16 February 2021
doi: 10.3389/fncel.2021.598230

Neuroprotective Effects of Exercise Postconditioning After Stroke *via* SIRT1-Mediated Suppression of Endoplasmic Reticulum (ER) Stress

Fengwu Li[1], Xiaokun Geng[1,2,3], Hangil Lee[3], Melissa Wills[3] and Yuchuan Ding[3,4]**

[1]China-America Institute of Neuroscience, Luhe Hospital, Capital Medical University, Beijing, China, [2]Department of Neurology, Beijing Luhe Hospital, Capital Medical University, Beijing, China, [3]Department of Neurosurgery, Wayne State University School of Medicine, Detroit, MI, United States, [4]Department of Research and Development Center, John D. Dingell VA Medical Center, Detroit, MI, United States

While it is well-known that pre-stroke exercise conditioning reduces the incidence of stroke and the development of comorbidities, it is unclear whether post-stroke exercise conditioning is also neuroprotective. The present study investigated whether exercise postconditioning (PostE) induced neuroprotection and elucidated the involvement of SIRT1 regulation on the ROS/ER stress pathway. Adult rats were subjected to middle cerebral artery occlusion (MCAO) followed by either: (1) resting; (2) mild exercise postconditioning (MPostE); or (3) intense exercise postconditioning (IPostE). PostE was initiated 24 h after reperfusion and performed on a treadmill. At 1 and 3 days thereafter, we determined infarct volumes, neurological defects, brain edema, apoptotic cell death through measuring pro- (BAX and Caspase-3) and anti-apoptotic (Bcl-2) proteins, and ER stress through the measurement of glucose-regulated protein 78 (GRP78), inositol-requiring 1α (IRE1α), protein kinase RNA-like endoplasmic reticulum kinase (PERK), activating transcription factor 6 (ATF6), C/EBP homologous protein (CHOP), Caspase-12, and SIRT1. Proteins were measured by Western blot. ROS production was detected by flow cytometry. Compared to resting rats, both MPostE and IPostE significantly decreased brain infarct volumes and edema, neurological deficits, ROS production, and apoptotic cell death. MPostE further increased Bcl-2 expression and Bcl-2/BAX ratio as well as BAX and Caspase-3 expressions and ROS production ($^*p < 0.05$). Both PostE groups saw decreases in ER stress proteins, while MPostE demonstrated a further reduction in GRP78 ($^{***}p < 0.001$) and Caspase-12 ($^*p < 0.05$) expressions at 1 day and IRE1α ($^{**}p < 0.01$) and CHOP ($^*p < 0.05$) expressions at 3 days. Additionally, both PostE groups saw significant increases in SIRT1 expression. In this study, both mild and intense PostE levels induced neuroprotection after stroke through SIRT1 and ROS/ER stress pathway. Additionally, the results may provide a base for our future study regarding the regulation of SIRT1 on the ROS/ER stress pathway in the biochemical processes underlying post-stroke neuroprotection. The results suggest that mild exercise postconditioning might play a similar neuroprotective role as intensive exercise and could be an effective exercise strategy as well.

Keywords: ischemia/reperfusion, exercise intensity, ER stress, apoptosis, caspase-12, CHOP

OPEN ACCESS

Edited by:
Rinki Minakshi, University of Delhi, India

Reviewed by:
Mustafa Caglar Beker, Istanbul Medipol University, Turkey
Jiangwen Yin, Sichuan University, China

****Correspondence:***
Xiaokun Geng
xgeng@ccmu.edu.cn
Yuchuan Ding
yding@med.wayne.edu

Specialty section:
This article was submitted to Cellular Neuropathology, a section of the journal Frontiers in Cellular Neuroscience

Received: *24 August 2020*
Accepted: *25 January 2021*
Published: *16 February 2021*

Citation:
Li F, Geng X, Lee H, Wills M and Ding Y (2021) Neuroprotective Effects of Exercise Postconditioning After Stroke via SIRT1-Mediated Suppression of Endoplasmic Reticulum (ER) Stress. Front. Cell. Neurosci. 15:598230. doi: 10.3389/fncel.2021.598230

INTRODUCTION

Stroke is the third leading cause of mortality and disability worldwide (Xiang et al., 2019; Turon et al., 2020). Despite growing approaches to treatment, many patients are left with a lifelong disability. Various conditioning strategies play important roles in reducing ischemic and reperfusion injury from stroke (Serviddio et al., 2008; Lemoine et al., 2017; Wang J. L. et al., 2020) to improve the prognosis and quality of life in stroke victims. Ischemic postconditioning is one of the strategies widely used to attenuate stroke-induced neural damage in animals and humans (Landman et al., 2019). In this rehabilitative method, cycles of transient ischemia to the distal limbs after a vascular accident, such as a stroke, stimulate physiologic responses that confer protection to the ischemic brain (Zhao J. J. et al., 2018). Alternatively, exercise conditioning is believed to be an effective strategy that attenuates the detrimental effects of ischemia and enhances various cognitive abilities, such as motor function (Thijssen et al., 2018). More specifically, prophylactic exercise, known as exercise preconditioning, has been widely reported to confer rehabilitative benefits in the post-stroke brain, such as the reduction of brain infarct volume and the promotion of angiogenesis, synaptogenesis, and neurogenesis after ischemia (Hafez et al., 2019; Lee et al., 2019; Terashi et al., 2019). Similarly, the benefits of post-ischemic exercise intervention were initially established in the context of myocardial injury in animal models. It has since been established that exercise postconditioning exerts beneficial effects in improving cardiovascular outcomes after myocardial ischemia (Szabo et al., 2019; Lee et al., 2020). However, the short-term effect of exercise postconditioning on the outcome of ischemic stroke has not been established. A growing body of evidence has demonstrated that higher intensity post-cerebral ischemia exercise yields beneficial effects in reducing brain infarct size, is an effective strategy for ameliorating physical disability, and leads to favorable outcomes after 3 months, which suggest that this exercise strategy has potential neuroprotective effects after stroke (Boyne et al., 2016; Luo et al., 2019; Andrews et al., 2020). Other studies suggest that mild exercise after stroke is superior in promoting recovery and improvement from brain damage (Zhu et al., 2015; Nie et al., 2016). The present conflicting conclusion elucidates the vital principle that exercise postconditioning intensity is an important determinant of neurological outcome after a stroke that merits close investigation. Patients may differ in their abilities and may be more vulnerable to harm from exercise, and thus prescribing the appropriately intense exercise and minimizing superfluous therapy is vital to their safe and successful rehabilitation. The appropriate intensities of exercise postconditioning and an understanding of its associated mechanisms need to be explored, as it may help direct the clinical application of exercise-based neuroprotection.

Many recent studies have demonstrated that cerebral ischemic injury is correlated to stress in the endoplasmic reticulum (ER), a multifunctional organelle responsible for protein synthesis and processing (Gong et al., 2017). Certain stressors, such as ischemia, disrupt homeostasis and cause ER stress, which triggers the unfolded protein response to minimize levels of unfolded proteins and to maximize cell viability (Ahsan et al., 2019). Prolonged environmental stress triggers signal transduction pathways that lead to apoptosis and thereby heighten pathological processes, leading to cerebral damage (Chi et al., 2019). Endoplasmic reticulum stress exerts its vital role in stroke-induced neural apoptosis (Mohammed Thangameeran et al., 2020) through activation of downstream CCAATenhancer-binding protein homologous protein (CHOP) and caspase-12 (Chi et al., 2019; Chu et al., 2019; Li Y. et al., 2020). SIRT1 is a nicotine adenine dinucleotide (NAD+)-dependent enzyme that deacetylates numerous transcription factors in response to ischemic stress and is involved in various biological pathways (Chen et al., 2005). Notably, it suppresses ER stress signals through the eEF2K/eEF2 pathway (Pires Da Silva et al., 2020) by increasing the expression of protective molecular chaperones (Wang F. et al., 2020) and by decreasing ROS production, which are potent ER stress agonists (Park et al., 2020). Its expression has also been shown to be elevated by post-stroke exercise, which suggests that exercise protects against ischemic damage by limiting ER stress (El Hayek et al., 2019; Jia et al., 2019). However, the precise mechanism by which exercise postconditioning affects the SIRT1/ER stress signal after stroke remains undetermined. The relationship between various exercise intensities and SIRT1/ER stress levels may help elucidate the mechanism of exercise-induced neuroprotection after ischemic stroke and guide efforts to optimize exercise intensity in postconditioning after stroke. We used an ischemia/reperfusion rat model to define the effect of exercise postconditioning after stroke and determine the relationship between SIRT1 and ROS/ER stress. Although the present study did not determine this relation, as the first step, we intended to assess the expression of SIRT1 and ER stress proteins following ischemia/reperfusion injury. These results might suggest a potential association of these molecules and provide a base for our future study regarding the regulation of SIRT1 on the ER stress pathway. The results of this study suggest a pathway for neuroprotection mediated by exercise postconditioning after stroke.

MATERIALS AND METHODS

Animals

A total of 175 adult male Sprague–Dawley rats (280–300 g, Vital River Laboratory Animal Technology Company, Limited, Beijing, China) were used in this study. The protocol, following the NIH Guide for the Care and Use of Laboratory Animals, was approved by the Animal Care and Use Committee of Capital Medical University (20180901). Animals were randomly divided into four groups: control ($n = 7$), middle cerebral artery occlusion (MCAO) without exercise ($n = 56$), MCAO with IPostE ($n = 56$), and MCAO with MPostE ($n = 56$). Both PostE protocols were initiated after 24 h of reperfusion and select animals from every group were sacrificed on days 1 and 3 after exercise for further biochemical analysis, as shown in **Figure 1A**. Seven rats from each group were used for the histological assay, Western Blotting, ROS detection, or brain edema analysis.

Focal Cerebral Ischemia and Reperfusion

The animals were subjected to transient right MCA occlusion according to the method we described previously (Chen et al., 2020). Briefly, rats were anesthetized in a chamber using 3% isoflurane and a mixture of 70% nitrous oxide and 30% oxygen. The rats were then transferred to a surgical table, where anesthesia was maintained with a facemask that delivered 1% isoflurane from a calibrated precision vaporizer. Poly-L-lysine-coated nylon (4.0) sutures were used to generate infarcts with minimal inter-animal variability. During the unilateral, two-hour MCAO procedure, cerebral blood flow (CBF) and rectal temperature were monitored continuously. CBF was monitored using the laser speckle technique according to the manufacturer's instructions. CBF before MCAO was defined as the baseline. Quantitative measurement of CBF 2 min before, immediately after MCAO, and at reperfusion were recorded as a percentage of baseline levels. Rectal temperatures were maintained between 36.5 and 37.5°C using a heating pad and a heating lamp. Ipsilateral ischemic hemispheres were used for further molecular analysis.

Exercise Postconditioning

All ischemic animals were randomly assigned to intense exercise, mild exercise, or non-exercise control groups. Exercise animals were run on a four-lane treadmill (ZS-PT-II, ZS Dichuang Instruments, Inc., Beijing, China), at a constant speed of 30 m/min for 30 min each day for the IPostE; or at 12 m/min for 30 min each day for the MPostE (Li F. et al., 2020). The rats were well enough for the exercise protocols at 24 h of spontaneous recovery, with recovery comparable to the performances on the treadmill at 3 days. For pre-conditioning to exercise, rats were required to perform treadmill training at a constant speed (10 m/min) for 10 min/day for 3 days before MCA occlusion. Although typical motor function impairment (movement in a circle) was observed, the animals moved around in the cage and were able to run on the treadmill for 30 min. Our previous studies, as well as others, have performed the exercise programs 24 h after MCAO, in which most animals were able to run continuously for 30 min (Li et al., 2017a,b,c; Pin-Barre et al., 2017; Li F. et al., 2020). From the beginning of group assignments until 1 or 3 days thereafter, all animals were housed in groups of threes in standard cages for equal times.

Cerebral Infarct Volume

After one or 3 days of exercise or non-exercise, the rats' brains were dissected, cut into 2-mm-thick slices with a brain matrix, and treated with 2,3,5-triphenyltetrazolium chloride (TTC, Sigma, USA) for staining. An indirect method for calculating infarct volume was used to minimize error caused by edema, as described previously by us (Liu et al., 2020).

Neurological Deficit

The modified scoring systems (5 and 12 scores) proposed by Zea Longa (5 scores) and Belayev et al (12 scores) were used to examine the severity of neurological deficits in rats before and after 24 h reperfusion (Li et al., 2019a). After MCAO, the modified scoring systems for neurological deficits were used to confirm brain injury. If the scores were 1 or below, the MCAO was considered unsuccessful and the rats were excluded (19, about 10%) from further studies. The exclusion was confirmed by an autopsy that lacked a core.

Brain Edema

Brain edema was evaluated through measurements of tissue water content to demonstrate brain swelling, as described previously by us (Li et al., 2019b). Following animal sacrifice, separated right and left hemispheres were immediately weighed to obtain wet weight (WW). The tissue was then dried in an oven at 70°C for 72 h and weighed again to obtain the dry weight (DW). The formula $(WW - DW)/WW \times 100\%$ was used to calculate the water content and is expressed here as a percentage of WW.

Apoptotic Cell Death

For the quantification of apoptosis-related DNA fragmentation, a commercial enzyme immunoassay was used to determine the cytoplasmic histone-associated DNA fragments (Cell Death Detection ELISA; MLBIO, Shanghai, China). The degree of apoptosis was quantified by the amount of cytoplasmic histone-associated DNA fragments in the stroke and variable groups at 1 or 3 days after PostE.

ROS Assay

As described previously by us (Chen et al., 2018), an adult brain dissociation kit (Miltenyi Biotec, Bergisch Gladbach, Germany) was used for brain cell isolation. Cell pellets were stained with ROS probes (S0063, Dihydroethidium, Biyuntian, Shanghai, China) and analyzed on a FACS Calibur flow cytometer with the Cell Quest software (BD, San Jose, CA, USA).

Protein Expression

After 1 or 3 days of exercise or non-exercise, rats were sacrificed for Western blot analysis. Tissue samples from the ipsilesional ischemic hemispheres were harvested and processed as described previously by us (Li et al., 2019a). Briefly, samples were incubated with a primary antibody rabbit anti-BAX (1:1,000, ab32503, Abcam, MA, USA), rabbit anti-Bcl-2 (1:500, ab196495, Abcam), rabbit anti-caspase-3 (1:1,000, ab13847, Abcam), rabbit anti-IRE1 (1:1,000, 14C10, CST, MA, USA), rabbit anti-GRP78 (1:1,000, 3183S, CST), rabbit anti-PERK (1:1,000, 27528-1-AP, PROTEINTECH, IL, USA), rabbit anti-ATF6 (1:1,000, ab203119, Abcam), rabbit anti-caspase-12 (1:1,000, ab62484, Abcam) and rabbit anti-CHOP (1:1,000, 2895S, CST) for 24 h at 4°C. The samples were further incubated with goat anti-rabbit IgG-HRP secondary antibody (1:1,000, sc-2004, Santa Cruz, Dallas, TX, USA) for all primary antibodies. Western blot images for molecules were analyzed using an image analysis program (ImageJ 1.42, National Institutes of Health, Bethesda, MD, USA) to quantify protein expressions according to relative image density. The calculations of Western blotting images were normalized according to their corresponding β-actin.

Statistical Analysis

Statistical analyses were performed with SPSS Statistics for Windows, Version 17.0 (SPSS Inc., Chicago, IL, USA).

Differences among groups were assessed using one-way ANOVA with significance levels of $p < 0.05$. *Post hoc* comparisons among groups were performed using the least significant difference method.

RESULTS

Cerebral Blood Flow (CBF)

Compared to CBF before ischemia, a significant decrease was observed after ischemia (**Figures 1B–D**).

Brain Infarction and Neurological Defects

Stroke-induced brain infarction and the infarct volumes were decreased significantly ($^{*}p < 0.05$) in both PostE groups at 1 and 3 days ($n = 7$ respectively, **Figures 1E,F**). Infarct volumes observed in the stroke groups were 42.5% at 1 day and 47.2% at 3 days ($n = 7$ respectively, **Figures 1E,F**). Infarction was significantly decreased by both exercise protocols, with IPostE decreasing to 32.3% and 19.7% on days 1 and 3, respectively ($^{**}p < 0.01$), and MPostE decreasing to 26.3% and 24.8% on days 1 and 3, respectively ($^{*}p < 0.05$). Neurological deficits detected by the 5- ($n = 7$, **Figure 1G**) and 12-point ($n = 7$, **Figure 1H**) score systems were 3.3 and 7.1 points (1 day), then 3.2 and 6.7 points (3 days) in the stroke groups. The 5-point score was decreased significantly after MPostE ($^{**}p < 0.01$, 2.6 points at 1 day; $^{*}p < 0.05$, 2.2 points at 3 days) and IPostE ($^{*}p < 0.05$, 2.9 points at 1 day; $^{**}p < 0.01$, 2.1 points at 3 days). The same trends were also seen in the 12-point score.

Brain Edema

On the ipsilateral side, a significant ($^{***}p < 0.001$) increase in water content was observed in ischemic rats (85.4% at 1 day and 84.0% at 3 days) as compared to control rats (76.1%) ($n = 7$ respectively, **Figures 1I,J**). Brain edema was significantly decreased by both exercise protocols, with IPostE decreasing to 80.1% and 79.1% on day 1 and 3, respectively ($^{*}p < 0.05$), and MPostE decreasing to 79.0% and 79.7% on days 1 and 3, respectively ($^{*}p < 0.05$; $n = 7$ respectively, **Figures 1I,J**). PostE made no significant difference to the water levels when compared with the control group in the contralateral hemisphere of ischemic rats.

Apoptosis and Apoptotic Proteins

Apoptotic cell death was detected at 1 and 3 days ($n = 7$ respectively, **Figures 2A,B**). Both mild and intense exercise significantly decreased cell death ($^{***}p < 0.001$), with further significant decrease observed in the mild exercise group at 3 days ($^{###}p < 0.001$; **Figure 2B**). Levels of BAX, Bcl-2, and Caspase-3 were detected by Western blot ($n = 7$ respectively, **Figures 2C–F**). Compared to the stroke group, MPostE significantly decreased pro-apoptotic protein expressions, such as BAX ($^{*}p < 0.05$ at 1 day and $^{***}p < 0.001$ at 3 days, **Figure 2C**) and Caspase-3 ($^{***}p < 0.001$ at 1 day and $^{***}p < 0.001$ at 3 days, **Figure 2F**), and increased anti-apoptotic protein expression, such as Bcl-2 ($^{***}p < 0.001$ at 1 day and $^{***}p < 0.001$, 1.1 at 3 days, **Figure 2D**). The same trends were also seen in the IPostE group. Additionally, we found that MPostE further significantly increased Bcl-2 level ($^{\#}p < 0.05$, 1 day; $^{\#\#\#}p < 0.001$, 3 days, **Figure 2D**) and decreased Caspase-3 level ($^{\#\#}p < 0.01$, 1 day; $^{\#\#\#}p < 0.001$, 3 days, **Figure 2F**) as compared to IPostE group. Moreover, the Bcl-2/BAX ratio in the stroke groups was 0.4 at both 1 and 3 days but significantly increased in both IPostE ($^{***}p < 0.001$, 1.8 at 1 day and 0.9 at 3 days) and MPostE groups ($^{***}p < 0.001$, 2.2 at 1 day and 1.9 at 3 days, **Figure 2E**). A further significant Bcl-2/BAX ratio increase was noted in the MPostE group at 3 days compared to the IPostE group ($^{\#\#\#}p < 0.001$, **Figure 2E**).

Expression of ER Stress

The levels of ER stress proteins in the stroke group were increased, including GRP78 (1.3, 1 day; 1.5, 3 days, **Figure 3A**), IRE1α (1.0, 1 and 3 days, **Figure 3B**), PERK (0.4, 1 day; 0.8, 3 days, **Figure 3C**), ATF6 (0.6, 1 day; 0.7, 3 days, **Figure 3D**), CHOP (0.7, 1 day; 0.9, 3 days, **Figure 3E**) and Caspase-12 (1.5, 1 day; 1.1, 3 days, **Figure 3F**). As compared to the stroke group, MPostE and IPostE significantly decreased expressions of GRP78 (**Figure 3A**), IRE1α (**Figure 3B**), PERK (**Figure 3C**), ATF6 (**Figure 3D**), CHOP (**Figure 3E**), and Caspase-12 (**Figure 3F**) ($n = 7$ respectively). MPostE was shown to significantly further reduce the levels of ER stress proteins compared to IPostE. These results demonstrate that the ER stress pathway may be involved in the regulation of apoptosis induced by ischemia/reperfusion and that varying degrees of exercise intensity may preferentially affect this pathway.

ROS Production and SIRT1 Expression

ROS production levels, measured by flow cytometry assay, were significantly decreased by exercise when compared to the levels raised after stroke ($^{*}p < 0.05$; $n = 7$ respectively, **Figures 4A,B**). The fluorescence intensity of ROS level in the stroke group was 23, 733.1 at 1 day and 20, 132.9 at 3 days (**Figure 4B**). Compared to the stroke group, MPostE ($^{**}p < 0.01$, 5, 856.8 at 1 day and 6, 131.9 at 3 days, **Figure 4B**) and IPostE ($^{*}p < 0.05$, 9, 376.6 at 1 day and 10, 920.1 at 3 days, **Figure 4B**) significantly decreased ROS production. MPostE further significantly decreased ROS production ($^{\#}p < 0.05$) at 1 and 3 days compared to IPostE. Furthermore, both PostE enhanced SIRT1 expressions in ischemic rats (**Figure 4C**). Protein expression of SIRT1 was significantly enhanced by MPostE ($^{**}p < 0.01$, 2.0 at 1 day and 0.7 at 3 days, **Figure 4C**) and IPostE ($^{*}p < 0.05$, 1.7 at 1 day, **Figure 4C**; $n = 7$ respectively). The present data indicate that SIRT1 and ROS may be involved in the ER stress pathway and exercise postconditioning.

DISCUSSION

In this study, we demonstrated that recovery from ischemic brain damage is enhanced by exercise postconditioning after stroke. Our results show that both mild and intense exercise regimes performed after stroke reduce brain edema and infarct size, neurological deficits, ROS production, and apoptotic cell death. Mild exercise induced a greater degree of apoptosis prevention in comparison to intense exercise.

Reduced brain injury was associated with an increase of anti-apoptotic proteins (Bcl-2) and Bcl-2/BAX ratio, and a decrease of pro-apoptotic proteins (BAX and caspase-3) and ER stress (GRP78, IRE1, PERK, ATF6, Caspase-12, CHOP). Furthermore, post-stroke exercise increased SIRT1 expression and had an inverse relationship with ROS levels.

Ischemic conditioning, which includes pre-and post-conditioning, is a nonpharmacological approach to inducing neuroprotection that is performed by the induction of intermittent blood flow restriction to non-vital organs. It has been widely reported to ameliorate brain and myocardial injury after an ischemic event (Guo et al., 2019). It's characterization of periodic ischemic induction is similar to the periodically

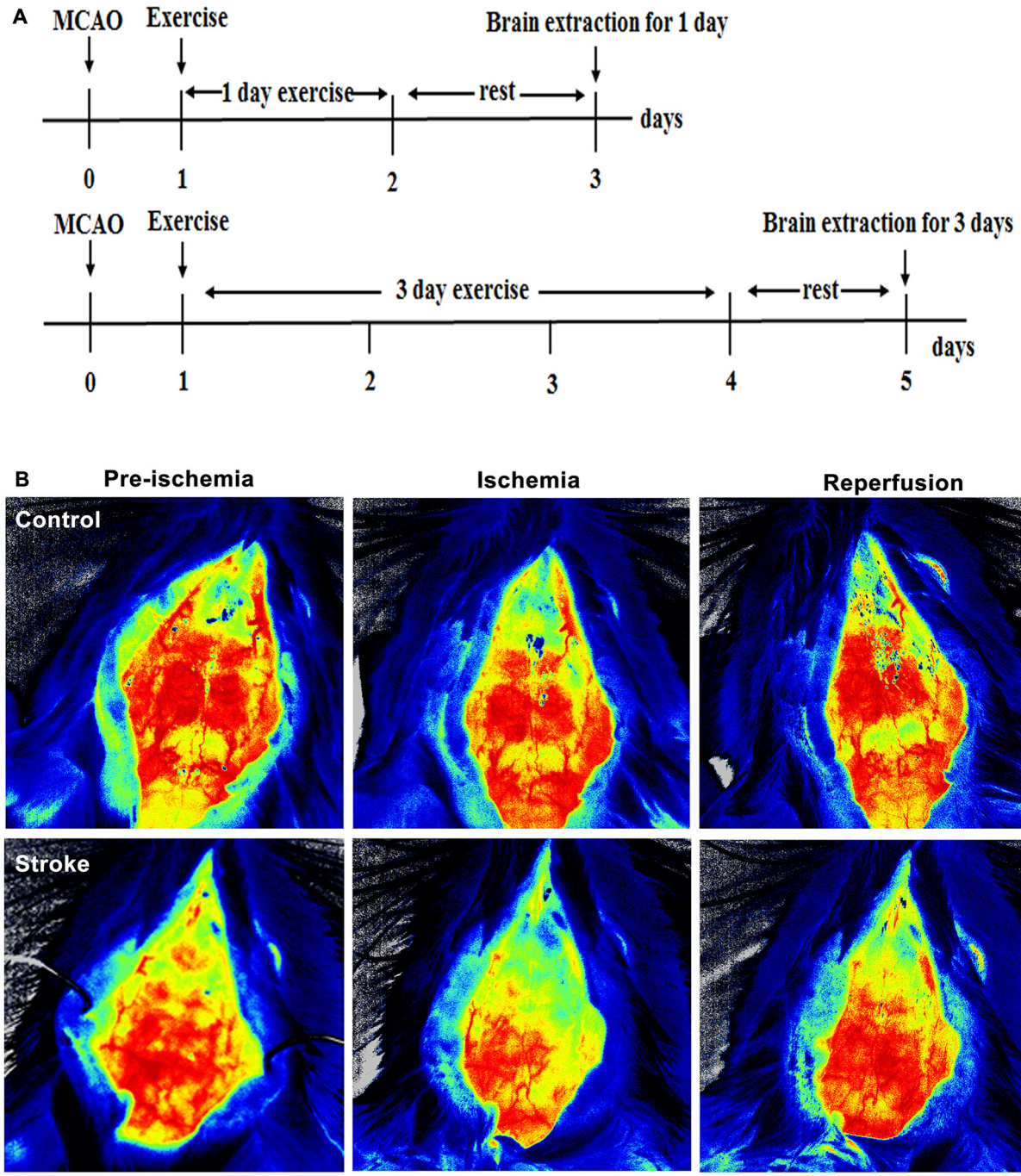

FIGURE 1 | Continued.

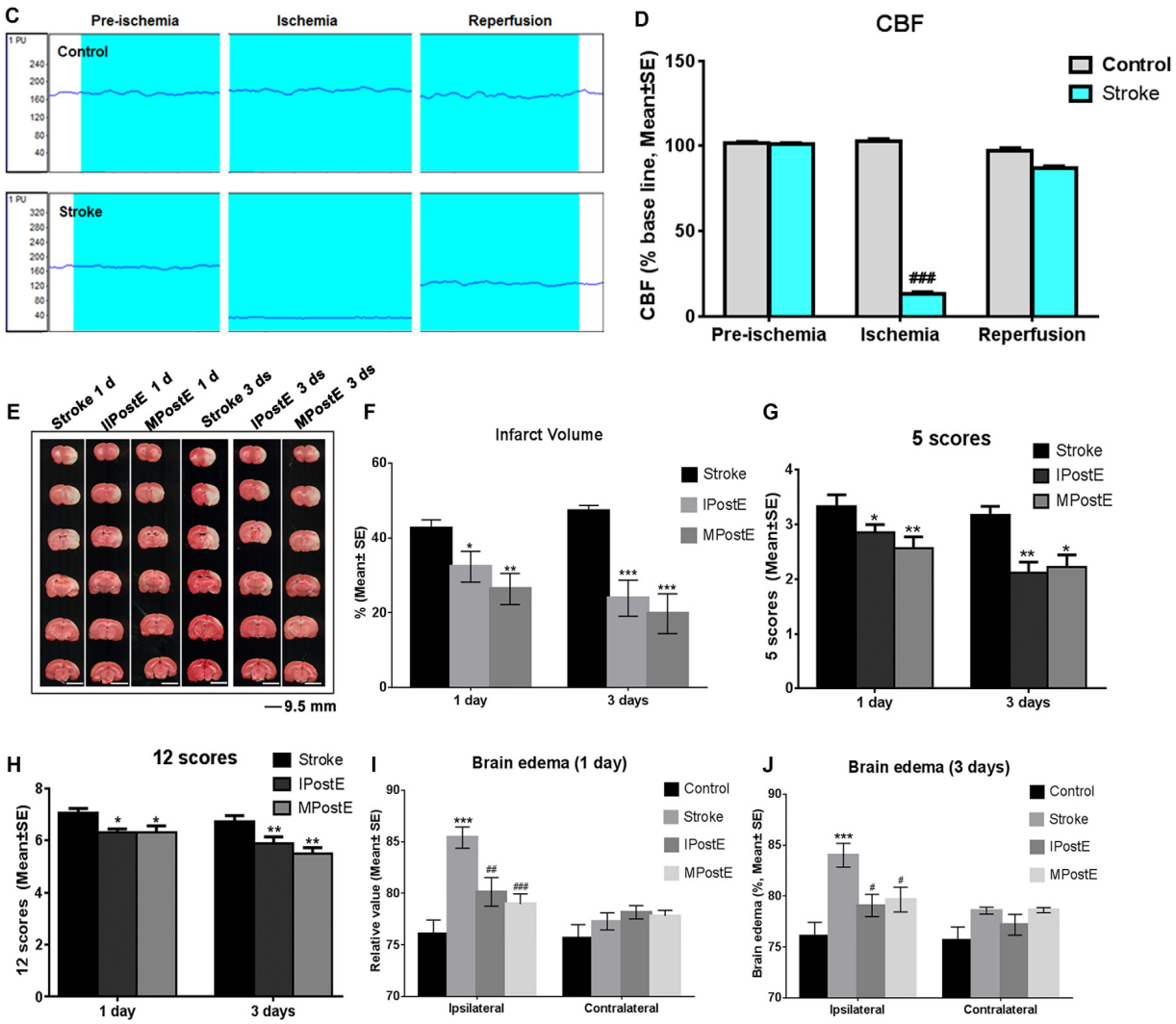

FIGURE 1 | Brain infarct and neurological deficits. **(A)** Illustration of the experimental timelines. Rats were subjected to 2 h middle cerebral artery occlusion (MCAO), followed by treadmill exercise 1 day after reperfusion for up to 2 or 4 days. **(B–D)** Representative images of monitored cerebral blood flow (CBF). **(E)** 2,3,5-triphenyltetrazolium chloride (TTC) histology demonstrating exercise postconditioning (PostE)-induced infarct volume reduction in the penumbra region of the ischemic territory supplied by the middle cerebral artery. **(F)** Quantification of infarct volume reduction by exercise conditioning. Compared to the stroke group, brain infarct ($n = 7$ respectively, $^{*}p < 0.05$, 1 day; $^{***}p < 0.001$, 3 days) significantly decreased in both intense and mild PostE groups. Neurological deficits after both PostE in 2 h MCAO, measured using the 5 score **(G)** and 12 score systems **(H)**, were decreased significantly ($^{*}p < 0.05$) after either mild or intense PostE. **(I–J)** PostE attenuated ipsilateral stroke-induced brain edema significantly vs. ipsilateral stroke group without exercise ($^{\#}P < 0.05$) at day 1 **(I)** and days 3 **(J)**. *, **, and *** represent MPostE or IPostE vs. stroke; $^{\#}$, $^{\#\#}$, and $^{\#\#\#}$ represent IPostE vs. MPostE.

scheduled exercise procedure that is also used as a form of cardioprotective conditioning (Thijssen et al., 2018). Chronic remote ischemic conditioning and regular exercise may share similar underlying cellular protective mechanisms such as increased antioxidant capacity, inhibition of autophagy, and the involvement of the NO pathway and inflammatory system (Zhao W. et al., 2018). Indeed, both exercise and ischemic conditioning are likely to employ similar mechanisms to enhance endogenous angiogenesis, synaptogenesis, and neurogenesis to improve recovery from ischemic injury. In light of these parallels, it is likely that regular post-stroke exercise conditioning, just like ischemic conditioning, has widespread health benefits and the potential for enhancing rehabilitation from cerebrovascular events. Though initially described through the scope of cardioprotection, there is growing literature substantiating the beneficial effects of exercise conditioning in restoring brain function after ischemic injury (Otsuka et al., 2016; Sakakima, 2019). Prophylactic exercise such as pre-ischemic exercise has been studied in stroke medicine and has been found in our previous studies to exert neuroprotective effects by improving recovery from blood-brain barrier (BBB) dysfunction and reducing brain infarct size (Davis et al., 2007; Otsuka et al., 2019). The present study's results further suggest that post-ischemic exercise conditioning, similar to

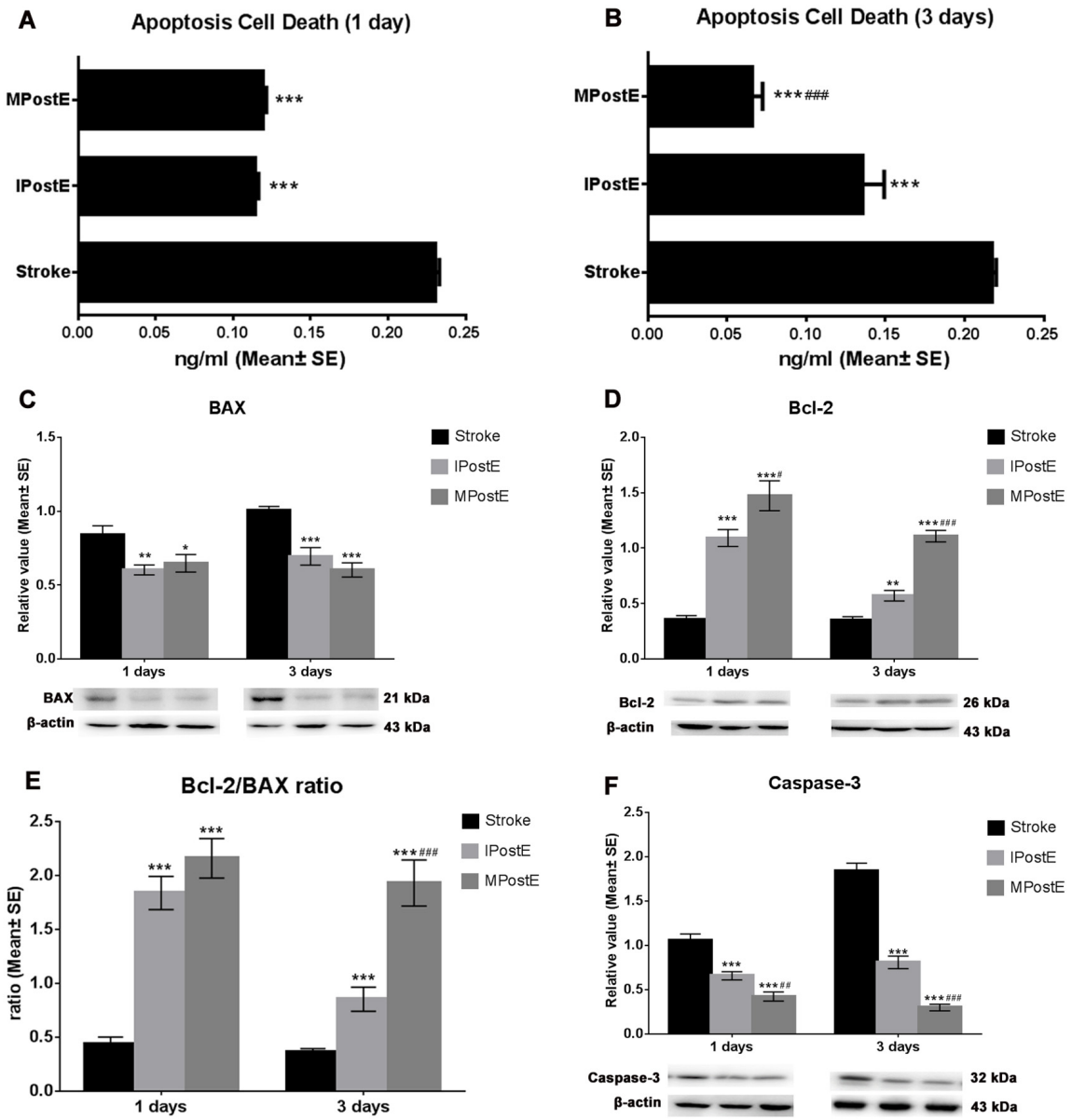

FIGURE 2 | Apoptosis and apoptotic proteins. **(A,B)** Cell death reduction due to PostE at 1 and 3 days, represented by apoptotic protein levels. Apoptotic cell death was detected at 1 and 3 days; both mild and intense PostE significantly ($n = 7$ respectively, $^{***}p < 0.001$) decreased cell death (**Figures 1H,I**), and a further significant decrease was noted ($^{\#\#\#}p < 0.001$) in the mild exercise group. **(C–F)** Representative images of BAX, Bcl-2, and Caspase-3 detected by Western Blot. Both intense ($^{**}p < 0.01$) and mild ($^{*}p < 0.05$) PostE ($n = 7$ respectively) decreased expressions of BAX **(C)** and Caspase-3 **(F)** at 1 and 3 days; significantly decreased Caspase-3 expression was seen with mild PostE ($^{\#\#\#}p < 0.001$). Compared to the stroke group, both mild and intense PostE significantly increased protein expression of Bcl-2 and Bcl-2/BAX ratio at 1 and 3 days **(D,E)**. Levels of Bcl-2 ($^{**}p < 0.01$; **D**) and Bcl-2/BAX ratio ($^{***}p < 0.001$; **E**) were found to be increased in IPostE rats at 1 and 3 days; similar results were seen with MPostE. $^{\#}$ and $^{\#\#}$ represent IPostE vs. MPostE.

pre-ischemic exercise conditioning, is also capable of inducing neuroprotective effects.

Previous studies have demonstrated that post-myocardial injury exercise exerted beneficial postconditioning effects by decreasing inflammatory reactions and ameliorating antioxidative statuses (Szabo et al., 2019), and also played a beneficial role in reducing liver carcinogenesis (Aguiar e Silva et al., 2012). A recent study indicated that exercise postconditioning after doxorubicin suppressed doxorubicin-induced cardiotoxicity (Lee et al., 2020). Another indicated the involvement of the BDNF/TrkB pathway in the increased myocardial angiogenesis and improved cardiac function seen in rats the exercised after myocardial infarction (Wang et al., 2018). These pieces of evidence imply the role of exercise postconditioning as a beneficial post-stroke intervention. Our previous

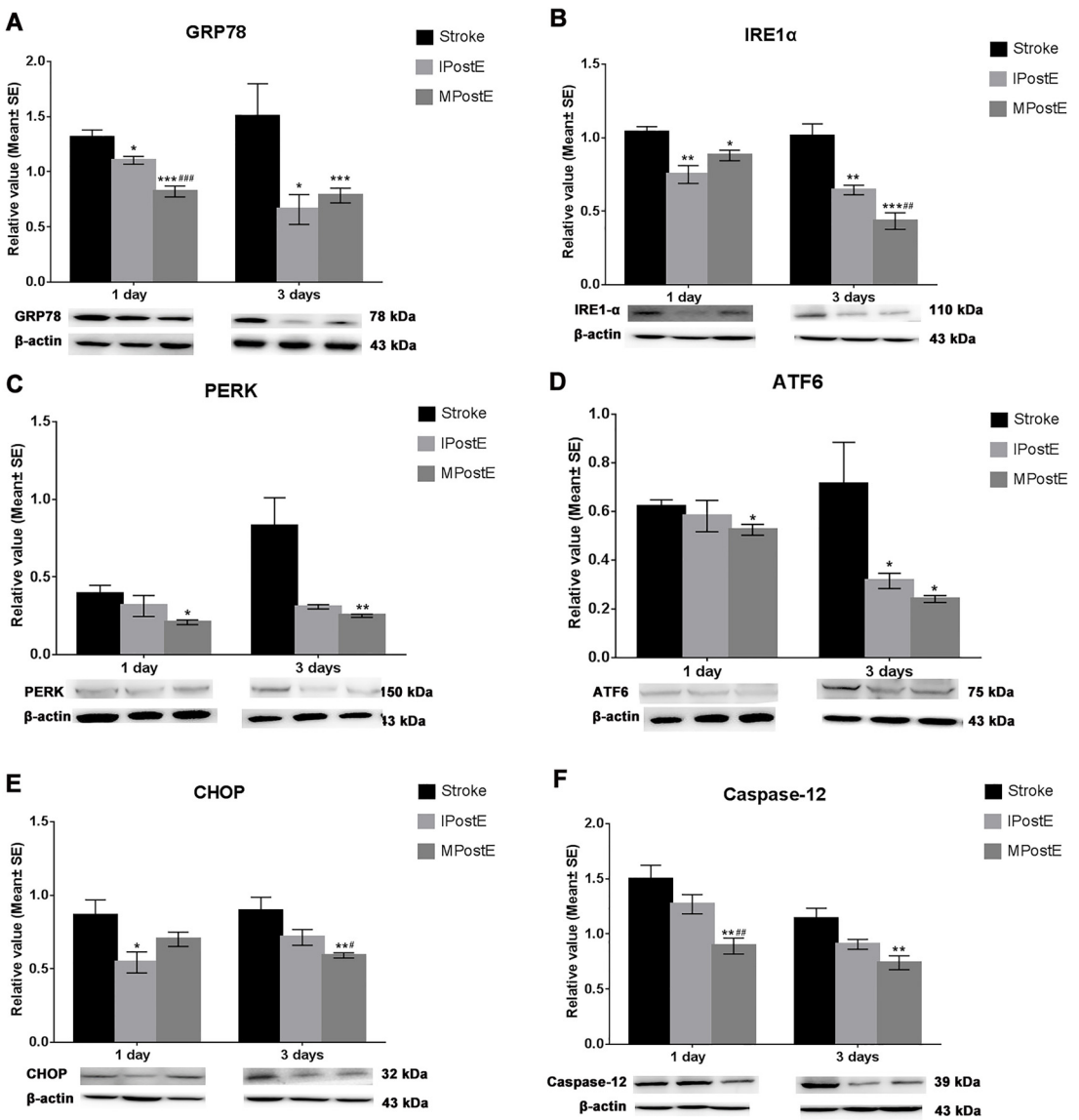

FIGURE 3 | Expression of endoplasmic reticulum (ER) stress. Both mild and intense PostE yielded a significant decrease in ER stress protein levels at 1 and 3 days. Compared to the stroke group, levels of **(A)** GRP78 (*$p < 0.05$, 1 and 3 days), **(B)** IRE1α (**$p < 0.01$, 1 and 3 days), **(C)** PERK, **(D)** ATF6 (*$p < 0.05$, 3 days), **(E)** CHOP (*$p < 0.05$, 1 day) and **(F)** Caspase-12 were significantly decreased in IPostE groups ($n = 7$ respectively). Similar results were also seen in the MPostE group. The protein levels were further decreased in the MPostE group compared to the IPostE group. The significance of the decreases were as follows: **(A)** GRP78 ($^{\#\#\#}p < 0.001$, 1 day), **(B)** IRE1α ($^{\#\#}p < 0.01$, 3 days), **(E)** CHOP (*$p < 0.05$, 3 days) and **(F)** Caspase-12 (*$p < 0.05$, 1 day). *** represents MPostE or IPostE vs. stroke; $^{\#}$ represents IPostE vs. MPostE.

studies support these findings and this notion as they demonstrated that exercise improved metabolism and decreased neuroinflammation at 1 and 3 days after stroke (Li et al., 2017a; Li F. et al., 2020). Although a rota-rod exercise style was used, both early intense and mild exercise conferred the similar neuroprotective effect by minimizing brain damage and apoptosis (Li et al., 2017c). The present results were further supported by the results of other groups, which indicated that various types and intensities of early exercise postconditioning accelerated CBF (Pianta et al., 2019), decreased infarct volume (Tian et al., 2013; Pan et al., 2020) and improved functional outcomes (Pianta et al., 2019). However, a few studies claimed that no obvious improvements were found after post-stroke exercise treatment on brain infarct and recovery (Matsuda et al., 2011; Cui et al., 2020). These studies employed models of 90-min ischemia or permanent MCAO models in their exercise procedures, whereas we used a model of 120 min temporary ischemia and induced a relatively small size of infarction. These differences may explain the lack of significant differences observed after exercise. Also, the relatively low intensity of the

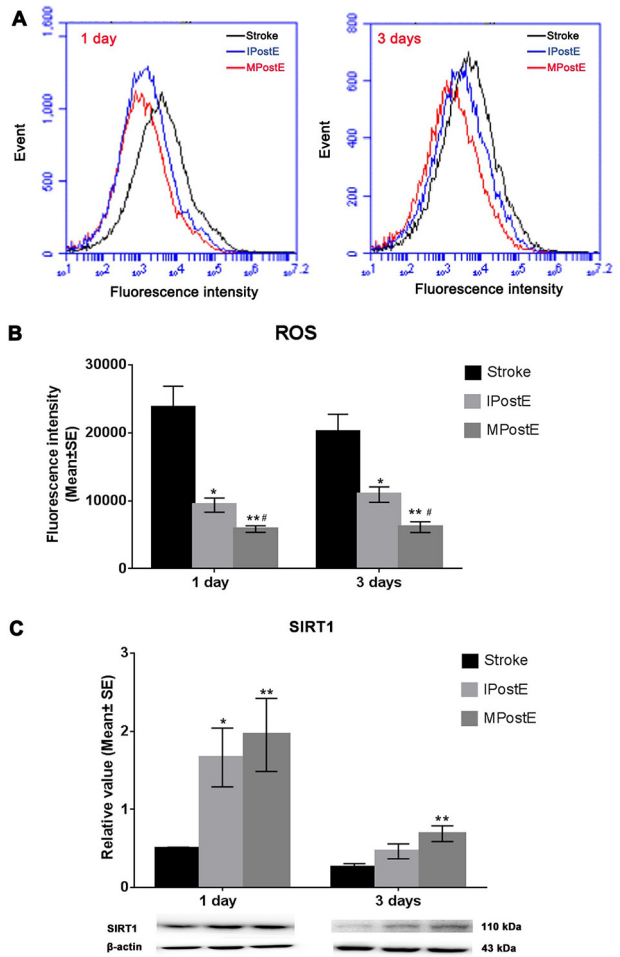

FIGURE 4 | ROS production and SIRT1 expression. **(A,B)** Flow cytometry assay demonstrated that both mild and intense PostE groups observed decreased ROS production at 1 and 3 days ($n = 7$ respectively, $^{*}p < 0.05$); between the two groups, MPostE further significantly decreased ROS production ($^{*}p < 0.05$). **(C)** Compared to the stroke group, levels of SIRT1 in MPostE groups were significantly increased ($n = 7$ respectively, $^{*}p < 0.05$, 1 day; $^{**}p < 0.01$, 3 days). Similar results were also seen with IPostE. $^{\#}$represents IPostE vs. MPostE.

rota-rod training model or insufficient exercise duration used in their exercise procedures may contribute to the discrepancy of these conclusions with our present results. This perspective was also supported by our previous studies, in which the early high-intensity rota-rod exercise exacerbated brain damage in the short-term. We demonstrated that early post-stroke exercise enhanced apoptosis through the expression of proapoptotic proteins (Li et al., 2017c) and aggravated brain damage through hyperglycolysis and NOX activation (Shen et al., 2016). Thus, the apparent inconsistencies in the effect of exercise training on brain infarct and recovery may due to the discrepancies in the duration, timing, or style of post-stroke exercise (Li et al., 2017a). Future studies are necessary to fully elucidate the effect of post-stroke exercise on brain injury and the optimal parameters for this proposed therapy. Additionally, future studies are needed to examine the impact of varying exercise intensities on other markers and participants of ER stress, such as molecular chaperones (e.g., GRP78) and caspases (e.g., caspase-9 and 12).

Previous studies have also found that the neurological outcomes of post-stroke exercise differed according to the exercise regimen intensities (Bell et al., 2015; Xing et al., 2018). Of these, some claimed that higher intensity exercise post-stroke yielded better functional recovery (Luo et al., 2019; Andrews et al., 2020), while others suggested that mild exercise resulted in superior neuroprotection (Lee et al., 2009; Shih et al., 2013), citing that exercise that is too intense may cause spikes in endogenous corticosteroid levels that limit post-stroke neurogenesis (Yagita et al., 2006). In no strong agreement with either of these findings, the present results indicated similar neuroprotective effects of both mild and intense doses of exercise postconditioning, although mild exercise did periodically have greater protection against apoptotic cell death. The protocol with two doses utilized in the present study was partially based on the previous studies on exercise intensity from us (Curry et al., 2010; Li F. et al., 2020) and others (Zhang et al., 2012; Gronwald et al., 2019). Following the principle that physical exercise regimens are reproducible (Gronwald et al., 2019), we set the highest achievable exercise training intensity to be the speed at which the rats could no longer run due to fatigue within 3 min of exercise onset. The therapeutic doses of physical exercise training used in our study were calculated as 40% of this maximum velocity for mild exercise training, which amounted to approximately 15 m/min, and 80% of the maximum velocity for intense exercise training, which was about 32 m/min (Zhang et al., 2012; Li F. et al., 2020). To further accentuate the difference between the two categories, we reduced the mild exercise group's speed to a maximum of 12 m/min as done by previous studies (Tian et al., 2013; Zhang et al., 2017; Tang et al., 2018; Li F. et al., 2020). For the high-intensity group, we selected 30 m/min because we have employed this speed in our previous work, in which we found that it reduced brain damage (Ding et al., 2006), blood-brain barrier dysfunction (Guo et al., 2008), and brain inflammation in stroke (Curry et al., 2010). Another key finding from our previous work was the influence of initiation time on post-stroke rehabilitation outcomes: initiation of exercise 6 h post-stroke exacerbated brain damage, while exercise deferment for 1–3 days avoided exacerbation of brain damage (Li et al., 2017a, Li F. et al., 2020). Therefore, an initiation time of 24 h after stroke was selected for this study.

In this study, we aimed to observe the short-term neuroprotective effect of post-stroke exercise conditioning on the infarcted brain. Previous studies have indicated that post-stroke days 1–3 are critical timepoints at which exercise both decreases brain damage and improves functional outcomes. Indeed, this time range avoids the brain damage exacerbation seen in very early exercise interventions while preserving the benefit of prompt post-stroke rehabilitation (Li et al., 2017a). Also, in our recent reports (Li F. et al., 2020), we have compared the long-term effects of these two exercise procedures for up to 28 days, which is the commonly used time point for long-term outcomes. In our future study, we may explore the

long-term effect of the exercise protocol by expanding it to 60 days after focal cerebral ischemia to investigate the benefits of expanding the therapeutic timeframe. This will allow us to determine whether postconditioning can also impact the remodeling processes that are crucial to long-term recovery from a cerebrovascular event.

The alterations in apoptotic death protein levels observed in the present study aligned with the current understanding of brain injury reduction, which is accomplished by time-sensitive, early suppression of neural apoptosis in the penumbra during the early stages of ischemia (Uzdensky, 2020). Previous studies have reported that ischemic or exercise conditioning suppresses neural apoptosis by regulating the expression of pro-and anti-apoptotic proteins (Zhou et al., 2011; Terashi et al., 2019). Our previous studies have indicated that early transient post-stroke exercise also reduces brain infarct in the penumbra by mediating the expression of pro-and anti-apoptotic proteins to favor functional recovery (Li et al., 2017a,c). Upregulation of anti-apoptotic proteins such as Bcl-2 in conjunction with an increased Bcl-2/BAX ratio appears to play a key role in reducing damage from ischemic injury and enabling rehabilitation (Ruan et al., 2020). Bcl-2 serves as a regulator of apoptosis-regulatory proteins such as caspase-3, which is an aspartate-specific cysteine protease that serves as an important executioner in cell death (Yang et al., 2019). Exercise preconditioning has been reported to reduce brain damage and neuronal apoptosis through enhancing the Bcl-2/Bax ratio and suppressing caspase-3 after focal brain ischemia in rats (Otsuka et al., 2019; Terashi et al., 2019). A series of studies have also shown that ischemic pre- or postconditioning alleviated ischemia/reperfusion injury by suppressing BAX-mediated apoptosis (Zhou et al., 2011; Zhang et al., 2018). Hence, the concurrent enhancement of Bcl-2 and suppression of proapoptotic factors such as caspase-3 and BAX may be contributing to the decrease of neuronal cell death following ischemic stroke. Therapies that catalyze the restorative mechanisms and suppress the apoptotic processes are thereby likely to encourage recovery from ischemic stroke and minimize acquired disability.

ER stress is one of the complex sets of mechanisms involved in apoptosis (Zheng et al., 2018). Activation of ER stress is stimulated by the upregulation of GRP78, which subsequently induces apoptosis signaling mediated by CHOP and caspase-12 through IRE1α-XBP-1, PERK-ATF4, and ATF6-dependent pathways (Zhang and Kaufman, 2008). Caspase-12 regulates ER stress-induced apoptosis signaling by activating caspase-9, which consequently activates caspase-3 (Datta et al., 2018; Rong et al., 2020). CHOP, a transcription factor, activates the expression of anti-apoptotic and pro-apoptotic proteins including those of the Bcl-2 family (Coker-Gurkan et al., 2019). Previous studies showed that ischemic postconditioning ameliorated cerebral ischemic injury by favoring these ER-stress-mediated anti-apoptotic, rather than pro-apoptotic mechanisms (Mahfoudh-Boussaid et al., 2012; Liu et al., 2014). Exercise preconditioning also exerted a cardioprotective effect *via* alleviating apoptosis regulated by ER stress (Korzeniowska Kubacka, 2011). These results are as per the present study, which showed that exercise post-conditioning mediated a decrease in the ER stress pathway, suggesting a potential anti-apoptotic mechanism of neuroprotection after stroke.

The cause-effect relationship between ROS and ER stress signaling has been well studied (Cao et al., 2018; Park et al., 2020); ROS was reported to be a potent trigger of ER stress and to subsequently induce apoptosis in cerebral ischemic stroke (Shi et al., 2019; Wei et al., 2019). SIRT1 was reported to suppress ROS release (Park et al., 2020), which protects the heart from ER stress-induced apoptosis (Pires Da Silva et al., 2020). The protective effects of ischemic postconditioning and post-myocardial infarction exercise were accomplished by enhancing SIRT1 expression (Ahsan et al., 2019; Ding et al., 2019), indicating its potential regulative role in protective post-stroke exercise. These previous studies and the strong inverse correlation of SIRT1 and ER stress protein expression observed in the present study suggests an association of SIRT1 and ER stress pathway in exercise postconditioning-induced neuroprotection. The link of SIRT1 to ER stress molecules was relatively weak in the present study. Our further investigation will additionally address the cause-and-effect link between SIRT1 and ER stress pathways by using both SIRT1 gene knockout animals and a SIRT1 inhibitor. This will enable us to examine the extent of the impact of SIRT1 on ER stress. Also, the interaction of these molecules will be determined, which will clarify the mechanisms that facilitate the ER stress pathway. Although we did not explicitly study the regulation of SIRT1 on the ER stress pathway, our results suggest a potential link between the molecules. Our findings could be a basis to further clarify the participation of SIRT1 in ER stress in stroke.

In conclusion, this study confirmed the beneficial effect of exercise postconditioning with either intense or mild doses after stroke. Our results further demonstrated that intense exercise postconditioning did not confer superior benefits to its milder counterpart, suggesting that an easier procedure with mild exercise conditions would be an appropriate protocol for stroke rehabilitation procedure. Moreover, the results may provide a base for our future study regarding the regulation of SIRT1 on the ER stress pathway in the biochemical processes underlying exercise postconditioning-induced neuroprotection.

DATA AVAILABILITY STATEMENT

The raw data supporting the conclusions of this article will be made available by the authors, without undue reservation.

ETHICS STATEMENT

The animal study was reviewed and approved by the Animal Care and Use Committee of the Capital Medical University.

AUTHOR CONTRIBUTIONS

FL conducted the animal and biochemical experiments employed in this research. FL, XG, HL, and MW were instrumental in preparing and revising the manuscript. YD was responsible

for the experimental design, manuscript preparation, and revision. All authors contributed to the article and approved the submitted version.

FUNDING

This work was partially supported by the National Natural Science Foundation of China (81802231, 81871838, 82002382), the Organization Department of Beijing talents project (2018000082595G485), the Beijing Tongzhou District Financial Fund, and the Science and Technology Plan of Beijing Tongzhou District (KJ2020CX002).

ACKNOWLEDGMENTS

The authors thank Yanna Tong, Sainan Wang, Menglei Liu, Yanlong Zhao, and Chencheng Zhang for technical assistance.

SUPPLEMENTARY MATERIAL

The Supplementary Material for this article can be found online at: https://www.frontiersin.org/articles/10.3389/fncel.2021.598230/full#supplementary-material.

REFERENCES

Aguiar e Silva, M. A., Vechetti-Junior, I. J., Nascimento, A. F., Furtado, K. S., Azevedo, L., Ribeiro, D. A., et al. (2012). Effects of swim training on liver carcinogenesis in male Wistar rats fed a low-fat or high-fat diet. *Appl. Physiol. Nutr. Metab.* 37, 1101–1109. doi: 10.1139/h2012-129

Ahsan, A., Zheng, Y. R., Wu, X. L., Tang, W. D., Liu, M. R., Ma, S. J., et al. (2019). Urolithin A-activated autophagy but not mitophagy protects against ischemic neuronal injury by inhibiting ER stress *in vitro* and *in vivo*. *CNS Neurosci. Ther.* 25, 976–986. doi: 10.1111/cns.13136

Andrews, S. C., Curtin, D., Hawi, Z., Wongtrakun, J., Stout, J. C., and Coxon, J. P. (2020). Intensity matters: high-intensity interval exercise enhances motor cortex plasticity more than moderate exercise. *Cereb. Cortex* 30, 101–112. doi: 10.1093/cercor/bhz075

Bell, J. A., Wolke, M. L., Ortez, R. C., Jones, T. A., and Kerr, A. L. (2015). Training intensity affects motor rehabilitation efficacy following unilateral ischemic insult of the sensorimotor cortex in C57BL/6 mice. *Neurorehabil. Neural Repair* 29, 590–598. doi: 10.1177/1545968314553031

Boyne, P., Dunning, K., Carl, D., Gerson, M., Khoury, J., Rockwell, B., et al. (2016). High-intensity interval training and moderate-intensity continuous training in ambulatory chronic stroke: feasibility study. *Phys. Ther.* 96, 1533–1544. doi: 10.2522/ptj.20150277

Cao, R., Wang, G., Qian, K., Chen, L., Ju, L., Qian, G., et al. (2018). TM4SF1 regulates apoptosis, cell cycle and ROS metabolism *via* the PPARγ-SIRT1 feedback loop in human bladder cancer cells. *Cancer Lett.* 414, 278–293. doi: 10.1016/j.canlet.2017.11.015

Chen, C., Chencheng, Z., Cuiying, L., and Xiaokun, G. (2020). Plasmacytoid dendritic cells protect against middle cerebral artery occlusion induced brain injury by priming regulatory T cells. *Front. Cell. Neurosci.* 14:8. doi: 10.3389/fncel.2020.00008

Chen, C., Jiang, W., Liu, Z., Li, F., Yang, J., Zhao, Y., et al. (2018). Splenic responses play an important role in remote ischemic preconditioning-mediated neuroprotection against stroke. *J. Neuroinflammation* 15:167. doi: 10.1186/s12974-018-1190-9

Chen, W. Y., Wang, D. H., Yen, R. C., Luo, J., Gu, W., and Baylin, S. B. (2005). Tumor suppressor HIC1 directly regulates SIRT1 to modulate p53-dependent DNA-damage responses. *Cell* 123, 437–448. doi: 10.1016/j.cell.2005.08.011

Chi, L., Jiao, D., Nan, G., Yuan, H., Shen, J., and Gao, Y. (2019). MiR-9-5p attenuates ischemic stroke through targeting ERMP1-mediated endoplasmic reticulum stress. *Acta Histochem.* 121:151438. doi: 10.1016/j.acthis.2019.08.005

Chu, Q., Martinez, T. F., Novak, S. W., Donaldson, C. J., Tan, D., Vaughan, J. M., et al. (2019). Regulation of the ER stress response by a mitochondrial microprotein. *Nat. Commun.* 10:4883. doi: 10.1038/s41467-019-12816-z

Coker-Gurkan, A., Ayhan-Sahin, B., Keceloglu, G., Obakan-Yerlikaya, P., Arisan, E. D., and Palavan-Unsal, N. (2019). Atiprimod induce apoptosis in pituitary adenoma: endoplasmic reticulum stress and autophagy pathways. *J. Cell. Biochem.* 120, 19749–19763. doi: 10.1002/jcb.29281

Cui, J., Kim, C. S., Kim, Y., Sohn, M. K., and Jee, S. (2020). Effects of repetitive transcranial magnetic stimulation (rTMS) combined with aerobic exercise on the recovery of motor function in ischemic stroke rat model. *Brain Sci.* 10:186. doi: 10.3390/brainsci10030186

Curry, A., Guo, M., Patel, R., Liebelt, B., Sprague, S., Lai, Q., et al. (2010). Exercise pre-conditioning reduces brain inflammation in stroke *via* tumor necrosis factor-alpha, extracellular signal-regulated kinase 1/2 and matrix metalloproteinase-9 activity. *Neurol. Res.* 32, 756–762. doi: 10.1179/174313209X459101

Datta, D., Khatri, P., Singh, A., Saha, D. R., Verma, G., Raman, R., et al. (2018). Mycobacterium fortuitum-induced ER-Mitochondrial calcium dynamics promotes calpain/caspase-12/caspase-9 mediated apoptosis in fish macrophages. *Cell Death Discov.* 4:30. doi: 10.1038/s41420-018-0034-9

Davis, W., Mahale, S., Carranza, A., Cox, B., Hayes, K., Jimenez, D., et al. (2007). Exercise pre-conditioning ameliorates blood-brain barrier dysfunction in stroke by enhancing basal lamina. *Neurol. Res.* 29, 382–387. doi: 10.1179/016164107X204701

Ding, M., Hu, L., Yang, H., Gao, C., Zeng, K., Yu, M., et al. (2019). Reduction of SIRT1 blunts the protective effects of ischemic post-conditioning in diabetic mice by impairing the Akt signaling pathway. *Biochim. Biophys. Acta Mol. Basis Dis.* 1865, 1677–1689. doi: 10.1016/j.bbadis.2019.04.005

Ding, Y. H., Mrizek, M., Lai, Q., Wu, Y., and Reyes, R. Jr. (2006). Exercise preconditioning reduces brain damage and inhibits TNF-α receptor expression after hypoxia/reoxygenation: an *in vivo* and *in vitro* study. *Curr. Neurovasc. Res.* 3, 263–271. doi: 10.2174/156720206778792911

El Hayek, L., Khalifeh, M., Zibara, V., Abi Assaad, R., Emmanuel, N., Karnib, N., et al. (2019). Lactate mediates the effects of exercise on learning and memory through SIRT1-dependent activation of hippocampal brain-derived neurotrophic factor (BDNF). *J. Neurosci.* 39, 2369–2382. doi: 10.1523/JNEUROSCI.1661-18.2019

Gong, L., Tang, Y., An, R., Lin, M., Chen, L., and Du, J. (2017). RTN1-C mediates cerebral ischemia/reperfusion injury *via* ER stress and mitochondria-associated apoptosis pathways. *Cell Death Dis.* 8:e3080. doi: 10.1038/cddis.2017.465

Gronwald, T., de Bem Alves, A. C., Murillo-Rodriguez, E., Latini, A., Schuette, J., and Budde, H. (2019). Standardization of exercise intensity and consideration of a dose-response is essential. Commentary on "exercise-linked FNDC5/irisin rescues synaptic plasticity and memory defects in Alzheimer's models", by Lourenco et al., published 2019 in nature medicine. *J. Sport Health Sci.* 8, 353–354. doi: 10.1016/j.jshs.2019.03.006

Guo, M., Lin, V., Davis, W., Huang, T., Carranza, A., Sprague, S., et al. (2008). Preischemic induction of TNF-α by physical exercise reduces blood-brain barrier dysfunction in stroke. *J. Cereb. Blood Flow Metab.* 28, 1422–1430. doi: 10.1038/jcbfm.2008.29

Guo, L., Zhou, D., Wu, D., Ding, J., He, X., Shi, J., et al. (2019). Short-term remote ischemic conditioning may protect monkeys after ischemic stroke. *Ann. Clin. Transl. Neurol.* 6, 310–323. doi: 10.1002/acn3.705

Hafez, S., Khan, M. B., Awad, M. E., Wagner, J. D., and Hess, D. C. (2019). Short-term acute exercise preconditioning reduces neurovascular injury after stroke through induced eNOS activation. *Transl. Stroke Res.* 11, 851–860. doi: 10.1007/s12975-019-00767-y

Jia, D., Hou, L., Lv, Y., Xi, L., and Tian, Z. (2019). Postinfarction exercise training alleviates cardiac dysfunction and adverse remodeling *via* mitochondrial biogenesis and SIRT1/PGC-1α/PI3K/Akt signaling. *J. Cell. Physiol.* 234, 23705–23718. doi: 10.1002/jcp.28939

Korzeniowska Kubacka, I. (2011). Physical training as an effective way to protect the heart against ischaemia. *Kardiol. Pol.* 69, 75–79.

Landman, T., Schoon, Y., Warle, M., De Leeuw, F. E., and Thijssen, D. (2019). The effect of repeated remote ischemic postconditioning on infarct size in patients with an ischemic stroke (REPOST): study protocol for a randomized clinical trial. *Trials* 20:167. doi: 10.1186/s13063-019-3264-0

Lee, J. M., Baek, S. S., Kim, T. W., Park, H. S., Park, S. S., Park, J. M., et al. (2019). Preischemic treadmill exercise improves short-term memory by inhibiting hypoperfusion-induced disruption of blood-brain barrier after bilateral common carotid arteries occlusion. *J. Exerc. Rehabil.* 15, 370–376. doi: 10.12965/jer.1938274.137

Lee, S. U., Kim, D. Y., Park, S. H., Choi, D. H., Park, H. W., and Han, T. R. (2009). Mild to moderate early exercise promotes recovery from cerebral ischemia in rats. *Can. J. Neurol. Sci.* 36, 443–449. doi: 10.1017/s0317167100007769

Lee, Y., Kwon, I., Jang, Y., Cosio-Lima, L., and Barrington, P. (2020). Endurance exercise attenuates doxorubicin-induced cardiotoxicity. *Med. Sci. Sports Exerc.* 52, 25–36. doi: 10.1249/MSS.0000000000002094

Lemoine, S., Blanchart, K., Souplis, M., Lemaitre, A., Legallois, D., Coulbault, L., et al. (2017). Argon exposure induces postconditioning in myocardial ischemia-reperfusion. *J. Cardiovasc. Pharmacol. Ther.* 22, 564–573. doi: 10.1177/1074248417702891

Li, F., Geng, X., Huber, C., Stone, C., and Ding, Y. (2020). In search of a dose: the functional and molecular effects of exercise on post-stroke rehabilitation in rats. *Front. Cell. Neurosci.* 14:186. doi: 10.3389/fncel.2020.00186

Li, F., Geng, X., Khan, H., Pendy, J. T. Jr., Peng, C., Li, X., et al. (2017a). Exacerbation of brain injury by post-stroke exercise is contingent upon exercise initiation timing. *Front. Cell. Neurosci.* 11:311. doi: 10.3389/fncel.2017.00311

Li, F., Pendy, J. T. Jr., Ding, J. N., Peng, C., Li, X., Shen, J., et al. (2017b). Exercise rehabilitation immediately following ischemic stroke exacerbates inflammatory injury. *Neurol. Res.* 39, 530–537. doi: 10.1080/01616412.2017.1315882

Li, F., Shi, W., Zhao, E. Y., Geng, X., Li, X., Peng, C., et al. (2017c). Enhanced apoptosis from early physical exercise rehabilitation following ischemic stroke. *J. Neurosci. Res.* 95, 1017–1024. doi: 10.1002/jnr.23890

Li, F., Geng, X., Yip, J., and Ding, Y. (2019a). Therapeutic target and cell-signal communication of chlorpromazine and promethazine in attenuating blood-brain barrier disruption after ischemic stroke. *Cell Transplant.* 28, 145–156. doi: 10.1177/0963689718819443

Li, F., Yang, Z., Stone, C., Ding, J. Y., Previch, L., Shen, J., et al. (2019b). Phenothiazines enhance the hypothermic preservation of liver grafts: a pilot *in vitro* study. *Cell. Transplant* 28, 318–327. doi: 10.1177/0963689718824559

Li, Y., Zhang, Y., Fu, H., Huang, H., Lu, Q., Qin, H., et al. (2020). Hes1 knockdown exacerbates ischemic stroke following tMCAO by increasing ER stress-dependent apoptosis *via* the PERK/eIF2alpha/ATF4/CHOP signaling pathway. *Neurosci. Bull.* 36, 134–142. doi: 10.1007/s12264-019-00411-7

Liu, C., Yang, J., Zhang, C., Geng, X., and Zhao, H. (2020). Remote ischemic conditioning reduced cerebral ischemic injury by modulating inflammatory responses and ERK activity in type 2 diabetic mice. *Neurochem. Int.* 135:104690. doi: 10.1016/j.neuint.2020.104690

Liu, X., Zhao, S., Liu, F., Kang, J., Xiao, A., Li, F., et al. (2014). Remote ischemic postconditioning alleviates cerebral ischemic injury by attenuating endoplasmic reticulum stress-mediated apoptosis. *Transl. Stroke Res.* 5, 692–700. doi: 10.1007/s12975-014-0359-5

Luo, L., Li, C., Deng, Y., Wang, Y., Meng, P., and Wang, Q. (2019). High-intensity interval training on neuroplasticity, balance between brain-derived neurotrophic factor and precursor brain-derived neurotrophic factor in poststroke depression rats. *J. Stroke Cerebrovasc. Dis.* 28, 672–682. doi: 10.1016/j.jstrokecerebrovasdis.2018.11.009

Mahfoudh-Boussaid, A., Zaouali, M. A., Hauet, T., Hadj-Ayed, K., Miled, A. H., Ghoul-Mazgar, S., et al. (2012). Attenuation of endoplasmic reticulum stress and mitochondrial injury in kidney with ischemic postconditioning application and trimetazidine treatment. *J. Biomed. Sci.* 19:71. doi: 10.1186/1423-0127-19-71

Matsuda, F., Sakakima, H., and Yoshida, Y. (2011). The effects of early exercise on brain damage and recovery after focal cerebral infarction in rats. *Acta Physiol.* 201, 275–287. doi: 10.1111/j.1748-1708.2010.02174.x

Mohammed Thangameeran, S. I., Tsai, S. T., Hung, H. Y., Hu, W. F., Pang, C. Y., Chen, S. Y., et al. (2020). A role for endoplasmic reticulum stress in intracerebral hemorrhage. *Cells* 9:750. doi: 10.3390/cells9030750

Nie, J., Yang, X., Tang, Q., Shen, Q., and Li, S. (2016). Willed-movement training reduces brain damage and enhances synaptic plasticity related proteins synthesis after focal ischemia. *Brain Res. Bull.* 120, 90–96. doi: 10.1016/j.brainresbull.2015.11.004

Otsuka, S., Sakakima, H., Sumizono, M., Takada, S., Terashi, T., and Yoshida, Y. (2016). The neuroprotective effects of preconditioning exercise on brain damage and neurotrophic factors after focal brain ischemia in rats. *Behav. Brain Res.* 303, 9–18. doi: 10.1016/j.bbr.2016.01.049

Otsuka, S., Sakakima, H., Terashi, T., Takada, S., Nakanishi, K., and Kikuchi, K. (2019). Preconditioning exercise reduces brain damage and neuronal apoptosis through enhanced endogenous 14-3-3γ after focal brain ischemia in rats. *Brain Struct. Funct.* 224, 727–738. doi: 10.1007/s00429-018-1800-4

Pan, G., Jin, L., Shen, W., Zhang, J., Pan, J., Cheng, J., et al. (2020). Treadmill exercise improves neurological function by inhibiting autophagy and the binding of HMGB1 to Beclin1 in MCAO juvenile rats. *Life Sci.* 243:117279. doi: 10.1016/j.lfs.2020.117279

Park, S., Shin, J., Bae, J., Han, D., Park, S. R., Shin, J., et al. (2020). SIRT1 alleviates LPS-induced IL-1β production by suppressing NLRP3 inflammasome activation and ROS production in trophoblasts. *Cells* 9:728. doi: 10.3390/cells9030728

Pianta, S., Lee, J. Y., Tuazon, J. P., Castelli, V., Mantohac, L. M., Tajiri, N., et al. (2019). A short bout of exercise prior to stroke improves functional outcomes by enhancing angiogenesis. *Neuromolecular Med.* 21, 517–528. doi: 10.1007/s12017-019-08533-x

Pin-Barre, C., Constans, A., Brisswalter, J., Pellegrino, C., and Laurin, J. (2017). Effects of high- versus moderate-intensity training on neuroplasticity and functional recovery after focal ischemia. *Stroke* 48, 2855–2864. doi: 10.1161/STROKEAHA.117.017962

Pires Da Silva, J., Monceaux, K., Guilbert, A., Gressette, M., Piquereau, J., Novotova, M., et al. (2020). SIRT1 protects the heart from ER stress-induced injury by promoting eEF2K/eEF2-dependent autophagy. *Cells* 9:426. doi: 10.3390/cells9020426

Rong, C., Wei, W., and Yu-Hong, T. (2020). Asperuloside exhibits a novel anti-leukemic activity by triggering ER stress-regulated apoptosis *via* targeting GRP78. *Biomed. Pharmacother.* 125:109819. doi: 10.1016/j.biopha.2020.109819

Ruan, W., Hu, J., Zhou, H., Li, Y., Xu, C., Luo, Y., et al. (2020). Intranasal wnt-3a alleviates neuronal apoptosis in early brain injury post subarachnoid hemorrhage *via* the regulation of wnt target PPAN mediated by the moonlighting role of aldolase C. *Neurochem. Int.* 134:104656. doi: 10.1016/j.neuint.2019.104656

Sakakima, H. (2019). Endogenous neuroprotective potential due to preconditioning exercise in stroke. *Phys. Ther. Res.* 22, 45–52. doi: 10.1298/ptr.R0006

Serviddio, G., Romano, A. D., Gesualdo, L., Tamborra, R., Di Palma, A. M., Rollo, T., et al. (2008). Postconditioning is an effective strategy to reduce renal ischaemia/reperfusion injury. *Nephrol. Dial. Transplant.* 23, 1504–1512. doi: 10.1093/ndt/gfm779

Shen, J., Huber, M., Zhao, E. Y., Peng, C., Li, F., Li, X., et al. (2016). Early rehabilitation aggravates brain damage after stroke *via* enhanced activation of nicotinamide adenine dinucleotide phosphate oxidase (NOX). *Brain Res.* 1648, 266–276. doi: 10.1016/j.brainres.2016.08.001

Shi, W. Z., Tian, Y., and Li, J. (2019). GCN2 suppression attenuates cerebral ischemia in mice by reducing apoptosis and endoplasmic reticulum (ER) stress through the blockage of FoxO3a-regulated ROS production. *Biochem. Biophys. Res. Commun.* 516, 285–292. doi: 10.1016/j.bbrc.2019.05.181

Shih, P. C., Yang, Y. R., and Wang, R. Y. (2013). Effects of exercise intensity on spatial memory performance and hippocampal synaptic plasticity in transient brain ischemic rats. *PLoS One* 8:e78163. doi: 10.1371/journal.pone.0078163

Szabo, R., Borzsei, D., Karacsonyi, Z., Gesztelyi, R., Nemes, K., Berko, A. M., et al. (2019). Postconditioning-like effect of exercis: new paradigm in experimental menopause. *Am. J. Physiol. Heart Circ. Physiol.* 316, H400–H407. doi: 10.1152/ajpheart.00485.2018

Tang, Y., Zhang, Y., Zheng, M., Chen, J., Chen, H., and Liu, N. (2018). Effects of treadmill exercise on cerebral angiogenesis and MT1-MMP expression after cerebral ischemia in rats. *Brain Behav.* 8:e01079. doi: 10.1002/brb3.1079

Terashi, T., Otsuka, S., Takada, S., Nakanishi, K., Ueda, K., Sumizono, M., et al. (2019). Neuroprotective effects of different frequency preconditioning exercise on neuronal apoptosis after focal brain ischemia in rats. *Neurol. Res.* 41, 510–518. doi: 10.1080/01616412.2019.1580458

Thijssen, D. H. J., Redington, A., George, K. P., Hopman, M. T. E., and Jones, H. (2018). Association of exercise preconditioning with immediate cardioprotection: a review. *JAMA Cardiol.* 3, 169–176. doi: 10.1001/jamacardio.2017.4495

Tian, S., Zhang, Y., Tian, S., Yang, X., Yu, K., Zhang, Y., et al. (2013). Early exercise training improves ischemic outcome in rats by cerebral hemodynamics. *Brain Res.* 1533, 114–121. doi: 10.1016/j.brainres.2013.07.049

Turon, M., Abraira, L., Cazorla, S., Fonseca, E., Quintana, M., Toledo, M., et al. (2020). Vascular risk factors as independent predictors of neurocognitive impairments in patients with late-onset epilepsy who have small-vessel disease. *Epilepsy Behav.* 104:106443. doi: 10.1016/j.yebeh.2019.106443

Uzdensky, A. B. (2020). Regulation of apoptosis in the ischemic penumbra in the first day post-stroke. *Neural Regen. Res.* 15, 253–254. doi: 10.4103/1673-5374.265546

Wang, B. L., Jin, H., Han, X. Q., Xia, Y., and Liu, N. F. (2018). Involvement of brain-derived neurotrophic factor in exerciseinduced cardioprotection of post-myocardial infarction rats. *Int. J. Mol. Med.* 42, 2867–2880. doi: 10.3892/ijmm.2018.3841

Wang, J. L., Li, Y. Z., Tao, T. Q., Wang, X. R., Wang, Y., Song, D. D., et al. (2020). Postconditioning with calreticulin attenuates myocardial ischemia/reperfusion injury and improves autophagic flux. *Shock* 53, 363–372. doi: 10.1097/SHK.0000000000001387

Wang, F., Yao, S., and Xia, H. (2020). SIRT1 is a key regulatory target for the treatment of the endoplasmic reticulum stress-related organ damage. *Biomed. Pharmacother.* 130:110601. doi: 10.1016/j.biopha.2020.110601

Wei, J., Wu, X., Luo, P., Yue, K., Yu, Y., Pu, J., et al. (2019). Homer1a attenuates endoplasmic reticulum stress-induced mitochondrial stress after ischemic reperfusion injury by inhibiting the PERK pathway. *Front. Cell. Neurosci.* 13:101. doi: 10.3389/fncel.2019.00101

Xiang, B., Zhong, P., Fang, L., Wu, X., Song, Y., and Yuan, H. (2019). MiR-183 inhibits microglia activation and expression of inflammatory factors in rats with cerebral ischemia reperfusion *via* NF-kappaB signaling pathway. *Exp. Ther. Med.* 18, 2540–2546. doi: 10.3892/etm.2019.7827

Xing, Y., Yang, S. D., Dong, F., Wang, M. M., Feng, Y. S., and Zhang, F. (2018). The beneficial role of early exercise training following stroke and possible mechanisms. *Life Sci.* 198, 32–37. doi: 10.1016/j.lfs.2018.02.018

Yagita, Y., Kitagawa, K., Sasaki, T., Terasaki, Y., Todo, K., Omura-Matsuoka, E., et al. (2006). Postischemic exercise decreases neurogenesis in the adult rat dentate gyrus. *Neurosci. Lett.* 409, 24–29. doi: 10.1016/j.neulet.2006.09.040

Yang, X., Feng, P., Zhang, X., Li, D., Wang, R., Ji, C., et al. (2019). The diabetes drug semaglutide reduces infarct size, inflammation and apoptosis and normalizes neurogenesis in a rat model of stroke. *Neuropharmacology* 158:107748. doi: 10.1016/j.neuropharm.2019.107748

Zhang, A., Bai, Y., Hu, Y., Zhang, F., Wu, Y., Wang, Y., et al. (2012). The effects of exercise intensity on p-NR2B expression in cerebral ischemic rats. *Can. J. Neurol. Sci.* 39, 613–618. doi: 10.1017/s0317167100015341

Zhang, K., and Kaufman, R. J. (2008). From endoplasmic-reticulum stress to the inflammatory response. *Nature* 454, 455–462. doi: 10.1038/nature07203

Zhang, J., Xiao, F., Zhang, L., Wang, X., Lai, X., Shen, Y., et al. (2018). Alpha-lipoic acid preconditioning and ischaemic postconditioning synergistically protect rats from cerebral injury induced by ischemia and reperfusion partly *via* inhibition TLR4/MyD88/NF-κB signaling pathway. *Cell. Physiol. Biochem.* 51, 1448–1460. doi: 10.1159/000495593

Zhang, Q., Zhang, J., Yan, Y., Zhang, P., Zhang, W., and Xia, R. (2017). Proinflammatory cytokines correlate with early exercise attenuating anxiety-like behavior after cerebral ischemia. *Brain Behav.* 7:e00854. doi: 10.1002/brb3.854

Zhao, W., Li, S., Ren, C., Meng, R., and Ji, X. (2018). Chronic remote ischemic conditioning may mimic regular exercise:perspective from clinical studies. *Aging Dis.* 9, 165–171. doi: 10.14336/AD.2017.1015

Zhao, J. J., Xiao, H., Zhao, W. B., Zhang, X. P., Xiang, Y., Ye, Z. J., et al. (2018). Remote ischemic postconditioning for ischemic stroke: a systematic review and meta-analysis of randomized controlled trials. *Chin. Med. J.* 131, 956–965. doi: 10.4103/0366-6999.229892

Zheng, P., Chen, Q., Tian, X., Qian, N., Chai, P., Liu, B., et al. (2018). DNA damage triggers tubular endoplasmic reticulum extension to promote apoptosis by facilitating ER-mitochondria signaling. *Cell Res.* 28, 833–854. doi: 10.1038/s41422-018-0065-z

Zhou, Y., Fathali, N., Lekic, T., Ostrowski, R. P., Chen, C., Martin, R. D., et al. (2011). Remote limb ischemic postconditioning protects against neonatal hypoxic-ischemic brain injury in rat pups by the opioid receptor/Akt pathway. *Stroke* 42, 439–444. doi: 10.1161/STROKEAHA.110.592162

Zhu, X., Hu, H., Li, Z., Lin, R., Mao, J., and Chen, L. (2015). Gua Lou Gui Zhi decoction attenuates poststroke spasticity *via* the modulation of $GABA_B$ receptors. *Mol. Med. Rep.* 12, 5957–5962. doi: 10.3892/mmr.2015.4207

Conflict of Interest: The authors declare that the research was conducted in the absence of any commercial or financial relationships that could be construed as a potential conflict of interest.

frontiers in Aging Neuroscience

MINI REVIEW
published: 11 June 2021
doi: 10.3389/fnagi.2021.682633

The Unfolded Protein Response in Immune Cells as an Emerging Regulator of Neuroinflammation

*Dominique Fernández, Antonia Geisse, Jose Ignacio Bernales, Alonso Lira and Fabiola Osorio**

Laboratory of Immunology and Cellular Stress, Program of Immunology, Institute of Biomedical Sciences, Faculty of Medicine, Universidad de Chile, Santiago, Chile

Immune surveillance is an essential process that safeguards the homeostasis of a healthy brain. Among the increasing diversity of immune cells present in the central nervous system (CNS), microglia have emerged as a prominent leukocyte subset with key roles in the support of brain function and in the control of neuroinflammation. In fact, impaired microglial function is associated with the development of neurodegenerative diseases, including Alzheimer's disease (AD) and Parkinson's disease (PD). Interestingly, these pathologies are also typified by protein aggregation and proteostasis dysfunction at the level of the endoplasmic reticulum (ER). These processes trigger activation of the unfolded protein response (UPR), which is a conserved signaling network that maintains the fidelity of the cellular proteome. Remarkably, beyond its role in protein folding, the UPR has also emerged as a key regulator of the development and function of immune cells. However, despite this evidence, the contribution of the UPR to immune cell homeostasis, immune surveillance, and neuro-inflammatory processes remains largely unexplored. In this review, we discuss the potential contribution of the UPR in brain-associated immune cells in the context of neurodegenerative diseases.

Keywords: UPR, neurodegeneration, microglia, inflammation, neuroinflammation, protein misfolding, ER stress, immune system

OPEN ACCESS

Edited by:
Safikur Rahman, Babasaheb Bhimrao Ambedkar Bihar University, India

Reviewed by:
Naeem Khan, Western Michigan University, United States
Balaji Banoth, St. Jude Children's Research Hospital, United States

***Correspondence:**
Fabiola Osorio
fabiolaosorio@med.uchile.cl

Received: *18 March 2021*
Accepted: *10 May 2021*
Published: *11 June 2021*

Citation:
Fernández D, Geisse A, Bernales JI, Lira A and Osorio F (2021) The Unfolded Protein Response in Immune Cells as an Emerging Regulator of Neuroinflammation. Front. Aging Neurosci. 13:682633. doi: 10.3389/fnagi.2021.682633

INTRODUCTION

Protein homeostasis, also known as "proteostasis," is a set of coordinated processes that govern synthesis, quality, control and localization of cellular proteins. Up to a third of protein biosynthesis takes place in the endoplasmic reticulum (ER; Brodsky and Skach, 2011) and thereby, cells possess regulatory mechanisms that maintain proteostasis in conditions that overload the folding capacity of the organelle (a process known as "ER stress").

The main mechanism counteracting the detrimental effects of ER stress is the unfolded protein response (UPR), a signal transduction pathway that maintains the balance between the folding capacity and the secretory demand of the cell. The UPR is integrated by three ER transmembrane sensors: Inositol-Requiring Enzyme (lRE1), Protein kinase R-like ER Kinase (PERK), and Activating Transcription Factor-6 (ATF6), which are triggered by the accumulation of misfolded proteins in the ER lumen (**Figure 1**). The UPR transducers act in concert to activate transcription factors and cytosolic signaling modules aiming to restore proteostasis and increase ER biogenesis (Walter and Ron, 2011). Once activated, ATF6 translocates to the Golgi apparatus where it is cleaved by site-1 and site-2 proteases, releasing a transcription

factor termed "ATF6-N" that controls expression of ER chaperones, ER-Associated protein degradation (ERAD) components, and lipid biosynthetic genes (Ron and Walter, 2007). PERK, on the other hand, mediates protein translation shutdown *via* phosphorylation of eukaryotic initiation factor-2α (p-eIF2α), which favors selective translation of mRNAs coding for proteins involved in cell survival, ER homeostasis, and antioxidant responses (Kranz et al., 2017). One of these mRNAs encodes ATF4, a transcription factor that controls the expression of the pro-apoptotic factor CHOP (C/EBP homologous protein), and GADD34 (also known as PPP1R15a), a phosphatase 1 cofactor that mediates dephosphorylation of p-eIF2α (Novoa et al., 2001; Hetz and Papa, 2018). Finally, IRE1 is the most conserved sensor of the UPR consisting of a transmembrane protein with two domains: a serine/threonine kinase domain and an endoribonuclease (RNase) domain (Grootjans et al., 2016). The IRE1 RNase domain mediates an unconventional splicing of the mRNA coding for X-box binding protein 1 (XBP1), removing a 26-nucleotide intron, followed by ligation by RtcB ligase (Hetz and Papa, 2018). XBP1 processing results in a shift in the coding reading frame, resulting in translation of the transcription factor "XBP1 spliced" (XBP1s), a master regulator of lipid biosynthesis, ER chaperones, ER biogenesis, and ERAD genes (Lee et al., 2003; Shoulders et al., 2013). Notably, ATF6 and XBP1s can also form heterodimers, amplifying the spectra of proteostatic genes particularly ERAD components (Yamamoto et al., 2007; Shoulders et al., 2013).

Furthermore, in contexts of prolonged ER stress or upon XBP1 deficiency, IRE1 RNase broadens its substrate repertoire and cleaves additional mRNAs/microRNAs through a process termed "Regulated IRE1-Dependent Decay" (RIDD; Lu et al., 2014; Maurel et al., 2014), which regulates mRNAs related to apoptosis and inflammation, among other processes (Maurel et al., 2014). In addition, IRE1 kinase can initiate inflammatory responses through recruitment of TRAF2 (TNF receptor-associated factor 2) protein and the transcription factor NF-κB (Urano et al., 2000; Hu et al., 2006), and it also facilitates apoptosis *via* mobilization of ER Ca^{2+} (Sprooten et al., 2019).

Remarkably, the capacity of the UPR to set the threshold between cell survival and death has associated the pathway with several neurodegenerative diseases that are typified by abnormal protein aggregation (Hetz, 2021). Nevertheless, despite this evidence, it is unclear if the UPR is selectively regulated at the level of supporting cells, nerve cells, and immune cells residing in the brain. In this review, we discuss the potential role of the UPR in controlling neuroinflammation and immunity in the central nervous system (CNS).

IMMUNE-SURVEILLANCE MECHANISMS IN THE CNS

The advent of single-cell analysis has revolutionized our understanding of tissue immunity, demonstrating that the brain contains a broad diversity of immune cell types with roles in homeostasis, aging, and disease (Korin et al., 2017; Mrdjen et al., 2018).

Microglia is the most prominent resident macrophage of the brain parenchyma, where these cells coordinate synaptic pruning, neuron survival/plasticity, and apoptotic cell clearance (Colonna and Butovsky, 2017; Herz et al., 2017). Microglia initiate inflammation through pattern-recognition receptors (PRRs) that recognize noxious stimuli in the CNS (such as protein aggregates, cancer cells, or neurotropic viruses), and the signal for transcription of proinflammatory genes (Colonna and Butovsky, 2017; Prinz et al., 2019), *via* NF-κB or interferon-regulatory factors (IRFs; Reverendo et al., 2019). Relevant PRRs initiating brain inflammation include Toll-like receptors (TLR) such as TLR4 and TLR2, NOD-like receptors (NLRs), and C-type lectins including CLEC7A (Colonna and Butovsky, 2017). Additional mechanisms regulating inflammation are the signaling platforms termed "inflammasomes", which control the secretion of interleukin-1β (IL-1β) and IL-18 (Swanson et al., 2019). In fact, the inflammasome coordinated by the intracellular sensor NLRP3 (NOD-, LRR- and pyrin domain-containing protein 3) has emerged as a critical regulator of neuroinflammation (Colonna and Butovsky, 2017). As such, microglia adapt to challenges by fine-tuning inflammation, although this response deteriorates with age contributing to neurodegeneration (Scheiblich et al., 2020).

Outside the parenchymal region, there is active immune-surveillance by border-associated macrophages (BAMs), monocytes, T cells, Natural Killer (NK) cells, NKT cells, dendritic cells (DCs), and B cells (Ransohoff and Cardona, 2010; Korin et al., 2017; Mrdjen et al., 2018). BAMs carry out scavenging/patrolling functions, whereas DCs are composed of plasmacytoid DCs (pDCs), type 1 conventional DCs (cDC1s), and type 2 conventional DCs (cDC2s; Mrdjen et al., 2018). pDCs produce type-I interferons (IFN-I) to viral infection, whereas cDC1s and cDC2s elicit long–term immunity *via* antigen presentation to cytotoxic $CD8^+$ T cells and $CD4^+$ T helper cells, respectively (Mundt et al., 2019; Cabeza-Cabrerizo et al., 2021). T cells in turn protect the brain against antigens found in neurodegenerative diseases and are critical for imprinting the functional maturation of microglia (Pasciuto et al., 2020). Notably, upon inflammation, aging, and neurodegeneration, resident immune cells become activated, and the parenchyma is infiltrated by leukocytes from the periphery, which can perpetuate inflammatory responses and propagate the progression of tissue damage (Scheiblich et al., 2020; Yang et al., 2020). This evidence indicates that the CNS contains a diverse immune microenvironment that can be targeted for intervention of neurodegenerative diseases. Finally, astrocytes are CNS glial cells that also contribute to inflammation (Giovannoni and Quintana, 2020) by expressing PRRs that trigger innate immunity, including TLR4 (Sofroniew, 2020).

Notably, although the UPR is known to control the development and function of immune cells including macrophages, DCs, B cells, eosinophils, NK cells, and T cells in physiological and pathological models (Martinon et al., 2010; Cubillos-Ruiz et al., 2015; Grootjans et al., 2016; Song et al., 2018; Dong et al., 2019), little is known about how the UPR regulates

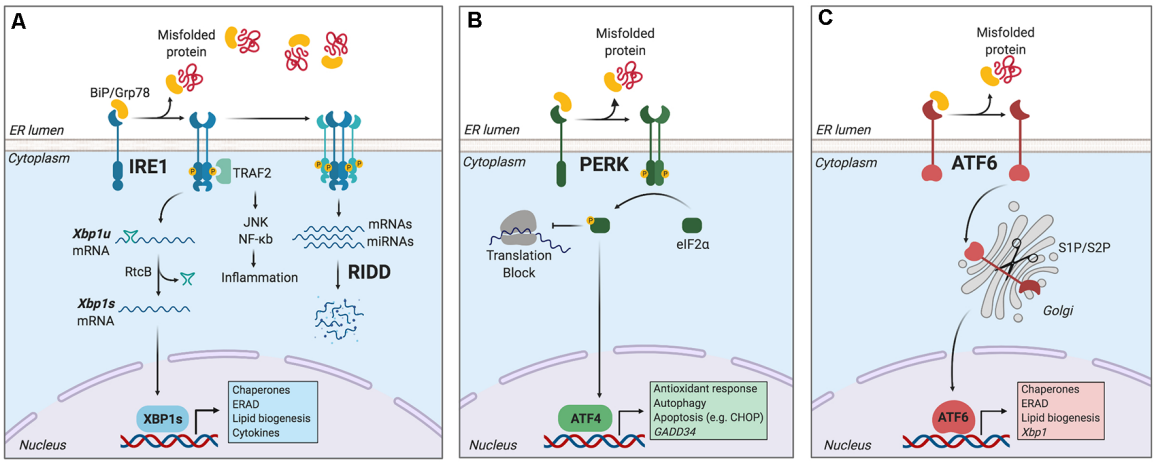

FIGURE 1 | The unfolded protein response (UPR). Endoplasmic reticulum (ER) stress induces an adaptive response known as the unfolded protein response (UPR), which is controlled by three main ER-resident sensors: IRE1, PERK, and activating transcription factor-6 (ATF6). **(A)** IRE1 is activated by oligomerization and trans-phosphorylation upon binding of unfolded proteins and release of the chaperone BiP. IRE1 autophosphorylation leads to the activation of its RNase domain and the processing of the mRNA encoding for X-box binding protein 1 (XBP1s), a transcriptional factor that upregulates genes involved in protein folding and quality control, in addition to regulating ER/Golgi biogenesis and ER-mediated degradation (ERAD), lipid biogenesis and cytokine production. Additionally, IRE1 RNase also degrades a subset of specific RNAs and microRNAs, a process termed Regulated IRE1-Dependent Decay (RIDD). **(B)** Upon activation, PERK phosphorylates the eukaryotic initiation factor-2α (eIF2α), decreasing the synthesis of proteins and the overload of misfolded proteins at the ER. PERK phosphorylation also leads to the specific translation of ATF4, a transcription factor that promotes the expression of genes related to amino acid metabolism, antioxidant response, autophagy, and apoptosis. **(C)** ATF6 is activated upon release of BiP and is translocated to the Golgi, where it undergoes sequential cleavage and removal of its luminal domain. The remaining transactivation domain of ATF6 moves to the nucleus and coordinates the expression of genes encoding ER chaperones, ER-associated protein degradation (ERAD) components, and molecules involved in lipid biogenesis. Figure created with BioRender.com.

immunity in the CNS. This is a relevant area considering that neurodegenerative diseases including Alzheimer's disease (AD), Parkinson's disease (PD), and multiple sclerosis (MS) display altered functions of several immune cell types, many of which are associated with disease progression (Ajami et al., 2018; Mrdjen et al., 2018; Scheiblich et al., 2020). Thus, modulating the UPR in immune cells during the progression of neurodegenerative diseases may have relevant implications for therapy.

THE UPR IN IMMUNE CELL FUNCTION IN PHYSIOLOGICAL AND INFLAMMATORY STATES

Although most studies connecting the UPR with immunity have focused on organs outside the CNS, some of these findings could be applied to neurodegenerative diseases.

IRE1 *via* XBP1s controls eosinophil, DC, and plasma cell development (Reimold et al., 2001; Iwakoshi et al., 2007; Bettigole et al., 2015), which contribute to neuroinflammation in MS and Experimental Autoimmune Encephalomyelitis (EAE), the mouse model of MS (Greter et al., 2005; Wensky et al., 2005; Mundt et al., 2019; Pröbstel et al., 2020). Furthermore, DCs and plasma cells show constitutive UPR activation and display an elevated protein synthesis rate in steady state (Osorio et al., 2014; Khalsa et al., 2019; Mendes et al., 2020). In these cell types, XBP1s maintains ER architecture, whereas RIDD controls functional aspects, including antigen cross-presentation and cDC1s survival, or immunoglobulin production by plasma cells (Benhamron et al., 2014; Osorio et al., 2014; Tavernier et al., 2017). PERK signaling is also active in DCs (Mendes et al., 2020), whereas ATF6 remains understudied in immunity. These findings suggest that IRE1 and PERK signaling could be targets in neuroinflammatory pathologies involving DCs and plasma cell function, such as EAE (Greter et al., 2005; Mundt et al., 2019; Pröbstel et al., 2020).

The UPR also regulates inflammation (Bettigole and Glimcher, 2015; Grootjans et al., 2016; Flores-Santibáñez et al., 2019), by mechanisms that could be extended to neurodegeneration (Reverendo et al., 2019). Innate recognition *via* TLRs triggers ER stress in leukocytes and UPR components amplify the inflammatory program elicited by these receptors (Goodall et al., 2010; Martinon et al., 2010). ER stress also licenses macrophages to secrete the proinflammatory factors IL-1β, IL-6, TNF, and iNOS (Rao et al., 2014; Shenderov et al., 2014; Yang F. et al., 2018; Yang et al., 2019). Upon bacterial infection, IRE1/XBP1s promotes optimal production of IL-6 and TNF (Martinon et al., 2010; Qiu et al., 2013) and XBP1s favors the synthesis of IL-23, exacerbating psoriasis-like inflammation (Mogilenko et al., 2019). XBP1s also controls prostaglandin synthesis regulating pain behavior (Chopra et al., 2019). In addition, IRE1 RNase activates the inflammasome through degradation of the microRNA miR-17, which is a destabilizer of an NLRP3 activator termed TXNIP (Thioredoxin-Interacting Protein; Lerner et al., 2012; Bronner et al., 2015; Chen D. et al., 2018). Furthermore, IRE1 RNase regulates IFN-I production in microglia, providing a direct connection between IRE1 signaling

in CNS-resident immune cells (Studencka-Turski et al., 2019). In fact, XBP1s can bind to IFNβ enhancer and promoter sequences, augmenting IFNβ production (Zeng et al., 2010; Dias-Teixeira et al., 2016). On the other hand, IRE1 kinase also activates innate immunity *via* NOD1/2 receptors and NF-κB (Keestra-Gounder et al., 2016). As such, IRE1 has emerged as an inflammatory regulator through its RNase and Kinase domains (Janssens et al., 2014).

Given its potential, there is interest in targeting IRE1 through the modulation of interacting regulators. Sigma-1 receptor (Sigmar1) is an ER-resident chaperone that regulates IRE1 function (Hayashi and Su, 2007; Mori et al., 2013), and that can be targeted through high-affinity agonists including fluvoxamine, an antidepressant that prevents IRE1-dependent hyperinflammation in sepsis models (Rosen et al., 2019). Thus, IRE1 can be modulated by administration of repurposed medicines.

Furthermore, PERK regulates pro-inflammatory phenotypes of macrophages by activating JAK2-STAT1 signaling pathways (Yang et al., 2019). PERK also controls IL-23 synthesis *via* CHOP (Goodall et al., 2010), and it promotes IL-6, CCL2, and CCL20 production in astrocytes *via* JAK1-STAT3 (Meares et al., 2014; Sanchez et al., 2019). PERK also promotes IFN-I production in DCs (Mendes et al., 2020), and it controls macrophage/myeloid cell function in atherosclerosis and cancer models (DeVries-Seimon et al., 2005; Erbay et al., 2009; Thevenot et al., 2014; Mohamed et al., 2020).

Although little is known about the role of ATF6 in myeloid cells, the UPR sensor regulates pro-inflammatory cytokine production by Kupffer cells in liver ischemia (Rao et al., 2014; So, 2018) and it enhances the pro-inflammatory effect of TLR4 by enhancing NF-κB signaling in macrophages (Rao et al., 2014).

POTENTIAL CROSSTALK BETWEEN THE UPR IN IMMUNE CELLS AND NEUROINFLAMMATION

Besides the documented roles in immunity, the UPR is also a hallmark of neurodegenerative diseases (Hetz and Saxena, 2017). Although studies have associated the UPR with the function of neurons and glial cells such as astrocytes and oligodendrocytes (Clayton and Popko, 2016; Godin et al., 2016; Wheeler et al., 2019), the role of the immune-associated UPR during neurodegeneration remains an emerging field. In this section, we highlight potential mechanisms by which the UPR in immune cells could influence CNS pathologies (**Figure 2**).

Neurodegenerative diseases share protein misfolding, neuronal, loss and inflammation as common mechanisms (Scheiblich et al., 2020). However, evidence demonstrates that AD, PD, and MS are critically regulated by immune-signaling networks, providing a rationale for the study of immunity in these disorders. AD is an age-related disease and common cause of dementia, characterized by a decline in memory and cognitive abilities, neuronal loss, and accumulation of amyloid-β (Aβ) plaques (Holtzman et al., 2011; Efthymiou and Goate, 2017). Mutations in genes coding for amyloid precursor protein and presenilin-1/2 are identified as causes of rare familial AD (Ulland and Colonna, 2018). Nevertheless, most patients with late-onset AD do not carry familial AD mutations and instead, express genetic risk factors associated with immune-related networks, particularly in genes expressed by microglia such as TREM2, CD33, and C1R (Efthymiou and Goate, 2017; Hansen et al., 2018; Schwabe et al., 2020). On the other hand, PD is a progressive disorder characterized by selective degeneration of neuromelanin-containing neurons, especially substantia nigra dopaminergic neurons, and accumulation of α-synuclein (α-syn) aggregates (Zhang et al., 2011). Dopaminergic neuron destruction in PD is connected to genetic, environmental, and immunologic conditions (Koutsilieri et al., 2013). Finally, MS is an inflammatory demyelinating disease displaying three clinical manifestations: a pre-clinical stage; a relapsing-remitting stage, characterized by episodes of neurologic dysfunction and resolution; and a progressive stage (Baecher-Allan et al., 2018). MS pathology is typified by four pathological features: inflammation, demyelination, axonal loss, and gliosis (Constantinescu et al., 2011).

Post-mortem tissue analysis revealed that AD, PD, and MS patients display increased levels of UPR markers including CHOP, BiP, pPERK, p-eIF2α, pIRE1, and XBP1 (Hoozemans et al., 2007, 2009; Mháille et al., 2008; Wheeler et al., 2019). Interestingly, UPR activation in these pathologies is connected to immune cells. Microglia from post-mortem AD patients upregulate transcriptional signatures associated with protein folding and response to unfolded proteins (Mathys et al., 2019). Also, microglia from MS patients show increased expression of BIP, CHOP, and p-eIF2α (Mháille et al., 2008; Cunnea et al., 2011; McMahon et al., 2012), and microglia from animals with EAE also express BiP, GRP94, CHOP, and p-eIF2α (Ní Fhlathartaigh et al., 2013; Ta et al., 2016). Despite this evidence, the relevance of microglial UPR to neurodegeneration remains to be elucidated. In addition, T cells isolated from MS lesions express CHOP (Mháille et al., 2008), whereas spinal cord-infiltrating $CD4^+$ T cells from EAE mice display ATF6 activation (Ta et al., 2016).

From an inflammatory perspective, increased levels of IL-6, TNF, and IL-1β are detected in the brain, cerebrospinal fluid, and serum of patients with AD, PD, and MS, although these responses have not been yet linked to IRE1 or PERK activation (Swardfager et al., 2010; Qin et al., 2016; Chen X. et al., 2018; Stampanoni Bassi et al., 2020). Analogous to peripheral macrophages, microglia initiate inflammation upon recognition of Aβ, α-syn, and neuromelanin through TLR2 and TLR4 (Reed-Geaghan et al., 2009; Zhang et al., 2011; Kim et al., 2013). Considering that TLR2 and TLR4 engage the IRE1/XBP1s axis to sustain the production of pro-inflammatory cytokines (Martinon et al., 2010), it is plausible that this UPR branch may initiate neuroinflammation in AD and PD.

Injections of TLR4 agonists are used as a microglial-dependent model of neuroinflammation (Qin et al., 2007; Zhao et al., 2019) and interestingly, this effect can be ameliorated by administration of the pharmacological activator of the UPR, tunicamycin (Wang et al., 2017). It is proposed that mild ER stress induces a reparative phenotype in microglia that

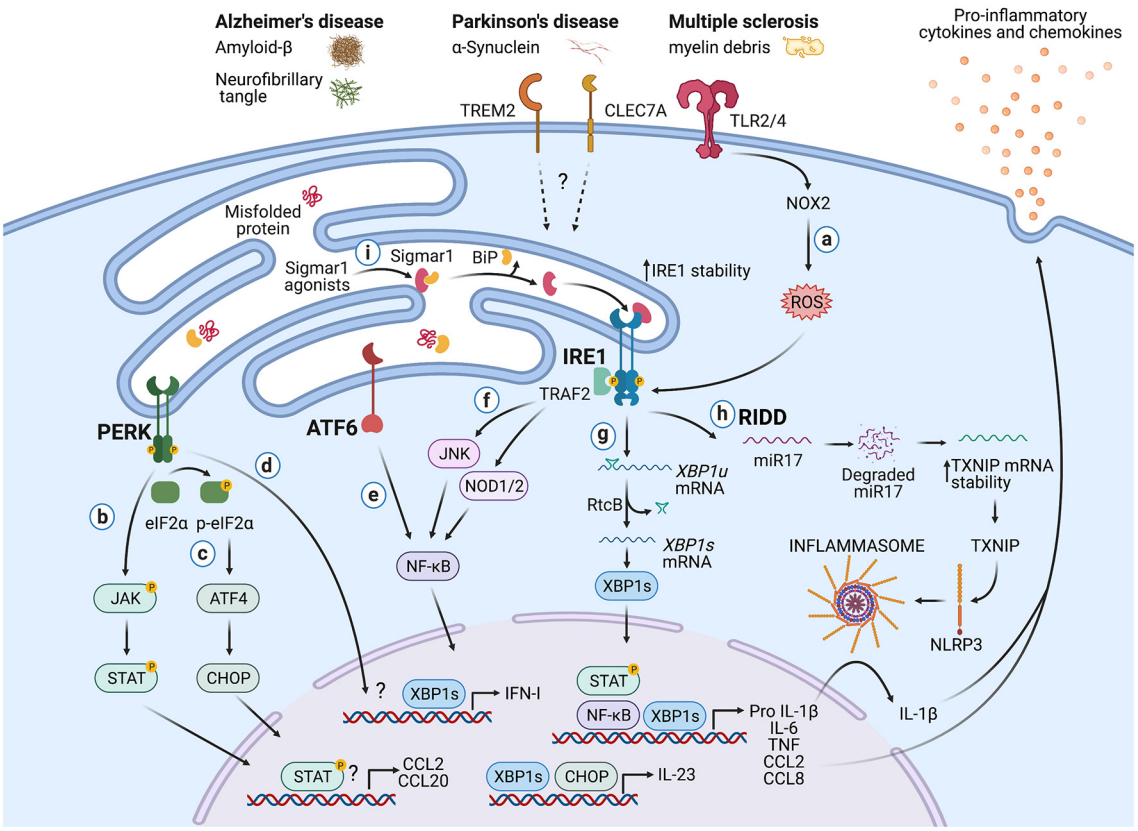

FIGURE 2 | Potential roles of the UPR in immune cells during neurodegeneration. Protein aggregates and myelin debris can promote inflammation *via* triggering of innate receptors and activation of the UPR, which in turn could increase inflammation in neurodegenerative diseases mainly by enhancing the production of proinflammatory cytokines and chemokines. **(a)** Detection of proteins aggregates (Amyloid-β, α-synuclein, neurofibrillary tangles) and myelin debris through TLR2 and TLR4 (and probably others pattern recognition receptors) present on immune cells can activate the IRE1/XBP1s axis through reactive oxygen species (ROS) production by NOX2. **(b)** PERK can modulate the production of the pro-inflammatory cytokines IL-6, TNF, IL-1β, and the chemokines CCL2 and CCL20 through activation of JAK1-STAT3 and JAK2-STAT1 signaling pathways. **(c)** PERK also can control the synthesis of IL-23 *via* CHOP. **(d)** Additionally, PERK could control the synthesis of type I interferons. **(e)** ATF6 *via* NF-κB can enhance the production of the cytokines IL-6, TNF, and the chemokines CCL2 and CCL8. **(f)** The kinase domain of IRE1 can modulate the production of IL-6, TNF, and IL-1β through activation of NF-κB *via* JNK and NOD1/2 receptors. **(g)** BP1s can promote optimal production of IL-6, TNF, and type I IFNs and also favors the synthesis of IL-23. **(h)** IRE1 RNase *via* RIDD activates the NLRP3 inflammasome through degradation of the TXNIP-destabilizing microRNA miR-17, leading to IL-1β production. **(i)** Sigmar1 forms a complex with binding immunoglobulin protein (BiP) under normal conditions, but Sigmar1 agonists can dissociate Sigmar1 from Bip to induce its action as a chaperone protein. Sigmar1 interacts with IRE1 and stabilizes it, prolonging IRE1/XBP1s signaling. Figure created with BioRender.com.

protects against neuroinflammation (Wang et al., 2017), and mild ER stress in neurons has also shown to be protective in PD and AD models (Casas-Tinto et al., 2011; Fouillet et al., 2012; Valdés et al., 2014). As such, genetic/pharmacological manipulation of the UPR can have distinct and even opposite effects on neurodegenerative diseases depending on the cell type (Hetz and Saxena, 2017) and thus, it becomes relevant to address the UPR roles in specific cell lineages of the CNS. In fact, the importance of this topic is underscored in studies that show that selective UPR activation *via* the PERK axis in astrocytes results in neuronal degeneration (Smith et al., 2020).

Another regulatory node between the UPR and neurodegeneration is the NLRP3 inflammasome, which is implicated in the pathogenesis of AD, PD, and MS (Song et al., 2017; Zhou et al., 2020). Recognition of Aβ and α-syn activates the NLRP3 inflammasome in microglia (Halle et al., 2008; Codolo et al., 2013; Panicker et al., 2019), and the relevance of this complex is underscored in studies with *Nlrp3*$^{-/-}$ mice, which are protected from spatial memory loss in a model of familial AD (Heneka et al., 2013). Considering that IRE1 regulates the NLRP3 inflammasome and that IRE1 is activated in microglia from AD patients (Lerner et al., 2012; Bronner et al., 2015), it is plausible that the UPR sensor contributes to IL-1β secretion during neurodegeneration.

Perhaps the best-documented link between the UPR and neuroinflammation is in MS (Stone and Lin, 2015). Selective PERK deletion in oligodendrocytes protects against EAE (Lin et al., 2013) and XBP1 deletion in CD4^{+} T cells

curtails the differentiation into T helper 17 (Th17) cells, delaying the onset of EAE signs (Brucklacher-Waldert et al., 2017). However, the opposite effect is noticed under ATF4 deficiency, which increases Th17 differentiation and worsens EAE (Yang X. et al., 2018). ATF6 on the other hand is required for transcription of Nos2, Ccl2, and Ccl8 in microglia in this model (Ta et al., 2016). Finally, the IRE1-XBP1s pathway promotes astrocyte-intrinsic pro-inflammatory activities during EAE, which is coordinated by the activity of Sigmar1 (Wheeler et al., 2019). XBP1s promote Nos2 and Csf2 expression in astrocytes and knock-down of Xbp1 in astrocytes ameliorates the disease (Wheeler et al., 2019), providing formal connections between IRE1 activation and CNS inflammation.

CONCLUDING REMARKS

The UPR is a central proteostatic pathway coordinating immunity and inflammation, emerging as a novel therapeutic option for neurodegenerative diseases. Despite the promising advances in the field, the interplay between the UPR and immune cells in the CNS remains to be fully uncovered. Relevant questions should aim to reveal the contribution of UPR transducers and regulators in microglia and additional immune cells contributing to neuroinflammation. Consideration should be given to the aging process, which is regulated by XBP1s in *C. elegans* (Taylor and Dillin, 2013).

AUTHOR CONTRIBUTIONS

DF, AG, JB, AL, and FO provided scientific input and wrote the manuscript. All authors contributed to the article and approved the submitted version.

FUNDING

This work was supported by an International Research Scholar grant from the Howard Hughes Medical Institute (HHMI#55008744), FONDECYT grant No. 1200793 (Fondo Nacional de Desarrollo Científico y Tecnológico), and ECOS-CONICYT grant (ECOS180052).

ACKNOWLEDGMENTS

We thank Maria Francisca Gutierrez for conceptual insights on the manuscript. We apologize to all of the authors whose work could not be referenced due to space constraints.

REFERENCES

Ajami, B., Samusik, N., Wieghofer, P., Ho, P. P., Crotti, A., Bjornson, Z., et al. (2018). Single-cell mass cytometry reveals distinct populations of brain myeloid cells in mouse neuroinflammation and neurodegeneration models. *Nat. Neurosci.* 21, 541–551. doi: 10.1038/s41593-018-0100-x

Baecher-Allan, C., Kaskow, B. J., and Weiner, H. L. (2018). Multiple sclerosis: mechanisms and immunotherapy. *Neuron* 97, 742–768. doi: 10.1016/j.neuron.2018.01.021

Benhamron, S., Hadar, R., Iwawaky, T., So, J. S., Lee, A. H., and Tirosh, B. (2014). Regulated IRE1-dependent decay participates in curtailing immunoglobulin secretion from plasma cells. *Eur. J. Immunol.* 44, 867–876. doi: 10.1002/eji.201343953

Bettigole, S. E., and Glimcher, L. H. (2015). Endoplasmic reticulum stress in immunity. *Annu. Rev. Immunol.* 33, 107–138. doi: 10.1146/annurev-immunol-032414-112116

Bettigole, S. E., Lis, R., Adoro, S., Lee, A. H., Spencer, L. A., Weller, P. F., et al. (2015). The transcription factor XBP1 is selectively required for eosinophil differentiation. *Nat. Immunol.* 16, 829–837. doi: 10.1038/ni.3225

Brodsky, J. L., and Skach, W. R. (2011). Protein folding and quality control in the endoplasmic reticulum: recent lessons from yeast and mammalian cell systems. *Curr. Opin. Cell Biol.* 23, 464–475. doi: 10.1016/j.ceb.2011.05.004

Bronner, D. N., Abuaita, B. H., Chen, X., Fitzgerald, K. A., Nuñez, G., He, Y., et al. (2015). Endoplasmic reticulum stress activates the inflammasome *via* NLRP3- and caspase-2-driven mitochondrial damage. *Immunity* 43, 451–462. doi: 10.1016/j.immuni.2015.08.008

Brucklacher-Waldert, V., Ferreira, C., Stebegg, M., Fesneau, O., Innocentin, S., Marie, J. C., et al. (2017). Cellular stress in the context of an inflammatory environment supports TGF-β-independent T helper-17 differentiation. *Cell Rep.* 19, 2357–2370. doi: 10.1016/j.celrep.2017.05.052

Cabeza-Cabrerizo, M., Cardoso, A., Minutti, C. M., Pereira, M., and Reis e Sousa, C. (2021). Dendritic cells revisited. *Annu. Rev. Immunol.* 39, 131–166. doi: 10.1146/annurev-immunol-061020-053707

Casas-Tinto, S., Zhang, Y., Sanchez-Garcia, J., Gomez-Velazquez, M., Rincon-Limas, D. E., and Fernandez-Funez, P. (2011). The ER stress factor XBP1s prevents amyloid-β neurotoxicity. *Hum. Mol. Genet.* 20, 2144–2160. doi: 10.1093/hmg/ddr100

Chen, D., Dixon, B. J., Doycheva, D. M., Li, B., Zhang, Y., Hu, Q., et al. (2018). IRE1α inhibition decreased TXNIP/NLRP3 inflammasome activation through miR-17–5p after neonatal hypoxic-ischemic brain injury in rats. *J. Neuroinflammation* 15:32. doi: 10.1186/s12974-018-1077-9

Chen, X., Hu, Y., Cao, Z., Liu, Q., and Cheng, Y. (2018). Cerebrospinal fluid inflammatory cytokine aberrations in Alzheimer's disease, Parkinson's disease and amyotrophic lateral sclerosis: a systematic review and meta-analysis. *Front. Immunol.* 9:2122. doi: 10.3389/fimmu.2018.02122

Chopra, S., Giovanelli, P., Alvarado-Vazquez, P. A., Alonso, S., Song, M., Sandoval, T. A., et al. (2019). IRE1α-XBP1 signaling in leukocytes controls prostaglandin biosynthesis and pain. *Science* 365:eaau6499. doi: 10.1126/science.aau6499

Clayton, B. L. L., and Popko, B. (2016). Endoplasmic reticulum stress and the unfolded protein response in disorders of myelinating glia. *Brain Res.* 1648, 594–602. doi: 10.1016/j.brainres.2016.03.046

Codolo, G., Plotegher, N., Pozzobon, T., Brucale, M., Tessari, I., Bubacco, L., et al. (2013). Triggering of inflammasome by aggregated α-synuclein, an inflammatory response in synucleinopathies. *PLoS One* 8:e55375. doi: 10.1371/journal.pone.0055375

Colonna, M., and Butovsky, O. (2017). Microglia function in the central nervous system during health and neurodegeneration. *Annu. Rev. Immunol.* 35, 441–468. doi: 10.1146/annurev-immunol-051116-052358

Constantinescu, C. S., Farooqi, N., O'Brien, K., and Gran, B. (2011). Experimental autoimmune encephalomyelitis (EAE) as a model for multiple sclerosis (MS). *Br. J. Pharmacol.* 164, 1079–1106. doi: 10.1111/j.1476-5381.2011.01302.x

Cubillos-Ruiz, J. R., Silberman, P. C., Rutkowski, M. R., Chopra, S., Perales-Puchalt, A., Song, M., et al. (2015). ER stress sensor XBP1 controls anti-tumor immunity by disrupting dendritic cell homeostasis. *Cell* 161, 1527–1538. doi: 10.1016/j.cell.2015.05.025

Cunnea, P., Mháille, A. N., McQuaid, S., Farrell, M., McMahon, J., and Fitzgerald, U. (2011). Expression profiles of endoplasmic reticulum stress-related molecules in demyelinating lesions and multiple sclerosis. *Mult. Scler.* 17, 808–818. doi: 10.1177/1352458511399114

DeVries-Seimon, T., Li, Y., Pin, M. Y., Stone, E., Wang, Y., Davis, R. J., et al. (2005). Cholesterol-induced macrophage apoptosis requires ER stress pathways and engagement of the type A scavenger receptor. *J. Cell Biol.* 171, 61–73. doi: 10.1083/jcb.200502078

Dias-Teixeira, K. L., Calegari-Silva, T. C., Dos Santos, G. R. R. M., Vitorino Dos Santos, J., Lima, C., Medina, J. M., et al. (2016). The integrated endoplasmic reticulum stress response in Leishmania amazonensis macrophage infection: the role of X-box binding protein 1 transcription factor. *FASEB J.* 30, 1557–1565. doi: 10.1096/fj.15-281550

Dong, H., Adams, N. M., Xu, Y., Cao, J., Allan, D. S. J., Carlyle, J. R., et al. (2019). The IRE1 endoplasmic reticulum stress sensor activates natural killer cell immunity in part by regulating c-Myc. *Nat. Immunol.* 20, 865–878. doi: 10.1038/s41590-019-0388-z

Efthymiou, A. G., and Goate, A. M. (2017). Late onset alzheimer's disease genetics implicates microglial pathways in disease risk. *Mol. Neurodegener.* 12:43. doi: 10.1186/s13024-017-0184-x

Erbay, E., Babaev, V. R., Mayers, J. R., Makowski, L., Charles, K. N., Snitow, M. E., et al. (2009). Reducing endoplasmic reticulum stress through a macrophage lipid chaperone alleviates atherosclerosis. *Nat. Med.* 15, 1383–1391. doi: 10.1038/nm.2067

Flores-Santibáñez, F., Medel, B., Bernales, J. I., and Osorio, F. (2019). Understanding the role of the unfolded protein response sensor IRE1 in the biology of antigen presenting cells. *Cells* 8:1563. doi: 10.3390/cells8121563

Fouillet, A., Levet, C., Virgone, A., Robin, M., Dourlen, P., Rieusset, J., et al. (2012). ER stress inhibits neuronal death by promoting autophagy. *Autophagy* 8, 915–926. doi: 10.4161/auto.19716

Giovannoni, F., and Quintana, F. J. (2020). The role of astrocytes in CNS inflammation. *Trends Immunol.* 41, 805–819. doi: 10.1016/j.it.2020.07.007

Godin, J. D., Creppe, C., Laguesse, S., and Nguyen, L. (2016). Emerging roles for the unfolded protein response in the developing nervous system. *Trends Neurosci.* 39, 394–404. doi: 10.1016/j.tins.2016.04.002

Goodall, J. C., Wu, C., Zhang, Y., McNeill, L., Ellis, L., Saudek, V., et al. (2010). Endoplasmic reticulum stress-induced transcription factor, CHOP, is crucial for dendritic cell IL-23 expression. *Proc. Natl. Acad. Sci. U S A* 107, 17698–17703. doi: 10.1073/pnas.1011736107

Greter, M., Heppner, F. L., Lemos, M. P., Odermatt, B. M., Goebels, N., Laufer, T., et al. (2005). Dendritic cells permit immune invasion of the CNS in an animal model of multiple sclerosis. *Nat. Med.* 11, 328–334. doi: 10.1038/nm1197

Grootjans, J., Kaser, A., Kaufman, R. J., and Blumberg, R. S. (2016). The unfolded protein response in immunity and inflammation. *Nat. Rev. Immunol.* 16, 469–484. doi: 10.1038/nri.2016.62

Halle, A., Hornung, V., Petzold, G. C., Stewart, C. R., Monks, B. G., Reinheckel, T., et al. (2008). The NALP3 inflammasome is involved in the innate immune response to amyloid-β. *Nat. Immunol.* 9, 857–865. doi: 10.1038/ni.1636

Hansen, D. V., Hanson, J. E., and Sheng, M. (2018). Microglia in Alzheimer's disease. *J. Cell Biol.* 217, 459–472. doi: 10.1083/jcb.201709069

Hayashi, T., and Su, T. P. (2007). Sigma-1 receptor chaperones at the ER-mitochondrion interface regulate Ca^{2+} signaling and cell survival. *Cell* 131, 596–610. doi: 10.1016/j.cell.2007.08.036

Heneka, M. T., Kummer, M. P., Stutz, A., Delekate, A., Schwartz, S., Vieira-Saecker, A., et al. (2013). NLRP3 is activated in Alzheimer's disease and contributes to pathology in APP/PS1 mice. *Nature* 493, 674–678. doi: 10.1038/nature11729

Hetz, C. (2021). Adapting the proteostasis capacity to sustain brain healthspan. *Cell* 184, 1545–1560. doi: 10.1016/j.cell.2021.02.007

Herz, J., Filiano, A. J., Smith, A., Yogev, N., and Kipnis, J. (2017). Myeloid cells in the central nervous system. *Immunity* 46, 943–956. doi: 10.1016/j.immuni.2017.06.007

Hetz, C., and Papa, F. R. (2018). The unfolded protein response and cell fate control. *Mol. Cell* 69, 169–181. doi: 10.1016/j.molcel.2017.06.017

Hetz, C., and Saxena, S. (2017). ER stress and the unfolded protein response in neurodegeneration. *Nat. Rev. Neurol.* 13, 477–491. doi: 10.1038/nrneurol.2017.99

Holtzman, D. M., Morris, J. C., and Goate, A. M. (2011). Alzheimer's disease: the challenge of the second century. *Sci. Transl. Med.* 3:77sr1. doi: 10.1126/scitranslmed.3002369

Hoozemans, J. J. M., van Haastert, E. S., Eikelenboom, P., de Vos, R. A. I., Rozemuller, J. M., and Scheper, W. (2007). Activation of the unfolded protein response in Parkinson's disease. *Biochem. Biophys. Res. Commun.* 354, 707–711. doi: 10.1016/j.bbrc.2007.01.043

Hoozemans, J. J. M., Van Haastert, E. S., Nijholt, D. A. T., Rozemuller, A. J. M., Eikelenboom, P., and Scheper, W. (2009). The unfolded protein response is activated in pretangle neurons in Alzheimer's disease hippocampus. *Am. J. Pathol.* 174, 1241–1251. doi: 10.2353/ajpath.2009.080814

Hu, P., Han, Z., Couvillon, A. D., Kaufman, R. J., and Exton, J. H. (2006). Autocrine tumor necrosis factor alpha links endoplasmic reticulum stress to the membrane death receptor pathway through IRE1alpha-mediated NF-kappaB activation and down-regulation of TRAF2 expression. *Mol. Cell. Biol.* 26, 3071–3084. doi: 10.1128/MCB.26.8.3071-3084.2006

Iwakoshi, N. N., Pypaert, M., and Glimcher, L. H. (2007). The transcription factor XBP-1 is essential for the development and survival of dendritic cells. *J. Exp. Med.* 204, 2267–2275. doi: 10.1084/jem.20070525

Janssens, S., Pulendran, B., and Lambrecht, B. N. (2014). Emerging functions of the unfolded protein response in immunity. *Nat. Immunol.* 15, 910–919. doi: 10.1038/ni.2991

Keestra-Gounder, A. M., Byndloss, M. X., Seyffert, N., Young, B. M., Chávez-Arroyo, A., Tsai, A. Y., et al. (2016). NOD1 and NOD2 signalling links ER stress with inflammation. *Nature* 532, 394–397. doi: 10.1038/nature17631

Khalsa, J. K., Chawla, A. S., Prabhu, S. B., Vats, M., Dhar, A., Dev, G., et al. (2019). Functionally significant metabolic differences between B and T lymphocyte lineages. *Immunology* 158, 104–120. doi: 10.1111/imm.13098

Kim, C., Ho, D.-H., Suk, J. E., You, S., Michael, S., Kang, J., et al. (2013). Neuron-released oligomeric α-synuclein is an endogenous agonist of TLR2 for paracrine activation of microglia. *Nat. Commun.* 4:1562. doi: 10.1038/ncomms2534

Korin, B., Ben-shaanan, T. L., Schiller, M., Dubovik, T., Azulay-debby, H., Boshnak, N. T., et al. (2017). High-dimensional, single-cell characterization of the brain's immune compartment. *Nat. Neurosci.* 20, 1300–1309. doi: 10.1038/nn.4610

Koutsilieri, E., Lutz, M. B., and Scheller, C. (2013). Autoimmunity, dendritic cells and relevance for Parkinson's disease. *J. Neural Transm.* 120, 75–81. doi: 10.1007/s00702-012-0842-7

Kranz, P., Neumann, F., Wolf, A., Classen, F., Pompsch, M., Ocklenburg, T., et al. (2017). PDI is an essential redox-sensitive activator of PERK during the unfolded protein response (UPR). *Cell Death Dis.* 8, e2986–e2986. doi: 10.1038/cddis.2017.369

Lee, A.-H., Iwakoshi, N. N., and Glimcher, L. H. (2003). XBP-1 regulates a subset of endoplasmic reticulum resident chaperone genes in the unfolded protein response. *Mol. Cell. Biol.* 23, 7448–7459. doi: 10.1128/mcb.23.21.7448-7459.2003

Lerner, A. G., Upton, J. P., Praveen, P. V. K., Ghosh, R., Nakagawa, Y., Igbaria, A., et al. (2012). IRE1α induces thioredoxin-interacting protein to activate the NLRP3 inflammasome and promote programmed cell death under irremediable ER stress. *Cell Metab.* 16, 250–264. doi: 10.1016/j.cmet.2012.07.007

Lin, W., Lin, Y., Li, J., Fenstermaker, A. G., Way, S. W., Clayton, B., et al. (2013). Oligodendrocyte-specific activation of PERK signaling protects mice against experimental autoimmune encephalomyelitis. *J. Neurosci.* 33, 5980–5991. doi: 10.1523/JNEUROSCI.1636-12.2013

Lu, M., Lawrence, D. A., Marsters, S., Acosta-Alvear, D., Kimmig, P., Mendez, A. S., et al. (2014). Opposing unfolded-protein-response signals converge on death receptor 5 to control apoptosis. *Science* 345, 98–101. doi: 10.1126/science.1254312

Martinon, F., Chen, X., Lee, A.-H., and Glimcher, L. H. (2010). TLR activation of the transcription factor XBP1 regulates innate immune responses in macrophages. *Nat. Immunol.* 11, 411–418. doi: 10.1038/ni.1857

Mathys, H., Davila-Velderrain, J., Peng, Z., Gao, F., Mohammadi, S., Young, J. Z., et al. (2019). Single-cell transcriptomic analysis of Alzheimer's disease. *Nature* 570, 332–337. doi: 10.1038/s41586-019-1195-2

Maurel, M., Chevet, E., Tavernier, J., and Gerlo, S. (2014). Getting RIDD of RNA: IRE1 in cell fate regulation. *Trends Biochem. Sci.* 39, 245–254. doi: 10.1016/j.tibs.2014.02.008

McMahon, J. M., McQuaid, S., Reynolds, R., and Fitzgerald, U. F. (2012). Increased expression of ER stress- and hypoxia-associated molecules in grey matter lesions in multiple sclerosis. *Mult. Scler.* 18, 1437–1447. doi: 10.1177/1352458512438455

Meares, G. P., Liu, Y., Rajbhandari, R., Qin, H., Nozell, S. E., Mobley, J. A., et al. (2014). PERK-dependent activation of JAK1 and STAT3 contributes to endoplasmic reticulum stress-induced inflammation. *Mol. Cell. Biol.* 34, 3911–3925. doi: 10.1128/MCB.00980-14

Mendes, A., Gigan, J. P., Rodrigues, C. R., Choteau, S. A., Sanseau, D., Barros, D., et al. (2020). Proteostasis in dendritic cells is controlled by the PERK signaling axis independently of ATF4. *Life Sci. Alliance* 4:e202000865. doi: 10.26508/lsa.202000865

Mháille, A. N., McQuaid, S., Windebank, A., Cunnea, P., McMahon, J., Samali, A., et al. (2008). Increased expression of endoplasmic reticulum stress-related signaling pathway molecules in multiple sclerosis lesions. *J. Neuropathol. Exp. Neurol.* 67, 200–211. doi: 10.1097/NEN.0b013e318165b239

Mogilenko, D. A., Haas, J. T., L'homme, L., Fleury, S., Quemener, S., Levavasseur, M., et al. (2019). Metabolic and innate immune cues merge into a specific inflammatory response *via* the UPR. *Cell* 177, 1201.e19–1216.e19. doi: 10.1016/j.cell.2019.03.018

Mohamed, E., Sierra, R. A., Trillo-Tinoco, J., Cao, Y., Innamarato, P., Payne, K. K., et al. (2020). The unfolded protein response mediator PERK governs myeloid cell-driven immunosuppression in tumors through inhibition of STING signaling. *Immunity* 52, 668.e7–682.e7. doi: 10.1016/j.immuni.2020.03.004

Mori, T., Hayashi, T., Hayashi, E., and Su, T. P. (2013). Sigma-1 receptor chaperone at the ER-mitochondrion interface mediates the mitochondrion-ER-nucleus signaling for cellular survival. *PLoS One* 8:e76941. doi: 10.1371/journal.pone.0076941

Mrdjen, D., Pavlovic, A., Hartmann, F. J., Schreiner, B., Utz, S. G., Leung, B. P., et al. (2018). High-dimensional single-cell mapping of central nervous system immune cells reveals distinct myeloid subsets in health, aging, and disease. *Immunity* 48, 380.e6–395.e6. doi: 10.1016/j.immuni.2018.01.011

Mundt, S., Mrdjen, D., Utz, S. G., Greter, M., Schreiner, B., and Becher, B. (2019). Conventional DCs sample and present myelin antigens in the healthy CNS and allow parenchymal T cell entry to initiate neuroinflammation. *Sci. Immunol.* 4:eaau8380. doi: 10.1126/sciimmunol.aau8380

Ní Fhlathartaigh, M., McMahon, J., Reynolds, R., Connolly, D., Higgins, E., Counihan, T., et al. (2013). Calreticulin and other components of endoplasmic reticulum stress in rat and human inflammatory demyelination. *Acta Neuropathol. Commun.* 1:37. doi: 10.1186/2051-5960-1-37

Novoa, I., Zeng, H., Harding, H. P., and Ron, D. (2001). Feedback inhibition of the unfolded protein response by GADD34-mediated dephosphorylation of eIF2alpha. *J. Cell Biol.* 153, 1011–1022. doi: 10.1083/jcb.153.5.1011

Osorio, F., Tavernier, S. J., Hoffmann, E., Saeys, Y., Martens, L., Vetters, J., et al. (2014). The unfolded-protein-response sensor IRE-1α regulates the function of CD8α + dendritic cells. *Nat. Immunol.* 15, 248–257. doi: 10.1038/ni.2808

Panicker, N., Sarkar, S., Harischandra, D. S., Neal, M., Kam, T. I., Jin, H., et al. (2019). Fyn kinase regulates misfolded α-synuclein uptake and NLRP3 inflammasome activation in microglia. *J. Exp. Med.* 216, 1411–1430. doi: 10.1084/jem.20182191

Pasciuto, E., Burton, O. T., Roca, C. P., Fitzgerald, D. C., Dooley, J., Liston, A., et al. (2020). Microglia require CD4 T cells to complete the fetal- to-adult transition microglia require CD4 T cells to complete the fetal-to-adult transition. *Cell* 182, 625.e24–640.e24. doi: 10.1016/j.cell.2020.06.026

Pröbstel, A., Zhou, X., Baumann, R., Wischnewski, S., Kutza, M., Rojas, O. L., et al. (2020). Gut microbiota-specific IgA + B cells traffic to the CNS in active multiple sclerosis. *Sci. Immunol.* 5:eabc7191. doi: 10.1126/sciimmunol.abc7191

Prinz, M., Jung, S., and Priller, J. (2019). Microglia biology: one century of evolving concepts. *Cell* 179, 292–311. doi: 10.1016/j.cell.2019.08.053

Qin, L., Wu, X., Block, M. L., Liu, Y., Breese, G. R., Hong, J.-S., et al. (2007). Systemic LPS causes chronic neuroinflammation and progressive neurodegeneration. *Glia* 55, 453–462. doi: 10.1002/glia.20467

Qin, X.-Y., Zhang, S.-P., Cao, C., Loh, Y. P., and Cheng, Y. (2016). Aberrations in peripheral inflammatory cytokine levels in Parkinson disease: a systematic review and meta-analysis. *JAMA Neurol.* 73, 1316–1324. doi: 10.1001/jamaneurol.2016.2742

Qiu, Q., Zheng, Z., Chang, L., Zhao, Y. S., Tan, C., Dandekar, A., et al. (2013). Toll-like receptor-mediated IRE1α activation as a therapeutic target for inflammatory arthritis. *EMBO J.* 32, 2477–2490. doi: 10.1038/emboj.2013.183

Ransohoff, R. M., and Cardona, A. E. (2010). The myeloid cells of the central nervous system parenchyma. *Nature* 468, 253–262. doi: 10.1038/nature09615

Rao, J., Yue, S., Fu, Y., Zhu, J., Wang, X., Busuttil, R. W., et al. (2014). ATF6 mediates a pro-inflammatory synergy between ER stress and TLR activation in the pathogenesis of liver ischemia-reperfusion injury. *Am. J. Transplant.* 14, 1552–1561. doi: 10.1111/ajt.12711

Reed-Geaghan, E. G., Savage, J. C., Hise, A. G., and Landreth, G. E. (2009). CD14 and toll-like receptors 2 and 4 are required for fibrillar Aβ-stimulated microglial activation. *J. Neurosci.* 29, 11982–11992. doi: 10.1523/JNEUROSCI.3158-09.2009

Reimold, A. M., Iwakoshi, N. N., Manis, J., Vallabhajosyula, P., Szomolanyi-Tsuda, E., Gravallese, E. M., et al. (2001). Plasma cell differentiation requires the transcription factor XBP-1. *Nature* 412, 300–307. doi: 10.1038/35085509

Reverendo, M., Mendes, A., Argüello, R. J., Gatti, E., and Pierre, P. (2019). At the crossway of ER-stress and proinflammatory responses. *FEBS J.* 286, 297–310. doi: 10.1111/febs.14391

Ron, D., and Walter, P. (2007). Signal integration in the endoplasmic reticulum unfolded protein response. *Nat. Rev. Mol. Cell Biol.* 8, 519–529. doi: 10.1038/nrm2199

Rosen, D. A., Seki, S. M., Fernández-Castañeda, A., Beiter, R. M., Eccles, J. D., Woodfolk, J. A., et al. (2019). Modulation of the sigma-1 receptor-IRE1 pathway is beneficial in preclinical models of inflammation and sepsis. *Sci. Transl. Med.* 11:eaau5266. doi: 10.1126/scitranslmed.aau5266

Sanchez, C. L., Sims, S. G., Nowery, J. D., and Meares, G. P. (2019). Endoplasmic reticulum stress differentially modulates the IL-6 family of cytokines in murine astrocytes and macrophages. *Sci. Rep.* 9:14931. doi: 10.1038/s41598-019-51481-6

Scheiblich, H., Trombly, M., Ramirez, A., and Heneka, M. T. (2020). Neuroimmune connections in aging and neurodegenerative diseases. *Trends Immunol.* 41, 300–312. doi: 10.1016/j.it.2020.02.002

Schwabe, T., Srinivasan, K., and Rhinn, H. (2020). Shifting paradigms: the central role of microglia in Alzheimer's disease. *Neurobiol. Dis.* 143:104962. doi: 10.1016/j.nbd.2020.104962

Shenderov, K., Riteau, N., Yip, R., Mayer-Barber, K. D., Oland, S., Hieny, S., et al. (2014). Cutting edge: endoplasmic reticulum stress licenses macrophages to produce mature IL-1β in response to TLR4 stimulation through a caspase-8- and TRIF-dependent pathway. *J. Immunol.* 192, 2029–2033. doi: 10.4049/jimmunol.1302549

Shoulders, M. D., Ryno, L. M., Genereux, J. C., Moresco, J. J., Tu, P. G., Wu, C., et al. (2013). Stress-independent activation of XBP1s and/or ATF6 reveals three functionally diverse ER proteostasis environments. *Cell Rep.* 3, 1279–1292. doi: 10.1016/j.celrep.2013.03.024

Smith, H. L., Freeman, O. J., Butcher, A. J., Holmqvist, S., Humoud, I., Schätzl, T., et al. (2020). Astrocyte unfolded protein response induces a specific reactivity state that causes non-cell-autonomous neuronal degeneration. *Neuron* 105, 855.e5–866.e5. doi: 10.1016/j.neuron.2019.12.014

So, J.-S. (2018). Roles of endoplasmic reticulum stress in immune responses. *Mol. Cells* 41, 705–716. doi: 10.14348/molcells.2018.0241

Sofroniew, M. V. (2020). Astrocyte reactivity: subtypes, states, and functions in CNS innate immunity. *Trends Immunol.* 41, 758–770. doi: 10.1016/j.it.2020.07.004

Song, L., Pei, L., Yao, S., Wu, Y., and Shang, Y. (2017). NLRP3 inflammasome in neurological diseases, from functions to therapies. *Front. Cell. Neurosci.* 11:63. doi: 10.3389/fncel.2017.00063

Song, M., Sandoval, T. A., Chae, C.-S., Chopra, S., Tan, C., Rutkowski, M. R., et al. (2018). IRE1α-XBP1 controls T cell function in ovarian cancer by regulating mitochondrial activity. *Nature* 562, 423–428. doi: 10.1038/s41586-018-0597-x

Sprooten, J., Agostinis, P., and Garg, A. D. (2019). "Type I interferons and dendritic cells in cancer immunotherapy," in *International Review of Cell and Molecular Biology*, eds Claire Lhuillier and Lorenzo Galluzzi (Oxford, UK: Elsevier Inc.), 217–262.

Stampanoni Bassi, M., Iezzi, E., Drulovic, J., Pekmezovic, T., Gilio, L., Furlan, R., et al. (2020). IL-6 in the cerebrospinal fluid signals disease activity in multiple sclerosis. *Front. Cell. Neurosci.* 14:120. doi: 10.3389/fncel.2020.00120

Stone, S., and Lin, W. (2015). The unfolded protein response in multiple sclerosis. *Front. Neurosci.* 9:264. doi: 10.3389/fnins.2015.00264

Studencka-Turski, M., Çetin, G., Junker, H., Ebstein, F., and Krüger, E. (2019). Molecular insight into the IRE1α-mediated type I interferon response induced by proteasome impairment in myeloid cells of the brain. *Front. Immunol.* 10:2900. doi: 10.3389/fimmu.2019.02900

Swanson, K. V., Deng, M., and Ting, J. P.-Y. (2019). The NLRP3 inflammasome: molecular activation and regulation to therapeutics. *Nat. Rev. Immunol.* 19, 477–489. doi: 10.1038/s41577-019-0165-0

Swardfager, W., Lanctôt, K., Rothenburg, L., Wong, A., Cappell, J., and Herrmann, N. (2010). A meta-analysis of cytokines in Alzheimer's disease. *Biol. Psychiatry* 68, 930–941. doi: 10.1016/j.biopsych.2010.06.012

Ta, H. M., Le, T. M., Ishii, H., Takarada-Iemata, M., Hattori, T., Hashida, K., et al. (2016). Atf6α deficiency suppresses microglial activation and ameliorates pathology of experimental autoimmune encephalomyelitis. *J. Neurochem.* 139, 1124–1137. doi: 10.1111/jnc.13714

Tavernier, S. J., Osorio, F., Vandersarren, L., Vetters, J., Vanlangenakker, N., Van Isterdael, G., et al. (2017). Regulated IRE1-dependent mRNA decay sets the threshold for dendritic cell survival. *Nat. Cell Biol.* 19, 698–710. doi: 10.1038/ncb3518

Taylor, R. C., and Dillin, A. (2013). XBP-1 Is a cell-nonautonomous regulator of stress resistance and longevity. *Cell* 153, 1435–1447. doi: 10.1016/j.cell.2013.05.042

Thevenot, P. T., Sierra, R. A., Raber, P. L., Al-Khami, A. A., Trillo-Tinoco, J., Zarreii, P., et al. (2014). The stress-response sensor chop regulates the function and accumulation of myeloid-derived suppressor cells in tumors. *Immunity* 41, 389–401. doi: 10.1016/j.immuni.2014.08.015

Ulland, T. K., and Colonna, M. (2018). TREM2—a key player in microglial biology and Alzheimer disease. *Nat. Rev. Neurol.* 14, 667–675. doi: 10.1038/s41582-018-0072-1

Urano, F., Wang, X., Bertolotti, A., Zhang, Y., Chung, P., Harding, H. P., et al. (2000). Coupling of stress in the ER to activation of JNK protein kinases by transmembrane protein kinase IRE1. *Science* 287, 664–666. doi: 10.1126/science.287.5453.664

Valdés, P., Mercado, G., Vidal, R. L., Molina, C., Parsons, G., Court, F. A., et al. (2014). Control of dopaminergic neuron survival by the unfolded protein response transcription factor XBP1. *Proc. Natl. Acad. Sci. U S A* 111, 6804–6809. doi: 10.1073/pnas.1321845111

Walter, P., and Ron, D. (2011). The unfolded protein response: from stress pathway to homeostatic regulation. *Science* 334, 1081–1086. doi: 10.1126/science.1209038

Wang, Y.-W., Zhou, Q., Zhang, X., Qian, Q.-Q., Xu, J.-W., Ni, P.-F., et al. (2017). Mild endoplasmic reticulum stress ameliorates lipopolysaccharide-induced neuroinflammation and cognitive impairment *via* regulation of microglial polarization. *J. Neuroinflammation* 14:233. doi: 10.1186/s12974-017-1002-7

Wensky, A. K., Furtado, G. C., Garibaldi Marcondes, M. C., Chen, S., Manfra, D., Lira, S. A., et al. (2005). IFN-γ determines distinct clinical outcomes in autoimmune encephalomyelitis. *J. Immunol.* 174, 1416–1423. doi: 10.4049/jimmunol.174.3.1416

Wheeler, M. A., Jaronen, M., Covacu, R., Zandee, S. E. J., Scalisi, G., Rothhammer, V., et al. (2019). Environmental control of astrocyte pathogenic activities in CNS inflammation. *Cell* 176, 581–596. doi: 10.1016/j.cell.2018.12.012

Yamamoto, K., Sato, T., Matsui, T., Sato, M., Okada, T., Yoshida, H., et al. (2007). Transcriptional induction of mammalian ER quality control proteins is mediated by single or combined action of ATF6α and XBP1. *Dev. Cell* 13, 365–376. doi: 10.1016/j.bcp.2019.113744

Yang, F., Liu, Y., Ren, H., Zhou, G., Yuan, X., and Shi, X. (2019). ER-stress regulates macrophage polarization through pancreatic EIF-2alpha kinase. *Cell. Immunol.* 336, 40–47. doi: 10.1016/j.cellimm.2018.12.008

Yang, F., Wang, S., Liu, Y., Zhou, Y., Shang, L., Feng, M., et al. (2018). IRE1α aggravates ischemia reperfusion injury of fatty liver by regulating phenotypic transformation of kupffer cells. *Free Radic. Biol. Med.* 124, 395–407. doi: 10.1016/j.freeradbiomed.2018.06.043

Yang, Q., Wang, G., and Zhang, F. (2020). Role of peripheral immune cells-mediated inflammation on the process of neurodegenerative diseases. *Front. Immunol.* 11:2511. doi: 10.3389/fimmu.2020.582825

Yang, X., Xia, R., Yue, C., Zhai, W., Du, W., Yang, Q., et al. (2018). ATF4 regulates CD4 + T cell immune responses through metabolic reprogramming. *Cell Rep.* 23, 1754–1766. doi: 10.1016/j.celrep.2018.04.032

Zeng, L., Liu, Y.-P., Sha, H., Chen, H., Qi, L., and Smith, J. (2010). XBP-1 couples endoplasmic reticulum stress to augmented IFNβ induction *via* a cis-acting enhancer in macrophages. *J. Immunol.* 185, 2324–2330. doi: 10.4049/jimmunol.0903052

Zhang, W., Phillips, K., Wielgus, A. R., Liu, J., Albertini, A., Zucca, F. A., et al. (2011). Neuromelanin activates microglia and induces degeneration of dopaminergic neurons: implications for progression of parkinson's disease. *Neurotox. Res.* 19, 63–72. doi: 10.1007/s12640-009-9140-z

Zhao, J., Bi, W., Xiao, S., Lan, X., Cheng, X., Zhang, J., et al. (2019). Neuroinflammation induced by lipopolysaccharide causes cognitive impairment in mice. *Sci. Rep.* 9:5790. doi: 10.1038/s41598-019-42286-8

Zhou, Y., Tong, Z., Jiang, S., Zheng, W., Zhao, J., and Zhou, X. (2020). The roles of endoplasmic reticulum in nlrp3 inflammasome activation. *Cells* 9:1219. doi: 10.3390/cells9051219

Conflict of Interest: The authors declare that the research was conducted in the absence of any commercial or financial relationships that could be construed as a potential conflict of interest.

frontiers in Aging Neuroscience

MINI REVIEW
published: 19 November 2021
doi: 10.3389/fnagi.2021.767493

The Interplay of the Unfolded Protein Response in Neurodegenerative Diseases: A Therapeutic Role of Curcumin

Sitabja Mukherjee[1†], Awdhesh Kumar Mishra[2†], G. D. Ghouse Peer[3†], Sali Abubaker Bagabir[4], Shafiul Haque[5,6], Ramendra Pati Pandey[3], V. Samuel Raj[3], Neeraj Jain[7], Atul Pandey[8,9] and Santosh Kumar Kar[10]**

[1] School of Biotechnology, KIIT University, Bhubaneswar, India, [2] Department of Biotechnology, Yeungnam University, Gyeongsan, South Korea, [3] Department of Biotechnology, Sri Ramaswamy Memorial (SRM) University, Sonepat, India, [4] Department of Medical Laboratory Technology, Faculty of Applied Medical Sciences, Jazan University, Jazan, Saudi Arabia, [5] Research and Scientific Studies Unit, College of Nursing and Allied Health Sciences, Jazan University, Jazan, Saudi Arabia, [6] Faculty of Medicine, Bursa Uludağ University, Bursa, Turkey, [7] Division of Cancer Biology, Council of Scientific and Industrial Research (CSIR)-Central Drug Research Institute, Lucknow, India, [8] Department of Ecology and Evolutionary Biology, University of Michigan, Ann Arbor, MI, United States, [9] Department of Ecology, Evolution and Behavior, The Alexander Silberman Institute of Life Science, The Hebrew University of Jerusalem, Jerusalem, Israel, [10] Nano Herb Research Laboratory, Kalinga Institute of Industrial Technology (KIIT) Technology Business Incubator, KIIT University, Bhubaneswar, India

OPEN ACCESS

Edited by:
Rinki Minakshi, University of Delhi, India

Reviewed by:
Niraj Kumar Jha, Sharda University, India
Upendra Kumar Singh, La Jolla Institute for Immunology (LJI), United States

***Correspondence:**
Atul Pandey
atulkp@umich.edu
Santosh Kumar Kar
santoshkariis@rediffmail.com

† These authors have contributed equally to this work and share first authorship

Received: 30 August 2021
Accepted: 18 October 2021
Published: 19 November 2021

Citation:
Mukherjee S, Mishra AK, Peer GDG, Bagabir SA, Haque S, Pandey RP, Raj VS, Jain N, Pandey A and Kar SK (2021) The Interplay of the Unfolded Protein Response in Neurodegenerative Diseases: A Therapeutic Role of Curcumin. Front. Aging Neurosci. 13:767493. doi: 10.3389/fnagi.2021.767493

Abnormal accumulation of misfolded proteins in the endoplasmic reticulum and their aggregation causes inflammation and endoplasmic reticulum stress. This promotes accumulation of toxic proteins in the body tissues especially brain leading to manifestation of neurodegenerative diseases. The studies suggest that deregulation of proteostasis, particularly aberrant unfolded protein response (UPR) signaling, may be a common morbific process in the development of neurodegeneration. Curcumin, the mixture of low molecular weight polyphenolic compounds from turmeric, *Curcuma longa* has shown promising response to prevents many diseases including current global severe acute respiratory syndrome coronavirus 2 (SARS-CoV-2) infection and neurodegenerative disorders. The UPR which correlates positively with neurodegenerative disorders were found affected by curcumin. In this review, we examine the evidence from many model systems illustrating how curcumin interacts with UPR and slows down the development of various neurodegenerative disorders (ND), e.g., Alzheimer's and Parkinson's diseases. The recent global increase in ND patients indicates that researchers and practitioners will need to develop a new pharmacological drug or treatment to manage and cure these neurodegenerative diseases.

Keywords: Alzheimer's disease, Parkinson's disease, neurodegenaration, unfolded protein response, ER stress, curcumin, ROS—reactive oxygen species, cell death

INTRODUCTION

The global burden of neurological diseases are rising, and considered as one of the leading causes of mortality and disability across the globe (Gammon, 2014; Feigin et al., 2019). The correct folding and packaging of the proteins are essential in regulation of many neurological diseases. All proteins bound to organelles and extracellular spaces are subject to proteostasis (Wang and Kaufman, 2016).

The abundance of too many secretory proteins in the endoplasmic reticulum (ER) induces the unfolded protein response (UPR) and in case of chronic ER-stress this leads to apoptotic cell death (Taniguchi and Yoshida, 2011; Hetz et al., 2013; Shah et al., 2015; **Figure 1**). Thus, the UPR protects cells against deformed proteins and maintains cellular homeostasis (Smith and Mallucci, 2016). There are three signal transducers inside the ER, which are inositol requiring enzymes 1 (IRE1) α and β, protein kinase R-like ER kinase (PERK) categorized as type I, and activating transcription factor 6 (ATF6), α and β as type II (Shah et al., 2015; Hetz and Papa, 2018). Various transcription factors activate these signal transducers to restore proteostasis and enhance ER and Golgi biogenesis (Hetz et al., 2020). Neurodegenerative diseases (NDs) are characterized by the degeneration and death of neurons (Pohl et al., 2018). While, the misfolded proteins cause ER-stress-induced neuronal apoptosis in progressive neurodegenerative diseases like Alzheimer's disease (AD), Parkinson's disease (PD) (Hetz and Mollereau, 2014; Scheper and Hoozemans, 2015; **Figure 1**). AD which accounts for 60–80% and other forms of dementia are the world's fifth leading cause of death, and its prevalence is expected to triple by 2050, according to WHO (Voulgaropoulou et al., 2019). While, PD is the most common neurodegenerative disease (20–30%) after Alzheimer's, with a prevalence of 150/100,000 (Schapira, 1999).

Curcumin, a primary natural polyphenol derived from *Curcuma longa* rhizome is found affecting a number of diseases including current SARS-CoV-2 infection (Gupta et al., 2013; Noorafshan and Ashkani-Esfahani, 2013; Marton et al., 2020; Sharifi-Rad et al., 2020; Ahmadi et al., 2021). The antioxidant, anti-inflammatory, anti-mutagenic, anti-parasitic, antimicrobial and anti-cancerous properties of curcumin are quite explored (Reddy et al., 2005; Aggarwal and Harikumar, 2009; Gupta et al., 2013; Vera-Ramirez et al., 2013; Lestari and Indrayanto, 2014; Hewlings and Kalman, 2017). Recently curcumin was characterized as a pharmacophore by X-ray micro-crystallography of fiber-forming tau fragments with small molecule binders, binding to the β-pleated layer in tau's paired helical filaments (Landau et al., 2011). Reports suggest that curcumin further scavenges the toxic reactive oxygen species (ROS) and increases Superoxide dismutase (SOD), Na^{+}-K^{+} ATPase, catalase, glutathione, and mitochondrial complex enzyme levels (Reeta et al., 2010; Barzegar and Moosavi-Movahedi, 2011; Li et al., 2020). It also reduces lipid peroxidation by reducing Malondialdehyde, nitrite, and acetylcholinesterase (Abdel-Diam et al., 2019; Kheirouri and Alizadeh, 2019). Curcumin affects neurogenesis in brain regions involving the Canonical Wnt/-Catenin Pathway (Tiwari et al., 2014). It activates nuclear factor erythroid 2-related factor (Nrf2), the antioxidant master regulator, to protect dopaminergic

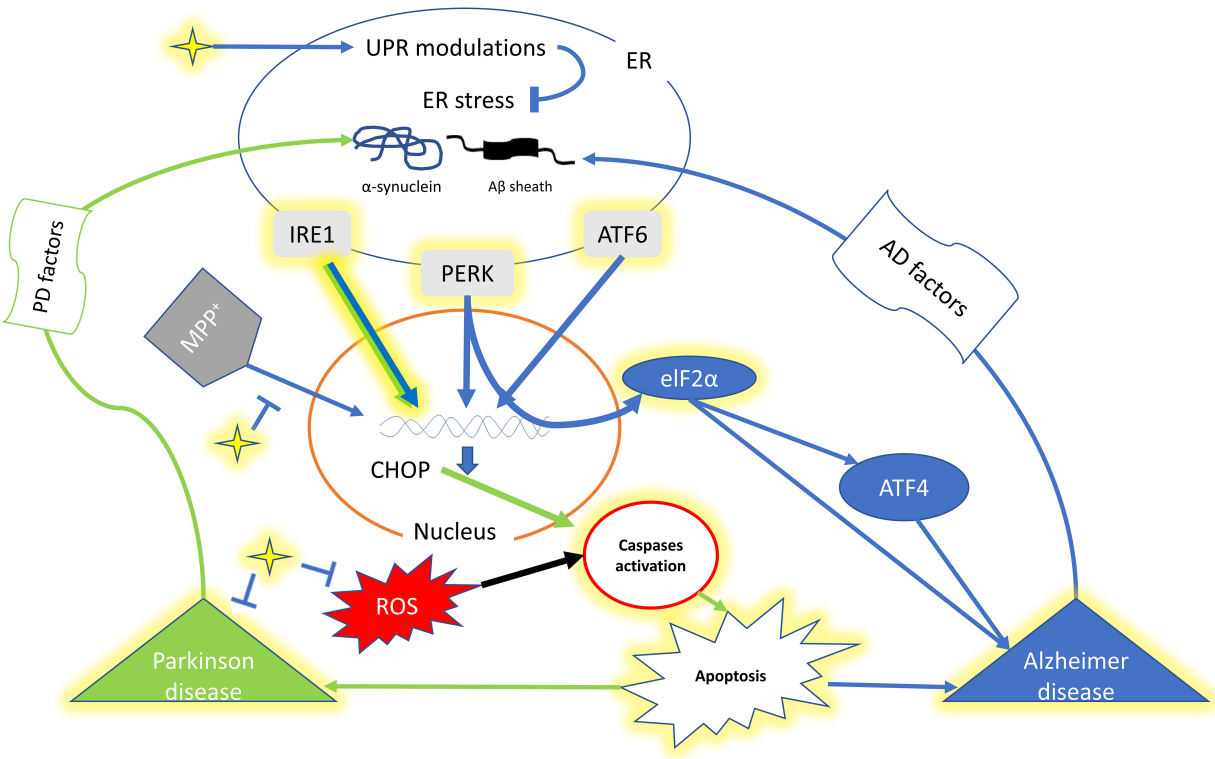

FIGURE 1 | A schematic representation of interplay of curcumin, UPR and factors of Alzheimer's disease and Parkinson's disease. The yellow highlighted genes, component and pathway represents the effect of Curcumin. The star shape (yellow) denotes curcumin. Green arrow shows signaling pathway for PD while Blue of AD. ER, endoplasmic reticulum; IRE1, inositol requiring enzymes 1; PERK, protein kinase R-like ER kinase; ATF4, Activating transcription factor 4; ATF6, Activating transcription factor 6; CHOP, C/EBP Homologous Protein; eIF2a, Eukaryotic translation initiation factor 2 alpha.

neurons (Dong et al., 2018). Furthermore, curcumin increases the expression of β-tubulin, neuroD1, doublecortin, neurogenic, neuroligin, and neuregulin while decreases the expression of the signal transducer and activator of transcription 3 (STAT3) (Karlstetter et al., 2011). Curcumin further helps in inhibition of neuroinflammation possibly by binding to the sensile plaques, inhibiting Aβ plaque aggregation, plaque pathology, and decreasing amyloid levels (Lim et al., 2001; McClure et al., 2017; Mei et al., 2020). It also inhibits several dysregulated cell-signaling pathways (Su et al., 2020; Ege, 2021). Curcumin also safeguards against AD (Desai and Patravale, 2018; Nebrisi et al., 2020). Recently, curcumin and curcuminoids were reported as a promising candidate against NDs (Gregory et al., 2021; Ryskalin et al., 2021; Silvestro et al., 2021; Simeonova et al., 2021). Here we review the curcumin's potential role in NDs and UPR regulations. Given the volume of literature, we chosen to focus on with common NDs like AD and PD in relation to UPR.

UNFOLDED PROTEIN RESPONSE AND NEURODEGENERATIVE DISEASES: A COMMON CONNECTION AND CONSEQUENCES

UPR activation has been observed in many NDs (Scheper and Hoozemans, 2015). Activated astrogliosis, brain aggravation, and microglial multiplication cause ADs (Haass and Selkoe, 2007). The amyloid-β (Aβ) peptide aggregates in specific brain areas like the neocortex, hippocampus, and limbic region which further causes synaptic failure and neuronal death (Chyung et al., 2005). UPR is a cellular stress reaction caused by misfolded proteins in the ER, while misfolded proteins accumulate in PD (Taylor et al., 2002). Thus, the UPR is linked to PD in cell models (Hoozemans et al., 2007). In PD, Lewy bodies and protein incorporation in neurites were increased (Mahul-Mellier et al., 2020). Synuclein, a small presynaptic protein, is a major component of Lewy bodies (Clayton and George, 1999; Breydo et al., 2012). The PD patients were also found correlated with higher levels of pPERK, peIF2, and pIRE1 than non-neurological controls (Hoozemans et al., 2007). pPERK-positive neurons had increased diffuse cytoplasmic synuclein immunoreactivity. These findings suggest a link between synuclein accumulation and ER stress in dopaminergic neurons. Further, heat shock reactions and ER or mitochondrial unfolded protein reactions are examples of misfold UPR (Lee et al., 2011; Kakkar et al., 2014; Chiti and Dobson, 2017; Shamsi et al., 2017). By upregulating atomic chaperones and proteasome components, the authors reported the increase in the ability to unfold and refold misfolded proteins, as well as eliminate misfolded proteins (Ciechanover and Kwon, 2017).

CURCUMIN AND NEURODEGENERATIVE DISEASES: INTERVENTIONS AND MODALITIES

This section reviews curcumin's use and effects on NDs, while focusing on PD and AD. Curcumin's neurological effects make it one of the most promising natural therapies for AD (Noorafshan and Ashkani-Esfahani, 2013; Eghbaliferiz et al., 2020). The lower prevalence of AD in India among adults aged 70–79 years (4.4 times lower than in the US) is attributed to higher curcumin use (Ganguli et al., 2000; Yang et al., 2005). Curcumin's ability to bind to Aβ-pleated structure reduces plaque stress in most AD plaque pathogenesis models (Yang et al., 2005; Garcia-Alloza et al., 2007; Cheng et al., 2013). Curcumin is also known for directly binding and inhibiting the aggregation of Aβ-sheet conformations found in many NDs (Cole et al., 2007; Mishra and Palanivelu, 2008; Forouzanfar et al., 2020; Radbakhsh et al., 2021).

Curcumin inhibits tau aggregation by binding to neurofibrillary tangles (Brunden et al., 2010; Mohorko et al., 2010; Mutsuga et al., 2012). Several β-pleated layer complexes, such as huntingtin, prion aggregates and α-synuclein, are found interacting with curcumin (Caughey et al., 2003; Ono et al., 2004; Pandey et al., 2008). Curcumin interacts directly with heat shock proteins (HSPs), such as HSP90 and HSP70, in Aβ-infused rats, tau transgenic mice and human models (Ma et al., 2013). It affects phagocytic cell association with plaque structures and stimulates clearance of Aβ aggregates in human cell lines and rodent AD models, similar to the amyloid vaccine (Frautschy et al., 2001; Cole et al., 2004). Curcumin also inhibits NF-κ *B* and Activator Protein 1 (AP1). A dysfunctional transcription factor pathway limits the resolution of inflammation in AD. Curcumin's inhibition of AP1 transcription results in hyperphosphorylation of tau (Singh and Aggarwal, 1995; Xu et al., 1997; Cho et al., 2007). According to recent research, curcumin seems to decrease peroxisome proliferator activated receptor (PPAR) activation by inhibiting Toll-like receptor 4 complex homodimerization. Wang et al. (2010) report that curcumin directly increases PPAR expression. The PPAR forms heterodimers with Retinoid X receptor alpha to control microglial activation and phagocytosis (Heneka et al., 2005). PPAR inhibits pro-inflammatory cytokines that promote tau kinase hyperactivity, pTau buildup, and oxidative damage. Curcumin also promotes oligodendrocyte progenitor (OP) differentiation and inhibits tumor necrosis factor-induced OP maturation arrest through PPAR (Bernardo et al., 2021). Curcumin directly inhibits β-site amyloid precursor protein-cleaving enzyme 1 (BACE1), which catalyzes the N terminal cleavage of transmembrane amyloid precursor protein (APP) (Lin et al., 2008), which further indirectly inhibits BACE1 (Huang et al., 2020). Curcumin also reduce Aβ levels by delaying APP maturation in the secretory route (Zhang et al., 2010). The anti-inflammatory properties of curcumin have been linked to improved learning and memory in ApoE4 mice (Kou et al., 2021).

Curcumin combats AD in various ways, according to recent research (Serafini et al., 2017; Su et al., 2020). It inhibits the production of β-amyloid, tau, and acetylcholinesterase, controls microglia, and chelates metals (Tang et al., 2017; Voulgaropoulou et al., 2019). Curcumin binds to Aβ and inhibits harmful aggregate formation (Ono et al., 2004; Kim et al., 2005; Yang et al., 2005). However, the diketone bridge in curcumin is not necessary for curcumin's anti-inflammatory actions, since reduced curcumin (tetrahydro curcumin) has strong anti-inflammatory characteristics (Begum et al., 2008). By deactivating Glycogen synthase kinase 3 (GSK-3), it reduced Aβ generation

and plaque formation by downregulating the ROS/JNK pathway. Curcumins inhibition of BACE1 by GSK3 resulted in reduction of Aβ plaques (Durairajan et al., 2012). The precise means by which curcumin regulates these processes are unknown. It seems like that curcumin is a potential antioxidant for treating AD, and that combining carriers and targeting agents to enhance brain delivery is highly effective. In future, more research on curcumin's mechanism of action related to NDs are required.

INTERPLAY OF CURCUMIN AND UNFOLDED PROTEIN RESPONSE

The ER has vital cellular functions including protein folding, post-translational modification, protein translocation, lipid synthesis, and Ca^{2+} storage (Schwarz and Blower, 2016). Under ER-stress, evolutionarily conserved UPR response system corrects ER homeostasis by activating transcription factors (ATF4, ATF6, and XBP1) that inhibit protein translation, and promotes unfolded protein destruction (Zhao and Ackerman, 2006; Limonta et al., 2019). In cases of persistent ER stress, the UPR initiates intrinsic apoptotic pathway and cell death (Sano and Reed, 2013). UPR may also be triggered by non-ER stress associated mechanisms (Hetz et al., 2020). For example, vascular endothelial growth factor signaling promotes angiogenesis through the UPR pathway (Urra and Hetz, 2014). Considering the vastness of this topic, we have chosen to concentrate on curcumin's role in UPR regulation in NDs.

Curcumin as a Suppressor or Inducer of Unfolded Protein Response in Neurological Diseases

Curcumin Function in Brain Injury

Diffuse axonal injury (DAI) associated with abnormally expressed β-APP and p-tau proteins in neurons leds to ER-stress induced cell death. Curcumin treatment in rat DAI model increased PERK phosphorylation and decreased CHOP expression and therefore prevented aberrant protein accumulation and inhibited UPR pathway activation (Huang et al., 2018). In another study, curcumin protected against glutamate-induced hippocampus neurotoxicity. The therapeutic role of curcumin against various human diseases are well explored (Shakeri et al., 2019).

Mutation Associated Neuropathies

Besides having a protective impact on brain injuries, curcumin treatment has also improved peripheral neuropathies. For example, Trembler-J is caused by accumulation of mutated myelin proteins (PMP22) that led to ER stress, UPR activation, and Schwann cell death, which were minimized by curcumin treatment (Okamoto et al., 2013). The second most prevalent autosomal dominant hereditary demyelinating neuropathy is Charcot–Marie–Tooth disease type 1B (CMT1B), caused by activation of UPR components coupled with accumulation of mutant protein myelin protein Zero (P0, MPZ), as a consequence of ER stress (Santoro et al., 2004; Khajavi et al., 2005; Saporta et al., 2011). Using the CMT1B mouse model of human neuropathy, researchers discovered that these mice exhibited motor impairment and axonal abnormalities linked with aberrant UPR activation (Patzkó et al., 2012). It was noted that curcumin formulation could influence the treatment outcomes. Oral curcumin in sesame oil enhanced neurophysiological state and Schwann cell myelination in CMT1B mouse model with decreased UPR signaling (Patzkó et al., 2012). Using the HT22 mouse hippocampus cell line, Chhunchha et al. (2013) discovered that curcumin has anti-oxidative and anti-ER stress properties. Curcumin therapy increased peroxiredoxin 6 (Prdx6) expressions and decreased ER stress in hypoxic HT22 cells (Chhunchha et al., 2013). ApoE4 is the major genetic risk factor for AD associated with dementia. Kou et al. (2021) found that ApoE4 transgenic mice had impaired cognitive capacity, which is linked to ER stress and activation of inflammatory signaling in the nervous system; these were reversed by curcumin treatment in AD mice. Curcumin is also found effective in Pelizaeus-Merzbacher disease of mice model (Gow et al., 1998; Hübner et al., 2005; Yu et al., 2012).

Analogs of Curcumin and Unfolded Protein Response in Neurological Diseases

The low bioavailability of curcumin leads to its poor absorption, requiring large doses of curcumin to reach a definite level in plasma. Curcumin plasma levels have been improved by dissolving it in various solutions, coating it with nanoparticles, forming emulsions and by creating its analogs (Sasaki et al., 2011; Zhongfa et al., 2012; Ramalingam and Ko, 2015). There are multiple curcumin analogs have been generated those presented profound effect in modulating ER stress in various cancers model including ovarian, colon, lung, prostrate, gastric, acute promyelocytic leukemia, glioblastoma, melanoma, and triple negative breast cancer cells (Zhang et al., 2012; Qu et al., 2013; Tan et al., 2014; Yoon et al., 2014; Zheng et al., 2014; Chen et al., 2016; Gao et al., 2017; He et al., 2021). However, curcumin mimics' effects on neurodegenerative disorders are poorly documented.

Treatment with CNB-001, a curcumin derivative, reduced intracellular soluble-amyloid build up in AD transgenic mice by activating the UPR's eIF2/ATF4 signaling (Valera et al., 2013). Protein disulfide isomerase (PDI) is an ER-resident chaperone that is modified to S-nitroso-PDI in the presence of high levels of nitric oxide (NO), which disrupts PDI's redox activity and resulted in the accumulation of misfolded in AD and PD model (Uehara et al., 2006). Curcumin analog 3,5-bis (2-flurobenzylidene) piperidin-4-one (EF-24) pretreatment of neuroblastoma cell line SHSY-5Y cells prevented rotenone-induced (a mitochondrial reactive oxygen species elevator) reduction in PDI expression and ER stress associated protein aggregation (Pal et al., 2011). Glioblastoma is the most common, highly invasive and malignant form of brain cancer currently treated with surgery, radiotherapy and chemotherapy. In a study published by Sansalone et al. (2019) have generated 19 curcumin analogs, out of which 4 have induced glioma stem cells (GSC) death and prevented neurosphere formation. Mechanistically, curcumin analog robustly induced UPR signaling as detected by

TABLE 1 | Curcumin and its analogs are associated with UPR modulation in neurological disorders.

Compound	Disease type/cell line	Effects on ER stress markers and UPR signaling	References
Curcumin	DAI model of rat	↑ (Nrf2, p-PERK), ↓ (CHOP)	Huang et al., 2018
Curcumin	Hippocampus or SH-SY5Y cells	↑ (AMPK), ↓ (p-IRE1α, p-PERK, NLRP3, TXNIP/NLRP3)	Li et al., 2015
Curcumin	Mouse hippocampus cell HT22	↑ Prdx6, CHOP, Grp78), ↓ (ROS)	Valera et al., 2013
Curcumin	Pmp22 Trembler-J mice	↓ (Atf3 and Ero1-lβ)	Okamoto et al., 2013
Curcumin dissolved in sesame oil or phosphatidylcholine	MPZ^{R98C} knock-in mice	↓ (Bip, ATF6, spliced XBP1), no change in CHOP expression	Patzkó et al., 2012
Curcumin	ApoE4 transgenic mice (SCXK2016-0004)	↓ (NFkβ, APoE4, Grp78, IRE1α)	Kou et al., 2021
Curcumin	Transgenic myelin synthesis deficient model	No changes in expression of Grp78, CHOP, Gadd45a, calnexin, calreticulin, Herpud1	Yu et al., 2012
CNB-001 (Curcumin analog)	huAPPswe/PS1E9 transgenic mice and MC65 cells	↑ (p-PERK, eIF2α, HSP90, ATF4), ↓ (5-LOX, β-amyloid)	Valera et al., 2013
EF-24 (Curcumin analog)	SHSY-5Y	↑ (PDI expression), ↓ (AD associated protein aggregation)	Pal et al., 2011
Bis-chalcone 4j (Curcumin analog)	GSC lines Glio3, Glio4, Glio9, Glio11 and Glio14	↑ (CHOP, p-jun and caspase 12)	Sansalone et al., 2019
C-150 (Curcumin analog)	GBM1-6, U87 MG, U251 MG and U373 MG	↑ (Grp78, GADD153, ATF4, XBP1), ↓ (NFkβ, Akt, PKCα kinase activity)	Hackler et al., 2016

DAI, diffuse axonal injury; Nrf2, nuclear factor erythroid-derived 2-like 2; CHOP, CCAAT-enhancer-binding protein homologous protein; AMPK, AMP-activated protein kinase; NLRP3, NLR family pyrin domain containing 3; ApoE4, Apolipoprotein E4; GSC, glioma stem cells; AD, Alzheimer's disease; XBP1, X-binding protein-1; ATF, activating transcription factor; Grp78, 78-kDa glucose-regulated protein; PDI, protein disulfide-isomerase; HSP90, heat shock protein 90; GADD153, growth arrest- and DNA damage-inducible gene 153; PKCα, protein kinase C; eIF2α, eukaryotic translation initiation factor 2A; Bip, binding immunoglobulin protein; Ero1, endoplasmic oxidoreductin-1; Prdx6, peroxiredoxin-6; ROS, reactive oxygen species.

increased expression of CHOP, p-jun and caspase 12 markers (Sansalone et al., 2019). Another study by Hackler et al. (2016) has demonstrated the cytotoxic effect of curcumin derivative C-150 (Mannich-type) on eight glioma cell lines. C-150 treatment in gliomas cells significantly affected expression of UPR proteins, Akt, and PKCα activity.

Overall, curcumin and its derivatives are neuroprotective in various neurological disorders and kill cancer cells via modulating UPR signaling (**Table 1**). The main difficulty is to formulate curcumin or its counterpart in the correct dosage and administer it in a proper manner. This includes undoubtedly to overcome poor absorption, rapid metabolism and poor bioavailability of curcumin and substantially improve its beneficial activities.

CURCUMIN, UNFOLDED PROTEIN RESPONSE AND NEURODEGENERATIVE DISEASES: A TRIVIAL CONNECTION AND FUTURE PERSPECTIVES

The studies suggest that deregulation of proteostasis, particularly aberrant UPR signaling, may be a common pathogenic mechanism in the development of ND. While modulation of the UPR in animal illness models, including AD, has shown early promises. To determine whether UPR signaling is a protective mechanism or actively contributes to disease development, neuropathological data alone cannot be used. The idea of targeting the UPR, and specifically the PERK signaling is extremely interesting (Das et al., 2015). Some protein misfolding in NDs appear to benefit from selectively increasing protein synthesis upstream or downstream of eIF2a-P to avoid pancreatic toxicity associated with systemic PERK inhibition.

Researchers also discovering novel UPR activation methods, e.g., mitochondria-associated ER membranes are gaining popularity as a possible therapeutic target in NDs. Disrupted connections between the ER and mitochondria have been identified were curcumin seems to influence ER-mitochondrial interactions (Paillusson et al., 2016). Curcumin as licensed drug delaying the development of dementia in different model systems, this is an intriguing idea and a major step forward in the quest for a therapeutic agent for neurodegeneration. The next issue will be identifying how best and when to regulate the PERK pathway in patients, given that there are many proven therapeutic targets along the route. What remains unclear if curcumin may directly interfere in neurodegeneration without engaging UPR components?

Curcumin affect the action of many factors such as NF-κ B and AP-1 (Han et al., 2002). Curcumin binds to different proteins and enzymes and modulate their conformation and biological activities. Curcumin's linker length and flexibility make it ideal for binding to Aβ aggregates. Curcumin's unique structure, which consists of an, α, β-unsaturated β-diketone moiety linked by a seven carbon heptadiene chain, allows it to remain in keto–enol tautomeric forms in solution depending on the pH. When the pH is between 3 and 7, it is in the keto form, whereas the enol form is found around pH 8. Curcumin retains its coplanarity

and extends the double-bond conjugation through six membered hydrogen bonding at the center when it is in the enol form which has strong Aβ aggregate binding activities. Curcumin, on the other hand, has very low binding activities for Aβ aggregates when it is in the keto form. Studies have shown that to be able to bind to Aβ aggregates, compounds need to be coplanar and have a double-bond conjugation of certain length. Curcumin, however, has certain disadvantages too, which includes its low water solubility and bioavailability. Dissolving it into organic solvent improves it solubility but its absorption remains poor (Ege, 2021; Jia et al., 2021). Some recent articles addressed the methods to enhance curcumin's effectiveness in treating AD (Fan et al., 2018; Francesco et al., 2019; Ege, 2021). In future curcumin compounds must be chemically screened on target enzymes and proteins to facilitate more information.

Overall, the studies suggest that curcumin may prevents or postpones the onset of NDs by decreasing ER stress which seems to be responsible for NDs through a complicated processes (**Figure 1**). Additional mechanistic studies are needed to establish curcumin's role in reducing ER stress. Despite promising preclinical findings, there are currently no clinical data to support curcumin as part of a drug therapy against NDs. The recent rise in the number of NDs patients across the globe suggests that researchers and practitioners will need to discover an effective pharmaceutical medication or therapy to successfully treat these illnesses in the future. Curcumin's interaction and mechanism of action against NDs warrants a more research to accomplish this goal.

AUTHOR CONTRIBUTIONS

NJ, RP, AP, and SK contributed to the conception and design of the study. SM, AM, GP, NJ, and AP organized the material and wrote the first draft of the manuscript. SM, GP, SB, SH, NJ, and AP wrote sections of the manuscript. RP, VR, NJ, AP, and SK helped with manuscript editing and formatting. All authors contributed to manuscript revision, read, and approved the submitted version.

FUNDING

NJ was supported by the Ramalingaswami grant (BT/RLF/Re-entry/18/2017) from the Department of Biotechnology, Ministry of Science and Technology, Government of India. AP was supported by the Planning and Budgeting Committee (PBC) outstanding postdoctoral fellowship, Israel.

REFERENCES

Abdel-Diam, M. M., Samak, D. H., El-Sayed, Y. S., Aleya, L., Alarifi, S., and Alkahtani, S. (2019). Curcumin and quercetin synergistically attenuate subacute diazinon-induced inflammation and oxidative neurohepatic damage, and acetylcholinesterase inhibition in albino rats. *Environ. Sci. Pollut. Res. Int.* 26, 3659–3665. doi: 10.1007/S11356-018-3907-9

Aggarwal, B. B., and Harikumar, K. B. (2009). Potential therapeutic effects of curcumin, the anti-inflammatory agent, against neurodegenerative, cardiovascular, pulmonary, metabolic, autoimmune and neoplastic diseases. *Int. J. Biochem. Cell Biol.* 41, 40–59. doi: 10.1016/j.biocel.2008.06.010

Ahmadi, R., Salari, S., Sharifi, M. D., Reihani, H., Rostamiani, M. B., Behmadi, M., et al. (2021). Oral nano-curcumin formulation efficacy in the management of mild to moderate outpatient COVID-19: A randomized triple-blind placebo-controlled clinical trial. *Food Sci. Nutr.* 9, 4068–4075. doi: 10.1002/FSN3.2226

Barzegar, A., and Moosavi-Movahedi, A. A. (2011). Intracellular ROS protection efficiency and free radical-scavenging activity of curcumin. *PLoS One* 6:26012. doi: 10.1371/journal.pone.0026012

Begum, A. N., Jones, M. R., Lim, G. P., Morihara, T., Kim, P., Heath, D. D., et al. (2008). Curcumin structure-function, bioavailability, and efficacy in models of neuroinflammation and Alzheimer's disease. *J. Pharmacol. Exp. Ther.* 326, 196–208. doi: 10.1124/jpet.108.137455

Bernardo, A., Plumitallo, C., De Nuccio, C., Visentin, S., and Minghetti, L. (2021). Curcumin promotes oligodendrocyte differentiation and their protection against TNF-α through the activation of the nuclear receptor PPAR-γ. *Sci. Rep.* 11:4952.

Breydo, L., Wu, J. W., and Uversky, V. N. (2012). A-synuclein misfolding and Parkinson's disease. *Biochim. Biophys. Acta* 1822, 261–285. doi: 10.1016/J.BBADIS.2011.10.002

Brunden, K. R., Ballatore, C., Crowe, A., Smith, A. B., Lee, V. M. Y., and Trojanowski, J. Q. (2010). Tau-directed drug discovery for Alzheimer's disease and related tauopathies: A focus on tau assembly inhibitors. *Exp. Neurol.* 223, 304–310. doi: 10.1016/j.expneurol.2009.08.031

Caughey, B., Raymond, L. D., Raymond, G. J., Maxson, L., Silveira, J., and Baron, G. S. (2003). Inhibition of Protease-Resistant Prion Protein Accumulation In Vitro by Curcumin. *J. Virol.* 77, 5499–5502. doi: 10.1128/jvi.77.9.5499-5502.2003

Chen, W., Zou, P., Zhao, Z., Weng, Q., Chen, X., Ying, S., et al. (2016). Selective killing of gastric cancer cells by a small molecule via targeting TrxR1 and ROS-mediated ER stress activation. *Oncotarget* 7, 16593–16609. doi: 10.18632/oncotarget.7565

Cheng, K. K., Yeung, C. F., Ho, S. W., Chow, S. F., Chow, A. H. L., and Baum, L. (2013). Highly stabilized curcumin nanoparticles tested in an in vitro blood-brain barrier model and in alzheimer's disease Tg2576 Mice. *AAPS J.* 15, 324–336. doi: 10.1208/s12248-012-9444-4

Chhunchha, B., Fatma, N., Kubo, E., Rai, P., Singh, S. P., and Singh, D. P. (2013). Curcumin abates hypoxia-induced oxidative stress based-ER stress-mediated cell death in mouse hippocampal cells (HT22) by controlling Prdx6 and NF-κB regulation. *Am. J. Physiol. Cell Physiol.* 304, C636–C655. doi: 10.1152/ajpcell.00345.2012

Chiti, F., and Dobson, C. (2017). Protein Misfolding amyloid formation, and Human Disease: a summary of progress over the last decade. *Annu. Rev. Biochem.* 86, 27–68. doi: 10.1146/ANNUREV-BIOCHEM-061516-045115

Cho, J. W., Lee, K. S., and Kim, C. W. (2007). Curcumin attenuates the expression of IL-1β, IL-6, and TNF-α as well as cyclin E in TNF-α-treated HaCaT cells; NF-κB and MAPKs as potential upstream targets. *Int. J. Mol. Med.* 19, 469–474. doi: 10.3892/ijmm.19.3.469

Chyung, J. H., Raper, D. M., and Selkoe, D. J. (2005). Gamma-secretase exists on the plasma membrane as an intact complex that accepts substrates and effects intramembrane cleavage. *J. Biol. Chem.* 280, 4383–4392. doi: 10.1074/jbc.M409272200

Ciechanover, A., and Kwon, Y. (2017). Protein Quality Control by Molecular Chaperones in Neurodegeneration. *Front. Neurosci* 11:185. doi: 10.3389/FNINS.2017.00185

Clayton, D. F., and George, J. M. (1999). Synucleins in Synaptic Plasticity and Neurodegenerative Disorders. *J. Neurosci. Res* 58, 120–129. doi: 10.1002/(SICI)1097-4547(19991001)58

Cole, G. M., Morihara, T., Lim, G. P., Yang, F., Begum, A., and Frautschy, S. A. (2004). NSAID and antioxidant prevention of Alzheimer's disease: lessons from in vitro and animal models. *Ann. N. Y. Acad. Sci.* 1035, 68–84. doi: 10.1196/annals.1332.005

Cole, G. M., Teter, B., and Frautschy, S. A. (2007). Neuroprotective effects of curcumin. *Adv. Exp. Med. Biol.* 595, 197–212. doi: 10.1007/978-0-387-46401-5_8

Das, I., Krzyzosiak, A., Schneider, K., Wrabetz, L., D'Antonio, M., Barry, N., et al. (2015). Preventing proteostasis diseases by selective inhibition of a phosphatase regulatory subunit. *Science* 348, 239–242. doi: 10.1126/science.aaa4484

Desai, P. P., and Patravale, V. B. (2018). Curcumin Cocrystal Micelles—Multifunctional Nanocomposites for Management of Neurodegenerative Ailments. *J. Pharm. Sci.* 107, 1143–1156. doi: 10.1016/j.xphs.2017.11.014

Dong, W., Yang, B., Wang, L., Li, B., Guo, X., Zhang, M., et al. (2018). Curcumin plays neuroprotective roles against traumatic brain injury partly via Nrf2 signaling. *Toxicol. Appl. Pharmacol.* 346, 28–36. doi: 10.1016/j.taap.2018.03.020

Durairajan, S. S. K., Liu, L.-F., Lu, J.-H., Chen, L.-L., Yuan, Q., Chung, S. K., et al. (2012). Berberine ameliorates β-amyloid pathology, gliosis, and cognitive impairment in an Alzheimer's disease transgenic mouse model. *Neurobiol. Aging* 33, 2903–2919. doi: 10.1016/j.neurobiolaging.2012.02.016

Ege, D. (2021). Action Mechanisms of Curcumin in Alzheimer's Disease and Its Brain Targeted Delivery. *Mater*14:332. doi: 10.3390/MA14123332

Eghbaliferiz, S., Farhadi, F., Barreto, G. E., Majeed, M., and Sahebkar, A. (2020). Effects of curcumin on neurological diseases: focus on astrocytes. *Pharmacol. Rep.* 72, 769–782. doi: 10.1007/s43440-020-00112-3

Fan, Y., Yi, J., Zhang, Y., and Yokoyama, W. (2018). Fabrication of curcumin-loaded bovine serum albumin (BSA)-dextran nanoparticles and the cellular antioxidant activity. *Food Chem.* 239, 1210–1218. doi: 10.1016/j.foodchem.2017.07.075

Feigin, V., Emma, N., Tahiya, A., Marlena, S. B., and Gbd 2016 Neurology Collaborators. (2019). Global, regional, and national burden of neurological disorders, 1990–2016: a systematic analysis for the Global Burden of Disease Study 2016. *Lancet Neurol.* 18, 459–480. doi: 10.1016/S1474-4422(18)30499-X

Forouzanfar, F., Read, M. I., Barreto, G. E., and Sahebkar, A. (2020). Neuroprotective effects of curcumin through autophagy modulation. *IUBMB Life* 72, 652–664. doi: 10.1002/iub.2209

Francesco, D. M., Margarucci, S., Galderisi, U., Crispi, S., and Peluso, G. (2019). Curcumin, gut microbiota, and neuroprotection. *Nutrients* 11:2426. doi: 10.3390/nu11102426

Frautschy, S. A., Hu, W., Kim, P., Miller, S. A., Chu, T., Harris-White, M. E., et al. (2001). Phenolic anti-inflammatory antioxidant reversal of Aβ-induced cognitive deficits and neuropathology. *Neurobiol. Aging* 22, 993–1005. doi: 10.1016/S0197-4580(01)00300-1

Gammon, K. (2014). Neurodegenerative disease: brain windfall. *Nature* 515, 299–300. doi: 10.1038/NJ7526-299A

Ganguli, M., Chandra, V., Kamboh, M. I., Johnston, J. M., Dodge, H. H., Thelma, B. K., et al. (2000). Apolipoprotein E polymorphism and Alzheimer disease: The Indo-US Cross-National Dementia Study. *Arch. Neurol.* 57, 824–830. doi: 10.1001/archneur.57.6.824

Gao, J., Fan, M., Peng, S., Zhang, M., Xiang, G., Li, X., et al. (2017). Small-molecule RL71-triggered excessive autophagic cell death as a potential therapeutic strategy in triple-negative breast cancer. *Cell Death Dis.* 8:e3049. doi: 10.1038/cddis.2017.444

Garcia-Alloza, M., Borrelli, L. A., Rozkalne, A., Hyman, B. T., and Bacskai, B. J. (2007). Curcumin labels amyloid pathology in vivo, disrupts existing plaques, and partially restores distorted neurites in an Alzheimer mouse model. *J. Neurochem.* 102, 1095–1104. doi: 10.1111/j.1471-4159.2007.04613.x

Gow, A., Southwood, C. M., and Lazzarini, R. A. (1998). Disrupted proteolipid protein trafficking results in oligodendrocyte apoptosis in an animal model of Pelizaeus-Merzbacher disease. *J. Cell Biol.* 140, 925–934. doi: 10.1083/jcb.140.4.925

Gregory, J., Vengalasetti, Y. V., Bredesen, D. E., and Rao, R. V. (2021). Neuroprotective herbs for the management of alzheimer's disease. *Biomolecules* 11:543. doi: 10.3390/biom11040543

Gupta, S. C., Patchva, S., and Aggarwal, B. B. (2013). Therapeutic roles of curcumin: Lessons learned from clinical trials. *AAPS J.* 15, 195–218. doi: 10.1208/s12248-012-9432-8

Haass, C., and Selkoe, D. (2007). Soluble protein oligomers in neurodegeneration: lessons from the Alzheimer's amyloid beta-peptide. *Nat. Rev. Mol. Cell Biol.* 8, 101–112. doi: 10.1038/NRM2101

Hackler, L., Ózsvári, B., Gyuris, M., Sipos, P., Fábián, G., Molnár, E., et al. (2016). The Curcumin Analog C-150, Influencing NF-κB, UPR and Akt/Notch Pathways Has Potent Anticancer Activity In Vitro and In Vivo. *PLoS One* 11:e0149832. doi: 10.1371/journal.pone.0149832

Han, S.-S., Keum, Y.-S., Seo, H.-J., and Surh, Y.-J. (2002). Curcumin Suppresses Activation of NF-κB and AP-1 Induced by Phorbol Ester in Cultured Human Promyelocytic Leukemia Cells. *J. Biochem. Mol. Biol.* 35, 337–342.

He, Y., Li, W., Zhang, J., Yang, Y., Qian, Y.-W., and Zhou, D. (2021). The curcumin analog EF24 is highly active against chemotherapy-resistant melanoma cells. *Curr. Cancer Drug Targets* 21, 608–618. doi: 10.2174/1568009621666210303092921

Heneka, M. T., Sastre, M., Dumitrescu-Ozimek, L., Hanke, A., Dewachter, I., Kuiperi, C., et al. (2005). Acute treatment with the PPARgamma agonist pioglitazone and ibuprofen reduces glial inflammation and Abeta1-42 levels in APPV717I transgenic mice. *Brain* 128, 1442–1453. doi: 10.1093/brain/awh452

Hetz, C., Chevet, E., and Harding, H. P. (2013). Targeting the unfolded protein response in disease. *Nat. Rev. Drug Discov.* 129, 703–719. doi: 10.1038/nrd3976

Hetz, C., and Mollereau, B. (2014). Disturbance of endoplasmic reticulum proteostasis in neurodegenerative diseases. *Nat. Rev. Neurosci.* 15, 233–249. doi: 10.1038/NRN3689

Hetz, C., and Papa, F. (2018). The Unfolded Protein Response and Cell Fate Control. *Mol. Cell* 69, 169–181. doi: 10.1016/J.MOLCEL.2017.06.017

Hetz, C., Zhang, K., and Kaufman, R. J. (2020). Mechanisms, regulation and functions of the unfolded protein response. *Nat. Rev. Mol. Cell Biol.* 21, 421–438. doi: 10.1038/s41580-020-0250-z

Hewlings, S., and Kalman, D. (2017). Curcumin: A Review of Its Effects on Human Health. *Foods* 6:92. doi: 10.3390/FOODS6100092

Hoozemans, J. J. M., van Haastert, E. S., Eikelenboom, P., de Vos, R. A. I., Rozemuller, J. M., and Scheper, W. (2007). Activation of the unfolded protein response in Parkinson's disease. *Biochem. Biophys. Res. Commun.* 354, 707–711. doi: 10.1016/j.bbrc.2007.01.043

Huang, P., Zheng, N., Zhou, H.-B., and Huang, J. (2020). Curcumin inhibits BACE1 expression through the interaction between ERβ and NFκB signaling pathway in SH-SY5Y cells. *Mol. Cell. Biochem.* 463, 161–173. doi: 10.1007/s11010-019-03638-0

Huang, T., Zhao, J., Guo, D., Pang, H., Zhao, Y., and Song, J. (2018). Curcumin mitigates axonal injury and neuronal cell apoptosis through the PERK/Nrf2 signaling pathway following diffuse axonal injury. *Neuroreport* 29, 661–677. doi: 10.1097/WNR.0000000000001015

Hübner, C. A., Orth, U., Senning, A., Steglich, C., Kohlschütter, A., Korinthenberg, R., et al. (2005). Seventeen novel PLP1 mutations in patients with Pelizaeus-Merzbacher disease. *Hum. Mutat.* 25, 321–322. doi: 10.1002/humu.9314

Jia, F., Chibhabha, F., Yang, Y., Kuang, Y., Zhang, Q., Ullah, S., et al. (2021). Detection and monitoring of the neuroprotective behavior of curcumin micelles based on an AIEgen probe. *J. Mater. Chem. B* 9, 731–745. doi: 10.1039/d0tb02320e

Kakkar, V., Meister-Broekema, M., Minoia, M., Carra, S., and Kampinga, H. H. (2014). Barcoding heat shock proteins to human diseases: looking beyond the heat shock response. *Dis. Model. Mech.* 7, 421–434. doi: 10.1242/dmm.014563

Karlstetter, M., Lippe, E., Walczak, Y., Moehle, C., Aslanidis, A., Mirza, M., et al. (2011). Curcumin is a potent modulator of microglial gene expression and migration. *J. Neuroinfl.* 8, 1–12. doi: 10.1186/1742-2094-8-125

Khajavi, M., Inoue, K., Wiszniewski, W., Ohyama, T., Snipes, G. J., and Lupski, J. R. (2005). Curcumin treatment abrogates endoplasmic reticulum retention and aggregation-induced apoptosis associated with neuropathy-causing myelin protein zero-truncating mutants. *Am. J. Hum. Genet.* 77, 841–850. doi: 10.1086/497541

Kheirouri, S., and Alizadeh, M. (2019). Dietary Inflammatory Potential and the Risk of Neurodegenerative Diseases in Adults. *Epidemiol. Rev.* 41, 109–120. doi: 10.1093/EPIREV/MXZ005

Kim, H., Park, B. S., Lee, K. G., Cheol, Y. C., Sung, S. J., Kim, Y. H., et al. (2005). Effects of naturally occurring compounds on fibril formation and oxidative stress of β-amyloid. *J. Agric. Food Chem.* 53, 8537–8541. doi: 10.1021/jf051985c

Kou, J., Wang, M., Shi, J., Zhang, H., Pu, X., Song, S., et al. (2021). Curcumin Reduces Cognitive Deficits by Inhibiting Neuroinflammation through the Endoplasmic Reticulum Stress Pathway in Apolipoprotein E4 Transgenic Mice. *ACS Omega* 6, 6654–6662. doi: 10.1021/acsomega.0c04810

Landau, M., Sawaya, M. R., Faull, K. F., Laganowsky, A., Jiang, L., Sievers, S. A., et al. (2011). Towards a pharmacophore for amyloid. *PLoS Biol.* 9:e1001080. doi: 10.1371/journal.pbio.1001080

Lee, S.-J., Lim, H.-S., Masliah, E., and Lee, H.-J. (2011). Protein aggregate spreading in neurodegenerative diseases: problems and perspectives. *Neurosci. Res.* 70, 339–348. doi: 10.1016/j.neures.2011.05.008

Lestari, M. L. A. D., and Indrayanto, G. (2014). Curcumin.Profiles Drug Subst. *Excip. Relat. Methodol.* 39, 113–204. doi: 10.1016/B978-0-12-800173-8.00003-9

Li, H., Dai, Y., Wu, H., Luo, L., Wei, L., Zhou, L., et al. (2020). Predictors of Early Neurologic Deterioration in Acute Pontine Infarction. *Stroke* 51, 637–640. doi: 10.1161/STROKEAHA.119.027239

Li, Y., Li, J., Li, S., Li, Y., Wang, X., Liu, B., et al. (2015). Curcumin attenuates glutamate neurotoxicity in the hippocampus by suppression of ER stress-associated TXNIP/NLRP3 inflammasome activation in a manner dependent on AMPK. *Toxicol. Appl. Pharmacol.* 286, 53–63. doi: 10.1016/j.taap.2015.03.010

Lim, G. P., Chu, T., Yang, F., Beech, W., Frautschy, S. A., and Cole, G. M. (2001). The curry spice curcumin reduces oxidative damage and amyloid pathology in an Alzheimer transgenic mouse. *J. Neurosci.* 21, 8370–8377. doi: 10.1523/jneurosci.21-21-08370.2001

Limonta, P., Moretti, R. M., Marzagalli, M., Fontana, F., Raimondi, M., and Montagnani Marelli, M. (2019). Role of Endoplasmic Reticulum Stress in the Anticancer Activity of Natural Compounds. *Int. J. Mol. Sci.* 20:961. doi: 10.3390/ijms20040961

Lin, R., Chen, X., Li, W., Han, Y., Liu, P., and Pi, R. (2008). Exposure to metal ions regulates mRNA levels of APP and BACE1 in PC12 cells: Blockage by curcumin. *Neurosci. Lett.* 440, 344–347. doi: 10.1016/j.neulet.2008.05.070

Ma, Q.-L., Zuo, X., Yang, F., Ubeda, O. J., Gant, D. J., Alaverdyan, M., et al. (2013). Curcumin suppresses soluble tau dimers and corrects molecular chaperone, synaptic, and behavioral deficits in aged human tau transgenic mice. *J. Biol. Chem.* 288, 4056–4065. doi: 10.1074/jbc.M112.393751

Mahul-Mellier, A.-L., Burtscher, J., Maharjan, N., Weerens, L., Croisier, M., Kuttler, F., et al. (2020). The process of Lewy body formation, rather than simply α-synuclein fibrillization, is one of the major drivers of neurodegeneration. *Proc. Natl. Acad. Sci. U.S.A.* 117, 4971–4982. doi: 10.1073/pnas.1913904117

Marton, L. T., Barbalho, S. M., Sloan, K. P., Sloan, L. A., Goulart, R., de, A., et al. (2020). Curcumin, autoimmune and inflammatory diseases: going beyond conventional therapy - a systematic review. *Crit. Rev. Food Sci. Nutr.* 1, 1–19. doi: 10.1080/10408398.2020.1850417

McClure, R., Ong, H., Janve, V., Barton, S., Zhu, M., Li, B., et al. (2017). Aerosol Delivery of Curcumin Reduced Amyloid-β Deposition and Improved Cognitive Performance in a Transgenic Model of Alzheimer's Disease. *J. Alzheimer's Dis.* 55, 797–811. doi: 10.3233/JAD-160289

Mei, X., Zhu, L., Zhou, Q., Li, X., and Chen, Z. (2020). Interplay of curcumin and its liver metabolism on the level of Aβ in the brain of APPswe/PS1dE9 mice before AD onset. *Pharmacol. Rep.* 72, 1604–1613. doi: 10.1007/s43440-020-00116-z

Mishra, K., and Palanivelu, K. (2008). The effect of curcumin (turmeric) on Alzheimer's disease: An overview. *Ann. Indian Acad. Neurol.* 11, 13–19. doi: 10.4103/0972-2327.40220

Mohorko, N., Repovs, G., Popović, M., Kovacs, G. G., and Bresjanac, M. (2010). Curcumin labeling of neuronal fibrillar tau inclusions in human brain samples. *J. Neuropathol. Exp. Neurol.* 69, 405–414. doi: 10.1097/NEN.0b013e3181d709eb

Mutsuga, M., Chambers, J. K., Uchida, K., Tei, M., Makibuchi, T., Mizorogi, T., et al. (2012). Binding of curcumin to senile plaques and cerebral amyloid angiopathy in the aged brain of various animals and to neurofibrillary tangles in Alzheimer's brain. *J. Vet. Med. Sci.* 74, 51–57. doi: 10.1292/jvms.11-0307

Nebrisi, E., El, Javed, H., Ojha, S. K., Oz, M., and Shehab, S. (2020). Neuroprotective effect of curcumin on the nigrostriatal pathway in a 6-hydroxydopmine-induced rat model of parkinson's disease is mediated by α7-nicotinic receptors. *Int. J. Mol. Sci.* 21, 1–19. doi: 10.3390/ijms21197329

Noorafshan, A., and Ashkani-Esfahani, S. (2013). A Review of Therapeutic Effects of Curcumin. *Curr. Pharm. Des.* 19, 2032–2046. doi: 10.2174/138161213805289273

Okamoto, Y., Pehlivan, D., Wiszniewski, W., Beck, C. R., Snipes, G. J., Lupski, J. R., et al. (2013). Curcumin facilitates a transitory cellular stress response in Trembler-J mice. *Hum. Mol. Genet.* 22, 4698–4705. doi: 10.1093/hmg/ddt318

Ono, K., Hasegawa, K., Naiki, H., and Yamada, M. (2004). Curcumin has potent anti-amyloidogenic effects for Alzheimer's beta-amyloid fibrils in vitro. *J. Neurosci. Res.* 75, 742–750. doi: 10.1002/jnr.20025

Paillusson, S., Stoica, R., Gomez-Suaga, P., Lau, D. H. W., Mueller, S., Miller, T., et al. (2016). There's Something Wrong with my MAM; the ER-Mitochondria Axis and Neurodegenerative Diseases. *Trends Neurosci.* 39, 146–157. doi: 10.1016/j.tins.2016.01.008

Pal, R., Miranda, M., and Narayan, M. (2011). Nitrosative stress-induced Parkinsonian Lewy-like aggregates prevented through polyphenolic phytochemical analog intervention. *Biochem. Biophys. Res. Commun.* 404, 324–329. doi: 10.1016/j.bbrc.2010.11.117

Pandey, N., Strider, J., Nolan, W. C., Yan, S. X., and Galvin, J. E. (2008). Curcumin inhibits aggregation of α-synuclein. *Acta Neuropathol.* 115, 479–489. doi: 10.1007/s00401-007-0332-4

Patzkó, A., Bai, Y., Saporta, M. A., Katona, I., Wu, X., Vizzuso, D., et al. (2012). Curcumin derivatives promote Schwann cell differentiation and improve neuropathy in R98C CMT1B mice. *Brain* 135, 3551–3566. doi: 10.1093/brain/aws299

Pohl, F., Kong Thoo, and Lin, P. (2018). The Potential Use of Plant Natural Products and Plant Extracts with Antioxidant Properties for the Prevention/Treatment of Neurodegenerative Diseases: In Vitro, In Vivo and Clinical Trials. *Molecules* 23:3283. doi: 10.3390/MOLECULES23123283

Qu, W., Xiao, J., Zhang, H., Chen, Q., Wang, Z., Shi, H., et al. (2013). B19, a novel monocarbonyl analogue of curcumin, induces human ovarian cancer cell apoptosis via activation of endoplasmic reticulum stress and the autophagy signaling pathway. *Int. J. Biol. Sci.* 9, 766–777. doi: 10.7150/ijbs.5711

Radbakhsh, S., Barreto, G. E., Bland, A. R., and Sahebkar, A. (2021). Curcumin: A small molecule with big functionality against amyloid aggregation in neurodegenerative diseases and type 2 diabetes. *Biofactors* 47, 570–586. doi: 10.1002/biof.1735

Ramalingam, P., and Ko, Y. (2015). Enhanced oral delivery of curcumin from N-trimethyl chitosan surface-modified solid lipid nanoparticles: pharmacokinetic and brain distribution evaluations. *Pharm. Res.* 32, 389–402. doi: 10.1007/S11095-014-1469-1

Reddy, R. C., Vatsala, P. G., Keshamouni, V. G., Padmanaban, G., and Rangarajan, P. N. (2005). Curcumin for malaria therapy. *Biochem. Biophys. Res. Commun.* 326, 472–474. doi: 10.1016/j.bbrc.2004.11.051

Reeta, K. H., Mehla, J., and Gupta, Y. K. (2010). Curcumin ameliorates cognitive dysfunction and oxidative damage in phenobarbitone and carbamazepine administered rats. *Eur. J. Pharmacol.* 644, 106–112. doi: 10.1016/j.ejphar.2010.07.022

Ryskalin, L., Puglisi-Allegra, S., Lazzeri, G., Biagioni, F., Busceti, C. L., Balestrini, L., et al. (2021). Neuroprotective effects of curcumin in methamphetamine-induced toxicity. *Molecules* 26:2493. doi: 10.3390/molecules26092493

Sano, R., and Reed, J. (2013). ER stress-induced cell death mechanisms. *Biochim. Biophys. Acta* 1833, 3460–3470. doi: 10.1016/J.BBAMCR.2013.06.028

Sansalone, L., Veliz, E. A., Myrthil, N. G., Stathias, V., Walters, W., Torrens, I. I., et al. (2019). Novel Curcumin Inspired Bis-Chalcone Promotes Endoplasmic Reticulum Stress and Glioblastoma Neurosphere Cell Death. *Cancers* 11:E357. doi: 10.3390/cancers11030357

Santoro, L., Manganelli, F., Maria, E., Di, Bordo, D., Cassandrini, D., et al. (2004). A novel mutation of myelin protein zero associated with an axonal form of Charcot–Marie–Tooth disease. *J. Neurol. Neurosurg. Psychiatry* 75, 262–265. doi: 10.1136/JNNP.2003.012278

Saporta, A. S. D., Sottile, S. L., Miller, L. J., Feely, S. M. E., Siskind, C. E., and Shy, M. E. (2011). Charcot-Marie-Tooth disease subtypes and genetic testing strategies. *Ann. Neurol.* 69, 22–33. doi: 10.1002/ana.22166

Sasaki, H., Sunagawa, Y., Takahashi, K., Imaizumi, A., Fukuda, H., Hashimoto, T., et al. (2011). Innovative preparation of curcumin for improved oral bioavailability. *Biol. Pharm. Bull.* 34, 660–665. doi: 10.1248/bpb.34.660

Schapira, A. (1999). Science, medicine, and the future: Parkinson's disease. *BMJ* 318, 311–314. doi: 10.1136/BMJ.318.7179.311

Scheper, W., and Hoozemans, J. (2015). The unfolded protein response in neurodegenerative diseases: a neuropathological perspective. *Acta Neuropathol.* 130, 315–331. doi: 10.1007/S00401-015-1462-8

Schwarz, D., and Blower, M. (2016). The endoplasmic reticulum: structure, function and response to cellular signaling. *Cell. Mol. Life Sci.* 73, 79–94. doi: 10.1007/S00018-015-2052-6

Serafini, M. M., Catanzaro, M., Rosini, M., Racchi, M., and Lanni, C. (2017). Curcumin in Alzheimer's disease: Can we think to new strategies and perspectives for this molecule? *Pharmacol. Res.* 124, 146–155. doi: 10.1016/j.phrs.2017.08.004

Shah, S. Z. A., Zhao, D., Khan, S. H., and Yang, L. (2015). Unfolded Protein Response Pathways in Neurodegenerative Diseases. *J. Mol. Neurosci.* 57, 529–537. doi: 10.1007/s12031-015-0633-3

Shakeri, A., Zirak, M. R., Wallace Hayes, A., Reiter, R., and Karimi, G. (2019). Curcumin and its analogues protect from endoplasmic reticulum stress: Mechanisms and pathways. *Pharmacol. Res.* 146:104335. doi: 10.1016/J.PHRS.2019.104335

Shamsi, T. N., Athar, T., Parveen, R., and Fatima, S. (2017). A review on protein misfolding, aggregation and strategies to prevent related ailments. *Int. J. Biol. Macromol.* 105, 993–1000. doi: 10.1016/j.ijbiomac.2017.07.116

Sharifi-Rad, J., Rayess, Y., El, Rizk, A. A., Sadaka, C., Zgheib, R., et al. (2020). Turmeric and Its Major Compound Curcumin on Health: Bioactive Effects and Safety Profiles for Food, Pharmaceutical, Biotechnological and Medicinal Applications. *Front. Pharmacol.* 11:1021. doi: 10.3389/FPHAR.2020.01021

Silvestro, S., Sindona, C., Bramanti, P., and Mazzon, E. (2021). A state of the art of antioxidant properties of curcuminoids in neurodegenerative diseases. *Int. J. Mol. Sci.* 22, 1–26. doi: 10.3390/ijms22063168

Simeonova, R., Zheleva, D., Valkova, I., Stavrakov, G., Philipova, I., Atanasova, M., et al. (2021). A novel galantamine-curcumin hybrid as a potential multi-target agent against neurodegenerative disorders. *Molecules* 26:1865. doi: 10.3390/molecules26071865

Singh, S., and Aggarwal, B. B. (1995). Activation of transcription factor NF-κB is suppressed by curcumin (diferulolylmethane). *J. Biol. Chem.* 270, 24995–25000. doi: 10.1074/jbc.270.42.24995

Smith, H., and Mallucci, G. (2016). The unfolded protein response: mechanisms and therapy of neurodegeneration. *Brain* 139, 2113–2121. doi: 10.1093/BRAIN/AWW101

Su, I. J., Chang, H. Y., Wang, H. C., and Tsai, K. J. (2020). A curcumin analog exhibits multiple biologic effects on the pathogenesis of Alzheimer's disease and improves behavior, inflammation, and β-amyloid accumulation in a mouse model. *Int. J. Mol. Sci.* 21, 1–20. doi: 10.3390/ijms21155459

Tan, K.-L., Ali, A., Du, Y., Fu, H., Jin, H.-X., Chin, T.-M., et al. (2014). Synthesis and evaluation of bisbenzylidenedioxotetrahydrothiopranones as activators of endoplasmic reticulum (ER) stress signaling pathways and apoptotic cell death in acute promyelocytic leukemic cells. *J. Med. Chem.* 57, 5904–5918. doi: 10.1021/jm401352a

Tang, M., Taghibiglou, C., and Liu, J. (2017). The Mechanisms of Action of Curcumin in Alzheimer's Disease. *J. Alzheimer's Dis.* 58, 1003–1016. doi: 10.3233/JAD-170188

Taniguchi, M., and Yoshida, H. (2011). Unfolded Protein Response. *Compr. Biotechnol.* 1, 525–537. doi: 10.1016/B978-0-08-088504-9.00062-3

Taylor, J. P., Hardy, J., and Fischbeck, K. H. (2002). Toxic proteins in neurodegenerative disease. *Science* 296, 1991–1995. doi: 10.1126/science.1067122

Tiwari, S. K., Agarwal, S., Seth, B., Yadav, A., Nair, S., Bhatnagar, P., et al. (2014). Curcumin-loaded nanoparticles potently induce adult neurogenesis and reverse cognitive deficits in Alzheimer's disease model via canonical Wnt/β-catenin pathway. *ACS Nano* 8, 76–103. doi: 10.1021/nn405077y

Uehara, T., Nakamura, T., Yao, D., Shi, Z.-Q., Gu, Z., Ma, Y., et al. (2006). S-nitrosylated protein-disulphide isomerase links protein misfolding to neurodegeneration. *Nature* 441, 513–517. doi: 10.1038/nature04782

Urra, H., and Hetz, C. (2014). A novel ER stress-independent function of the UPR in angiogenesis. *Mol. Cell* 54, 542–544. doi: 10.1016/J.MOLCEL.2014.05.013

Valera, E., Dargusch, R., Maher, P. A., and Schubert, D. (2013). Modulation of 5-lipoxygenase in proteotoxicity and Alzheimer's disease. *J. Neurosci.* 33, 10512–10525. doi: 10.1523/JNEUROSCI.5183-12.2013

Vera-Ramirez, L., Pérez-Lopez, P., Varela-Lopez, A., Ramirez-Tortosa, M., Battino, M., and Quiles, J. L. (2013). Curcumin and liver disease. *BioFactors* 39, 88–100. doi: 10.1002/biof.1057

Voulgaropoulou, S. D., van Amelsvoort, T. A. M. J., Prickaerts, J., and Vingerhoets, C. (2019). The effect of curcumin on cognition in Alzheimer's disease and healthy aging: A systematic review of pre-clinical and clinical studies. *Brain Res.* 1725, 146476. doi: 10.1016/j.brainres.2019.146476

Wang, H. M., Zhao, Y. X., Zhang, S., Liu, G. D., Kang, W. Y., Tang, H. D., et al. (2010). PPARγ agonist curcumin reduces the amyloid-β-stimulated inflammatory responses in primary astrocytes. *J. Alzheimer's Dis.* 20, 1189–1199. doi: 10.3233/JAD-2010-091336

Wang, M., and Kaufman, R. (2016). Protein misfolding in the endoplasmic reticulum as a conduit to human disease. *Nature* 529, 326–335. doi: 10.1038/NATURE17041

Xu, Y. X., Pindolia, K. R., Janakiraman, N., Chapman, R. A., and Gautam, S. C. (1997). Curcumin inhibits IL1α and TNFα induction of AP-1 and NF-kB DNA-binding activity in bone marrow stromal cells. *Hematopathol. Mol. Hematol.* 11, 49–62.

Yang, F., Lim, G. P., Begum, A. N., Ubeda, O. J., Simmons, M. R., Ambegaokar, S. S., et al. (2005). Curcumin inhibits formation of amyloid β oligomers and fibrils, binds plaques, and reduces amyloid in vivo. *J. Biol. Chem.* 280, 5892–5901. doi: 10.1074/jbc.M404751200

Yoon, M. J., Kang, Y. J., Lee, J. A., Kim, I. Y., Kim, M. A., Lee, Y. S., et al. (2014). Stronger proteasomal inhibition and higher CHOP induction are responsible for more effective induction of paraptosis by dimethoxycurcumin than curcumin. *Cell Death Dis.* 5:e1112. doi: 10.1038/cddis.2014.85

Yu, L.-H., Morimura, T., Numata, Y., Yamamoto, R., Inoue, N., Antalfy, B., et al. (2012). Effect of curcumin in a mouse model of Pelizaeus-Merzbacher disease. *Mol. Genet. Metab.* 106, 108–114. doi: 10.1016/j.ymgme.2012.02.016

Zhang, C., Browne, A., Child, D., and Tanzi, R. E. (2010). Curcumin decreases amyloid-β peptide levels by attenuating the maturation of amyloid-β precursor protein. *J. Biol. Chem.* 285, 28472–28480. doi: 10.1074/jbc.M110.133520

Zhang, X., Zhang, H.-Q., Zhu, G.-H., Wang, Y.-H., Yu, X.-C., Zhu, X.-B., et al. (2012). A novel mono-carbonyl analogue of curcumin induces apoptosis in ovarian carcinoma cells via endoplasmic reticulum stress and reactive oxygen species production. *Mol. Med. Rep.* 5, 739–744. doi: 10.3892/mmr.2011.700

Zhao, L., and Ackerman, S. (2006). Endoplasmic reticulum stress in health and disease. *Curr. Opin. Cell Biol.* 18, 444–452. doi: 10.1016/J.CEB.2006.06.005

Zheng, A., Li, H., Wang, X., Feng, Z., Xu, J., Cao, K., et al. (2014). Anticancer effect of a curcumin derivative B63: ROS production and mitochondrial dysfunction. *Curr. Cancer Drug Targets* 14, 156–166. doi: 10.2174/1568009613666131126115444

Zhongfa, L., Chiu, M., Wang, J., Chen, W., Yen, W., Fan-Havard, P., et al. (2012). Enhancement of curcumin oral absorption and pharmacokinetics of curcuminoids and curcumin metabolites in mice. *Cancer Chemother. Pharmacol.* 69, 679–689. doi: 10.1007/s00280-011-1749-y

Conflict of Interest: The authors declare that the research was conducted in the absence of any commercial or financial relationships that could be construed as a potential conflict of interest.

Publisher's Note: All claims expressed in this article are solely those of the authors and do not necessarily represent those of their affiliated organizations, or those of the publisher, the editors and the reviewers. Any product that may be evaluated in this article, or claim that may be made by its manufacturer, is not guaranteed or endorsed by the publisher.

frontiers | Frontiers in Cellular Neuroscience

ORIGINAL RESEARCH
published: 06 April 2022
doi: 10.3389/fncel.2022.865005

Comprehensive Analysis of Endoplasmic Reticulum Stress in Intracranial Aneurysm

Bo Chen[1,2], Hongshu Zhou[1,2], Xiaoxi Zhou[1,2], Liting Yang[1,2], Yuanyuan Xiong[3] and Liyang Zhang[1,2]**

[1] Department of Neurosurgery, Xiangya Hospital, Central South University, Changsha, China, [2] National Clinical Research Center for Geriatric Disorders, Xiangya Hospital, Central South University, Changsha, China, [3] Department of Neurosurgery, The Second Affiliated Hospital of Nanchang University, Nanchang, China

Background: Aberrant endoplasmic reticulum stress (ERS) plays an important role in multiple cardiovascular diseases. However, their implication in intracranial aneurysms (IAs) remains unclear. We designed this study to explore the general expression pattern and potential functions of ERS in IAs.

Methods: Five Gene Expression Omnibus (GEO) microarray datasets were used as the training cohorts, and 3 GEO RNA sequencing (RNA-seq) datasets were used as the validating cohorts. Differentially expressed genes (DEGs), functional enrichment, Lasso regression, logistic regression, ROC analysis, immune cell profiling, vascular smooth muscle cell (VSMC) phenotyping, weighted gene coexpression network analysis (WGCNA), and protein-protein interaction (PPI) analysis were applied to investigate the role of ERS in IA. Finally, we predicted the upstream transcription factor (TF)/miRNA and potential drugs targeting ERS.

Results: Significant DEGs were majorly associated with ERS, autophagy, and metabolism. Eight-gene ERS signature and IRE1 pathway were identified during the IA formation. WGCNA showed that ERS was highly associated with a VSMC synthesis phenotype. Next, ERS-VSMC-metabolism-autophagy PPI and ERS-TF-miRNA networks were constructed. Finally, we predicted 9 potential drugs targeting ERS in IAs.

Conclusion: ERS is involved in IA formation. Upstream and downstream regulatory networks for ERS were identified in IAs. Novel potential drugs targeting ERS were also proposed, which may delay IA formation and progress.

Keywords: intracranial aneurysm, endoplasmic reticulum stress, bioinformatics, drug prediction, unfolded protein response

OPEN ACCESS

Edited by:
Safikur Rahman,
Babasaheb Bhimrao Ambedkar Bihar University, India

Reviewed by:
Esmerina Tili,
The Ohio State University, United States
Yujie Chen,
Army Medical University, China

****Correspondence:***
Yuanyuan Xiong
xiongyuanyuan_pub@126.com
Liyang Zhang
zhangliyang@csu.edu.cn

Specialty section:
This article was submitted to Cellular Neuropathology, a section of the journal Frontiers in Cellular Neuroscience

Received: *29 January 2022*
Accepted: *07 March 2022*
Published: *06 April 2022*

Citation:
Chen B, Zhou H, Zhou X, Yang L, Xiong Y and Zhang L (2022) Comprehensive Analysis of Endoplasmic Reticulum Stress in Intracranial Aneurysm. Front. Cell. Neurosci. 16:865005. doi: 10.3389/fncel.2022.865005

Abbreviations: ADD1, adducin 1; AUC, areas under the curve; CALR, calreticulin; CMAP, connectivity map; DEG, differential expression gene; ERS, endoplasmic reticulum stress; GEO, Gene Expression Omnibus; GO, Gene Ontology; GSEA, Gene Set Enrichment Analysis; GSVA, Gene Set Variation Analysis; IA, intracranial aneurysm; KEGG, Kyoto Encyclopedia of Genes and Genomes; PCA, principal components analysis; PPI, protein–protein Interaction; RNA-seq, RNA sequencing; SNP, single nucleotide polymorphism; TF, transcription factor; UPR, unfolded protein response; VSMC, vascular smooth muscle cell; WGCNA, weighted gene coexpression network analysis.

INTRODUCTION

Intracranial aneurysm (IA) is a life-threatening, complicated, and multifactorial disease that forms owing to the interaction among hemodynamics, genetics, and environmental factors. Immune/inflammation infiltration, cell death, lipid metabolism, oxidative stress, proteolytic activity, and iron accumulation are major histopathological features of IAs (Frösen et al., 2012). The recruitment and infiltration of immune cells have been confirmed to be a key phase in IA formation and development (Hosaka and Hoh, 2014; Signorelli et al., 2018). Recent studies suggest that vascular smooth muscle cell (VSMC) phenotype transformation is crucial to vascular wall remodeling of IA (Starke et al., 2014). Dysregulated autophagy can alter the VSMC phenotype, impair arterial wall function, and contribute to IA formation. Metabolism is also closely associated with the degeneration of IA arterial wall (Frösen et al., 2013). Therefore, it is urgent to investigate the complete mechanisms behind IA formation.

Endoplasmic reticulum stress (ERS) is various physiological or molecular disturbances that unbalance the unfolded-protein-response-regulated endoplasmic reticulum homeostasis (Ren et al., 2021). As a fundamental organelle, the dysfunction of the endoplasmic reticulum can affect multiple biological processes. Relevant studies show that ERS participates in the formation and development of cardiovascular diseases (Ren et al., 2021). Increased ERS markers have been reported in aortic aneurysm walls (Clément et al., 2019). Furthermore, stress-induced ERS can promote VSMC apoptosis, endothelial dysfunction, inflammation infiltration, and ultimately induce aortic aneurysm formation (Jia et al., 2015, 2017). Identifying the associations between ERS and IA may provide a better understanding of IA etiology.

In our study, 5 Gene Expression Omnibus (GEO) microarray datasets were selected as training cohorts, while 3 GEO RNA sequencing (RNA-seq) datasets were selected as validating cohorts. The association between ERS and IA formation was first confirmed by functional enrichment of differential expression genes (DEGs). Afterward, we constructed an ERS signature gene set, identified classical ERS pathways, generated an ERS-VSMC-metabolism-autophagy regulated network, predicted upstream transcription factor (TF) and microRNA targets of ERS genes, and explored the relationship between ERS and single nucleotide polymorphisms (SNPs) in IA diseases. Finally, potential drugs targeting ERS were predicted to inhibit IA formation and development.

MATERIALS AND METHODS

Intracranial Aneurysm Datasets and Preprocessing

Eight public IA datasets were downloaded from the GEO[1], including 5 microarray datasets (GSE75436, GSE54083, GSE26969, GSE13353, GSE15629) and 3 RNA-sequencing datasets (GSE158558, GSE122897 and GSE66240). The patients involved in the database have obtained ethical approval. The raw data were merged and normalized using the "limma" R package (Ritchie et al., 2015). Batch effects were eliminated using the Combat algorithm (Leek et al., 2012). Of the 181 samples enrolled in our study, microarray data (55IAs and 42 controls) were used as the training set, and RNA-seq data (53 IAs and 31 controls) were used as the validating sets.

Differentially Expressed Gene Screening and Functional Analysis

Principal components analysis (PCA) was employed to visualize the disparity between IA and control groups using the "factoextra" R package. DEG screening was conducted using the "limma" package ($P < 0.05$ and log2-fold change > 1 or < -1). Furthermore, we analyzed DEG functions by Gene Ontology (GO), Kyoto Encyclopedia of Genes and Genomes (KEGG), and Gene Set Enrichment Analysis (GSEA) analysis ($P < 0.05$).

Constructing Endoplasmic Reticulum Stress Signature

Two ERS-related gene sets (GO RESPONSE TO ENDOPLASMIC RETICULUM STRESS and GO REGULATION OF RESPONSE TO ENDOPLASMIC RETICULUM STRESS) were downloaded from Molecular Signature Database (MSigDB) v7.0. The Lasso regression was performed to identify the ERS-related DEGs with the highest IA predictive values. The predictive ability was further evaluated by univariate logistic analysis. Next, using these genes, we quantified ERS expression levels of all samples by Gene Set Variation Analysis (GSVA) scores (Hänzelmann et al., 2013).

Identifying Endoplasmic Reticulum Stress Pathways

Three ERS-related signaling pathways (GOBP ATF6 MEDIATED UNFOLDED PROTEIN RESPONSE, GOBP IRE1 MEDIATED UNFOLDED PROTEIN RESPONSE, GOBP PERK MEDIATED UNFOLDED PROTEIN RESPONSE) were downloaded from MsigDB v7.0. The GSVA scores were performed to quantify the expression level of these pathways in all samples. Pearson correlation analysis was performed between ERS pathways and signature genes.

Immunocyte Infiltration and Vascular Smooth Muscle Cell Phenotype Analysis

Immunocyte infiltration of arterial walls was estimated using the "xCell" R package, which uses gene expression profiles to predict enrichment of 64 immune and stromal cell types (Aran et al., 2017). The VSMC phenotype was identified by 7 feature genes [SDC1, RBP1, MMP14, CDH2, MGP, PDGFA, MYH9 (Nakahara et al., 1992; Shanahan et al., 1993; Orlandi et al., 2002; Lyon et al., 2010; Chaterji et al., 2014; Shao et al., 2020)] and quantified by GSVA scores.

[1]https://www.ncbi.nlm.nih.gov/geo/

Coexpression Analysis of Endoplasmic Reticulum Stress, Intracranial Aneurysm, Immune, and Vascular Smooth Muscle Cell Phenotype

Weighted gene coexpression network analysis (WGCNA) was performed using the "WGCNA" R package (Langfelder and Horvath, 2008). An optimal soft threshold β was set to attain a scale-free topology network. Next, we evaluated the correlation between "ERS" and other pathophysiological traits. "ERS," "VSMC synthesis," and "IA" traits had the same high-associated modules ($P < 0.001$ and $r > 0.45$), which were assumed to be the key modules involved in IA formation and progression. The gene function of key modules was analyzed using GO and KEGG enrichment.

Constructing Endoplasmic Reticulum Stress-Vascular Smooth Muscle Cell-Metabolism-Autophagy Protein-Protein Interaction and Endoplasmic Reticulum Stress-Transcription Factor-miRNA Networks

Apart from ERS, the DEG functions also included metabolism and autophagy. To evaluate the association between ERS, metabolism, and autophagy, we downloaded 948 metabolism-related genes from the KEGG database[2], and 232 autophagy-related genes from the HADb database[3]. GSVA scoring and Pearson correlation analysis were then performed. After identifying the correlation, the aforementioned genes, together with high ERS-VSMC-IA-associated module genes were then imported into the STRING database[4]. Protein-protein interaction (PPI) networks were further visualized by Cytoscape software (version 3.9.0). Furthermore, NetworkAnalyst[5] (Zhou et al., 2019), a comprehensive network visual analytics platform for gene expression analysis, was applied to predict upstream TFs and miRNAs of ERS. Finally, based on ERS signature genes, we constructed ERS-TF-miRNA networks.

Exploring the Relationship Between Endoplasmic Reticulum Stress and Non-coding Single Nucleotide Polymorphisms

The 80 TFs and 142 nearby genes of regulatory regions which overlapped with IA-associated SNPs, were downloaded from Laarman's study (Laarman et al., 2018). The integration analysis was used between TFs of the ERS signature and TFs of regulatory regions. The correlation analysis was performed between the ERS signature and genes in proximity to regulatory regions.

[2]https://www.kegg.jp/

[3]http://www.autophagy.lu/

[4]https://www.string-db.org/

[5]https://www.networkanalyst.ca/

Small Molecular Drug Analysis for Endoplasmic Reticulum Stress Signature Genes

The Connectivity Map (CMAP) website[6] was applied to explore small molecule drugs with the potential to inhibit IA formation and development. The drugs with negative Raw_cs and high fdr_q_nlog10 values were considered as potential therapeutic agents because they could suppress the expression of ERS signature genes.

Statistical Analysis

All statistical analyses were conducted using the R software (version 4.0.2). The Wilcox test was applied to compare the difference of continuous variables between the two groups. $P < 0.05$ was considered statistically significant. Data were visualized using the R package "ggplot2." Heatmaps were drawn using the "pheatmap" R package. Volcano plots were generated using the "ggrepel" R package.

RESULTS

Data Preprocessing and Differentially Expressed Gene Screening

The study was designed as indicated in the flow chart (**Figure 1**). We sought to explore the role of ERS in IA formation by comprehensive analysis based on microarray and RNA-sequencing datasets. In total, we collected 55 cases of IA and 42 cases of normal arteries as controls in microarray training cohorts, and 53 cases of IA and 31 cases of normal arteries as controls in RNA-seq validation cohorts (**Figure 2A**). For both training and validation cohorts, similar distributions of different samples were observed in normalized data after preprocessing (**Figure 2B**). PCA analysis showed that the IA group could be discriminated from the controls at the transcript level (**Figure 2C**). On filtering with the limma package, 1,628 up-regulated genes and 2,013 down-regulated genes were found in the training cohort. 590 up-regulated genes and 685 down-regulated genes were found in the validation cohort (**Figure 2D**). Heatmaps were used to visualize the expression of DEGs in all cases (**Figure 2E**).

Differentially Expressed Gene Functional Enrichment

To explore disease progression in IA, we performed functional enrichment analysis for intersected DEGs between the training and validation cohorts. Among GO enrichment terms, the most overrepresented were ERS, response to unfolded protein, autophagosome, and similar pathways (**Figure 3A**). In the KEGG pathway analysis, DEGs were notably enriched in protein processing in ER, metabolism process, phagosome, antigen processing and presentation, and others (**Figure 3B**). In GSEA biological process results, endomembrane system

[6]https://clue.io/

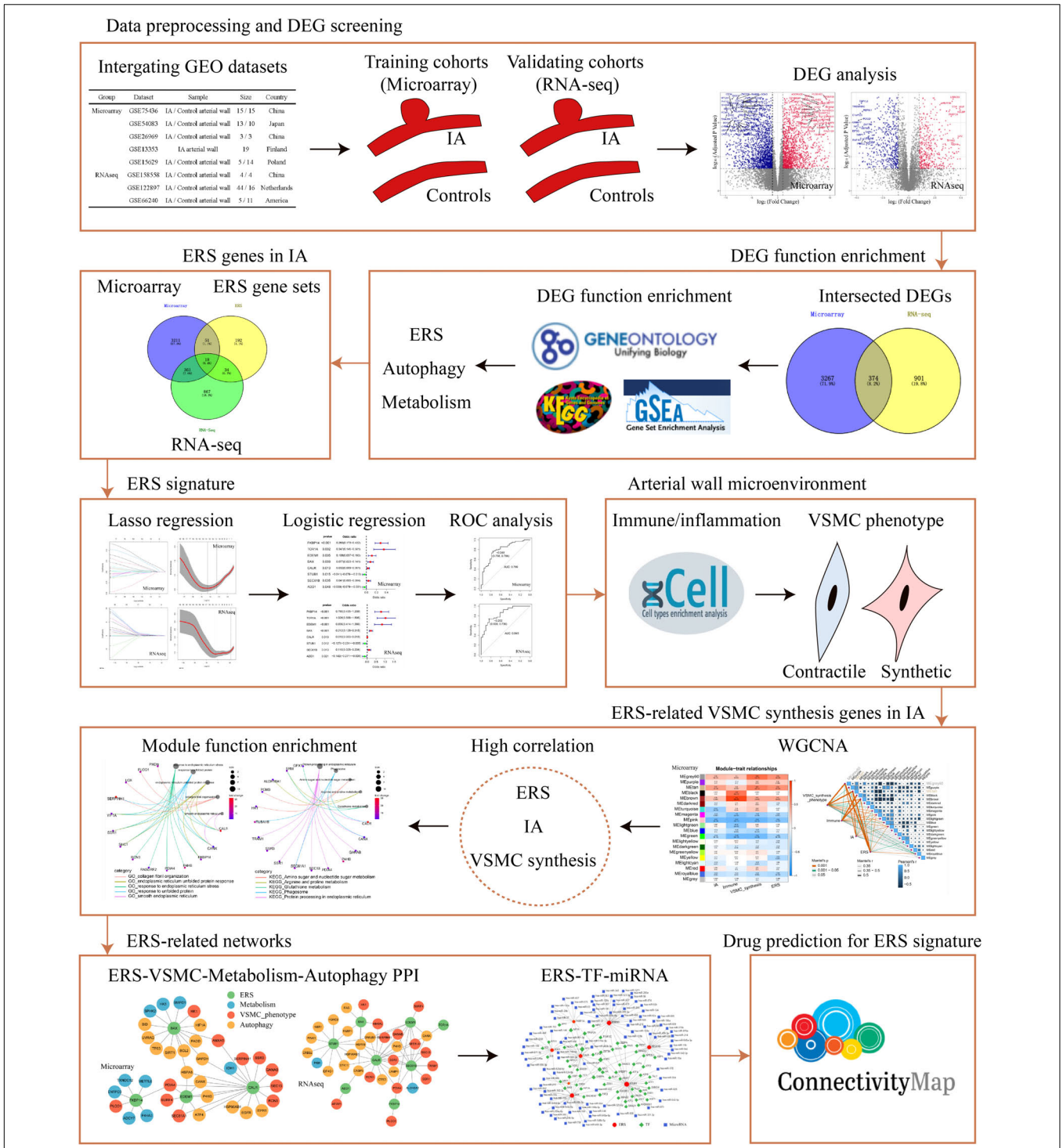

FIGURE 1 | The flow chart of data analysis. DEG, differential expression gene; RNA-seq, RNA sequencing; ERS, endoplasmic reticulum stress; ROC, receiver operating characteristic; VSMC, vascular smooth muscle cell; PPI, protein–protein Interaction; TF, transcription factor.

and response to stimulus terms showed higher expression in the IA group (**Figure 3C**), whereas cellular macromolecule metabolic process was more frequent in the normal artery control group (**Figure 3D**). Overall, DEGs were functionally enriched in ERS, autophagy, and metabolism-related processes. Further correlation analysis showed that the expression of autophagy and metabolism was positively associated with ERS, separately (**Supplementary Figures 1A,B**).

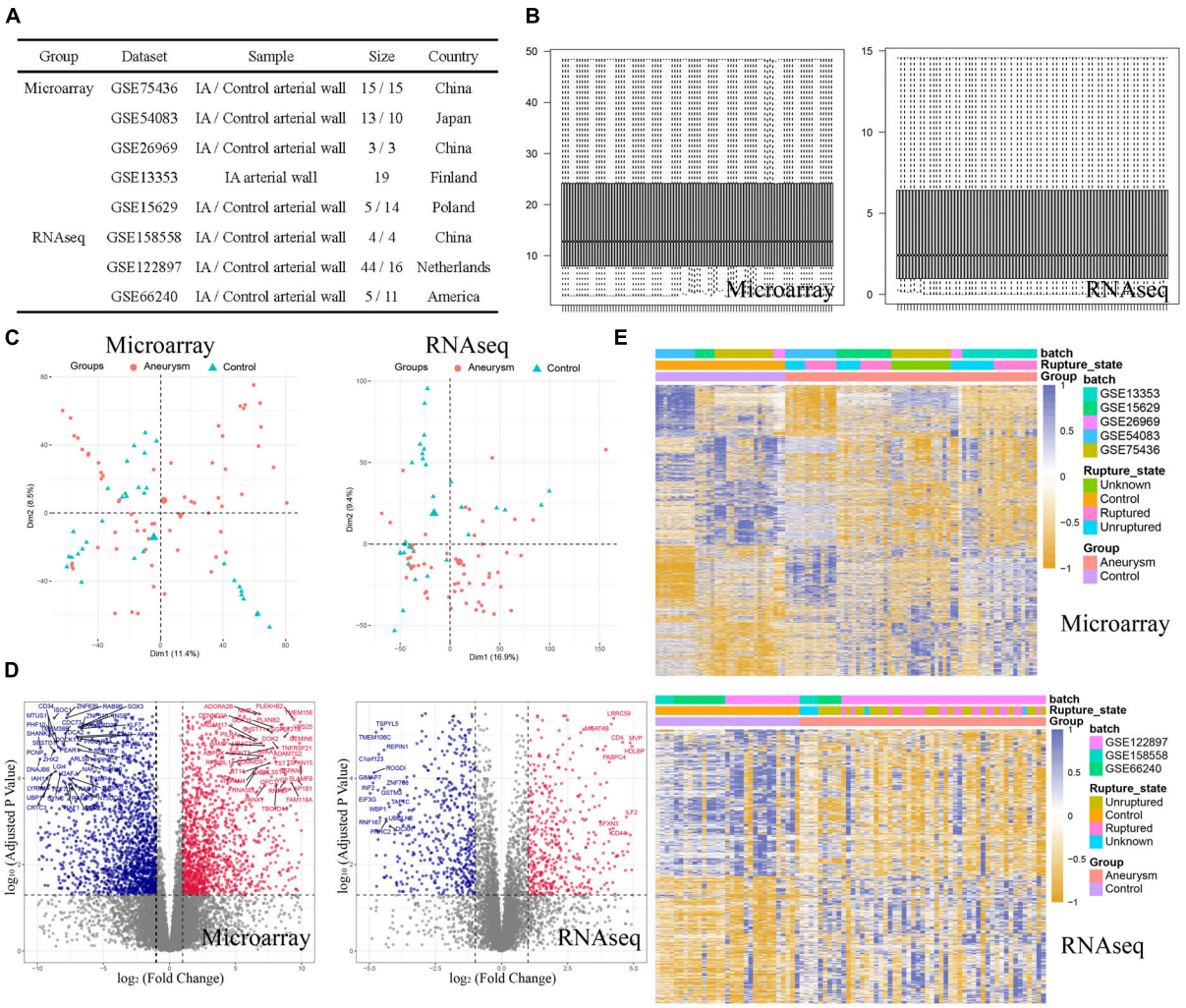

FIGURE 2 | Data preprocessing and DEG screening in both training and validating cohorts. **(A)** Basic information of included dataset. **(B)** Boxplots of normalized data showed similar distributions of different samples. **(C)** PCA plots showed the IA group could be discriminated from the controls. **(D)** Volcano plots visualized the fold change and *P*-value of all genes between the two groups. Red plots were upregulated genes and blue plots were downregulated genes. **(E)** Heatmaps visualized the expression level of DEGs.

Constructing the Endoplasmic Reticulum Stress Related Signature in Intracranial Aneurysm

Considering the prominent role of ERS in DEG functional enrichment, we sought to determine diagnostic values of ERS in IA by constructing an ERS signature. Firstly, we selected 18 IA-related ERS genes by intersecting ERS gene sets and DEGs of training and validation cohorts. Next, these 18 genes were used for LASSO regression to select the most valuable predictive genes, and an 8-gene ERS signature was constructed (**Figures 4A,B**). FKBP14, TOR1A, EDEM1, BAX, CALR, SEC61B were upregulated, whereas STUB1 and ADD1 were downregulated in IAs (**Supplementary Figure 3A**). Univariate Logistic regression showed FKBP14, TOR1A, EDEM1, BAX, CALR, and SEC61B may promote IA formation, while STUB1 and ADD1 can prevent it (**Figure 4C**). ROC curve analysis showed that GSVA scores of the ERS signature could predict IA formation, with areas under the curve (AUC) of 0.799 and 0.845 in the training and validation cohorts, respectively (**Figure 4D**). Heatmaps were used to visualize ERS signature expression in all cases (**Figure 4E**).

Identifying Signaling Pathways in Intracranial Aneurysm

There were 3 ERS-related classical signaling pathways, including the ATF6 pathway, IRE1 pathway, and Perk pathway. The expression of the IRE1 pathway was significantly higher in IAs than controls, whereas the ATF6 pathway and perk pathway did not show significant differences between the two groups (**Figure 5A**). IRE1 pathway showed high correlations to FKBP14, BAX, and SEC61B expression (Correlation coefficient > 0.3, **Figure 5B**).

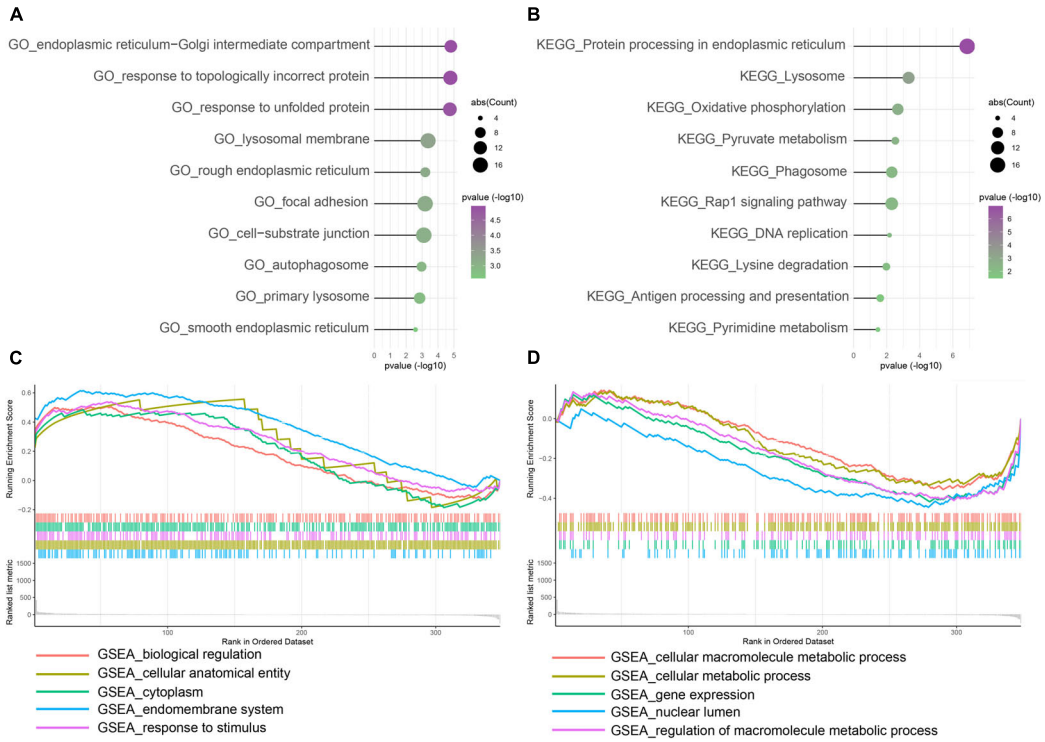

FIGURE 3 | Function enrichment of intersected DEGs between the training and control group. **(A)** Gene Ontology (GO) enrichment analysis. **(B)** Kyoto Encyclopedia of Genes and Genomes (KEGG) enrichment analysis. **(C,D)** Gene Set Enrichment Analysis (GSEA). Enrichment showed that DEG function mainly focused on ERS, unfolded protein response (UPR), autophagy, immune/inflammation, and metabolism.

Annotation of the Arterial Wall Microenvironment of Immune/Inflammation Infiltrating and Vascular Smooth Muscle Cell Phenotype

Since immune infiltration/inflammation and VSMC phenotype are tightly associated with IA formation and progression, we further investigated the arterial wall microenvironment. For both training and validation cohorts, Xcell immune profiling results showed more immune/inflammation-related cell types and higher immune scores in IA (**Figures 6A,B**). VSMC phenotype analysis revealed that IA cohorts expressed more VSMC-synthesis-phenotype-feature genes and higher synthesis-phenotype GSVA scores (**Figures 6C,D**).

Coexpression Analysis Identifying Endoplasmic Reticulum Stress-Related Vascular Smooth Muscle Cell Phenotype Genes

Considering ERS, immune/inflammation, and VSMC phenotype are all involved in IA formation, we sought to conduct WGCNA coexpression analysis to identify the relationship among those. Powers $\beta = 5$ or 4 were selected as the software threshold for scale-free network construction in training and validation cohorts, respectively (**Figure 7A** and **Supplementary Figure 2A**). In the training cohort, 20 modules were identified, and in the validation cohort, 13 modules were identified by clustering dendrogram (**Figure 7B** and **Supplementary Figure 2B**). IA, VSMC synthesis, and ERS had the same highest-correlated modules (MEgray60 and MEtan), indicating strong associations among these traits (**Figures 7C,D**). A similar result was also observed in the validation cohort (**Supplementary Figures 2C,D**). By intersecting the two most relevant modules in the training and validation group, we identified 85 ERS-related VSMC phenotype genes involved in IA formation. GO enrichment analysis showed these genes mainly focused on collagen fibril organization, smooth endoplasmic reticulum, and others (**Figure 7E**). KEGG pathway analysis showed metabolism, phagosome, and protein processing in the endoplasmic reticulum were more enriched among these genes (**Figure 7F**).

Constructing Endoplasmic Reticulum Stress-Vascular Smooth Muscle Cell-Metabolism-Autophagy Protein-Protein Interaction and Endoplasmic Reticulum Stress-Transcription Factor-miRNA Networks

After identifying the correlation among ERS, VSMC phenotype, metabolism, and autophagy in IA formation, we constructed PPI networks among those pathophysiological traits. Within DEGs

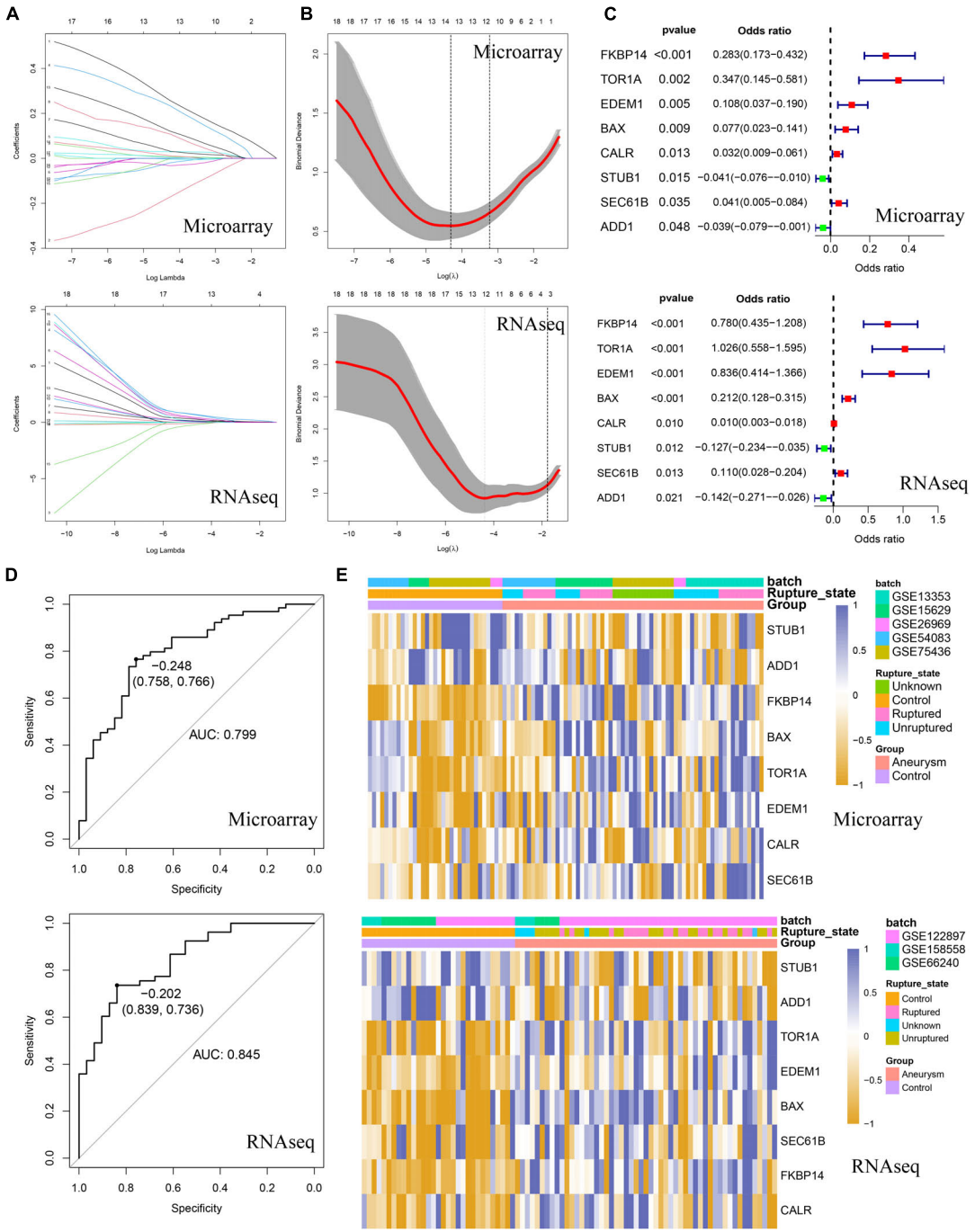

FIGURE 4 | Identification of the ERS-related signature in both training and validating cohorts. **(A)** The coefficient profiles of the LASSO regression model. **(B)** Cross-validation for tuning parameter screening in the LASSO regression model. **(C)** Univariate Logistic regression identified 8 ERS genes' odds ratios (ORs) and 95% confidence intervals (CIs) after LASSO regression filtration. **(D)** ROC curve analysis for Gene Set Variation Analysis (GSVA) scores of 8 ERS genes. **(E)** The heatmap visualized the expression level of 8 ERS genes.

targeting the ERS signature, a total of 11 were involved in the VSMC synthesis phenotype, 9 were correlated to metabolism, and 15 were associated with autophagy in the training cohort (**Figure 8A**). The validating cohort also showed similar ERS-VSMC-metabolism-autophagy PPI networks (**Figure 8B**).

The NetworkAnalyst online tool was used to predict ERS upstream TF and miRNA. Eight ERS signature genes had identified TFs. NFYA, TFAP2A, SP1, EGR1, MYC, GABPA, and USF1 were common TFs among at least 3 genes. ERS signature genes of EDEM1 and BAX had the most predicted

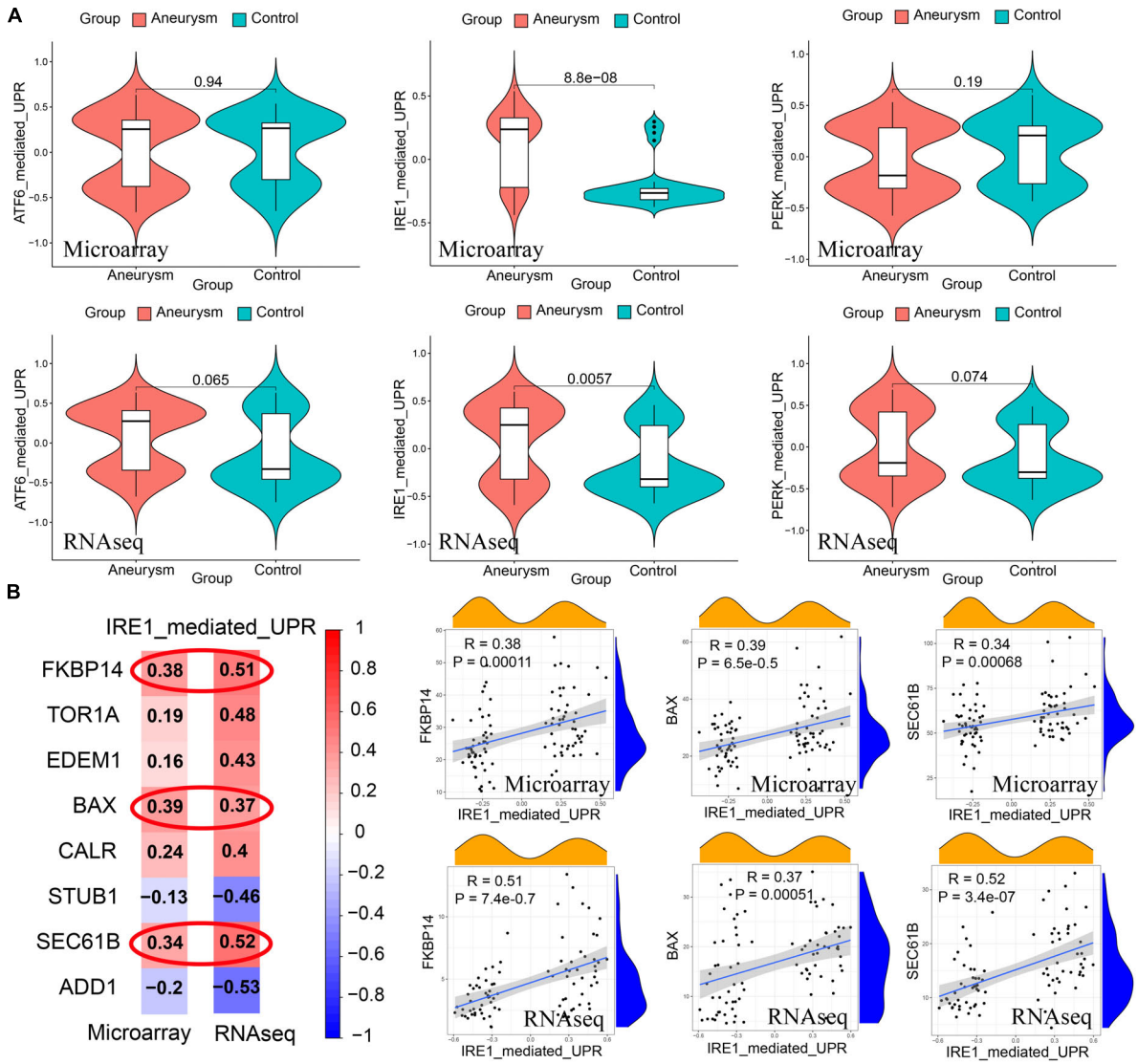

FIGURE 5 | Identification of ERS-related signaling pathways in both training and validating cohorts. **(A)** GSVA scores of 3 pathway expression. IRE1 pathway had a higher expression level in IAs than the level in controls. The expression of the ATF6 pathway and PERK pathway did not show significant differences between the two groups. **(B)** Pearson correlation between IRE1 pathway and signature genes. The expression of FKBP14, BAX, and SEC61B had high correlations to IRE1 pathway expression (Correlation coefficient > 0.3 in both training and validating cohorts).

miRNAs including hsa-miR-25, hsa-miR-32, hsa-miR-520d-5p, hsa-miR-524-5p, hsa-miR-637, hsa-miR-133b and hsa-miR-133a (**Figure 8C**).

Exploring the Relationship Between Endoplasmic Reticulum Stress and Non-coding Single Nucleotide Polymorphisms

We then investigated TFs and nearby genes of ERS-associated non-coding SNPs in IAs. Seventeen TFs were identified to co-regulate ERS and non-coding SNPs. Among these, MYC had the most ERS target genes and TF binding sites (**Supplementary Table 1**). Moreover, 6 nearby genes were found to differentially express (**Supplementary Figure 3B**). Correlation analysis showed the tight connectivity between 8 ERS signature genes and 6 nearby genes, in which KCTD15 had the most significant correlations with ERS (**Supplementary Figure 3C**).

Drug Prediction for Endoplasmic Reticulum Stress Signature

To predict small molecule drugs with the potential to inhibit IA ERS, we uploaded the ERS signature into the CMAP online tool. We identified 9 drugs (thioperamide, tracazolate, cephaeline, GW-843682X, aminopurvalanol-a, geranylgeraniol, hydroflumethiazide, BRD-K76674262, everolimus) with the negative Raw_cs and the top fdr_q_nlog10 values, suggesting

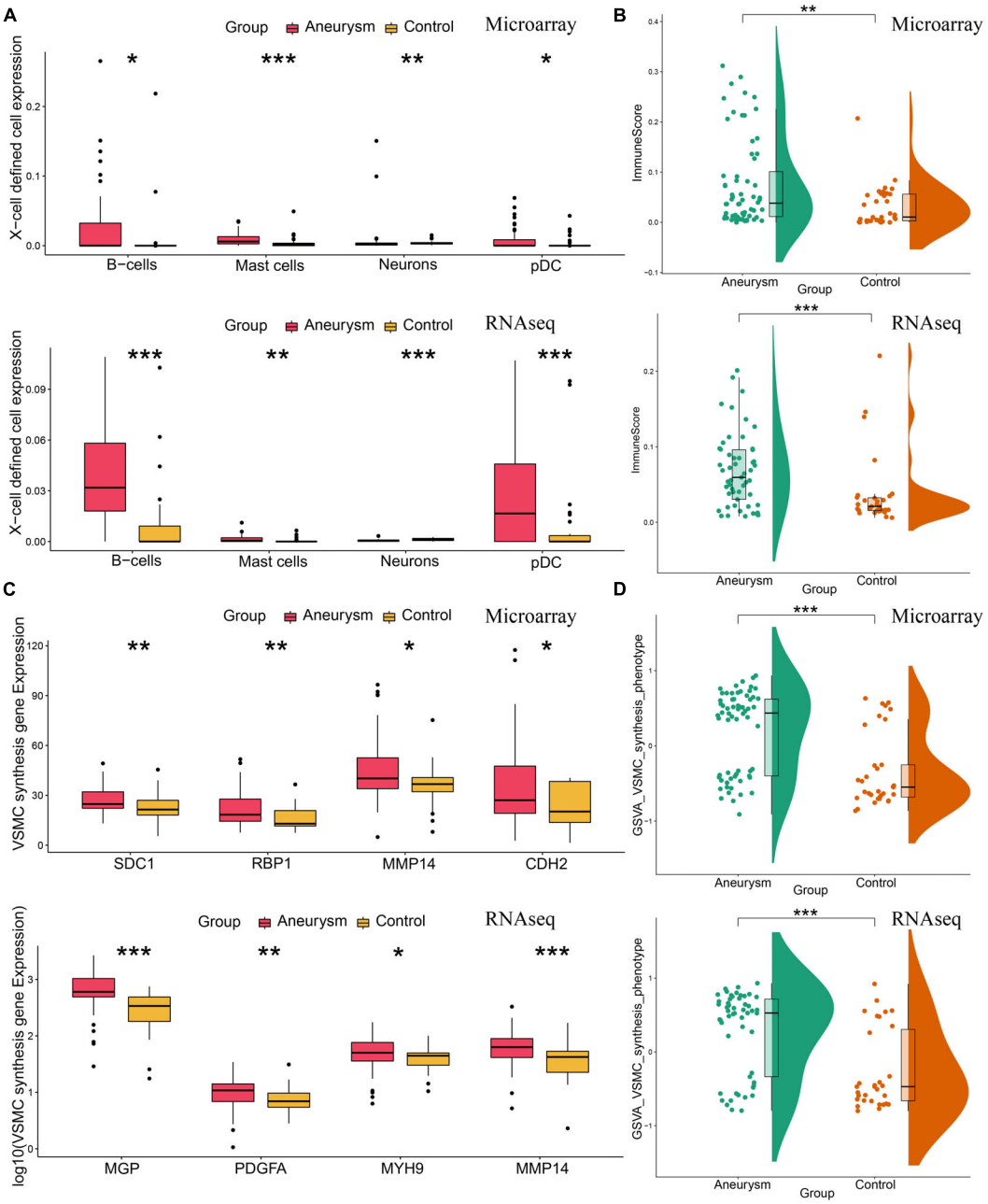

FIGURE 6 | Annotation of the arterial wall microenvironment of immune/inflammation infiltrating and VSMC phenotype in both training and validating cohorts. **(A)** The expression level of X cell-defined immunocytes and neurons. **(B)** The total enrichment scores of the immune microenvironment. IA lesions had higher immune expression than control arteries. **(C)** The expression of feature genes of VSMC synthesis phenotype. **(D)** The GSVA scores of VSMC synthesis phenotype. IA lesions had more VSMC synthesis phenotype than control arteries. *$P < 0.05$; **$P < 0.01$; ***$P < 0.001$.

they could inhibit the expression of the ERS signature (**Figure 9** and **Supplementary Table 2**).

DISCUSSION

Endoplasmic reticulum stress is an imbalance of the endoplasmic reticulum homeostasis caused by an accumulation of unfolded or misfolded proteins. Multiple pathologies can induce ERS, including pressure overload, metabolic disorders, atherosclerosis, ischemia-reperfusion injury, endothelial dysfunction, and others. Long-term ERS promotes abnormal inflammation and apoptosis in the vascular wall, leading to disturbances in cardiovascular function (Ren et al., 2021). Previous studies have shown that excessive ERS is closely associated with various cardiovascular diseases, including heart

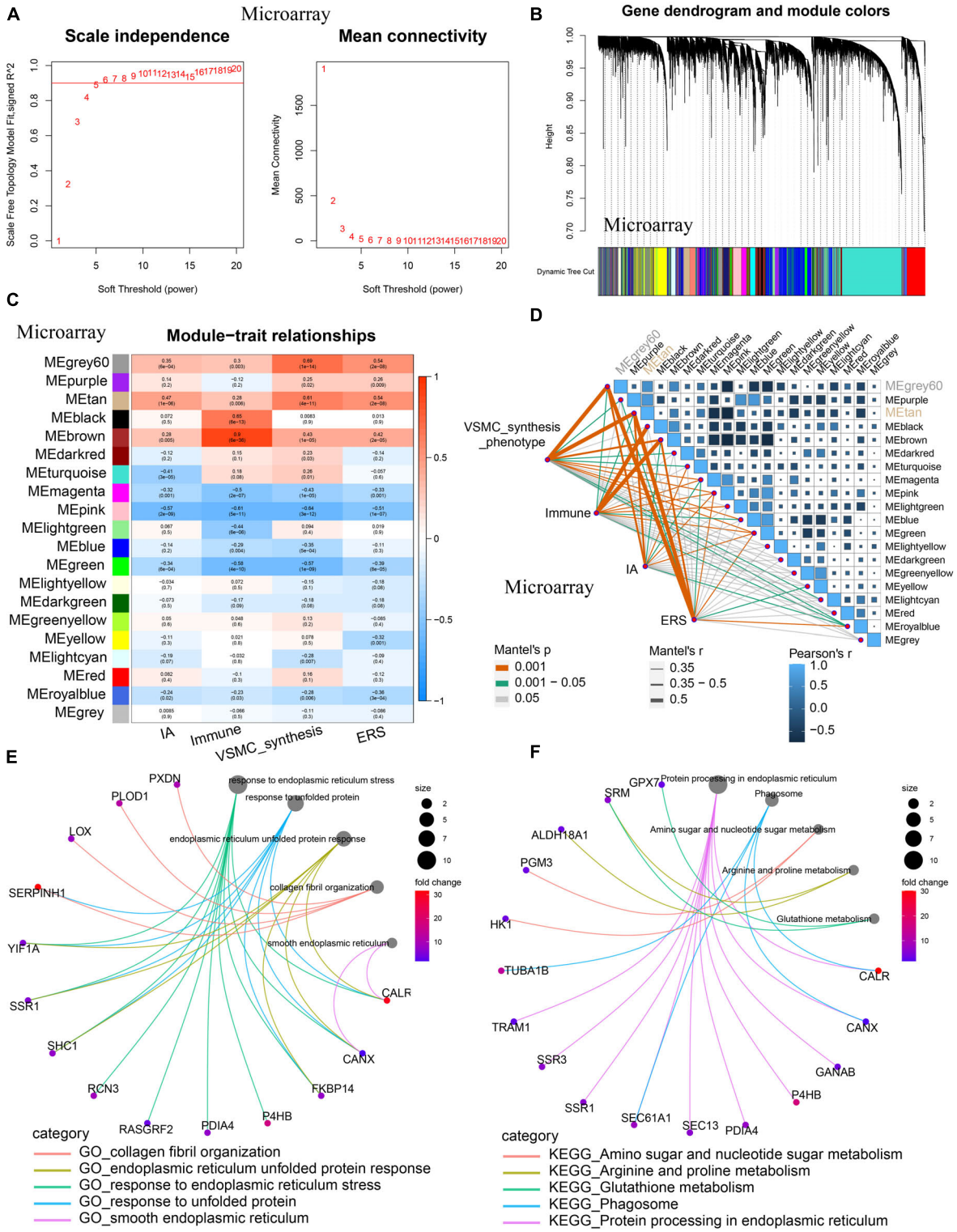

FIGURE 7 | Co-expression analysis identifying ERS-related VSMC phenotype genes in the training cohort. **(A)** A scale-free network construction (power threshold β = 5). **(B)** Gene dendrogram generating gene modules. **(C)** and **(D)** Correlation analysis between modules and pathophysiological traits. IA occurrence, VSMC synthesis, and ERS had the same two highest correlation modules (MEgray60 and MEtan). **(E)** GO enrichment analysis of the intersection between the training cohort (MEgray60 and MEtan) and the validating cohort (MEbrown and MEpink). **(F)** KEGG enrichment analysis of the intersection between the training cohort (MEgray60 and MEtan) and (MEbrown and MEpink). Function enrichment showed that these modules mainly focused on smooth endoplasmic reticulum, collagen fibril organization, metabolism, and phagosome.

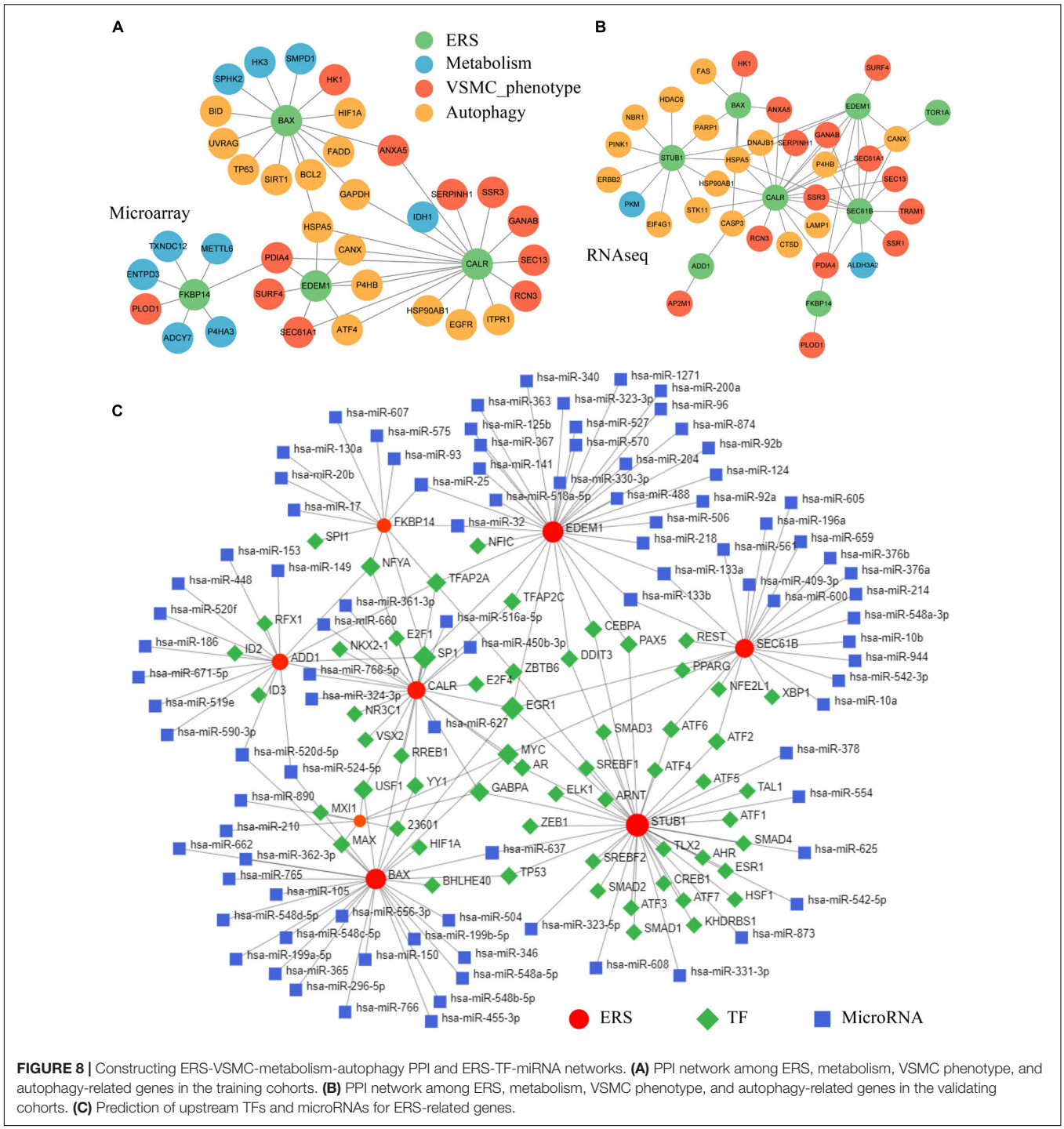

FIGURE 8 | Constructing ERS-VSMC-metabolism-autophagy PPI and ERS-TF-miRNA networks. **(A)** PPI network among ERS, metabolism, VSMC phenotype, and autophagy-related genes in the training cohorts. **(B)** PPI network among ERS, metabolism, VSMC phenotype, and autophagy-related genes in the validating cohorts. **(C)** Prediction of upstream TFs and microRNAs for ERS-related genes.

failure, cardiomyopathy, hypertension, stroke, and the like (Ren et al., 2021).

In the present study, the role of ERS in IA formation was explored using bioinformatics analysis for the first time. We firstly identified ERS by functional enrichment of DEGs, constructed an ERS signature gene set. Afterward, we generated ERS-VSMC-metabolism-autophagy PPI networks and predicted ERS-related upstream TF and microRNAs. The relationship between ERS and non-coding SNPs was then explored. Finally, potential drugs targeting ERS were predicted to inhibit IA formation and development.

Recently, accumulating evidence demonstrates that ERS plays an important role in aneurysm formation and development. In our research, multiple types of DEG functional enrichment analyses showed ERS was related to IA pathogenesis. Similarly, Clément et al. (2019) found increased expression of ERS markers

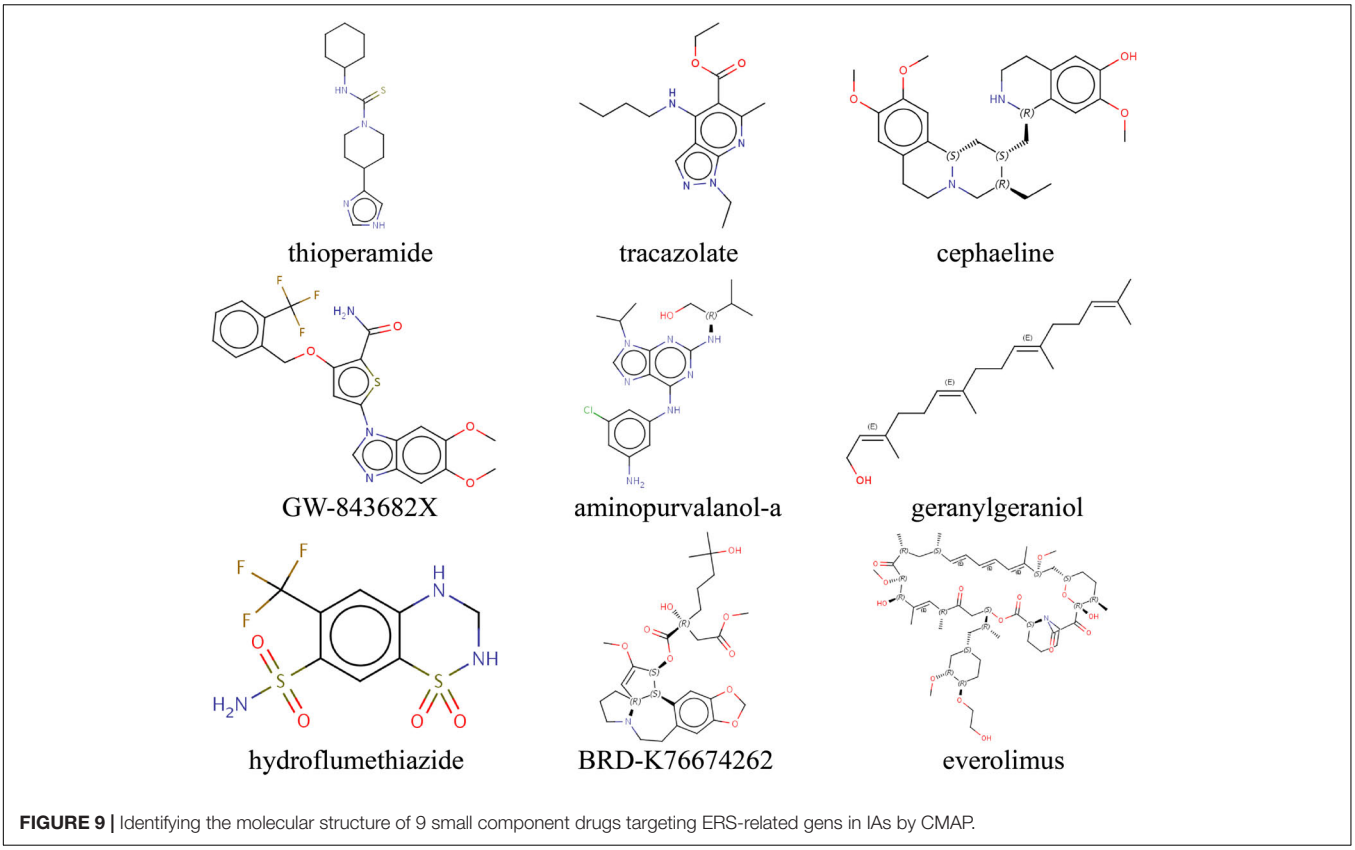

FIGURE 9 | Identifying the molecular structure of 9 small component drugs targeting ERS-related gens in IAs by CMAP.

in VSMCs of dissected aortic aneurysms. Jia et al. (2015) proved that stress-induced ERS contributed to thoracic aortic aneurysm and dissection formation. They also reported that ERS-dependent microparticles promote endothelial dysfunction during the formation process of thoracic aortic aneurysm and dissection (Jia et al., 2017). In addition, several studies showed that ERS inhibition could attenuate the formation and development of abdominal aortic aneurysms (Li et al., 2017; Ni et al., 2018).

The ERS signature gene set was then constructed in IA, including FKBP14, TOR1A, EDEM1, BAX, CALR, STUB1, SEC61B, and ADD1. These genes have been confirmed to be related to multiple cardiovascular diseases. Among those, BAX, whose protein belongs to the BCL2 family, is an apoptosis activator. One study showed that overexpressed Bax regulated intimal hyperplasia of VSMCs in arteriosclerosis (Hayakawa et al., 1999). Another study showed that upregulated Bax was associated with the presence of cystic medial degeneration of the aorta (Ihling et al., 1999). Calreticulin (CALR) encoded by the CALR gene, is a highly conserved chaperone protein primarily expressed in the endoplasmic reticulum. Previous studies indicate that CALR can coordinate vascular function and heterocellular calcium signaling (Biwer et al., 2018). STUB1, encoding the protein of STIP1 Homology And U-Box Containing Protein 1, was down-regulated during the IA process in our studies. A prior study showed that the decreased STUB1 in VSMCs inhibited thrombosis in flow loops (Shashar et al., 2017). Adducin 1 (ADD1), belonging to the cytoskeletal protein family, was also expressed at lower levels in vascular walls of IA patients. A sequencing study suggested that ADD1 polymorphism significantly increased the susceptibility to ischemic and hemorrhagic strokes (Kalita et al., 2011).

To update, there are three classic signaling pathways in ERS, including ATF6 pathway, IRE1 pathway, and Perk pathway. They act as proximal sensors of unfolded protein response (UPR) (Wu and Kaufman, 2006). Our results showed that the IRE1 pathway was highly expressed in IA lesions and had strong correlations to the gene expression of BAX, FKBP14, and SEC61B. Previous research has demonstrated that proapoptotic BAX moduled UPR by direct interaction with IRE (Hetz et al., 2006). The overexpression of BAX inhibitor-1 could inhibit IRE and reversed hyperglycemia in diet-induced obesity mice (Bailly-Maitre et al., 2010). Whether these ERS genes could promote IA formation by the IRE1 pathway deserves further basic experimental study.

VSMC phenotype transformation, from contractility to synthesis, is involved in IA formation and development. Our results suggest a strong association between ERS and VSMC synthesis in IA pathogenesis. This relationship has already been confirmed in a previous study. Zhang et al. (2020) showed that the microgravity regulated ERS to induce VSMC phenotype transform. Zhao et al. (2020) identified that Matrine inhibited VSMC phenotype transformation *via* ERS-dependent Notch signaling. Chattopadhyay et al. (2021) found that UPR could drive cholesterol-induced VSMC phenotype transformation.

Considering metabolism and autophagy were also enriched in IAs, we constructed ERS-VSMC-metabolism-autophagy PPI networks. Body metabolism disorders have been discovered to involve the pathological processes of IA. Frösen et al. (2013) found that lipid accumulation and its oxidation in the IA wall, together with low plasma levels of acquired antibodies against oxidized lipids, were associated with IA wall degeneration and rupture. Semmler et al. (2008) demonstrated that polymorphisms of homocysteine metabolism were possible risk factors for IA formation. Besides, growing evidence showed that autophagy was also involved in IA formation, development, and rupture. Sun et al. (2017) proved that ruptured IA tissues had more expression of autophagy-related genes, including LC3, Atg5, and Atg14, followed by unruptured IA and control artery tissues. *In vitro* experiments showed that activated VSMC autophagy could enhance the VSMC proliferation and migration, and induce IA formation (Zhang et al., 2019). Furthermore, the relationships among ERS, metabolism, and autophagy have been demonstrated in other diseases. There are mutual regulations between ERS and metabolism. Fu et al. (2011) showed that aberrant lipid metabolism would cause ERS in obesity. Henkel et al. (2017) proved that ERS regulated hepatic bile acid metabolism in mice. As for autophagy, it is generally considered the last means to restore the homeostasis of the endoplasmic reticulum (Henkel et al., 2017). Together, we speculated ERS can influence metabolism/autophagy/VSMC phenotype and thus contribute to IA formation, which needs further basic research.

The dysregulation of upstream TF and microRNA for ERS also has a crucial impact on the formation and development of cardiovascular diseases. Our TF prediction showed that NFYA, TFAP2A, SP1, EGR1, MYC, GABPA, and USF1 were common TFs with at least 3 ERS genes in IAs. Among these, SP1, whose encoding protein is involved in cell differentiation and growth, has been confirmed to be associated with ERS and VSMC phenotype switching. Dauer et al. (2017) proved that inhibition of SP1 prevented endoplasmic reticulum homeostasis. Hu et al. (2021) found that SP1 regulated migration and phenotype switching of VSMCs through the MAPK pathway in aortic dissections. Tang et al. (2017) identified that microRNA-124 controlled VSMC phenotypic switching *via* SP1. EGR, belonging to the early growth response family, was found to be related to ERS and aneurysm formation. Previous studies showed that ERS can activate EGR1 transcription *via* the MAPK pathway (Shan et al., 2019). Other studies prove that EGR1 upregulation leads to aortic aneurysm formation and EGR1 downregulation can reverse this process (Lin et al., 2020; Shin et al., 2020). In addition, we predicted 91 upstream microRNAs for ERS. Seven microRNAs had 2 target ERS genes. Among these, hsa-miR-25, hsa-miR-133b, and hsa-miR-133a have been confirmed to independently predict aneurysm occurrence or prevent aneurysm development (Li et al., 2014; Plana et al., 2020; Akerman et al., 2021). Furthermore, upregulated hsa-miR-637 can aggravate ERS-induced apoptosis (Kong et al., 2020).

IA-associated SNPs were reported to be enriched in Cow regulatory regions (Laarman et al., 2018). The relationship between non-coding SNPs and ERS was investigated. Integration analysis showed that 17 TFs co-regulated ERS and regulatory regions in IAs. Among these, MYC, whose encoded a nuclear phosphoprotein, with a role in cycle progression, apoptosis, and cellular transformation, had the most ERS target genes and TF binding sites. Previous research had confirmed that MYC was involved in ERS. Dong et al. (2019) found that the IRE1 ERS sensor could activate natural killer cell immunity by MYC regulation. Jayasooriya et al. (2018) found that camptothecin enhanced MYC-mediated ERS and led to autophagy. In addition, Li et al. (2020) proved that the downregulating MYC-mediated ENC1 could prevent IA formation. Correlation analysis showed the tight connectivity between ERS signature genes and nearby genes of regulatory regions. KCTD15, a potassium channel encoding gene, had the most significant associations with ERS. Previous research found that potassium channels have the modification of gating properties under the ERS and were involved in the cerebral vasospasm after subarachnoid hemorrhage (Sobey and Faraci, 1998; Khodaee et al., 2014). The role of KCTD15 in IA formation deserves further research.

Previous studies reported that ERS was the potential therapeutic target for aneurysms. In this research, we predicted 9 small molecule drugs for IAs. These drugs have shown the potential to inhibit ERS progress. Cephaeline and BRD-K76674262, belonging to protein synthesis inhibitors, could inhibit tumor viability, migration, and proliferation (Silva et al., 2021). Han et al. (2013) proved ERS increased protein synthesis leading to cell death, and presented, limiting protein synthesis would be therapeutic for ERS-caused diseases. Everolimus, an mTOR inhibitor, is used in immunosuppressive treatment after organ transplantation and anticancer treatment for advanced renal cell cancers (Patel and Kobashigawa, 2006; Mariniello et al., 2012). Previous studies have found bidirectional crosstalk between ERS and mTOR (Appenzeller-Herzog and Hall, 2012). Persistent mTOR activation could induce ERS occurrence (Wang et al., 2016). Of note, everolimus has been shown capable of limiting aortic aneurysm dilatation in apolipoprotein E-deficient mouse (Moran et al., 2013). IA progress may be delayed by these compounds.

Our study had some limitations. One major limitation was the lack of basic experimental data to confirm and support our findings. Another limitation was the lack of IA-associated clinical data, like size, location, number, and others, to further explore the association between ERS and IA. Additionally, the predicted TF, miRNA, and drugs remain to be further explored to understand their real-world roles in IA formation and development.

CONCLUSION

Our results strongly suggest that ERS is involved in IA formation. Upstream and downstream regulatory networks for ERS were identified in IAs. Novel potential drugs targeting ERS were also proposed, which may delay IA formation and progress.

DATA AVAILABILITY STATEMENT

The original contributions presented in the study are included in the article/**Supplementary Material**, further inquiries can be directed to the corresponding author/s.

ETHICS STATEMENT

The studies involving human participants were reviewed and approved by open-source GEO database. The patients/participants provided their written informed consent to participate in this study. Written informed consent was obtained from the individual(s) for the publication of any potentially identifiable images or data included in this article.

AUTHOR CONTRIBUTIONS

BC, YX, and LZ designed and drafted the manuscript. BC, HZ, LY, XZ, and LZ organized figure legends and revised the article. BC conducted data analysis. All authors have read and approved the final manuscript.

FUNDING

This work was supported by the Nature Science Foundation of China (No. 81402249 to LZ), the Natural Science Foundation of Hunan Province (No. 2019JJ50963 to LZ), and Fundamental Research Funds for the Central Universities of Central South University (No. 160171016 to BC).

ACKNOWLEDGMENTS

We acknowledge GEO databases for their platforms and contributors for uploading their meaningful datasets. We would like to express our very great appreciation to F. H. Chen for his valuable and constructive suggestions during the development of this research.

SUPPLEMENTARY MATERIAL

The Supplementary Material for this article can be found online at: https://www.frontiersin.org/articles/10.3389/fncel.2022.865005/full#supplementary-material

Supplementary Figure 1 | Correlation analysis among ERS, metabolism, and autophagy in both training and validating cohorts. Autophagy **(A)** and metabolism **(B)** were positively associated with ERS, separately.

Supplementary Figure 2 | Co-expression analysis identifying ERS-related VSMC phenotype genes in the validating cohort. **(A)** A scale-free network construction (power threshold $\beta = 4$). **(B)** Gene dendrogram generating gene modules. **(C,D)** Correlation analysis between modules and pathophysiological traits. IA occurrence, VSMC synthesis, and ERS had the same two highest correlation modules (MEbrown and MEpink).

Supplementary Figure 3 | Correlation analysis between ERS and nearby genes of regulatory regions in both training and validating cohorts. **(A)** The expression level of ERS signature genes. IA lesions had higher expression of FKBP14, TOR1A, EDEM1, BAX, CALR, SEC61B, and lower expression of STUB1 and ADD1. **(B)** Venn diagrams of differential expressed genes (DEGs) and nearby genes. Six nearby DEGs of regulatory regions were gained. **(C)** Correlation analysis between ERS signature genes and nearby genes. KCTD15 had the most significant associations with ERS.

Supplementary Table 1 | TF intersection between ERS signature genes and regulatory regions.

Supplementary Table 2 | Identified 9 small molecular drugs by CMAP.

REFERENCES

Akerman, A. W., Collins, E. N., Peterson, A. R., Collins, L. B., Harrison, J. K., DeVaughn, A., et al. (2021). miR-133a replacement attenuates thoracic aortic aneurysm in mice. *J. Am. Heart Assoc.* 10:e019862. doi: 10.1161/jaha.120.019862

Appenzeller-Herzog, C., and Hall, M. N. (2012). Bidirectional crosstalk between endoplasmic reticulum stress and mTOR signaling. *Trends Cell Biol.* 22, 274–282. doi: 10.1016/j.tcb.2012.02.006

Aran, D., Hu, Z., and Butte, A. J. (2017). xCell: digitally portraying the tissue cellular heterogeneity landscape. *Genome Biol.* 18:220. doi: 10.1186/s13059-017-1349-1

Bailly-Maitre, B., Belgardt, B. F., Jordan, S. D., Coornaert, B., von Freyend, M. J., Kleinridders, A., et al. (2010). Hepatic Bax inhibitor-1 inhibits IRE1alpha and protects from obesity-associated insulin resistance and glucose intolerance. *J. Biol. Chem.* 285, 6198–6207. doi: 10.1074/jbc.M109.056648

Biwer, L. A., Good, M. E., Hong, K., Patel, R. K., Agrawal, N., Looft-Wilson, R., et al. (2018). Non-Endoplasmic reticulum-based calr (Calreticulin) can coordinate heterocellular calcium signaling and vascular function. *Arterioscler. Thromb. Vasc. Biol.* 38, 120–130. doi: 10.1161/atvbaha.117.309886

Chaterji, S., Lam, C. H., Ho, D. S., Proske, D. C., and Baker, A. B. (2014). Syndecan-1 regulates vascular smooth muscle cell phenotype. *PLoS One* 9:e89824. doi: 10.1371/journal.pone.0089824

Chattopadhyay, A., Kwartler, C. S., Kaw, K., Li, Y., Kaw, A., Chen, J., et al. (2021). Cholesterol-Induced phenotypic modulation of smooth muscle cells to macrophage/fibroblast-like cells is driven by an unfolded protein response. *Arterioscler. Thromb. Vasc. Biol.* 41, 302–316. doi: 10.1161/atvbaha.120.315164

Clément, M., Chappell, J., Raffort, J., Lareyre, F., Vandestienne, M., Taylor, A. L., et al. (2019). Vascular smooth muscle cell plasticity and autophagy in dissecting aortic aneurysms. *Arterioscler. Thromb. Vasc. Biol.* 39, 1149–1159. doi: 10.1161/atvbaha.118.311727

Dauer, P., Gupta, V. K., McGinn, O., Nomura, A., Sharma, N. S., Arora, N., et al. (2017). Inhibition of Sp1 prevents ER homeostasis and causes cell death by lysosomal membrane permeabilization in pancreatic cancer. *Sci. Rep.* 7:1564. doi: 10.1038/s41598-017-01696-2

Dong, H., Adams, N. M., Xu, Y., Cao, J., Allan, D. S. J., Carlyle, J. R., et al. (2019). The IRE1 endoplasmic reticulum stress sensor activates natural killer cell immunity in part by regulating c-Myc. *Nat. Immunol.* 20, 865–878. doi: 10.1038/s41590-019-0388-z

Frösen, J., Tulamo, R., Heikura, T., Sammalkorpi, S., Niemelä, M., Hernesniemi, J., et al. (2013). Lipid accumulation, lipid oxidation, and low plasma levels of acquired antibodies against oxidized lipids associate with degeneration and rupture of the intracranial aneurysm wall. *Acta Neuropathol. Commun.* 1:71. doi: 10.1186/2051-5960-1-71

Frösen, J., Tulamo, R., Paetau, A., Laaksamo, E., Korja, M., Laakso, A., et al. (2012). Saccular intracranial aneurysm: pathology and mechanisms. *Acta Neuropathol.* 123, 773–786. doi: 10.1007/s00401-011-0939-3

Fu, S., Yang, L., Li, P., Hofmann, O., Dicker, L., Hide, W., et al. (2011). Aberrant lipid metabolism disrupts calcium homeostasis causing liver endoplasmic reticulum stress in obesity. *Nature* 473, 528–531. doi: 10.1038/nature09968

Han, J., Back, S. H., Hur, J., Lin, Y. H., Gildersleeve, R., Shan, J., et al. (2013). ER-stress-induced transcriptional regulation increases protein synthesis leading to cell death. *Nat. Cell Biol.* 15, 481–490. doi: 10.1038/ncb2738

Hänzelmann, S., Castelo, R., and Guinney, J. (2013). GSVA: gene set variation analysis for microarray and RNA-seq data. *BMC Bioinformatics* 14:7. doi: 10.1186/1471-2105-14-7

Hayakawa, Y., Takemura, G., Misao, J., Kanoh, M., Ohno, M., Ohashi, H., et al. (1999). Apoptosis and overexpression of bax protein and bax mRNA in smooth muscle cells within intimal hyperplasia of human radial arteries : analysis with arteriovenous fistulas used for hemodialysis. *Arterioscler. Thromb. Vasc. Biol.* 19, 2066–2077. doi: 10.1161/01.atv.19.9.2066

Henkel, A. S., LeCuyer, B., Olivares, S., and Green, R. M. (2017). Endoplasmic reticulum stress regulates hepatic bile acid metabolism in mice. *Cell Mol. Gastroenterol. Hepatol.* 3, 261–271. doi: 10.1016/j.jcmgh.2016.11.006

Hetz, C., Bernasconi, P., Fisher, J., Lee, A. H., Bassik, M. C., Antonsson, B., et al. (2006). Proapoptotic BAX and BAK modulate the unfolded protein response by a direct interaction with IRE1alpha. *Science* 312, 572–576. doi: 10.1126/science.1123480

Hosaka, K., and Hoh, B. L. (2014). Inflammation and cerebral aneurysms. *Transl. Stroke Res.* 5, 190–198. doi: 10.1007/s12975-013-0313-y

Hu, C., Huang, W., Xiong, N., and Liu, X. (2021). SP1-mediated transcriptional activation of PTTG1 regulates the migration and phenotypic switching of aortic vascular smooth muscle cells in aortic dissection through MAPK signaling. *Arch. Biochem. Biophys.* 711:109007. doi: 10.1016/j.abb.2021.109007

Ihling, C., Szombathy, T., Nampoothiri, K., Haendeler, J., Beyersdorf, F., Uhl, M., et al. (1999). Cystic medial degeneration of the aorta is associated with p53 accumulation, Bax upregulation, apoptotic cell death, and cell proliferation. *Heart* 82, 286–293. doi: 10.1136/hrt.82.3.286

Jayasooriya, R., Dilshara, M. G., Karunarathne, W., Molagoda, I. M. N., Choi, Y. H., and Kim, G. Y. (2018). Camptothecin enhances c-Myc-mediated endoplasmic reticulum stress and leads to autophagy by activating Ca(2+)-mediated AMPK. *Food Chem. Toxicol.* 121, 648–656. doi: 10.1016/j.fct.2018.09.057

Jia, L. X., Zhang, W. M., Li, T. T., Liu, Y., Piao, C. M., Ma, Y. C., et al. (2017). ER stress dependent microparticles derived from smooth muscle cells promote endothelial dysfunction during thoracic aortic aneurysm and dissection. *Clin. Sci. (Lond)* 131, 1287–1299. doi: 10.1042/cs20170252

Jia, L. X., Zhang, W. M., Zhang, H. J., Li, T. T., Wang, Y. L., Qin, Y. W., et al. (2015). Mechanical stretch-induced endoplasmic reticulum stress, apoptosis and inflammation contribute to thoracic aortic aneurysm and dissection. *J. Pathol.* 236, 373–383. doi: 10.1002/path.4534

Kalita, J., Somarajan, B. I., Kumar, B., Mittal, B., and Misra, U. K. (2011). A study of ACE and ADD1 polymorphism in ischemic and hemorrhagic stroke. *Clin. Chim. Acta* 412, 642–646. doi: 10.1016/j.cca.2010.12.022

Khodaee, N., Ghasemi, M., Saghiri, R., and Eliassi, A. (2014). Endoplasmic reticulum membrane potassium channel dysfunction in high fat diet induced stress in rat hepatocytes. *Excli J.* 13, 1075–1087.

Kong, Q., Zhang, Z., and Liang, Z. (2020). Upregulating miR-637 aggravates endoplasmic reticulum stress-induced apoptosis in gastric cancer cells by suppressing Calreticulin. *Anim. Cells Syst. (Seoul)* 24, 267–274. doi: 10.1080/19768354.2020.1816579

Laarman, M. D., Vermunt, M. W., Kleinloog, R., de Boer-Bergsma, J. J., Brain Bank, N., Rinkel, G. J. E., et al. (2018). Intracranial aneurysm-associated single-nucleotide polymorphisms alter regulatory DNA in the human circle of willis. *Stroke* 49, 447–453. doi: 10.1161/strokeaha.117.018557

Langfelder, P., and Horvath, S. (2008). WGCNA: an R package for weighted correlation network analysis. *BMC Bioinformatics* 9:559. doi: 10.1186/1471-2105-9-559

Leek, J. T., Johnson, W. E., Parker, H. S., Jaffe, A. E., and Storey, J. D. (2012). The sva package for removing batch effects and other unwanted variation in high-throughput experiments. *Bioinformatics* 28, 882–883. doi: 10.1093/bioinformatics/bts034

Li, P., Zhang, Q., Wu, X., Yang, X., Zhang, Y., Li, Y., et al. (2014). Circulating microRNAs serve as novel biological markers for intracranial aneurysms. *J. Am. Heart Assoc.* 3:e000972. doi: 10.1161/jaha.114.000972

Li, X., Zhao, H., Liu, J., and Tong, J. (2020). Long Non-coding RNA MIAT knockdown prevents the formation of intracranial aneurysm by downregulating ENC1 via MYC. *Front. Physiol.* 11:572605. doi: 10.3389/fphys.2020.572605

Li, Y., Lu, G., Sun, D., Zuo, H., Wang, D. W., and Yan, J. (2017). Inhibition of endoplasmic reticulum stress signaling pathway: a new mechanism of statins to suppress the development of abdominal aortic aneurysm. *PLoS One* 12:e0174821. doi: 10.1371/journal.pone.0174821

Lin, H., You, B., Lin, X., Wang, X., Zhou, D., Chen, Z., et al. (2020). Silencing of long non-coding RNA Sox2ot inhibits oxidative stress and inflammation of vascular smooth muscle cells in abdominal aortic aneurysm via microRNA-145-mediated Egr1 inhibition. *Aging (Albany NY)* 12, 12684–12702. doi: 10.18632/aging.103077

Lyon, C. A., Koutsouki, E., Aguilera, C. M., Blaschuk, O. W., and George, S. J. (2010). Inhibition of N-cadherin retards smooth muscle cell migration and intimal thickening via induction of apoptosis. *J. Vasc. Surg.* 52, 1301–1309. doi: 10.1016/j.jvs.2010.05.096

Mariniello, B., Rosato, A., Zuccolotto, G., Rubin, B., Cicala, M. V., Finco, I., et al. (2012). Combination of sorafenib and everolimus impacts therapeutically on adrenocortical tumor models. *Endocr. Relat. Cancer* 19, 527–539. doi: 10.1530/erc-11-0337

Moran, C. S., Jose, R. J., Moxon, J. V., Roomberg, A., Norman, P. E., Rush, C., et al. (2013). Everolimus limits aortic aneurysm in the apolipoprotein E-deficient mouse by downregulating C-C chemokine receptor 2 positive monocytes. *Arterioscler. Thromb. Vasc. Biol.* 33, 814–821. doi: 10.1161/atvbaha.112.301006

Nakahara, K., Nishimura, H., Kuro-o, M., Takewaki, S., Iwase, M., Ohkubo, A., et al. (1992). Identification of three types of PDGF-A chain gene transcripts in rabbit vascular smooth muscle and their regulated expression during development and by angiotensin II. *Biochem. Biophys. Res. Commun.* 184, 811–818. doi: 10.1016/0006-291x(92)90662-5

Ni, X. Q., Lu, W. W., Zhang, J. S., Zhu, Q., Ren, J. L., Yu, Y. R., et al. (2018). Inhibition of endoplasmic reticulum stress by intermedin1-53 attenuates angiotensin II-induced abdominal aortic aneurysm in ApoE KO Mice. *Endocrine* 62, 90–106. doi: 10.1007/s12020-018-1657-6

Orlandi, A., Francesconi, A., Clément, S., Ropraz, P., Spagnoli, L. G., and Gabbiani, G. (2002). High levels of cellular retinol binding protein-1 expression in leiomyosarcoma: possible implications for diagnostic evaluation. *Virchows Arch.* 441, 31–40. doi: 10.1007/s00428-001-0576-7

Patel, J. K., and Kobashigawa, J. A. (2006). Everolimus: an immunosuppressive agent in transplantation. *Expert Opin. Pharmacother.* 7, 1347–1355. doi: 10.1517/14656566.7.10.1347

Plana, E., Gálvez, L., Medina, P., Navarro, S., Fornés-Ferrer, V., Panadero, J., et al. (2020). Identification of novel microRNA profiles dysregulated in plasma and tissue of abdominal aortic aneurysm patients. *Int. J. Mol. Sci.* 21:4600. doi: 10.3390/ijms21134600

Ren, J., Bi, Y., Sowers, J. R., Hetz, C., and Zhang, Y. (2021). Endoplasmic reticulum stress and unfolded protein response in cardiovascular diseases. *Nat. Rev. Cardiol.* 18, 499–521. doi: 10.1038/s41569-021-00511-w

Ritchie, M. E., Phipson, B., Wu, D., Hu, Y., Law, C. W., Shi, W., et al. (2015). limma powers differential expression analyses for RNA-sequencing and microarray studies. *Nucleic Acids Res.* 43:e47. doi: 10.1093/nar/gkv007

Semmler, A., Linnebank, M., Krex, D., Götz, A., Moskau, S., Ziegler, A., et al. (2008). Polymorphisms of homocysteine metabolism are associated with intracranial aneurysms. *Cerebrovasc. Dis.* 26, 425–429. doi: 10.1159/000155638

Shan, J., Dudenhausen, E., and Kilberg, M. S. (2019). Induction of early growth response gene 1 (EGR1) by endoplasmic reticulum stress is mediated by the extracellular regulated kinase (ERK) arm of the MAPK pathways. *Biochim. Biophys. Acta Mol. Cell Res.* 1866, 371–381. doi: 10.1016/j.bbamcr.2018.09.009

Shanahan, C. M., Weissberg, P. L., and Metcalfe, J. C. (1993). Isolation of gene markers of differentiated and proliferating vascular smooth muscle cells. *Circ. Res.* 73, 193–204. doi: 10.1161/01.res.73.1.193

Shao, Y., Li, G., Huang, S., Li, Z., Qiao, B., Chen, D., et al. (2020). Effects of extracellular matrix softening on vascular smooth muscle cell dysfunction. *Cardiovasc. Toxicol.* 20, 548–556. doi: 10.1007/s12012-020-09580-8

Shashar, M., Belghasem, M. E., Matsuura, S., Walker, J., Richards, S., Alousi, F., et al. (2017). Targeting STUB1-tissue factor axis normalizes hyperthrombotic uremic phenotype without increasing bleeding risk. *Sci. Transl. Med.* 9:eaam8475. doi: 10.1126/scitranslmed.aam8475

Shin, S. J., Hang, H. T., Thang, B. Q., Shimoda, T., Sakamoto, H., Osaka, M., et al. (2020). Role of PAR1-Egr1 in the initiation of thoracic aortic aneurysm in Fbln4-Deficient mice. *Arterioscler. Thromb. Vasc. Biol.* 40, 1905–1917. doi: 10.1161/atvbaha.120.314560

Signorelli, F., Sela, S., Gesualdo, L., Chevrel, S., Tollet, F., Pailler-Mattei, C., et al. (2018). Hemodynamic stress, inflammation, and intracranial aneurysm

development and rupture: a systematic review. *World Neurosurg.* 115, 234–244. doi: 10.1016/j.wneu.2018.04.143

Silva, L. C., Borgato, G. B., Wagner, V. P., Martins, M. D., Rocha, G. Z., Lopes, M. A., et al. (2021). Cephaeline is an inductor of histone H3 acetylation and inhibitor of mucoepidermoid carcinoma cancer stem cells. *J. Oral Pathol. Med.* Online ahead of print. doi: 10.1111/jop.13252

Sobey, C. G., and Faraci, F. M. (1998). Subarachnoid haemorrhage: what happens to the cerebral arteries? *Clin. Exp. Pharmacol. Physiol.* 25, 867–876. doi: 10.1111/j.1440-1681.1998.tb02337.x

Starke, R. M., Chalouhi, N., Ding, D., Raper, D. M., McKisic, M. S., Owens, G. K., et al. (2014). Vascular smooth muscle cells in cerebral aneurysm pathogenesis. *Transl. Stroke Res.* 5, 338–346. doi: 10.1007/s12975-013-0290-1

Sun, L., Zhao, M., Zhang, J., Lv, M., Li, Y., Yang, X., et al. (2017). MiR-29b downregulation induces phenotypic modulation of vascular smooth muscle cells: implication for intracranial aneurysm formation and progression to rupture. *Cell Physiol. Biochem.* 41, 510–518. doi: 10.1159/000456887

Tang, Y., Yu, S., Liu, Y., Zhang, J., Han, L., and Xu, Z. (2017). MicroRNA-124 controls human vascular smooth muscle cell phenotypic switch via Sp1. *Am. J. Physiol. Heart Circ. Physiol.* 313, H641–H649. doi: 10.1152/ajpheart.00660.2016

Wang, J., Yang, X., and Zhang, J. (2016). Bridges between mitochondrial oxidative stress, ER stress and mTOR signaling in pancreatic β cells. *Cell. Signal.* 28, 1099–1104. doi: 10.1016/j.cellsig.2016.05.007

Wu, J., and Kaufman, R. J. (2006). From acute ER stress to physiological roles of the unfolded protein response. *Cell Death Differ.* 13, 374–384. doi: 10.1038/sj.cdd.4401840

Zhang, J., Jin, J., and Yang, W. (2019). [Autophagy regulates the function of vascular smooth muscle cells in the formation and rupture of intracranial aneurysms]. *Zhejiang Da Xue Xue Bao Yi Xue Ban* 48, 552–559.

Zhang, R., Jiang, M., Zhang, J., Qiu, Y., Li, D., Li, S., et al. (2020). Regulation of the cerebrovascular smooth muscle cell phenotype by mitochondrial oxidative injury and endoplasmic reticulum stress in simulated microgravity rats via the PERK-eIF2α-ATF4-CHOP pathway. *Biochim Biophys. Acta Mol. Basis Dis.* 1866:165799. doi: 10.1016/j.bbadis.2020.165799

Zhao, L., Cai, H., Tang, Z., Cui, Q., Liu, Z., and Lu, S. (2020). Matrine suppresses advanced glycation end products-induced human coronary smooth muscle cells phenotype conversion by regulating endoplasmic reticulum stress-dependent Notch signaling. *Eur. J. Pharmacol.* 882:173257. doi: 10.1016/j.ejphar.2020.173257

Zhou, G., Soufan, O., Ewald, J., Hancock, R. E. W., Basu, N., and Xia, J. (2019). NetworkAnalyst 3.0: a visual analytics platform for comprehensive gene expression profiling and meta-analysis. *Nucleic Acids Res.* 47, W234–W241. doi: 10.1093/nar/gkz240

Conflict of Interest: The authors declare that the research was conducted in the absence of any commercial or financial relationships that could be construed as a potential conflict of interest.

Publisher's Note: All claims expressed in this article are solely those of the authors and do not necessarily represent those of their affiliated organizations, or those of the publisher, the editors and the reviewers. Any product that may be evaluated in this article, or claim that may be made by its manufacturer, is not guaranteed or endorsed by the publisher.

frontiers | Frontiers in Aging Neuroscience

MINI REVIEW
published: 09 May 2022
doi: 10.3389/fnagi.2022.880167

Deciphering the Link Between ER^{UPR} Signaling and MicroRNA in Pathogenesis of Alzheimer's Disease

Nusrath Yasmeen[1], Manali Datta[1], Vikram Kumar[1], Fahad S. Alshehri[2], Atiah H. Almalki[3,4] and Shafiul Haque[5,6]*

[1] Amity Institute of Biotechnology, Amity University Rajasthan, Jaipur, India, [2] Department of Pharmacology and Toxicology, College of Pharmacy, Umm Al-Qura University, Makkah, Saudi Arabia, [3] Department of Pharmaceutical Chemistry, College of Pharmacy, Taif University, Taif, Saudi Arabia, [4] Addiction and Neuroscience Research Unit, College of Pharmacy, Taif University, Taif, Saudi Arabia, [5] Research and Scientific Studies Unit, College of Nursing and Allied Health Sciences, Jazan University, Jazan, Saudi Arabia, [6] Faculty of Medicine, Bursa Uludağ University, Bursa, Turkey

Alzheimer's disease (AD) is a neurodegenerative proteinopathic disease. The deposits of misfolded Amyloid β and Tau proteins in the brain of patients with AD suggest an imbalance in endoplasmic reticulum (ER) proteostasis. ER stress is due to accumulation of aberrant proteins in the ER lumen, which then leads to activation of three sensor protein pathways that ultimately evokes the adaptive mechanism of the unfolded protein response (UPR). The UPR mechanism operates *via* adaptive UPR and the apoptotic UPR. Adaptive UPR tries to restore imbalance in ER hemostasis by decreasing protein production, enhanced chaperone involvement to restore protein folding, misfolded protein decay by proteasome, and suppression of ribosomal translation ultimately relieving the excessive protein load in the ER. Subsequently, apoptotic UPR activated under severe ER stress conditions triggers cell death. MicroRNAs (miRNAs) are small non-coding protein causing dysregulated translational of mRNAs in a sequential manner. They are considered to be critical elements in the maintenance of numerous cellular activities, hemostasis, and developmental processes. Therefore, upregulation or downregulation of miRNA expression is implicated in several pathogenic processes. Evidence from scientific studies suggest a strong correlation between ER^{UPR} signaling and miRNA dysregulation but the research done is still dormant. In this review, we summarized the cross-talk between ER stress, and the UPR signaling processes and their role in AD pathology by scrutinizing and collecting information from original research and review articles.

Keywords: ER stress, unfolded protein response (UPR), microRNA, Alzheimer's disease, neurodegeneration

OPEN ACCESS

Edited by:
Rinki Minakshi,
University of Delhi, India

Reviewed by:
Zeenat Mirza,
King Abdulaziz University, Saudi Arabia
Niraj Kumar Jha,
Sharda University, India

****Correspondence:***
Vikram Kumar
vikramyadav05@gmail.com;
vkumar3@jpr.amity.edu

Specialty section:
This article was submitted to Alzheimer's Disease and Related Dementias, a section of the journal Frontiers in Aging Neuroscience

Received: *21 February 2022*
Accepted: *23 March 2022*
Published: *09 May 2022*

Citation:
Yasmeen N, Datta M, Kumar V, Alshehri FS, Almalki AH and Haque S (2022) Deciphering the Link Between ER^{UPR} Signaling and MicroRNA in Pathogenesis of Alzheimer's Disease. Front. Aging Neurosci. 14:880167. doi: 10.3389/fnagi.2022.880167

INTRODUCTION

The endoplasmic reticulum (ER) is a cellular organelle with an imperative role in the processes of folding, modification, and trafficking of nascent proteins (Plácido et al., 2014). ER dysfunction leads to an imbalance in the proteostasis that results in accumulation of abnormal (unfolded/misfolded) proteins, consequently, such proteins trigger a stress response called ER stress (Scheper and Hoozemans, 2015; Rahman et al., 2017). ER dysfunctions/ER stress is considered to be involved in several pathological conditions like metabolic disorders,

such as diabetes, neurodegenerative diseases, cancer, atherosclerosis, lung, and renal diseases (Lindholm et al., 2017). ER stress in turn triggers unfolded protein response (UPR), an adaptive rescuer mechanism, through upregulation of molecular chaperones (Fu and Gao, 2014; Alshareef et al., 2021). The UPR acts as *two-edged sword* it can either exhibit cytoprotective action or cytotoxic action. Cytoprotection is exhibited through the revival of proteostatic balance, and cellular adaptations essential for ER protein folding. However, prolonged ER stress-related perturbations might enhance UPR led cytotoxicity and hence apoptosis (Gardner et al., 2013).

Proteostatic defects augment the accretion of misfolded protein, to which neuronal cells are sensitive. Consequently, they survive and evade toxicity by utilizing the ER-induced UPR mechanism (Remondelli and Renna, 2017). Misfolded protein aggregates may cause neuronal toxicity, which is regarded as the crucial step in the pathogenesis of neurodegenerative diseases (Spires-Jones et al., 2017). Alzheimer's disease (AD) is a type of misfolded-protein disease. AD is an age-related neurodegenerative disease regarded as the most common cause of dementia (Abduljaleel et al., 2014; Scheper and Hoozemans, 2015; Rahman et al., 2018). The prominent neuropathological features of AD include Neuritic plaque (NP) besides neurofibrillary tangle (NFT). NPs are extracellular aggregates of amyloid-β (Aβ) peptides (Labban et al., 2021). Furthermore, dystrophic neurites and neuropil threads along with interneuronal aggregates of hyperphosphorylated Tau proteins in neurofibrillary tangles are other hallmark features of AD (Tanprasertsuk et al., 2019). Katayama et al., in their study, reported that mutation in presenilin-1 (PS1), and induction of high-mobility group A1a (HMGA1a) protein by Presenilin-2 (PS2) isoform, i.e., PS2V, along with the activation of Caspase-4 are all responsible for the neuronal cell death in AD. Eventually, this is attributed to hyperactivity of the protein translation mechanism accompanied by Aβ accumulation in neurons all of which lead to aberrant ER stress (Katayama et al., 2004; Wu Q. et al., 2016; Hashimoto and Saido, 2018).

MicroRNAs (miRNAs) are non-coding 19–25 nucleotides long, single-stranded protein molecules that are endogenously synthesized, evolutionarily conserved (Rahman et al., 2021; Yasmeen et al., 2021). miRNA mediates post-translational gene regulation either by promoting mRNA decay or repressing protein translation (Wang M. et al., 2019). The role of miRNAs is imperative in several cellular processes, such as cellular proliferation, cell differentiation, apoptosis, and in neural cell biology. Local protein synthesis to crucial to maintain neuronal function and synaptic plasticity. The existence of several hundreds of translationally silent mRNAs in axons their activation *via* stimuli leads to their subsequent protein synthesis specific to that cellular process (Kim and Jung, 2015). miRNAs are located in cell soma, dendrites, and synaptosomes, they control GluA1 or GluA2 subunits of AMPA-type glutamate receptor (AMPAR) along with $GABA_A$Rs (α1 and γ2) crucial for synaptic coordination and long-term potentiation. Hence, miRNAs are regarded as key regulators of local protein synthesis during synaptic plasticity. In short, neuronal protein translation is also regulated by miRNAs (Smalheiser and Lugli, 2009; Rajgor et al., 2021). Not only this, but they are also implicated in several pathological processes, such as cancer, diabetes, and neurodegenerative diseases (Grasso et al., 2014). The role of miRNAs in regulating ER stress is the foundation to unravel following several studies. However, significant contributions are required to understand the mechanism involved behind this. Numerous revelations are being made in recent times, regarding the influence of miRNA dysregulation in neuronal disease. Several miRNA families for instance miR-485 were found to be dysregulated in AD and other neurological diseases. In this review, we summarize the connection between miRNAs and ER^{UPR} signaling pathways that play a vital role in AD.

ER^{UPR} SIGNALING

The ER is a membrane-bound organelle that plays an important role in the synthesis, folding, maturation, proper trafficking, quality control, degradation, and post-translational modifications of nascent proteins. It is also involved in several other cellular events, such as calcium homeostasis, cholesterol homeostasis in endosomes, and in cytoplasmic streaming (Almanza et al., 2019). ER quality control helps in preserving proteostasis. ER-associated degradation (ERAD) is a process that helps in disposing of terminally misfolded proteins through ubiquitin–proteasome system (Oku et al., 2021). When the misfolded proteins are overloaded the prototypical ER-stress sensors located at the ER membrane activate UPR. The UPR activation is mediated by an intricate network of three main signaling pathways: inositol-requiring transmembrane kinase/endonucleases (IRE1α and -β), protein kinase RNA (PKR)-like endoplasmic reticulum kinase (PERK), and the activating transcription factor-6 (ATF6α and -β) (Dufey et al., 2014). Under normal physiological conditions, these stress-sensor proteins bind to BiP/GRP78 an ER-resident chaperone forming a complex, which remains dormant (Hoozemans et al., 2012). Whereas, following ER stress this complex dissociates and individual proteins are activated and influence downstream signaling. The signaling pathways involved in UPR are depicted in **Figure 1**.

IRE1 Pathway

Inositol-requiring transmembrane kinase/endonucleases 1 (IRE1) is a highly conserved, type I transmembrane protein. In ER-stress conditions, IRE1 self-associates during which BiP/GRP78 chaperone is displaced by Hsp47, from the complex called IRE1 UPRosome and promotes oligomerization (Almanza et al., 2019). The activation of cytosolic kinase domain and IRE1 RNase domain is through conformational change and autophosphorylation. Activation of IRE1 further activates UPR downstream signaling *via* the splicing of X-box binding protein 1 (Xbp-1) mRNA, which is a basic leucine zipper (bZIP) transcription factor (Gerakis and Hetz, 2018). Spliced XBP1 (sXBP1) mRNA mediates transactivation of genes, such as GRP78/BiP essential for proteostasis, lipid biosynthesis, redox metabolism, and glucose metabolism. Furthermore,

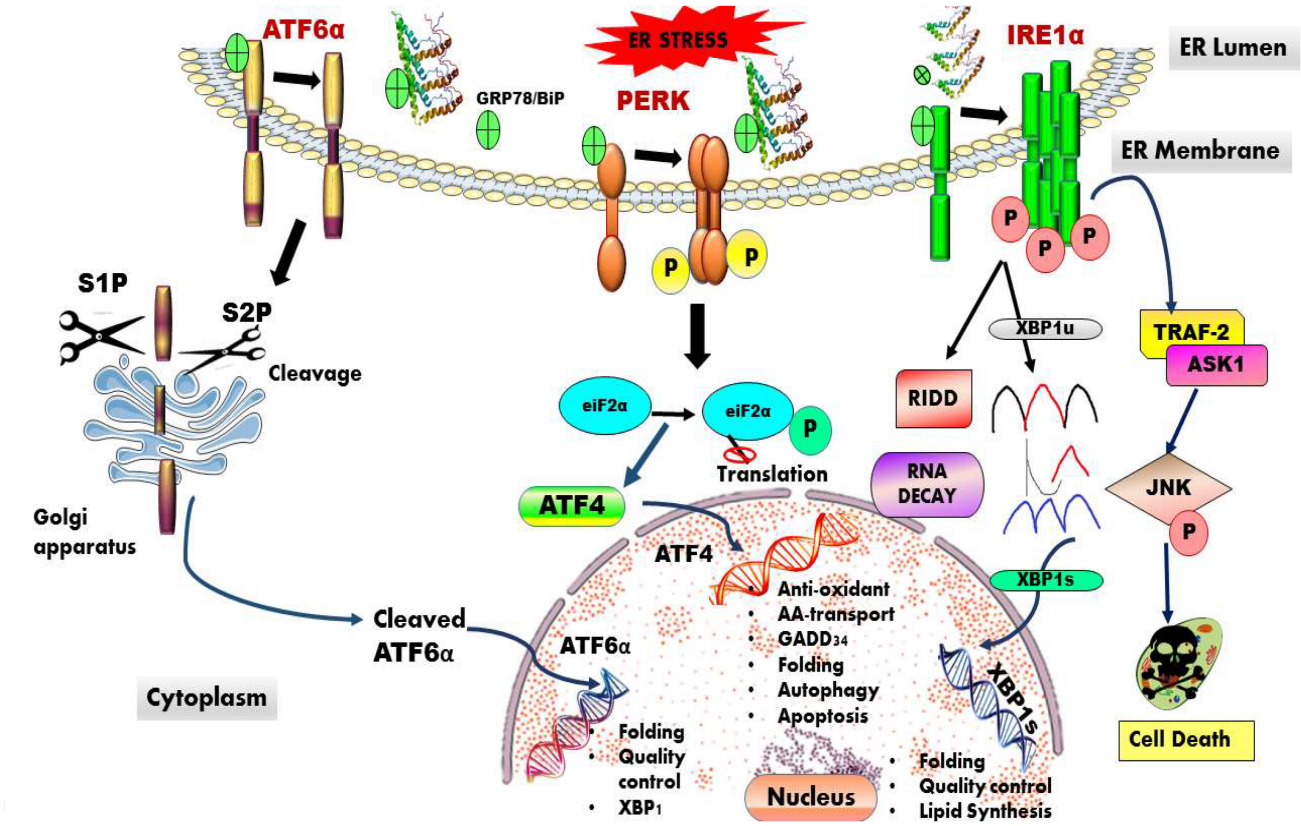

FIGURE 1 | Overview of ER-induced UPR stress signaling pathway. The UPR is an adaptive mechanism activated in response to ER stress. The three UPR stress sensing proteins that are activated are IRE1, PERK, and ATF6, which work independently with an aim to maintain protestatic balance *via* decreasing the load of misfolded proteins and restoring ER protein homeostasis.

the activated RNase domain of IRE1 leads to activation of regulated IRE1-dependent decay (RIDD). RIDD pathway activation degrades mRNAs and miRNAs, decreasing the load of nascent proteins entering ER. Hence, essential for preserving ER homeostasis and cell survival (Siwecka et al., 2021). Under ER stress conditions, IRE1α induces TRAF 2 and ASK1 [tumor necrosis factor (TNF) receptor-associated factor 2; apoptosis signal-regulating kinase 1], respectively. Subsequently, the IRE1α-TRAF2-ASK1 complex formed activates several other pathways, such as JNK (c-Jun N-terminal kinase), MAPK (p38 mitogen-activated protein kinase), and procaspase 12 pathways, which ultimately lead to apoptosis. Hence, IRE1α pathway is regarded as the main trigger of apoptosis (Chen and Brandizzi, 2013; Wu J. et al., 2016; Junjappa et al., 2018).

PERK Pathway

Protein kinase RNA (PKR)-like endoplasmic reticulum kinase is a kinase protein that is ubiquitously expressed lodges ER luminal domain and a cytoplasmic kinase domain. Under ER-stress conditions, the PERK pathway is activated when BiP/GRP78 chaperone and PERK complex dissociates, which leads to oligomerization, additionally, its cytosolic kinase domain is subjected to trans-auto phosphorylation. PERK activation phosphorylates eukaryotic translation initiation factor-2α(eIF2α) on serine 51 causing downstream signaling of eIF2α (Wang et al., 2018). Phosphorylation of eIF2α is involved in regulation of protein synthesis, also inhibits eIF2B activity, which blocks protein translation and hence reduces the protein load. eIF2α phosphorylation translates mRNA having short upstream open reading frames (uORFs) that activates ATF4, which in turn induces GADD34 (growth arrest and DNA damage-inducible34) and C/EBP homologous protein (CHOP) (Pakos-Zebrucka et al., 2016). GADD34 is a regulatory subunit of protein phosphatase (PP1C) complex, it acts as a negative feedback mechanism, as it dephosphorylates eIF2α in the PERK pathway, while CHOP is a proapoptotic factor. Overall PERK/ATF4 signaling is involved in redox homeostasis, protein folding, amino acid biosynthesis, autophagy, and apoptosis. PERK pathway is prosurvival and transitions to proapoptotic under critical ER-stress conditions (Gardner et al., 2013).

ATF6 Pathway

Activating transcription factor 6 a type II transmembrane protein has stress sensor carboxy-terminal luminal domain and an amino-terminal domain, which is a bZip transcription factor (Stauffer et al., 2020). ER-stress conditions activate ATF6, which translocate from the ER to the Golgi, where it is

cleaved sequentially by the site-1 and site-2 proteases (S1Pand S2P) releasing the cytosolic amino terminus ATF6-N fragment. ATF6-N later binds to cis-acting ER stress response elements (ERSE) in the nucleus. ATF6 up-regulates gene expression of foldases, chaperones, XBP-1, and ERAD pathway also facilitates cytoprotection, suppressing the UPR-induced apoptotic program (Ibe et al., 2021). **Figure 1** depicts the various pathways activated in ER proteotoxic stress conditions.

TABLE 1 | Depicts several microRNAs dysregulated in AD.

microRNA	Up/Down regulation	Description	Experimental model	Potential targets	References
miR-34c	Up regulated	Causes synaptic and memory deficits by targeting SYT1 through ROS-JNK-p53 pathway	HT-22 cells; SAMP8 mice and patients	Synaptotagmin 1 (SYT1)	Shi et al., 2020
miR-455-5p	Up regulated	Led to synaptic and memory deficits in AD	APP/PS1 mice	Cytoplasmic polyadenylation element-binding 1 (CPEB1)	Xiao et al., 2021
miR-361-3p	Up regulated	inhibits β-amyloid deposition and ameliorated AD progression	SH-SY5Y cell; APP/PS1 mice	BACE1	Ji Y. et al., 2019
miR-181a	Up regulated	mediates Aβ-induced synaptotoxicity; Leads to loss of functional synapses and cognitive impairment	C57BL6/J mice and 3xTg-AD	GluA2	Rodriguez-Ortiz et al., 2020
miR-200b/c	Up regulated	Exhibit defensive role against Aβ-induced toxicity by activating insulin signaling pathway	Tg2576 transgenic Mice	Ribosomal protein S6 kinase B1 (S6K1)	Higaki et al., 2018
miR-22-3p	Up regulated	reduced Aβ deposit reduce AD progression	AD mice model	Mitogen-activated protein kinase 14 (MAPK14)	Ji Q. et al., 2019
miR-26b	Up regulated	Activates Cell Cycle, Hyper phosphorylation of Tau and Apoptosis in Neurons	MCI and AD brains	IGF-1; Cdk5; Retinoblastoma protein (Rb1)	Absalon et al., 2013
miR-9	Up/down regulated	Helps in hyperphosphorylation of Tau		Fibroblast growth factor receptor 1 (FGFR1), NFkB and sirtuin 1 (SIRT1)	Delay et al., 2012; Almalki et al., 2021
miR-485-3p	Up regulated	Aβ plaque deposition, tau phosphorylation,	Transgenic mice and AD patients'	Synaptophysin	Koh et al., 2021
miR-200a-3p	Up regulated	inhibit cell apoptosis; reduced the production of Aβ1-42; neuroprotective effects	APP/PS1 and SAMP8 mice; AD patients	BACE1 and protein kinase cAMP-activated catalytic subunit beta (PRKACB)	Wang L. et al., 2019
miR-409-5p	Down regulated	impairs neurite outgrowth, decreases neuronal viability, and accelerates the progression of Aβ1 - 42-induced pathologies	APP/PS1 mice	Pleckstrin (Plek)	Guo et al., 2019
miR-106b	Down regulated	APP expression regulation; Cell cycle regulation; apoptosis and autophagy	SH-SY5Y cells	Rb1, p2; APP; p73; p62; Fyn	Liu et al., 2016
miR-384	Down regulated	decreased miR-384 levels might cause upregulation of APP and lead to progression of AD	SH-SY5Y cells; Patients with MCI and DAT	APP and BACE-1	Liu et al., 2014
miR-135a-5p	Down regulated	loss of miR-135a-5p, aberrant Rock2 activation. . .reduction of Foxd3 are induced by Tau and are associated with memory impairment and synaptic disorder	APP/PS1 mice and P301S	Foxd3	Zheng et al., 2021
miR-331-3p and miR-9-5p	down-regulated ….early-stage up-regulated late-stage of AD	Affected autophagy	APPswe/PS1dE9 mice	Sequestosome 1 (Sqstm1) and Optineurin (Optn)	Chen Y. et al., 2021
miR-335-5p	Down regulated	Aβ accumulation and AD progression, activate JNK pathway	APP/PS1 transgenic mice	c-jun-N-terminal kinase 3 (JNK3)	Wang et al., 2020
miR-16-5p	Up regulated	neuronal cell apoptosis in AD	5xFAD mice; SH-SY5Y cells	B cell lymphoma-2 (BCL-2)	Kim et al., 2020
miR-214-5p	Down regulated	Involved with hippocampal neuronal apoptosis, cognitive impairment and oxidative stress	APPswe/PS1dE9 mice	SUZ12	Hu et al., 2021
miR-124	Down regulated	alleviated Aβ-induced viability; decreased apoptosis	SH-SY5Y cells.	BACE1	An et al., 2017
miR-29a/b-1	Down regulated	AD progression	sporadic AD patients	BACE1	Hébert et al., 2008
miR-339-5p	Down regulated	AD progression	AD patients	BACE1	Long et al., 2014
miR-149	Down regulated	AD Progression	SH-SY5Y cells	BACE1	Du et al., 2021

MicroRNAs IMPLICATED IN ALZHEIMER'S DISEASE

Alzheimer's disease is a neurodegenerative disease with dual proteinopathy characterized by deposits of neuritic ß-amyloid (Aß) plaques and deposits of hyper-phosphorylated, microtubule stabilizing protein called tau protein in NFTs (Bejanin et al., 2017; Sultan et al., 2020). Neuropsychiatric symptoms (NPSs) are prevalent hallmark symptoms in patients with AD. Furthermore, AD is characterized by impairment in cognitive, behavioral, and functional domains with symptoms, such as depression, apathy, cognitive decline, delusion, motor disturbance, and agility (Chen M. L. et al., 2021). miRNAs exhibit crucial role in the pathogenesis of several neurodegenerative diseases, such as AD, they may be either upregulated or downregulated in AD. The onset of AD begins with synaptic dysfunction, which is accompanied by the dysregulation of several miRNAs. miRNAs serve as a promising biomarker to monitor initial, pre-symptomatic phases of AD pathogenesis. Evidence from previous studies suggests that several miRNAs are implicated in the AD pathogenesis by dysregulating functions of Aβ production, Cofilin, APP, BACE1, and Tau phosphorylation levels. There are numerous miRNAs implicated in the pathogenesis of AD some of them are elaborated in the following **Table 1**.

CONNECTION BETWEEN ER^{UPR} SIGNALING PATHWAYS AND miRNAs in ALZHEIMER'S DISEASE

MiRNAs are proven to be the most efficient modulators of several cellular pathways. They also play a regulatory role in the major ER-stress sensor pathways like IRE1, ATF6, and PERK pathways. miRNAs help in modulation of the cellular stress response, by regulating UPR key component levels. Krammes et al., 2020 reported that miR-34a-5p plays a vital role in the regulation of the IRE1α branch. Its overexpression targets *BIP*, *IRE1α*, and *XBP1* genes and subsequently leads to a reduction in IRE1α and XBP1s thereby modulating UPR signaling. In another study, it was reported that protection against Aβ-induced injury in SH-SY5Y cells can be enhanced by miR-34a upregulation and IRE1α inhibition (Li et al., 2019). It is also suggested that a plausible

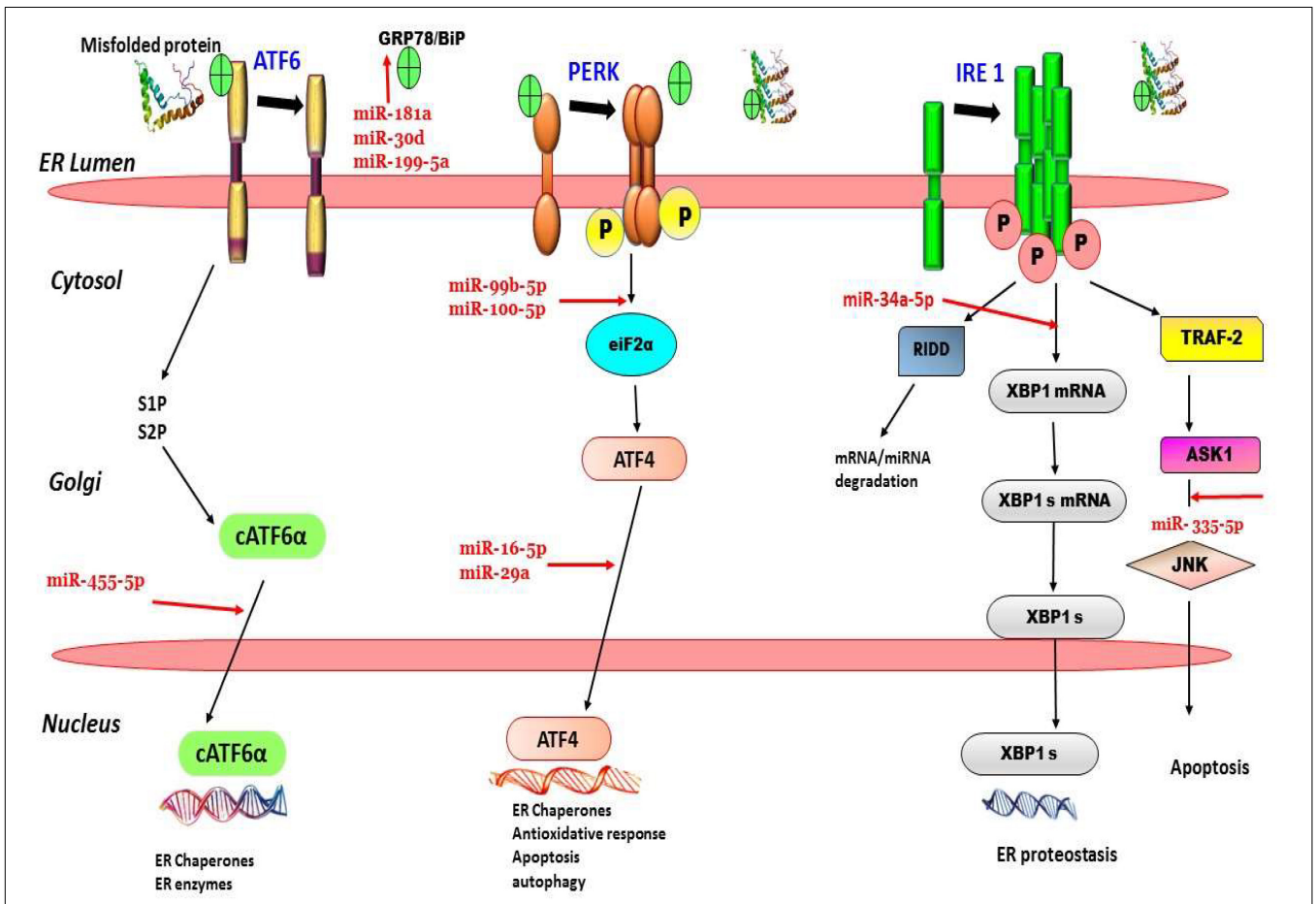

FIGURE 2 | ER stress, UPR, and microRNA relation in Alzheimer's disease. For instance, evidence suggests that, miR-199-5a, miR-30a and miR-181 suppress GRP78 expression. miR-34a-5p downregulates XBP-1 expression in. miR-335 is involved in activation of JNK pathway leading to apoptosis, etc., can be seen in the figure.

link exists between miR expression levels and Aβ-induced ER stress, they reported that upregulation of miR-200c induced by Aβ deposition is mediated *via* ER stress pathways, such as PERK and eIF2 α pathways, due to the activation of as XBP1, ATF4, and ATF6 transcriptional factors (Wu J. et al., 2016). The findings of a recent study reported significant alterations in the levels of two miR-99b-5p and miR100-5p *via* Aβ-induced ER-stress modulation along with alteration in the mTOR pathway. This proved the correlation between the ER stress–miRNAs–mTOR" axis in AD pathogenesis (Ye et al., 2015). **Figure 2** depicts ER stress and microRNA relation in AD. From the above studies, it is evident that a significant relationship exists between ER stress pathways—miRNAs axis but the exact mechanism still remains elusive and needs further elaborative research to gather substantial evidence.

Therapeutic Approaches Against Alzheimer's Disease Involving the ER^{UPR} Signaling Pathway and MicroRNA

Alzheimer's disease pathobiology is complex and still elusive. Although, NFT, Aβ, and tau proteins are regarded as the markers of this disease, treatment approaches are dormant. The first drug ever known to treat cognitive symptoms of AD is Tacrine, which is currently withdrawn due to toxicity issues. Later many drugs targeting cholinesterase, NMDA receptors were introduced which could only alleviate symptoms. The year 2021 saw a major breakthrough with the approval of drug, Aducanumab, an IgG1 monoclonal antibody targeted to treat the underlying cause of disease (Riscado et al., 2021). Another drug Verubecestat (MK-8931) targeting beta-secretase 1 (BACE1), was supposedly being investigated to treat AD; however, this was terminated due to no promising results (Kennedy et al., 2016). miRNAs are identified as efficient diagnostic biomarkers for AD, they target multiple genes and multiple pathologic pathways in one stance. Hence, miRNAs are regarded as potential therapeutic targets for several diseases, including AD. However, there are several limitations to develop miRNA-based therapeutic agents, like difficulty in identification of the functional target gene, factors influencing variations in miRNA expression, decay kinetics of miRNA in body fluids, passage across BBB, the delivery options of miRNA in their stable form, toxicity, and immune response (Madadi et al., 2019). Scientists around the world are working tremendously to overcome these hurdles. Currently, encouraging developments are seen targeting diseases, using miRNA mimics, miRNA sponges/decoys, antagomiRs, miRNA antisense nucleotides, antagoNAT and miRNA-based oligonucleotides (Bajan and Hutvagner, 2020). Also, delivery of these miRNA, which is a hurdle, is being worked on using novel targeted delivery approaches, such as conjugated nanoparticle, intra-nasal administration, intracerebroventricular infusion, lipid, and viral vectors (Fu et al., 2019). The first drug developed using miRNA targeting is Miravirsen, miRNA oligonucleotide to treat hepatitis C, which is currently in phase II clinical trials (Baek et al., 2014). Despite such incredible efforts by the scientific fraternity no approved disease-modifying miRNA-based AD therapies 0 exists, no drug have been FDA approved as yet. However, several miRNA-based drugs have managed to reach phase I and phase II clinical trials. These lacunae need to be addressed as early as possible so as to enable AD treatment with novel therapeutic approaches.

CONCLUSION AND FUTURE PERSPECTIVES

The endoplasmic reticulum has a very crucial role in several cellular processes with a focus on protein synthesis and transport, proteostasis, redox homeostasis, autophagy, and cellular apoptosis, supposedly disrupted in aberrant conditions ameliorating AD progression. Numerous studies have shown the role of regulatory non-coding proteins miRNA in several pathologies, such as AD. This article reviews the complex, interconnection between non-coding miRNA networks involved in the regulation of ER stress *via* UPR activation. Hundreds of miRNAs have been discovered and still there is scope for the discovery of miRNAs that are directly involved in altering and regulating ER-induced UPR stress pathways. miRNAs exhibit diversity in their actions, advancements in molecular and RNA sequencing technologies have provided significant insights into the dysregulation in miRNAs in AD and helped us unravel their role as potential diagnostic biomarkers and therapeutic agents. An elaborative analysis of individual miRNAs or clusters of miRNA families targeting ER^{UPR} or ER proteostasis along with miRNA quantification methods must be carried out to precisely know the miRNAs that can serve as excellent biomarkers and therapeutic targets to overcome the disease burden of AD.

AUTHOR CONTRIBUTIONS

NY, MD, VK, and FA conceptualized the idea of mini-review and were responsible for the entire manuscript in its final form. AA and SH checked the complete manuscript in terms of technical and scientific integrity. All authors contributed to manuscript writing, revision, read, and approved the submitted version.

FUNDING

The funding was provided by the Deanship of Scientific Research at Umm Al-Qura University for supporting this work by Grant Code: (22UQU4310453DSR01).

ACKNOWLEDGMENTS

We would like to thank Director, Amity Institute of Biotechnology, Amity University Rajasthan, Jaipur and the Deanship of Scientific Research at Umm Al-Qura University for providing the needful facilities to write this important manuscript. We also would like to thank the Deanship of Scientific Research at Umm Al-Qura University for supporting this work by Grant Code: (22UQU4310453DSR01).

REFERENCES

Abduljaleel, Z., Al-Allaf, F. A., Khan, W., Athar, M., Shahzad, N., Taher, M. M., et al. (2014). Evidence of trem2 variant associated with triple risk of Alzheimer's disease. *PLoS One* 9:e92648. doi: 10.1371/journal.pone.0092648

Absalon, S., Kochanek, D. M., Raghavan, V., and Krichevsky, A. M. (2013). MiR-26b, upregulated in Alzheimer's disease, activates cell cycle entry, tau-phosphorylation, and apoptosis in postmitotic neurons. *J. Neurosci.* 33, 14645–14659. doi: 10.1523/JNEUROSCI.1327-13.2013

Almalki, W. H., Alzahrani, A., Mahmoud El-Daly, M. E., and Fadel Ahmed, A. H. F. (2021). The emerging potential of SIRT-3 in oxidative stress-inflammatory axis associated increased neuroinflammatory component for metabolically impaired neural cell. *Chem. Biol. Interact.* 333:109328. doi: 10.1016/j.cbi.2020.109328

Almanza, A., Carlesso, A., Chintha, C., Creedican, S., Doultsinos, D., Leuzzi, B., et al. (2019). Endoplasmic reticulum stress signalling–from basic mechanisms to clinical applications. *FEBS J.* 286, 241–278. doi: 10.1111/febs.14608

Alshareef, M. H., Hartland, E. L., and McCaffrey, K. (2021). Effectors targeting the unfolded protein response during intracellular bacterial infection. *Microorganisms* 9:705. doi: 10.3390/microorganisms9040705

An, F., Gong, G., Wang, Y., Bian, M., Yu, L., and Wei, C. (2017). MiR-124 acts as a target for Alzheimer's disease by regulating BACE1. *Oncotarget* 8, 114065–114071. doi: 10.18632/oncotarget.23119

Baek, J., Kang, S., and Min, H. (2014). MicroRNA-targeting therapeutics for hepatitis C. *Arch. Pharm. Res.* 37, 299–305. doi: 10.1007/s12272-013-0318-9

Bajan, S., and Hutvagner, G. (2020). RNA-based therapeutics: from antisense oligonucleotides to miRNAs. *Cells* 9:137. doi: 10.3390/cells9010137

Bejanin, A., Schonhaut, D. R., La Joie, R., Kramer, J. H., Baker, S. L., Sosa, N., et al. (2017). Tau pathology and neurodegeneration contribute to cognitive impairment in Alzheimer's disease. *Brain* 140, 3286–3300. doi: 10.1093/brain/awx243

Chen, M. L., Hong, C. G., Yue, T., Li, H. M., Duan, R., Hu, W. B., et al. (2021). Inhibition of miR-331-3p and miR-9-5p ameliorates Alzheimer's disease by enhancing autophagy. *Theranostics* 11, 2395–2409. doi: 10.7150/thno.47408

Chen, Y., and Brandizzi, F. (2013). IRE1: ER stress sensor and cell fate executor. *Trends Cell Biol.* 23, 547–555. doi: 10.1016/j.tcb.2013.06.005

Chen, Y., Dang, M., and Zhang, Z. (2021). Brain mechanisms underlying neuropsychiatric symptoms in Alzheimer's disease: a systematic review of symptom-general and -specific lesion patterns. *Mol. Neurodegen.* 16:38. doi: 10.1186/s13024-021-00456-1

Delay, C., Mandemakers, W., and Hébert, S. S. (2012). MicroRNAs in Alzheimer's disease. *Neurobiol. Dis.* 46, 285–290. doi: 10.1016/j.nbd.2012.01.003

Du, W., Lei, C., and Dong, Y. (2021). MicroRNA-149 is downregulated in Alzheimer's disease and inhibits β-amyloid accumulation and ameliorates neuronal viability through targeting BACE1. *Genet. Mol. Biol.* 44:e20200064. doi: 10.1590/1678-4685-GMB-2020-0064

Dufey, E., Sepúlveda, D., Rojas-Rivera, D., and Hetz, C. (2014). Cellular mechanisms of endoplasmic reticulum stress signaling in health and disease. 1. An overview. *Am. J. Physiol. Cell Physiol.* 307, C582–C594. doi: 10.1152/ajpcell.00258.2014

Fu, X. L., and Gao, D. S. (2014). Endoplasmic reticulum proteins quality control and the unfolded protein response: the regulative mechanism of organisms against stress injuries. *Biofactors* 40, 569–585. doi: 10.1002/biof.1194

Fu, Y., Chen, J., and Huang, Z. (2019). Recent progress in microRNA-based delivery systems for the treatment of human disease. *ExRNA* 1, 1–14. doi: 10.1186/s41544-019-0024-y

Gardner, B. M., Pincus, D., Gotthardt, K., Gallagher, C. M., and Walter, P. (2013). Endoplasmic reticulum stress sensing in the unfolded protein response. *Cold Spring Harb. Perspect. Biol.* 5:a013169. doi: 10.1101/cshperspect

Gerakis, Y., and Hetz, C. (2018). Emerging roles of ER stress in the etiology and pathogenesis of Alzheimer's disease. *FEBS J.* 285, 995–1011. doi: 10.1111/febs.14332

Grasso, M., Piscopo, P., Confaloni, A., and Denti, M. A. (2014). Circulating miRNAs as biomarkers for neurodegenerative disorders. *Molecules (Basel, Switzerland)* 19, 6891–6910. doi: 10.3390/molecules19056891

Guo, J., Cai, Y., Ye, X., Ma, N., Wang, Y., Yu, B., et al. (2019). MiR-409-5p as a regulator of neurite growth is down regulated in APP/PS1 murine model of Alzheimer's disease. *Front. Neurosci.* 13:1264. doi: 10.3389/fnins.2019.01264

Hashimoto, S., and Saido, T. C. (2018). Critical review: involvement of endoplasmic reticulum stress in the aetiology of Alzheimer's disease. *Open Biol.* 8:180024. doi: 10.1098/rsob.180024

Hébert, S. S., Horré, K., Nicolaï, L., Papadopoulou, A. S., Mandemakers, W., Silahtaroglu, A. N., et al. (2008). Loss of microRNA cluster miR-29a/b-1 in sporadic Alzheimer's disease correlates with increased BACE1/beta-secretase expression. *Proc. Natl. Acad. Sci. U.S.A.* 105, 6415–6420. doi: 10.1073/pnas.0710263105

Higaki, S., Muramatsu, M., Matsuda, A., Matsumoto, K., Satoh, J. I., Michikawa, M., et al. (2018). Defensive effect of microRNA-200b/c against amyloid-beta peptide-induced toxicity in Alzheimer's disease models. *PLoS One* 13:e0196929. doi: 10.1371/journal.pone.0196929

Hoozemans, J. J., Van Haastert, E. S., Nijholt, D. A., Rozemuller, A. J., and Scheper, W. (2012). Activation of the unfolded protein response is an early event in Alzheimer's and Parkinson's disease. *Neurodegener. Dis.* 10, 212–215. doi: 10.1159/000334536

Hu, G., Shi, Z., Shao, W., and Xu, B. (2021). MicroRNA-214-5p involves in the protection effect of Dexmedetomidine against neurological injury in Alzheimer's disease via targeting the suppressor of zest 12. *Brain Res. Bull.* 178, 164–172. doi: 10.1016/j.brainresbull.2021.10.016

Ibe, N. U., Subramanian, A., and Mukherjee, S. (2021). Non-canonical activation of the ER stress sensor ATF6 by *Legionella pneumophila* effectors. *Life Sci. Alliance* 4:e202101247. doi: 10.26508/lsa.202101247

Ji, Q., Wang, X., Cai, J., Du, X., Sun, H., and Zhang, N. (2019). MiR-22-3p regulates amyloid β deposit in mice model of Alzheimer's disease by targeting mitogen-activated protein kinase 14. *Curr. Neurovasc. Res.* 16, 473–480. doi: 10.2174/1567202616666191111124516

Ji, Y., Wang, D., Zhang, B., and Lu, H. (2019). MiR-361-3p inhibits β-amyloid accumulation and attenuates cognitive deficits through targeting BACE1 in Alzheimer's disease. *J. Integr. Neurosci.* 18, 285–291. doi: 10.31083/j.jin.2019.03.1136

Junjappa, R. P., Patil, P., Bhattarai, K. R., Kim, H. R., and Chae, H. J. (2018). IRE1α implications in endoplasmic reticulum stress-mediated development and pathogenesis of autoimmune diseases. *Front. Immunol.* 9:1289. doi: 10.3389/fimmu.2018.01289

Katayama, T., Imaizumi, K., Manabe, T., Hitomi, J., Kudo, T., and Tohyama, M. (2004). Induction of neuronal death by ER stress in Alzheimer's disease. *J. Chem. Neuroanat.* 28, 67–78. doi: 10.1016/j.jchemneu.2003.12.004

Kennedy, M. E., Stamford, A. W., Chen, X., Cox, K., Cumming, J. N., Dockendorf, M. F., et al. (2016). The BACE1 inhibitor verubecestat (MK-8931) reduces CNS β-amyloid in animal models and in Alzheimer's disease patients. *Sci. Transl. Med.* 8:363ra150. doi: 10.1126/scitranslmed.aad9704

Kim, E., and Jung, H. (2015). Local protein synthesis in neuronal axons: why and how we study. *BMB Rep.* 48:139. doi: 10.5483/BMBRep.2015.48.3.010

Kim, Y. J., Kim, S. H., Park, Y., Park, J., Lee, J. H., Kim, B. C., et al. (2020). miR-16-5p is upregulated by amyloid β deposition in Alzheimer's disease models and induces neuronal cell apoptosis through direct targeting and suppression of BCL-2. *Exp. Gerontol.* 136:110954. doi: 10.1016/j.exger.2020.110954

Koh, H. S., Lee, S., Lee, H. J., Min, J. W., Iwatsubo, T., Teunissen, C. E., et al. (2021). Targeting MicroRNA-485-3p blocks Alzheimer's disease progression. *Int. J. Mol. Sci.* 22:13136. doi: 10.3390/ijms222313136

Krammes, L., Hart, M., Rheinheimer, S., Diener, C., Menegatti, J., Grässer, F., et al. (2020). Induction of the Endoplasmic-reticulum-stress response: MicroRNA-34a targeting of the IRE1α-branch. *Cells* 9:1442. doi: 10.3390/cells9061442

Labban, S., Alshehri, F. S., Kurdi, M., Alatawi, Y., and Alghamdi, B. S. (2021). Melatonin improves short-term spatial memory in a mouse model of Alzheimer's disease. *Degener. Neurol. Neuromuscul. Dis.* 11, 15–27. doi: 10.2147/DNND.S291172

Li, Q., Liu, T., Yang, S., and Zhang, Z. (2019). Upregulation of miR-34a by Inhibition of IRE1α has protective effect against Aβ-induced injury in SH-SY5Y cells by targeting caspase-2. *Oxid. Med. Cell. Longev.* 2019:2140427.

Lindholm, D., Korhonen, L., Eriksson, O., and Kõks, S. (2017). Recent insights into the role of unfolded protein response in ER stress in health and disease. *Front. Cell Dev. Biol.* 5:48. doi: 10.3389/fcell.2017.00048

Liu, C. G., Wang, J. L., Li, L. E. I., and Wang, P. C. (2014). MicroRNA-384 regulates both amyloid precursor protein and β-secretase expression and is a potential biomarker for Alzheimer's disease. *Int. J. Mol. Med.* 34, 160–166.

Liu, W., Zhao, J., and Lu, G. (2016). miR-106b inhibits tau phosphorylation at Tyr18 by targeting Fyn in a model of Alzheimer's disease. *Biochem. Biophys. Res. Commun.* 478, 852–857.

Long, J. M., Ray, B., and Lahiri, D. K. (2014). MicroRNA-339-5p down-regulates protein expression of β-site amyloid precursor protein-cleaving enzyme 1 (BACE1) in human primary brain cultures and is reduced in brain tissue specimens of Alzheimer disease subjects. *J. Biol. Chem.* 289, 5184–5198. doi: 10.1074/jbc.M113.518241

Madadi, S., Schwarzenbach, H., Saidijam, M., Mahjub, R., and Soleimani, M. (2019). Potential microRNA-related targets in clearance pathways of amyloid-β: novel therapeutic approach for the treatment of Alzheimer's disease. *Cell Biosci.* 9:91. doi: 10.1186/s13578-019-0354-3

Oku, Y., Kariya, M., Fujimura, T., Hoseki, J., and Sakai, Y. (2021). Homeostasis of the ER redox state subsequent to proteasome inhibition. *Sci. Rep.* 11, 1–9. doi: 10.1038/s41598-021-87944-y

Pakos-Zebrucka, K., Koryga, I., Mnich, K., Ljujic, M., Samali, A., and Gorman, A. M. (2016). The integrated stress response. *EMBO Rep.* 17, 1374–1395. doi: 10.15252/embr.201642195

Plácido, A. I., Pereira, C. M. F., Duarte, A. I., Candeias, E., Correia, S. C., Santos, R. X., et al. (2014). The role of endoplasmic reticulum in amyloid precursor protein processing and trafficking: implications for Alzheimer's disease. *Biochim. Biophys. Acta* 1842, 1444–1453. doi: 10.1016/j.bbadis.2014.05.003

Rahman, S., Archana, A., Jan, A. T., and Minakshi, R. (2018). Dissecting endoplasmic reticulum unfolded protein response (UPRER) in managing clandestine modus operandi of Alzheimer's disease. *Front. Aging Neurosci.* 10:30. doi: 10.3389/fnagi.2018.00030

Rahman, S., Jan, A. T., Ayyagari, A., Kim, J., Kim, J., and Minakshi, R. (2017). Entanglement of UPRER in aging driven neurodegenerative diseases. *Front. Aging Neurosci.* 9:341. doi: 10.3389/fnagi.2017.00341

Rahman, S., Kumar, V., Kumar, A., Abdullah, T. S., Rather, I. A., and Jan, A. T. (2021). Molecular perspective of nanoparticle mediated therapeutic targeting in breast cancer: an odyssey of endoplasmic reticulum unfolded protein response (UPRER) and beyond. *Biomedicines* 9:635. doi: 10.3390/biomedicines9060635

Rajgor, D., Welle, T. M., and Smith, K. R. (2021). The coordination of local translation, membranous organelle trafficking, and synaptic plasticity in neurons. *Front. Cell Dev. Biol.* 9:711446. doi: 10.3389/fcell.2021.711446

Remondelli, P., and Renna, M. (2017). The endoplasmic reticulum unfolded protein response in neurodegenerative disorders and its potential therapeutic significance. *Front. Mol. Neurosci.* 10:187. doi: 10.3389/fnmol.2017.00187

Riscado, M., Baptista, B., and Sousa, F. (2021). New RNA-based breakthroughs in Alzheimer's disease diagnosis and therapeutics. *Pharmaceutics* 13:1397. doi: 10.3390/pharmaceutics13091397

Rodriguez-Ortiz, C. J., Prieto, G. A., Martini, A. C., Forner, S., Trujillo-Estrada, L., LaFerla, F. M., et al. (2020). miR-181a negatively modulates synaptic plasticity in hippocampal cultures and its inhibition rescues memory deficits in a mouse model of Alzheimer's disease. *Aging Cell* 19:e13118. doi: 10.1111/acel.13118

Scheper, W., and Hoozemans, J. J. (2015). The unfolded protein response in neurodegenerative diseases: a neuropathological perspective. *Acta Neuropathol.* 130, 315–331. doi: 10.1007/s00401-015-1462-8

Shi, Z., Zhang, K., Zhou, H., Jiang, L., Xie, B., Wang, R., et al. (2020). Increased miR-34c mediates synaptic deficits by targeting synaptotagmin 1 through ROS-JNK-p53 pathway in Alzheimer's disease. *Aging Cell* 19:e13125. doi: 10.1111/acel.13125

Siwecka, N., Rozpędek-Kamińska, W., Wawrzynkiewicz, A., Pytel, D., Diehl, J. A., and Majsterek, I. (2021). The structure, activation and signaling of IRE1 and its role in determining cell fate. *Biomedicines* 9:156. doi: 10.3390/biomedicines9020156

Smalheiser, N. R., and Lugli, G. (2009). microRNA regulation of synaptic plasticity. *Neuromol. Med.* 11, 133–140. doi: 10.1007/s12017-009-8065-2

Spires-Jones, T. L., Attems, J., and Thal, D. R. (2017). Interactions of pathological proteins in neurodegenerative diseases. *Acta Neuropathol.* 134, 187–205. doi: 10.1007/s00401-017-1709-7

Stauffer, W. T., Arrieta, A., Blackwood, E. A., and Glembotski, C. C. (2020). Sledgehammer to scalpel: broad challenges to the heart and other tissues yield specific cellular responses via transcriptional regulation of the ER-stress master regulator ATF6α. *Int. J. Mol. Sci.* 21:1134. doi: 10.3390/ijms21031134

Sultan, S., Taimuri, U., Basnan, S. A., Ai-Orabi, W. K., Awadallah, A., Almowald, F., et al. (2020). Low vitamin D and its association with cognitive impairment and dementia. *J. Aging Res.* 2020:6097820. doi: 10.1155/2020/6097820

Tanprasertsuk, J., Johnson, E. J., Johnson, M. A., Poon, L. W., Nelson, P. T., Davey, A., et al. (2019). Clinico-neuropathological findings in the oldest old from the georgia centenarian study. *J. Alzheimers Dis.* 70, 35–49. doi: 10.3233/JAD-181110

Wang, D., Fei, Z., Luo, S., and Wang, H. (2020). MiR-335-5p inhibits β-amyloid (Aβ) accumulation to attenuate cognitive deficits through targeting c-jun-N-terminal kinase 3 in Alzheimer's disease. *Curr. Neurovasc. Res.* 17, 93–101. doi: 10.2174/1567202617666200128141938

Wang, L., Liu, J., Wang, Q., Jiang, H., Zeng, L., Li, Z., et al. (2019). MicroRNA-200a-3p mediates neuroprotection in alzheimer-related deficits and attenuates amyloid-beta overproduction and tau hyperphosphorylation via coregulating BACE1 and PRKACB. *Front. Pharmacol.* 10:806. doi: 10.3389/fphar.2019.00806

Wang, M., Qin, L., and Tang, B. (2019). MicroRNAs in Alzheimer's disease. *Front. Genet.* 10:153. doi: 10.3389/fgene.2019.00153

Wang, P., Li, J., Tao, J., and Sha, B. (2018). The luminal domain of the ER stress sensor protein PERK binds misfolded proteins and thereby triggers PERK oligomerization. *J. Biol. Chem.* 293, 4110–4121. doi: 10.1074/jbc.RA117.001294

Wu, J., He, G. T., Zhang, W. J., Xu, J., and Huang, Q. B. (2016). IRE1α signaling pathways involved in mammalian cell fate determination. *Cell Physiol. Biochem.* 2016, 847–858. doi: 10.1159/000443039

Wu, Q., Ye, X., Xiong, Y., Zhu, H., Miao, J., Zhang, W., et al. (2016). The protective role of microRNA-200c in Alzheimer's disease pathologies is induced by beta amyloid-triggered endoplasmic reticulum stress. *Front. Mol. Neurosci.* 9:140. doi: 10.3389/fnmol.2016.00140

Xiao, G., Chen, Q., and Zhang, X. (2021). MicroRNA-455-5p/CPEB1 pathway mediates Aβ-related learning and memory deficits in a mouse model of Alzheimer's disease. *Brain Res. Bull.* 177, 282–294. doi: 10.1016/j.brainresbull.2021.10.008

Yasmeen, N., Kumar, V., and Shaikh, K. D. (2021). "Impact of MicroRNA polymorphisms on breast cancer susceptibility," in *Genetic Polymorphism and Cancer Susceptibility*, eds A. S. Sameer, M. Z. Banday, and S. Nissar (Singapore: Springer), 53–77. doi: 10.1007/978-981-33-6699-2_3

Ye, X., Luo, H., Chen, Y., Wu, Q., Xiong, Y., Zhu, J., et al. (2015). MicroRNAs 99b-5p/100-5p regulated by endoplasmic reticulum stress are involved in abeta-induced pathologies. *Front. Aging Neurosci.* 7:210. doi: 10.3389/fnagi.2015.00210

Zheng, K., Hu, F., Zhou, Y., Zhang, J., Zheng, J., Lai, C., et al. (2021). miR-135a-5p mediates memory and synaptic impairments via the Rock2/Adducin1 signaling pathway in a mouse model of Alzheimer's disease. *Nat. Commun.* 12:1903. doi: 10.1038/s41467-021-22196-y

Conflict of Interest: The authors declare that the research was conducted in the absence of any commercial or financial relationships that could be construed as a potential conflict of interest.

Publisher's Note: All claims expressed in this article are solely those of the authors and do not necessarily represent those of their affiliated organizations, or those of the publisher, the editors and the reviewers. Any product that may be evaluated in this article, or claim that may be made by its manufacturer, is not guaranteed or endorsed by the publisher.

frontiers | Frontiers in Aging Neuroscience

REVIEW
published: 15 June 2022
doi: 10.3389/fnagi.2022.892518

Towards Understanding the Relationship Between ER Stress and Unfolded Protein Response in Amyotrophic Lateral Sclerosis

Chenxuan Zhao[1], *Yong Liao*[2]*, *Abdul Rahaman*[3] *and Vijay Kumar*[4]*†

[1]School of Engineering, College of Technology and Business, Guangzhou, China, [2]Center of Scientific Research, Maoming People's Hospital, Maoming, China, [3]School of Food Science and Engineering, South China University of Technology, Guangzhou, China, [4]Amity Institute of Neuropsychology & Neurosciences (AINN), Amity University, Noida, India

OPEN ACCESS

Edited by:
Khurshid Ahmad,
Yeungnam University, South Korea

Reviewed by:
Timir Tripathi,
North Eastern Hill University, India
Shafiul Haque,
Jamia Millia Islamia, India

***Correspondence:**
Yong Liao
liaoyong0668@163.com
Vijay Kumar
vkumar33@amity.edu

†ORCID:
Vijay Kumar
orcid.org/0000-0002-3621-5025

Specialty section:
This article was submitted to Alzheimer's Disease and Related Dementias, a section of the journal Frontiers in Aging Neuroscience

Received: 09 March 2022
Accepted: 18 May 2022
Published: 15 June 2022

Citation:
Zhao C, Liao Y, Rahaman A and Kumar V (2022) Towards Understanding the Relationship Between ER Stress and Unfolded Protein Response in Amyotrophic Lateral Sclerosis. Front. Aging Neurosci. 14:892518. doi: 10.3389/fnagi.2022.892518

Biological stress due to the aberrant buildup of misfolded/unfolded proteins in the endoplasmic reticulum (ER) is considered a key reason behind many human neurodegenerative diseases. Cells adapted to ER stress through the activation of an integrated signal transduction pathway known as the unfolded protein response (UPR). Amyotrophic lateral sclerosis (ALS) is a neurodegenerative disease characterized by degeneration of the motor system. It has largely been known that ER stress plays an important role in the pathogenesis of ALS through the dysregulation of proteostasis. Moreover, accumulating evidence indicates that ER stress and UPR are important players in TDP-43 pathology. In this mini-review, the complex interplay between ER stress and the UPR in ALS and TDP-43 pathology will be explored by taking into account the studies from *in vitro* and *in vivo* models of ALS. We also discuss therapeutic strategies to control levels of ER stress and UPR signaling components that have contrasting effects on ALS pathogenesis.

Keywords: ER stress, UPR, ALS, TDP-43, pharmacological modulator

INTRODUCTION

Amyotrophic lateral sclerosis (ALS), the most common type of motor neuron disease, is characterized by the progressive degeneration of both lower and upper motor neurons and eventually leads to death due to respiratory failure, typically within 2–5 years of symptom onset (van Es et al., 2017). While the majority of cases are sporadic (sALS), approximately 10% of ALS is inherited, usually in an autosomal dominant fashion (fALS). The proposed pathomechanisms of ALS include oxidative stress, dysfunction in mitochondria and axonal transport, excitotoxicity, damage to protein homeostasis, etc. (Ferraiuolo et al., 2011; Kumar et al., 2016a; Tsai and Manley, 2021). Studies of fALS cases have revealed several ALS-associated genes (Cooper-Knock et al., 2021; Shatunov and Al-Chalabi, 2021) which are involved in several important cellular and biological processes. Many of the fALS- genes have also been involved in different facets of the proteostasis network. Abnormal accumulation of misfolded or aggregated proteins to proteinaceous inclusions represents a common unifying pathological feature of ALS (Lin et al., 2017; Webster et al., 2017; Cicardi et al., 2021). These intracellular inclusions are found in both degenerating neurons and surrounding glia (Nishihira et al., 2009; Dugger and Dickson, 2017) as well as present in the different regions of the brain including the spinal cord, cerebellum, brainstem, hippocampus, and the frontal

and temporal lobes (Al-Chalabi et al., 2012). The most predominant inclusions observed in the motor neurons are of ubiquitinated proteins (Neumann et al., 2006), thus indicating the defects in protein homeostasis (Blokhuis et al., 2013). Ubiquitinated protein inclusions of Tar DNA-binding protein of 43 kDa (TDP-43) are positive for the majority of ALS cases (Arai et al., 2006; Neumann et al., 2006). TDP-43 was also identified as the pathological protein in a subset of neurodegenerative diseases commonly known as TDP-43 proteinopathies (Tziortzouda et al., 2021). In these diseases, the loss of nuclear TDP-43 and cytoplasmic inclusions of TDP-43 result in either loss or gain-of-function within neurons and affect several biological processes like autophagy, RNA synthesis, the ubiquitin-proteasome system, and axonal transport (Prasad et al., 2019). Several studies also indicate that endoplasmic reticulum (ER) stress plays a critical role in TDP-43 proteinopathies (Walker and Atkin, 2011; Walter and Ron, 2011; Walker et al., 2013; de Mena et al., 2021). Besides the presence of TDP-43 inclusions, inclusions for mutant Cu/Zn superoxide dismutase (SOD1) and fused in sarcoma protein (FUS) are also found in ALS patients (Mackenzie et al., 2007; Kwiatkowski et al., 2009; Vance et al., 2009). The other fALS-associated mutant proteins that aggregates are valosin-containing protein (VCP), dynactin-1 (DCTN1), optineurin (OPTN), and ubiquilin-2 (UBQLN2; Levy et al., 2006; Maruyama et al., 2010; Deng et al., 2011; Koppers et al., 2012). The characteristic observation of the protein aggregates is indicative of the breakdown of proteostasis in ALS. Consequently, a key proteostatic pathway identified as the Unfolded Protein Response (UPR) responds to the endoplasmic reticulum (ER) stress-induced protein aggregation by initiating either proadaptive and/or proapoptotic pathways. In this mini-review, we aim to provide insights into the complex interplay between ER stress, UPR, and TDP-43 in the context of ALS.

ER STRESS AND UPR PATHWAY

The ER is a membranous organelle involved in protein folding, post-translational modifications, and trafficking, and synthesizes about one-third of the total proteome (Schroder, 2008; Bernard-Marissal et al., 2015). Despite the quality control accomplished by ER chaperones to ensure proper folding and maturation of newly synthesized proteins, protein maturation mechanisms are sometimes perturbed which leads to the correct folding success in the cell to be under 20% (Kaushik and Cuervo, 2015). These misfolded/unfolded proteins are retained in the ER and are susceptible to undergoing proteasomal degradation through the ER-associated degradation (ERAD) pathway that recognizes, ubiquitinates, and relocates misfolded proteins to the cytosol for their degradation (Oakes and Papa, 2015). However, disruption of ER-calcium homeostasis, abnormal proteostasis, hypoxia, etc., decrease the protein-folding ability leading to ER stress (Lin et al., 2008). Upon detection of ER stress, the ER initiates UPR that decreases the burden of misfolded proteins and re-establishes proteostasis. This cellular response is achieved through coordinated transcriptional and translational activities, the increased expression of chaperones in the ERAD pathway, and a brief decrease in the protein flux entering the ER. The UPR has three proximal transmembrane protein sensors: Inositol-requiring kinase/endoribonuclease (IRE1), double-stranded RNA-activated protein kinase (PKR)-like ER kinase (PERK), and activating transcription factor 6 (ATF6) (Schroder, 2008; Hetz, 2012). Both IRE-1 and PERK are type I transmembrane proteins having kinase activity (Liu et al., 2002). On the other hand, ATF6 is a type II transmembrane protein, and its cytosolic domain can enter the nucleus and thus can activate UPR related genes (Haze et al., 1999). The UPR attempts to restore proteostasis by decreasing translation, increasing chaperones assisted protein folding, and up-regulation of ERAD and autophagy to get rid of misfolded proteins. If ER stress is brief, the UPR pathways work in parallel to organize a series of pro-adaptive cascades to restore proteostasis and the cell survives. However, in case of severe prolonged ER stress, the UPR activates the pro-apoptotic pathway (**Figure 1**; Hetz and Saxena, 2017; Hetz and Papa, 2018).

An immediate adaptive reaction to ER stress is started by translocation of ATF6 to the nucleus, where it modulates the genes involved in protein homeostasis (Haze et al., 1999). IRE1 by mediating the splicing of a transcription factor, X-Box-Binding protein 1 (XBP1), activates several genes of the protein homeostasis pathway along with the release of ERAD proteins (Acosta-Alvear et al., 2007). Whereas, PERK phosphorylates the eukaryotic initiation factor 2α (eIF2α), and thus decreases protein translation by overpowering a load of misfolded proteins (Harding et al., 1999). Also, eIF2α activates ATF4 which subsequently activates many UPR-targeted genes (Tabas and Ron, 2011). Ultimately, the UPR reduced the translation and increased the expression of genes of protein homeostasis including chaperones and ERAD proteins. Also, disruption of ER homeostasis leads to the activation of apoptotic pathways (Malhotra and Kaufman, 2007; Krebs et al., 2015).

ER STRESS AND UPR IN ALS

Long-term ER stress is a critical factor affecting cell survival in neurodegenerative diseases characterized by severe proteostatic imbalances (Scheper and Hoozemans, 2015). Many studies have reported the presence of ER stress in ALS and FTD patient's tissue samples, as well as cellular and animal models of fALS genes like SOD1, VAPB, or FUS (Kikuchi et al., 2006; Gitcho et al., 2009; Chen et al., 2010; Farg et al., 2012). The involvement of the UPR pathway in ALS has been shown in ALS patients' post-mortem spinal cord as well as in ALS mice (Ilieva et al., 2007; Atkin et al., 2008; Sasaki, 2010). Morphological alterations such as dilation and fragmentation of rough ER have been observed in sALS patients and the mutant $SOD1^{G93A}$ mice (Oyanagi et al., 2008; Lautenschlaeger et al., 2012). Sasaki (2010) has observed the accumulation of misfolded proteins as a granular or amorphous material in the ER of sALS patients.

Misfolding and aberrant deposition of SOD1 are thought to be responsible for ER stress in ALS cases since mutant SOD1 is prone to misfold, co-localize with ER resident markers like glucose-related protein 78 (Grp78) and calnexin (Wate et al., 2005; Kikuchi et al., 2006). Further evidence for a close association between UPR and misfolded SOD1 deposition

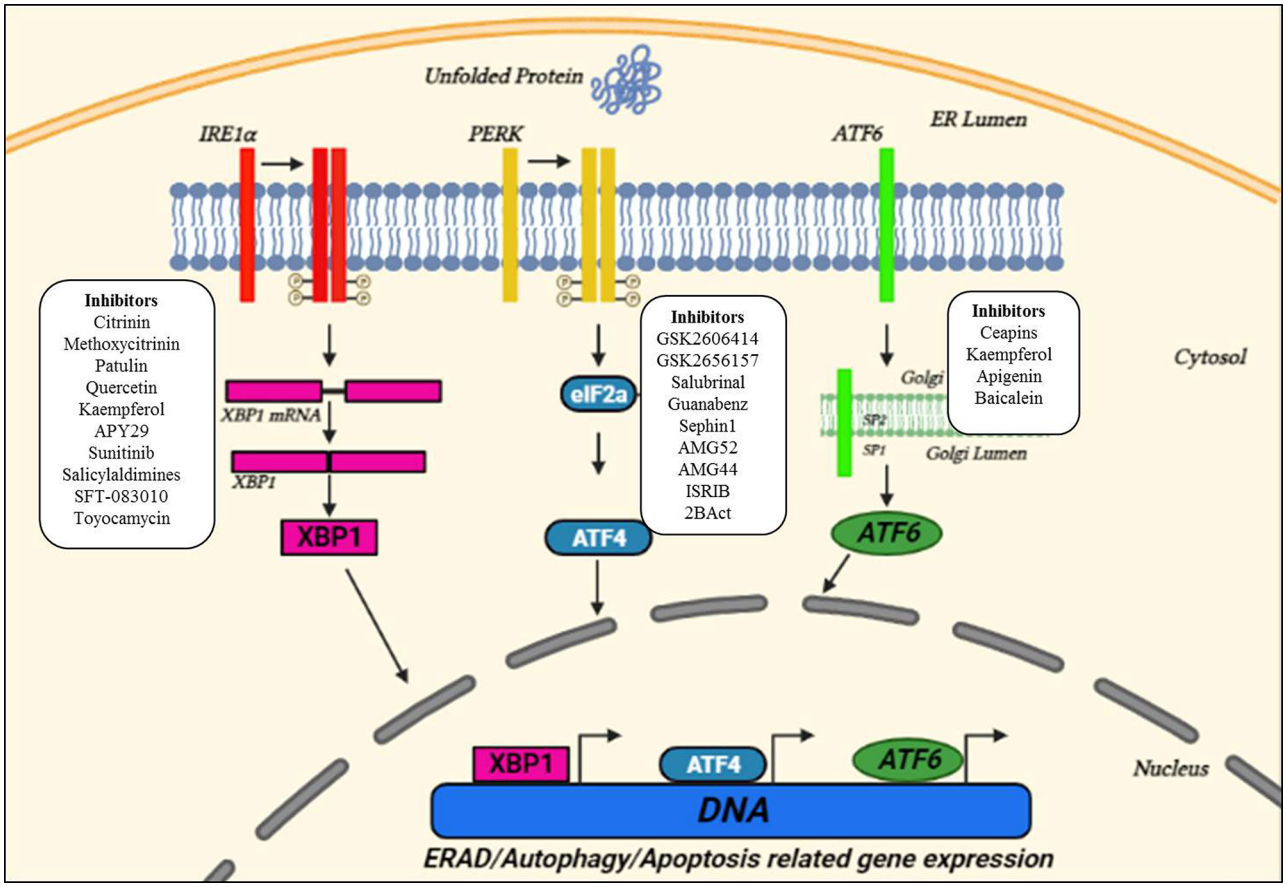

FIGURE 1 | Unfolded protein response (UPR) pathways in the ER and small molecule interventions. Upon ER stress, the ER launches three adaptive pathways through IRE1α, PERK, and activating transcription factor 6 (ATF6), collectively called as the UPR, to restore proteostasis. All these three ER stress sensors activate signaling cascades, increasing protein-folding ability and decreasing ER stress. Small molecules targeting three key UPR signaling components are also indicated in the figure suggesting the sites for therapeutic interventions. Adapted and modified from Webster et al. (2017).

was provided by the findings that showed the upregulation and subsequent co-localization of an ER chaperone, protein disulphideisomerase (PDI) in ALS patients, and SOD1^{G93A} mice (Atkin et al., 2006). Also, increased amounts of phosphorylated PERK (Atkin et al., 2006, 2008; Saxena et al., 2009), and phosphorylated eIF2α (Saxena et al., 2009) have been reported inSOD1^{G93A} mice as well as in Neuro2a cells transfected with mutant SOD1.

Interestingly, ER stress and subsequent activation of the UPR components have been observed in the primary motor neurons exposed to the CSF of sALS patients (Vijayalakshmi et al., 2009, 2011). The CSF-induced ER stress and neurodegeneration appear to involve caspase-12 activation by the UPR pathway (Nakagawa et al., 2000; Martinez et al., 2010). Increased levels of ATF6 have been reported in ALS patients and SOD1^{G93A} mice (Atkin et al., 2006, 2008). Oh et al. (2008) have shown the cleavage and movement of ATF6 in Neuro2a cells transfected with mutant SOD1^{G85R}. While, Hetz et al. (2008) showed that ATF6 knockdown in NSC-34 cells transfected with mutant SOD1 increases SOD1 aggregation. Also, ALS patients and ALS mice showed increased IRE1 expression before the onset of disease (Atkin et al., 2006, 2008).

Several studies showed the involvement of C9orf72 pathogenesis in the ER stress in cell culture, primary cortical neurons, and iPSC-derived human neurons (Zhang et al., 2014; Zhang Y. J. et al., 2018; Kramer et al., 2018; Wang et al., 2019). Also, ER stress inducer tunicamycin showed a dose-dependent increase in cell death in C9-ALS iPSC-derived motoneurons, indicating altered ER proteostasis (Haeusler et al., 2014). C9orf72-ALS transcriptome studies from the human cerebellum and frontal cortex showed the upregulation of UPR genes, indicating the activation of ER stress (Prudencio et al., 2015). Dafinca et al. (2016) showed improved ER stress along with altered mitochondrial morphology and membrane potential in an iPSC-derived motor neurons from C9-ALS patients. Furthermore, an RNA sequencing study of mouse neurons having poly (PR) dipeptide repeats showed the upregulation of genes involved in ER stress, indicating that poly (PR) activates the UPR pathway (Kramer et al., 2018).

In another study by Wang et al. (2019), synthetic poly (PR) induced ER stress and inhibited the UPR mediated cell survival.

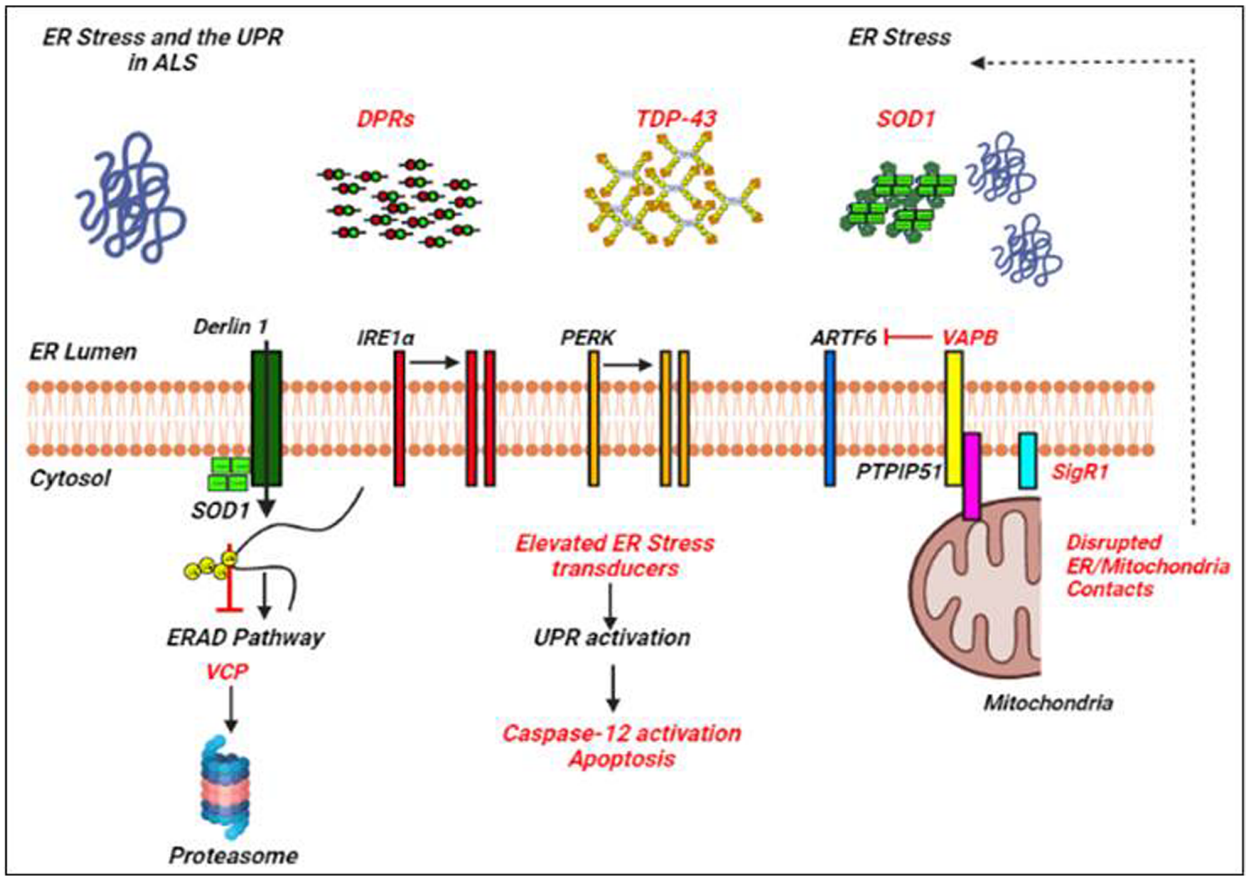

FIGURE 2 | ER stress and the UPR in amyotrophic lateral sclerosis (ALS). Examples of ALS-linked genes involved in ER stress and the UPR are shown in red text. ALS-associated defects to the UPR are also mentioned in red text. Adapted from Webster et al. (2017).

Moreover, ER stress also increased the RAN translation of the G4C2 expansion, and overexpression of the G4C2 repeats decreased the global translation while increasing the stress granules formation in an eIF2α-dependent manner (Green et al., 2017). Westergard et al. (2019) have also reported the increased RAN translation and ER stress due to excitotoxic stress and optogenetic neuronal stimulation of cortical and spinal motor neurons from a C9orf72 model with $(G4C2)_{188}$ repeat expansion.

A recent post-mortem study in C9-FTD patients showed increased levels of phosphorylated PERK and eIF2α in the hippocampus of C9-FTD patients and the increased levels were significantly correlated with the presence of poly (PR) pathology (Gami-Patel et al., 2021).

Therefore, integrated stress response (ISR) activation initiated by cellular stresses triggers RAN translation in cells and neurons and indicates a feed-forward loop between poly (PR) formation and the associated stress (Green et al., 2017; Cheng et al., 2018; Sonobe et al., 2018; Westergard et al., 2019). In this context, Sidrauski et al. (2013) reported that a small molecule inhibitor of ISR, ISRIB reduced poly (PR) induced toxicity. Moreover, Glineburg et al. (2021) have shown that activation of ISR by sodium arsenite-induced G4C2 repeat foci in C9orf72 patient fibroblasts. Administration of ISRIB or GSK2606414, PERK inhibitor showed strong neuroprotection in a fly model of C9orf72 pathogenesis (Zhang K. et al., 2018). Similar results were also shown in iPSC-derived motoneurons from C9-ALS cases (Zhang K. et al., 2018).

Importantly, inhibition of PKR largely reduced poly (PR) accumulation and improved behavior in C9-ALS/FTD transgenic mice (Zu et al., 2020). Overall, accumulating evidences indicate that inhibition of eIF2α phosphorylation or its downstream effects has neuroprotective consequences in the context of C9-ALS/FTD pathogenesis.

Similarly, the ER stress increased in NSC-34 cells with mutant FUS and in primary neurons expressing C9orf72-linked poly (GA) dipeptide repeats (Farg et al., 2012; Zhang et al., 2014).

Many of the ALS proteins significantly affect the UPR and/or proteostasis pathways as shown by different studies (Lin et al., 2017; Webster et al., 2017; Dafinca et al., 2021; **Figure 2**). ALS mutant SOD1 interacts with Derlin-1, an ER protein crucial for the ERAD pathway, and thus alters the ERAD which induces ER stress (Nishitoh et al., 2008). Vesicle-associated membrane protein-associated protein B (VAPB) is an important

ER protein which is involved in the UPR activation through the IRE1 and ATF6 pathways, and mutations in VAPB cause ALS8 (Gkogkas et al., 2008; Suzuki et al., 2009). Overexpressed WT and mutant VAPB^{P56S} interact strongly with ATF6 and decrease the transcription of XBP1, thus inducing ER stress (Suzuki et al., 2009). Indeed, knockdown of VAPB has been shown to inhibit the IRE1/XBP1 pathway, VAPB is thus involved in the activation of UPR in response to ER stress (Kanekura et al., 2006). Interestingly, Simmen et al. (2005) have shown that loss of ER/mitochondria contacts induces ER stress and the UPR, probably by disturbing some of the ER chaperones together with calnexin, calreticulin, and Sigma non-opioid intracellular receptor 1 (Sig1R; Hayashi and Su, 2007).

TDP-43 AND ER STRESS AND UPR

Aberrant misfolding and aggregation of TDP-43 along with TDP-43 posttranslational modifications play a crucial role in the development of neurodegenerative diseases including ALS and FTD (Arai et al., 2006; Neumann et al., 2006; Igaz et al., 2008; Kumar et al., 2016b, 2019). Also, pathological aggregation of TDP-43 causes increased ER stress following the activation of apoptosis (Suzuki et al., 2011; Dafinca et al., 2021). Nuclear depletion of TDP-43 correlates with increased mislocalization of TDP-43 to the rough ER and cytoplasmic inclusion formation, indicating a dynamic relationship between the TDP-43, ER, and pathological inclusion leading to neurodegeneration (Sasaki, 2010; Vaccaro et al., 2013; Wang et al., 2015a). Later, Suzuki and Matsuoka (2012) reported that the increased endogenous levels of TDP-43 result with the increase in the expression of C/EBP-homologous protein(CHOP), largely involved in ER-facilitated apoptosis and is regulated *via* the PERK/eIF2a/ATF4 pathway. Walker et al. (2013) showed that both WT and mutant TDP-43$^{Q331K/A315T}$ significantly activate the UPR pathways through increasing the expression of the key ER stress markers, XBP1 and ATF6 in Neuro2a cells. Moreover, overexpression of TDP-43 C-terminal fragments, TDP-35, and TDP-25 increased the levels of phosphorylated-eIF2α, CHOP, and truncated caspase-12 (Wang et al., 2015b). These findings were further established by Wang et al. (2015a), who showed that overexpression of WT and TDP-43^{A315T} in neural SH-SY5Y cells up-regulates the expression of the GRP-78, phosphorylated-eIF2α, CHOP, caspase-3, caspase-9, and caspase-12 fragments, as well as downregulates the Bcl-2 family proteins. Similarly, Hu et al. (2019) showed that overexpression of mutant TDP-43^{Q331K} in SH-SY5Ycellsleads to increased levels of GRP-78, ATF4, CHOP, PDI, and caspase 12. Also, TDP-43^{Q331K}mutant enhanced Beclin1 and p62 expression, and decreased the LC3-II/LC3-I ratio, an indicative of impaired autophagy normally observed in several neurodegenerative diseases.

PHARMACOLOGICAL TARGETING OF ER STRESS AND UPR

The fact that ER stress is involved in ALS pathogenesis and the UPR pathway which mitigates ER stress under physiological conditions represents a key therapeutic target for interventions. The activation of the UPR signaling pathway can lead to the activation of both pro-survival and pro-apoptotic activities. Thus, modulating the UPR pathways will either stimulate alleviation of protein misfolding, or stimulate apoptosis, which would have therapeutic effects in human diseases associated with ER stress. Many studies have identified small molecules that can be considered as a potential drug to selectively inhibit UPR components and have already been enrolled in preclinical trials of disease (Kanekura et al., 2009; Saxena et al., 2009; Ciechanover and Kwon, 2015; Ruegsegger and Saxena, 2016; Dalla Bella et al., 2021).

TABLE 1 | Pharmacological targeting of UPR pathway (Rivas et al., 2015; Hetz et al., 2019).

Small molecules	UPR pathway	ER-stress
GSK2656157	PERK arm	Inhibitor of PERK kinase
GSK2606414		Inhibitor of PERK kinase
Salubrinal		Binding GADD34 phosphatase complex, inhibitor of eIF2a dephosphorylation
ISRIB		Reduced ATF4 expression
Guanabenz		eIF2a phosphatase inhibitor
Sephin1		eIF2a phosphatase inhibitor
Salicylaldimines	IRE1 arm	Inhibitor of IRE1α RNase
SFT-083010		Inhibitor of IRE1α RNase
MKC-3946		Inhibitor of IRE1α RNase
Sunitinib		Inhibitor of IRE1α RNase
Toyocamycin		Inhibitor of IRE1α RNase
Methoxycitrinin		Increasing the XBP1 splicing levels
Citrinin		Increasing the XBP1 splicing levels
Patulin		Increasing the XBP1 splicing levels
Quercetin		Increase IRE1 nuclease activityand splicing of XBP1
Apigenin		Increasingthe IRE1α nuclease activity
Resveratrol		Decreasing DNA-binding capacity of XBP1 to the target genes
Apigenin	ATF6 arm	Upregulation of ATF6 expression
Baicalein		Upregulation of ATF6 expression
Kaempferol		Downregulation of ATF6 expression

Several small molecules targeting the different domains of the IRE1 pathway are in the preclinical stages against cancer, diabetes, neurodegenerative diseases, etc. The RNase domain inhibitors of IRE1 (e.g., MKC-3946, STF-083010) contain an aromatic aldehyde group in the core and adjacent hydroxyl group. The core aldehyde group reacts with the amino group of lysine and forms imine derivatives, and the hydroxyl group reacts with the tyrosine forming hydrogen bonds, and inhibiting the catalytic cleavage of IRE1α (Cross et al., 2012). The inhibitors targeting the kinase domain of IRE1 (e.g., KIRA6) disrupt the interfacial contacts and prevent the dimerization of IRE1α, thus making it inactive (Feldman et al., 2016). The small molecule inhibitors of the

PERK pathway (e.g., GSK2606414, GSK2656157) prevent the interaction of PERK with ATP and thus block the PERK induced signaling cascade. These ATP-competitive inhibitors contain an indoline core moiety that binds to the kinase domain in the ATP-binding site, leading to a conformational change that results in the inhibition of the kinase domain of PERK (Hetz et al., 2019). Similarly, the modulators of the PERK pathway (Salubrinal, Guanabenz, and Sephin1) inhibit the protein phosphatase complex and thus prevent the de-phosphorylation of eIF2α, a negative feedback loop to control protein translation during the ER stress (Boyce et al., 2005; Tsaytler et al., 2011). Also, Salubrinal protects $SOD1^{G93A}$ mouse motor neurons from ER stress (Saxena et al., 2009). Guanabenz, an FDA-approved alpha-2 adrenergic receptor agonist, decreased neuronal toxicity by decreasing the ER stress in worm and zebrafish models (Vaccaro et al., 2013). Guanabenz treatment delayed the disease onset, improved motor performance, decrease the loss of motor neurons, and improve the survival in a $SOD1^{G93A}$ mouse model by reducing ER stress due to extensive phosphorylation ofeIF2a (Jiang et al., 2014; Wang et al., 2014; Das et al., 2015; Dalla Bella et al., 2021). In mutant TDP-43 *C. elegans* and zebrafish models of ALS, guanabenz, and salubrinal decreased ER stress and subsequently reduced the neurodegeneration (Vieira et al., 2015).

A summary of small molecules that selectively target crucial UPR components and other players of the ER proteostasis network, and is used to target neurodegenerative disease models is elegantly reviewed in Charif et al. (2022), Hetz et al. (2019), and Rivas et al. (2015) and is further shown in **Figure 1** and **Table 1**.

CONCLUSION

In summary, growing evidences indicate that ER stress and UPRare largely involved in the pathogenesis of human diseases, including cancer and neurodegenerative diseases. Protein misfolding and aggregation in cells trigger the ER stress which is overpowered by an adaptive response of cells collectively known as UPR. The UPR pathways are facilitated by essential components like PERK, IRE1, and ATF6 which are important in maintaining protein homeostasis. This protective role becomes more important and beneficial in several neurodegenerative diseases including ALS. Studies from ALS and other neurodegenerative disease models indicate that treatments targeting ER proteostasis and UPR have shown protective roles. Further, a more clear and improved understanding of the genes involved in ALS and the associated mechanisms of proteostasis dysfunction in ALS will be essential and crucial for developing small molecule therapeutics to effectively target the ER proteostasis and UPR.

AUTHOR CONTRIBUTIONS

VK and YL designed the topics. CZ and AR wrote the main text with the contributions of YL and VK. All authors contributed to the article and approved the submitted version.

REFERENCES

Acosta-Alvear, D., Zhou, Y., Blais, A., Tsikitis, M., Lents, N. H., Arias, C., et al. (2007). XBP1 controls diverse cell type- and condition-specific transcriptional regulatory networks. *Mol. Cell* 27, 53–66. doi: 10.1016/j.molcel.2007.06.011

Al-Chalabi, A., Jones, A., Troakes, C., King, A., Al-Sarraj, S., and van den Berg, L. H. (2012). The genetics and neuropathology of amyotrophic lateral sclerosis. *Acta Neuropathol.* 124, 339–352. doi: 10.1007/s00401-012-1022-4

Arai, T., Hasegawa, M., Akiyama, H., Ikeda, K., Nonaka, T., Mori, H., et al. (2006). TDP-43 is a component of ubiquitin-positive tau-negative inclusions in frontotemporal lobar degeneration and amyotrophic lateral sclerosis. *Biochem. Biophys. Res. Commun.* 351, 602–611. doi: 10.1016/j.bbrc.2006.10.093

Atkin, J. D., Farg, M. A., Turner, B. J., Tomas, D., Lysaght, J. A., Nunan, J., et al. (2006). Induction of the unfolded protein response in familial amyotrophic lateral sclerosis and association of protein-disulfide isomerase with superoxide dismutase 1. *J. Biol. Chem.* 281, 30152–30165. doi: 10.1074/jbc.M603393200

Atkin, J. D., Farg, M. A., Walker, A. K., McLean, C., Tomas, D., and Horne, M. K. (2008). Endoplasmic reticulum stress and induction of the unfolded protein response in human sporadic amyotrophic lateral sclerosis. *Neurobiol. Dis.* 30, 400–407. doi: 10.1016/j.nbd.2008.02.009

Bernard-Marissal, N., Sunyach, C., Marissal, T., Raoul, C., and Pettmann, B. (2015). Calreticulin levels determine onset of early muscle denervation by fast motoneurons of ALS model mice. *Neurobiol. Dis.* 73, 130–136. doi: 10.1016/j.nbd.2014.09.009

Blokhuis, A. M., Groen, E. J., Koppers, M., van den Berg, L. H., and Pasterkamp, R. J. (2013). Protein aggregation in amyotrophic lateral sclerosis. *Acta Neuropathol.* 125, 777–794. doi: 10.1007/s00401-013-1125-6

Boyce, M., Bryant, K. F., Jousse, C., Long, K., Harding, H. P., Scheuner, D., et al. (2005). A selective inhibitor of eIF2α dephosphorylation protects cells from ER stress. *Science* 307, 935–939. doi: 10.1126/science.1101902

Charif, S. E., Vassallu, M. F., Salvanal, L., and Igaz, L. M. (2022). Protein synthesis modulation as a therapeutic approach for amyotrophic lateral sclerosis and frontotemporal dementia. *Neural Regen. Res.* 17, 1423–1430. doi: 10.4103/1673-5374.330593

Chen, H. J., Anagnostou, G., Chai, A., Withers, J., Morris, A., Adhikaree, J., et al. (2010). Characterization of the properties of a novel mutation in VAPB in familial amyotrophic lateral sclerosis. *J. Biol. Chem.* 285, 40266–40281. doi: 10.1074/jbc.M110.161398

Cheng, W., Wang, S., Mestre, A. A., Fu, C., Makarem, A., Xian, F., et al. (2018). C9ORF72 GGGGCC repeat-associated non-AUG translation is upregulated by stress through eIF2α phosphorylation. *Nat. Commun.* 9:51. doi: 10.1038/s41467-017-02495-z

Cicardi, M. E., Marrone, L., Azzouz, M., and Trotti, D. (2021). Proteostatic imbalance and protein spreading in amyotrophic lateral sclerosis. *EMBO J.* 40:e106389. doi: 10.15252/embj.2020106389

Ciechanover, A., and Kwon, Y. T. (2015). Degradation of misfolded proteins in neurodegenerative diseases: therapeutic targets and strategies. *Exp. Mol. Med.* 47:e147. doi: 10.1038/emm.2014.117

Cooper-Knock, J., Harvey, C., Zhang, S., Moll, T., Timpanaro, I. S., Kenna, K. P., et al. (2021). Advances in the genetic classification of amyotrophic lateral sclerosis. *Curr. Opin. Neurol.* 34, 756–764. doi: 10.1097/WCO.0000000000000986

Cross, B. C., Bond, P. J., Sadowski, P. G., Jha, B. K., Zak, J., Goodman, J. M., et al. (2012). The molecular basis for selective inhibition of unconventional mRNA splicing by an IRE1-binding small molecule. *Proc. Natl. Acad. Sci. U S A* 109, E869–878. doi: 10.1073/pnas.1115623109

Dafinca, R., Barbagallo, P., and Talbot, K. (2021). The role of mitochondrial dysfunction and ER stress in TDP-43 and C9ORF72 ALS. *Front. Cell Neurosci.* 15:653688. doi: 10.3389/fncel.2021.653688

Dafinca, R., Scaber, J., Ababneh, N., Lalic, T., Weir, G., Christian, H., et al. (2016). C9orf72 hexanucleotide expansions are associated with altered endoplasmic reticulum calcium homeostasis and stress granule formation in

induced pluripotent stem cell-derived neurons from patients with amyotrophic lateral sclerosis and frontotemporal dementia. *Stem Cells* 34, 2063–2078. doi: 10.1002/stem.2388

Dalla Bella, E., Bersano, E., Antonini, G., Borghero, G., Capasso, M., Caponnetto, C., et al. (2021). The unfolded protein response in amyotrophic later sclerosis: results of a phase 2 trial. *Brain* 144, 2635–2647. doi: 10.1093/brain/awab167

Das, I., Krzyzosiak, A., Schneider, K., Wrabetz, L., D'Antonio, M., Barry, N., et al. (2015). Preventing proteostasis diseases by selective inhibition of a phosphatase regulatory subunit. *Science* 348, 239–242. doi: 10.1126/science.aaa4484

de Mena, L., Lopez-Scarim, J., and Rincon-Limas, D. E. (2021). TDP-43 and ER stress in neurodegeneration: friends or foes? *Front. Mol. Neurosci.* 14:772226. doi: 10.3389/fnmol.2021.772226

Deng, H. X., Chen, W., Hong, S. T., Boycott, K. M., Gorrie, G. H., Siddique, N., et al. (2011). Mutations in UBQLN2 cause dominant X-linked juvenile and adult-onset ALS and ALS/dementia. *Nature* 477, 211–215. doi: 10.1038/nature10353

Dugger, B. N., and Dickson, D. W. (2017). Pathology of neurodegenerative diseases. *Cold Spring Harb. Perspect. Biol.* 9:a028035. doi: 10.1101/cshperspect.a028035

Farg, M. A., Soo, K. Y., Walker, A. K., Pham, H., Orian, J., Horne, M. K., et al. (2012). Mutant FUS induces endoplasmic reticulum stress in amyotrophic lateral sclerosis and interacts with protein disulfide-isomerase. *Neurobiol. Aging* 33, 2855–2868. doi: 10.1016/j.neurobiolaging.2012.02.009

Feldman, H. C., Tong, M., Wang, L., Meza-Acevedo, R., Gobillot, T. A., Lebedev, I., et al. (2016). Structural and functional analysis of the allosteric inhibition of IRE1alpha with ATP-competitive ligands. *ACS Chem. Biol.* 11, 2195–2205. doi: 10.1021/acschembio.5b00940

Ferraiuolo, L., Kirby, J., Grierson, A. J., Sendtner, M., and Shaw, P. J. (2011). Molecular pathways of motor neuron injury in amyotrophic lateral sclerosis. *Nat. Rev. Neurol.* 7, 616–630. doi: 10.1038/nrneurol.2011.152

Gami-Patel, P., van Dijken, I., Meeter, L. H., Melhem, S., Morrema, T. H. J., Scheper, W., et al. (2021). Unfolded protein response activation in C9orf72 frontotemporal dementia is associated with dipeptide pathology and granulovacuolar degeneration in granule cells. *Brain Pathol.* 31, 163–173. doi: 10.1111/bpa.12894

Gitcho, M. A., Strider, J., Carter, D., Taylor-Reinwald, L., Forman, M. S., Goate, A. M., et al. (2009). VCP mutations causing frontotemporal lobar degeneration disrupt localization of TDP-43 and induce cell death. *J. Biol. Chem.* 284, 12384–12398. doi: 10.1074/jbc.M900992200

Gkogkas, C., Middleton, S., Kremer, A. M., Wardrope, C., Hannah, M., Gillingwater, T. H., et al. (2008). VAPB interacts with and modulates the activity of ATF6. *Hum. Mol. Genet.* 17, 1517–1526. doi: 10.1093/hmg/ddn040

Glineburg, M. R., Zhang, Y., Krans, A., Tank, E. M., Barmada, S. J., and Todd, P. K. (2021). Enhanced detection of expanded repeat mRNA foci with hybridization chain reaction. *Acta Neuropathol. Commun.* 9:73. doi: 10.1186/s40478-021-01169-8

Green, K. M., Glineburg, M. R., Kearse, M. G., Flores, B. N., Linsalata, A. E., Fedak, S. J., et al. (2017). RAN translation at C9orf72-associated repeat expansions is selectively enhanced by the integrated stress response. *Nat. Commun.* 8:2005. doi: 10.1038/s41467-017-02200-0

Haeusler, A. R., Donnelly, C. J., Periz, G., Simko, E. A., Shaw, P. G., Kim, M. S., et al. (2014). C9orf72 nucleotide repeat structures initiate molecular cascades of disease. *Nature* 507, 195–200. doi: 10.1038/nature13124

Harding, H. P., Zhang, Y., and Ron, D. (1999). Protein translation and folding are coupled by an endoplasmic-reticulum-resident kinase. *Nature* 397, 271–274. doi: 10.1038/16729

Hayashi, T., and Su, T. P. (2007). Sigma-1 receptor chaperones at the ER-mitochondrion interface regulate Ca^{2+} signaling and cell survival. *Cell* 131, 596–610. doi: 10.1016/j.cell.2007.08.036

Haze, K., Yoshida, H., Yanagi, H., Yura, T., and Mori, K. (1999). Mammalian transcription factor ATF6 is synthesized as a transmembrane protein and activated by proteolysis in response to endoplasmic reticulum stress. *Mol. Biol. Cell* 10, 3787–3799. doi: 10.1091/mbc.10.11.3787

Hetz, C. (2012). The unfolded protein response: controlling cell fate decisions under ER stress and beyond. *Nat. Rev. Mol. Cell Biol.* 13, 89–102. doi: 10.1038/nrm3270

Hetz, C., Axten, J. M., and Patterson, J. B. (2019). Pharmacological targeting of the unfolded protein response for disease intervention. *Nat. Chem. Biol.* 15, 764–775. doi: 10.1038/s41589-019-0326-2

Hetz, C., Lee, A. H., Gonzalez-Romero, D., Thielen, P., Castilla, J., Soto, C., et al. (2008). Unfolded protein response transcription factor XBP-1 does not influence prion replication or pathogenesis. *Proc. Natl. Acad. Sci. U S A* 105, 757–762. doi: 10.1073/pnas.0711094105

Hetz, C., and Papa, F. R. (2018). The unfolded protein response and cell fate control. *Mol. Cell* 69, 169–181. doi: 10.1016/j.molcel.2017.06.017

Hetz, C., and Saxena, S. (2017). ER stress and the unfolded protein response in neurodegeneration. *Nat. Rev. Neurol.* 13, 477–491. doi: 10.1038/nrneurol.2017.99

Hu, W., Liu, X., Wang, S., Sun, G., Zhao, R., and Lu, H. (2019). SecinH3 attenuates TDP-43 p.Q331K-induced neuronal toxicity by suppressing endoplasmic reticulum stress and enhancing autophagic flux. *IUBMB Life* 71, 192–199. doi: 10.1002/iub.1951

Igaz, L. M., Kwong, L. K., Xu, Y., Truax, A. C., Uryu, K., Neumann, M., et al. (2008). Enrichment of C-terminal fragments in TAR DNA-binding protein-43 cytoplasmic inclusions in brain but not in spinal cord of frontotemporal lobar degeneration and amyotrophic lateral sclerosis. *Am. J. Pathol.* 173, 182–194. doi: 10.2353/ajpath.2008.080003

Ilieva, E. V., Ayala, V., Jove, M., Dalfo, E., Cacabelos, D., Povedano, M., et al. (2007). Oxidative and endoplasmic reticulum stress interplay in sporadic amyotrophic lateral sclerosis. *Brain* 130, 3111–3123. doi: 10.1093/brain/awm190

Jiang, H. Q., Ren, M., Jiang, H. Z., Wang, J., Zhang, J., Yin, X., et al. (2014). Guanabenz delays the onset of disease symptoms, extends lifespan, improves motor performance and attenuates motor neuron loss in the SOD1 G93A mouse model of amyotrophic lateral sclerosis. *Neuroscience* 277, 132–138. doi: 10.1016/j.neuroscience.2014.03.047

Kanekura, K., Nishimoto, I., Aiso, S., and Matsuoka, M. (2006). Characterization of amyotrophic lateral sclerosis-linked P56S mutation of vesicle-associated membrane protein-associated protein B (VAPB/ALS8). *J. Biol. Chem.* 281, 30223–30233. doi: 10.1074/jbc.M605049200

Kanekura, K., Suzuki, H., Aiso, S., and Matsuoka, M. (2009). ER stress and unfolded protein response in amyotrophic lateral sclerosis. *Mol. Neurobiol.* 39, 81–89. doi: 10.1007/s12035-009-8054-3

Kaushik, S., and Cuervo, A. M. (2015). Proteostasis and aging. *Nat. Med.* 21, 1406–1415. doi: 10.1038/nm.4001

Kikuchi, H., Almer, G., Yamashita, S., Guegan, C., Nagai, M., Xu, Z., et al. (2006). Spinal cord endoplasmic reticulum stress associated with a microsomal accumulation of mutant superoxide dismutase-1 in an ALS model. *Proc. Natl. Acad. Sci. U S A* 103, 6025–6030. doi: 10.1073/pnas.0509227103

Koppers, M., van Blitterswijk, M. M., Vlam, L., Rowicka, P. A., van Vught, P. W., Groen, E. J., et al. (2012). VCP mutations in familial and sporadic amyotrophic lateral sclerosis. *Neurobiol. Aging* 33, e7837–e7913. doi: 10.1016/j.neurobiolaging.2011.10.006

Kramer, N. J., Haney, M. S., Morgens, D. W., Jovicic, A., Couthouis, J., Li, A., et al. (2018). CRISPR-Cas9 screens in human cells and primary neurons identify modifiers of C9ORF72 dipeptide-repeat-protein toxicity. *Nat. Genet.* 50, 603–612. doi: 10.1038/s41588-018-0070-7

Krebs, J., Agellon, L. B., and Michalak, M. (2015). Ca^{2+} homeostasis and endoplasmic reticulum (ER) stress: an integrated view of calcium signaling. *Biochem. Biophys. Res. Commun.* 460, 114–121. doi: 10.1016/j.bbrc.2015.02.004

Kumar, V., Islam, A., Hassan, M. I., and Ahmad, F. (2016a). Therapeutic progress in amyotrophic lateral sclerosis-beginning to learning. *Eur. J. Med. Chem.* 121, 903–917. doi: 10.1016/j.ejmech.2016.06.017

Kumar, V., Sami, N., Kashav, T., Islam, A., Ahmad, F., and Hassan, M. I. (2016b). Protein aggregation and neurodegenerative diseases: from theory to therapy. *Eur. J. Med. Chem.* 124, 1105–1120. doi: 10.1016/j.ejmech.2016.07.054

Kumar, V., Wahiduzzaman, W., Prakash, A., Tomar, A. K., Srivastava, A., Kundu, B., et al. (2019). Exploring the aggregation-prone regions from structural domains of human TDP-43. *Biochim. Biophys. Acta Proteins Proteomics* 1867, 286–296. doi: 10.1016/j.bbapap.2018.10.008

Kwiatkowski, T. J., Jr., Bosco, D. A., Leclerc, A. L., Tamrazian, E., Vanderburg, C. R., Russ, C., et al. (2009). Mutations in the FUS/TLS gene on chromosome 16 cause familial amyotrophic lateral sclerosis. *Science* 323, 1205–1208. doi: 10.1126/science.1166066

Lautenschlaeger, J., Prell, T., and Grosskreutz, J. (2012). Endoplasmic reticulum stress and the ER mitochondrial calcium cycle in amyotrophic lateral sclerosis. *Amyotroph. Lateral Scler.* 13, 166–177. doi: 10.3109/17482968.2011.641569

Levy, J. R., Sumner, C. J., Caviston, J. P., Tokito, M. K., Ranganathan, S., Ligon, L. A., et al. (2006). A motor neuron disease-associated mutation in $p150^{Glued}$ perturbs dynactin function and induces protein aggregation. *J. Cell Biol.* 172, 733–745. doi: 10.1083/jcb.200511068

Lin, G., Mao, D., and Bellen, H. J. (2017). Amyotrophic lateral sclerosis pathogenesis converges on defects in protein homeostasis associated with TDP-43 mislocalization and proteasome-mediated degradation overload. *Curr. Top. Dev. Biol.* 121, 111–171. doi: 10.1016/bs.ctdb.2016.07.004

Lin, J. H., Walter, P., and Yen, T. S. (2008). Endoplasmic reticulum stress in disease pathogenesis. *Annu. Rev. Pathol.* 3, 399–425. doi: 10.1146/annurev.pathmechdis.3.121806.151434

Liu, C. Y., Wong, H. N., Schauerte, J. A., and Kaufman, R. J. (2002). The protein kinase/endoribonuclease IRE1α that signals the unfolded protein response has a luminal N-terminal ligand-independent dimerization domain. *J. Biol. Chem.* 277, 18346–18356. doi: 10.1074/jbc.M112454200

Mackenzie, I. R., Bigio, E. H., Ince, P. G., Geser, F., Neumann, M., Cairns, N. J., et al. (2007). Pathological TDP-43 distinguishes sporadic amyotrophic lateral sclerosis from amyotrophic lateral sclerosis with SOD1 mutations. *Ann. Neurol.* 61, 427–434. doi: 10.1002/ana.21147

Malhotra, J. D., and Kaufman, R. J. (2007). The endoplasmic reticulum and the unfolded protein response. *Semin. Cell Dev. Biol.* 18, 716–731. doi: 10.1016/j.semcdb.2007.09.003

Martinez, J. A., Zhang, Z., Svetlov, S. I., Hayes, R. L., Wang, K. K., and Larner, S. F. (2010). Calpain and caspase processing of caspase-12 contribute to the ER stress-induced cell death pathway in differentiated PC12 cells. *Apoptosis* 15, 1480–1493. doi: 10.1007/s10495-010-0526-4

Maruyama, H., Morino, H., Ito, H., Izumi, Y., Kato, H., Watanabe, Y., et al. (2010). Mutations of optineurin in amyotrophic lateral sclerosis. *Nature* 465, 223–226. doi: 10.1038/nature08971

Nakagawa, T., Zhu, H., Morishima, N., Li, E., Xu, J., Yankner, B. A., et al. (2000). Caspase-12 mediates endoplasmic-reticulum-specific apoptosis and cytotoxicity by amyloid-β. *Nature* 403, 98–103. doi: 10.1038/47513

Neumann, M., Sampathu, D. M., Kwong, L. K., Truax, A. C., Micsenyi, M. C., Chou, T. T., et al. (2006). Ubiquitinated TDP-43 in frontotemporal lobar degeneration and amyotrophic lateral sclerosis. *Science* 314, 130–133. doi: 10.1126/science.1134108

Nishihira, Y., Tan, C. F., Hoshi, Y., Iwanaga, K., Yamada, M., Kawachi, I., et al. (2009). Sporadic amyotrophic lateral sclerosis of long duration is associated with relatively mild TDP-43 pathology. *Acta Neuropathol.* 117, 45–53. doi: 10.1007/s00401-008-0443-6

Nishitoh, H., Kadowaki, H., Nagai, A., Maruyama, T., Yokota, T., Fukutomi, H., et al. (2008). ALS-linked mutant SOD1 induces ER stress- and ASK1-dependent motor neuron death by targeting Derlin-1. *Genes Dev.* 22, 1451–1464. doi: 10.1101/gad.1640108

Oakes, S. A., and Papa, F. R. (2015). The role of endoplasmic reticulum stress in human pathology. *Annu. Rev. Pathol.* 10, 173–194. doi: 10.1146/annurev-pathol-012513-104649

Oh, Y. K., Shin, K. S., Yuan, J., and Kang, S. J. (2008). Superoxide dismutase 1 mutants related to amyotrophic lateral sclerosis induce endoplasmic stress in neuro2a cells. *J. Neurochem.* 104, 993–1005. doi: 10.1111/j.1471-4159.2007.05053.x

Oyanagi, K., Yamazaki, M., Takahashi, H., Watabe, K., Wada, M., Komori, T., et al. (2008). Spinal anterior horn cells in sporadic amyotrophic lateral sclerosis show ribosomal detachment from and cisternal distention of the rough endoplasmic reticulum. *Neuropathol. Appl. Neurobiol.* 34, 650–658. doi: 10.1111/j.1365-2990.2008.00941.x

Prasad, A., Bharathi, V., Sivalingam, V., Girdhar, A., and Patel, B. K. (2019). Molecular mechanisms of TDP-43 misfolding and pathology in amyotrophic lateral sclerosis. *Front. Mol. Neurosci.* 12:25. doi: 10.3389/fnmol.2019.00025

Prudencio, M., Belzil, V. V., Batra, R., Ross, C. A., Gendron, T. F., Pregent, L. J., et al. (2015). Distinct brain transcriptome profiles in C9orf72-associated and sporadic ALS. *Nat. Neurosci.* 18, 1175–1182. doi: 10.1038/nn.4065

Rivas, A., Vidal, R. L., and Hetz, C. (2015). Targeting the unfolded protein response for disease intervention. *Expert Opin. Ther. Targets* 19, 1203–1218. doi: 10.1517/14728222.2015.1053869

Ruegsegger, C., and Saxena, S. (2016). Proteostasis impairment in ALS. *Brain Res.* 1648, 571–579. doi: 10.1016/j.brainres.2016.03.032

Sasaki, S. (2010). Endoplasmic reticulum stress in motor neurons of the spinal cord in sporadic amyotrophic lateral sclerosis. *J. Neuropathol. Exp. Neurol.* 69, 346–355. doi: 10.1097/NEN.0b013e3181d44992

Saxena, S., Cabuy, E., and Caroni, P. (2009). A role for motoneuron subtype-selective ER stress in disease manifestations of FALS mice. *Nat. Neurosci.* 12, 627–636. doi: 10.1038/nn.2297

Scheper, W., and Hoozemans, J. J. (2015). The unfolded protein response in neurodegenerative diseases: a neuropathological perspective. *Acta Neuropathol.* 130, 315–331. doi: 10.1007/s00401-015-1462-8

Schroder, M. (2008). Endoplasmic reticulum stress responses. *Cell. Mol. Life Sci.* 65, 862–894. doi: 10.1007/s00018-007-7383-5

Shatunov, A., and Al-Chalabi, A. (2021). The genetic architecture of ALS. *Neurobiol. Dis.* 147:105156. doi: 10.1016/j.nbd.2020.105156

Sidrauski, C., Acosta-Alvear, D., Khoutorsky, A., Vedantham, P., Hearn, B. R., Li, H., et al. (2013). Pharmacological brake-release of mRNA translation enhances cognitive memory. *eLife* 2:e00498. doi: 10.7554/eLife.00498

Simmen, T., Aslan, J. E., Blagoveshchenskaya, A. D., Thomas, L., Wan, L., Xiang, Y., et al. (2005). PACS-2 controls endoplasmic reticulum-mitochondria communication and Bid-mediated apoptosis. *EMBO J.* 24, 717–729. doi: 10.1038/sj.emboj.7600559

Sonobe, Y., Ghadge, G., Masaki, K., Sendoel, A., Fuchs, E., and Roos, R. P. (2018). Translation of dipeptide repeat proteins from the C9ORF72 expanded repeat is associated with cellular stress. *Neurobiol. Dis.* 116, 155–165. doi: 10.1016/j.nbd.2018.05.009

Suzuki, H., Kanekura, K., Levine, T. P., Kohno, K., Olkkonen, V. M., Aiso, S., et al. (2009). ALS-linked P56S-VAPB, an aggregated loss-of-function mutant of VAPB, predisposes motor neurons to ER stress-related death by inducing aggregation of co-expressed wild-type VAPB. *J. Neurochem.* 108, 973–985. doi: 10.1111/j.1471-4159.2008.05857.x

Suzuki, H., Lee, K., and Matsuoka, M. (2011). TDP-43-induced death is associated with altered regulation of BIM and Bcl-xL and attenuated by caspase-mediated TDP-43 cleavage. *J. Biol. Chem.* 286, 13171–13183. doi: 10.1074/jbc.M110.197483

Suzuki, H., and Matsuoka, M. (2012). TDP-43 toxicity is mediated by the unfolded protein response-unrelated induction of C/EBP homologous protein expression. *J. Neurosci. Res.* 90, 641–647. doi: 10.1002/jnr.22777

Tabas, I., and Ron, D. (2011). Integrating the mechanisms of apoptosis induced by endoplasmic reticulum stress. *Nat. Cell Biol.* 13, 184–190. doi: 10.1038/ncb0311-184

Tsai, Y. L., and Manley, J. L. (2021). Multiple ways to a dead end: diverse mechanisms by which ALS mutant genes induce cell death. *Cell Cycle* 20, 631–646. doi: 10.1080/15384101.2021.1886661

Tsaytler, P., Harding, H. P., Ron, D., and Bertolotti, A. (2011). Selective inhibition of a regulatory subunit of protein phosphatase 1 restores proteostasis. *Science* 332, 91–94. doi: 10.1126/science.1201396

Tziortzouda, P., Van Den Bosch, L., and Hirth, F. (2021). Triad of TDP43 control in neurodegeneration: autoregulation, localization and aggregation. *Nat. Rev. Neurosci.* 22, 197–208. doi: 10.1038/s41583-021-00431-1

Vaccaro, A., Patten, S. A., Aggad, D., Julien, C., Maios, C., Kabashi, E., et al. (2013). Pharmacological reduction of ER stress protects against TDP-43 neuronal toxicity *in vivo*. *Neurobiol. Dis.* 55, 64–75. doi: 10.1016/j.nbd.2013.03.015

van Es, M. A., Hardiman, O., Chio, A., Al-Chalabi, A., Pasterkamp, R. J., Veldink, J. H., et al. (2017). Amyotrophic lateral sclerosis. *Lancet* 390, 2084–2098. doi: 10.1016/S0140-6736(17)31287-4

Vance, C., Rogelj, B., Hortobagyi, T., De Vos, K. J., Nishimura, A. L., Sreedharan, J., et al. (2009). Mutations in FUS, an RNA processing protein, cause familial amyotrophic lateral sclerosis type 6. *Science* 323, 1208–1211. doi: 10.1126/science.1165942

Vieira, F. G., Ping, Q., Moreno, A. J., Kidd, J. D., Thompson, K., Jiang, B., et al. (2015). Guanabenz treatment accelerates disease in a mutant SOD1 mouse

model of ALS. *PLoS One* 10:e0135570. doi: 10.1371/journal.pone.0135570

Vijayalakshmi, K., Alladi, P. A., Ghosh, S., Prasanna, V. K., Sagar, B. C., Nalini, A., et al. (2011). Evidence of endoplasmic reticular stress in the spinal motor neurons exposed to CSF from sporadic amyotrophic lateral sclerosis patients. *Neurobiol. Dis.* 41, 695–705. doi: 10.1016/j.nbd.2010.12.005

Vijayalakshmi, K., Alladi, P. A., Sathyaprabha, T. N., Subramaniam, J. R., Nalini, A., and Raju, T. R. (2009). Cerebrospinal fluid from sporadic amyotrophic lateral sclerosis patients induces degeneration of a cultured motor neuron cell line. *Brain Res.* 1263, 122–133. doi: 10.1016/j.brainres.2009.01.041

Walker, A. K., and Atkin, J. D. (2011). Stress signaling from the endoplasmic reticulum: a central player in the pathogenesis of amyotrophic lateral sclerosis. *IUBMB Life* 63, 754–763. doi: 10.1002/iub.520

Walker, A. K., Soo, K. Y., Sundaramoorthy, V., Parakh, S., Ma, Y., Farg, M. A., et al. (2013). ALS-associated TDP-43 induces endoplasmic reticulum stress, which drives cytoplasmic TDP-43 accumulation and stress granule formation. *PLoS One* 8:e81170. doi: 10.1371/journal.pone.0081170

Walter, P., and Ron, D. (2011). The unfolded protein response: from stress pathway to homeostatic regulation. *Science* 334, 1081–1086. doi: 10.1126/science.1209038

Wang, L., Popko, B., Tixier, E., and Roos, R. P. (2014). Guanabenz, which enhances the unfolded protein response, ameliorates mutant SOD1-induced amyotrophic lateral sclerosis. *Neurobiol. Dis.* 71, 317–324. doi: 10.1016/j.nbd.2014.08.010

Wang, X., Ma, M., Teng, J., Che, X., Zhang, W., Feng, S., et al. (2015a). Valproate attenuates 25-kDa C-terminal fragment of TDP-43-induced neuronal toxicity *via* suppressing endoplasmic reticulum stress and activating autophagy. *Int. J. Biol. Sci.* 11, 752–761. doi: 10.7150/ijbs.11880

Wang, X., Zhou, S., Ding, X., Ma, M., Zhang, J., Zhou, Y., et al. (2015b). Activation of ER stress and autophagy induced by TDP-43 A315T as pathogenic mechanism and the corresponding histological changes in skin as potential biomarker for ALS with the mutation. *Int. J. Biol. Sci.* 11, 1140–1149. doi: 10.7150/ijbs.12657

Wang, R., Xu, X., Hao, Z., Zhang, S., Wu, D., Sun, H., et al. (2019). Poly-PR in C9ORF72-related amyotrophic lateral sclerosis/frontotemporal dementia causes neurotoxicity by clathrin-dependent endocytosis. *Neurosci. Bull.* 35, 889–900. doi: 10.1007/s12264-019-00395-4

Wate, R., Ito, H., Zhang, J. H., Ohnishi, S., Nakano, S., and Kusaka, H. (2005). Expression of an endoplasmic reticulum-resident chaperone, glucose-regulated stress protein 78, in the spinal cord of a mouse model of amyotrophic lateral sclerosis. *Acta Neuropathol.* 110, 557–562. doi: 10.1007/s00401-005-1080-y

Webster, C. P., Smith, E. F., Shaw, P. J., and De Vos, K. J. (2017). Protein homeostasis in amyotrophic lateral sclerosis: therapeutic opportunities? *Front. Mol. Neurosci.* 10:123. doi: 10.3389/fnmol.2017.00123

Westergard, T., McAvoy, K., Russell, K., Wen, X., Pang, Y., Morris, B., et al. (2019). Repeat-associated non-AUG translation in C9orf72-ALS/FTD is driven by neuronal excitation and stress. *EMBO Mol. Med.* 11:e9423. doi: 10.15252/emmm.201809423

Zhang, K., Daigle, J. G., Cunningham, K. M., Coyne, A. N., Ruan, K., Grima, J. C., et al. (2018). Stress granule assembly disrupts nucleocytoplasmic transport. *Cell* 173, 958–971.e17. doi: 10.1016/j.cell.2018.03.025

Zhang, Y. J., Gendron, T. F., Ebbert, M. T. W., O'Raw, A. D., Yue, M., Jansen-West, K., et al. (2018). Poly(GR) impairs protein translation and stress granule dynamics in C9orf72-associated frontotemporal dementia and amyotrophic lateral sclerosis. *Nat. Med.* 24, 1136–1142. doi: 10.1038/s41591-018-0071-1

Zhang, Y. J., Jansen-West, K., Xu, Y. F., Gendron, T. F., Bieniek, K. F., Lin, W. L., et al. (2014). Aggregation-prone c9FTD/ALS poly(GA) RAN-translated proteins cause neurotoxicity by inducing ER stress. *Acta Neuropathol.* 128, 505–524. doi: 10.1007/s00401-014-1336-5

Zu, T., Guo, S., Bardhi, O., Ryskamp, D. A., Li, J., Khoramian Tusi, S., et al. (2020). Metformin inhibits RAN translation through PKR pathway and mitigates disease in C9orf72 ALS/FTD mice. *Proc. Natl. Acad. Sci. U S A* 117, 18591–18599. doi: 10.1073/pnas.2005748117

Conflict of Interest: The authors declare that the research was conducted in the absence of any commercial or financial relationships that could be construed as a potential conflict of interest.

Publisher's Note: All claims expressed in this article are solely those of the authors and do not necessarily represent those of their affiliated organizations, or those of the publisher, the editors and the reviewers. Any product that may be evaluated in this article, or claim that may be made by its manufacturer, is not guaranteed or endorsed by the publisher.

Advantages of publishing in Frontiers

OPEN ACCESS
Articles are free to read for greatest visibility and readership

FAST PUBLICATION
Around 90 days from submission to decision

HIGH QUALITY PEER-REVIEW
Rigorous, collaborative, and constructive peer-review

TRANSPARENT PEER-REVIEW
Editors and reviewers acknowledged by name on published articles

Frontiers
Avenue du Tribunal-Fédéral 34
1005 Lausanne | Switzerland

Visit us: www.frontiersin.org
Contact us: frontiersin.org/about/contact

REPRODUCIBILITY OF RESEARCH
Support open data and methods to enhance research reproducibility

DIGITAL PUBLISHING
Articles designed for optimal readership across devices

FOLLOW US
@frontiersin

IMPACT METRICS
Advanced article metrics track visibility across digital media

EXTENSIVE PROMOTION
Marketing and promotion of impactful research

LOOP RESEARCH NETWORK
Our network increases your article's readership